Production of medium-chain-length polyhydroxyalkanoates from engineered bacteria

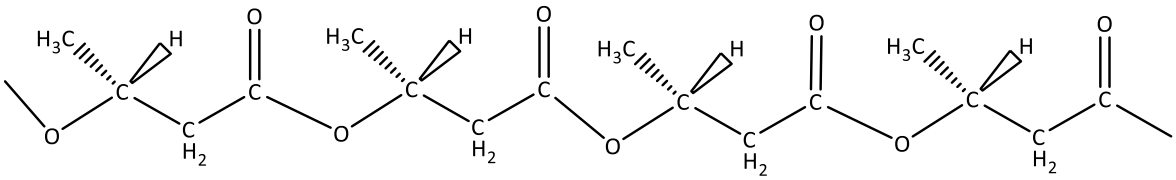

By: Isabel Vital Vilchis

A thesis submitted for the degree of Doctor of Philosophy

The University of Sheffield

Faculty of Engineering

Department of Chemical and Biological Engineering

May 2024

(*This page was left blank intentionally*)

DECLARATION

This thesis and the work presented in it is a product of original research conducted by me at the Department of Chemical and Biological Engineering, at The University of Sheffield. All sources of information presented in this work have been accordingly referenced. This thesis has been previously submitted at this University and this version is a re-submission. It has not been submitted at any other institution. Parts of this work may be presented elsewhere in the form of scientific publications.

This thesis is written in conformance to the rules of the Code Of Practice For Research Degree Program 2023-2024 of the University of Sheffield.

CONTENT

LIST OF FIGURES

LIST OF TABLES

LIST OF APPENDICES

LIST OF ANNEXES

LIST OF ABBREVIATIONS

Abbreviation	Meaning
µmol	Micromol
3HX,HX	Hydroxy x where
	X= butyrate (b), valerate(v), hexanoate(hx), octanoate (o)
	Decanoate(d), dodecanoate(dd), tetradecanoate(td).
A	Alanine
Å	Angstrom
aldB	Aldehyde dehydrogenase
alkk	Medium-chain-fatty acid-coa ligase
Arg	Arginine
Asn	Asparagine
Asp	Aspartic Acid
C, Cys	Cysteine
C. necator	*Cupriavidus necator*
Cad	Cadherin-like domain
Cam ^{R}	Chloramphenicol resistance
C-NMR	Carbon nuclear magnetic resonance
CO	Carbon monoxide
CO2	Carbon dioxide
CoA	Coenzyme a
dPHA	Extracellular pha
DTNB	5,5-dithio-bis (2 nitrobenzoic acid)
E. coli	*Escherichia coli*
fabG	Ketoacyl reductases
fadA	B-ketoacyl-coa thiolase
FadB	Multifunctional enzyme with hydratase and dehydrogenase

fadE	Acyl-coa dehydrogenase
FAME	Fatty acid methyl ester
FID	Flame ionization
Fn3	Fibronectin type 3
FRT	Flippase recognition target
G	Glycine
g	Gram
GC	Gas chromatography
Gln	Glutamine
H2	Hydrogen
HDPE	High density polyethylene
His	Histidine
H-NMR	Hydrogen-nuclear magnetic resonance
HPLC	High performance liquid chromatography
Kan^R	Kanamycin resistance
Kda	Kilodaltons
km	Michaelis constant
l	Liter
LA	Lactate
LCFA	Long carbon chain fatty acid(≥ c11).
LDPE	Low density polyethylene
Leu	Leucine
lys	Lysine
MCFA	Medium carbon chain length fatty acid (c7–c10)
mcl	Medium chain length
NADPH	Nicotinamide adenine dinucleotide
NH4OH	Ammonium hydroxide
nm	Nanometers
nPHA	Native intracellular pha

O2	Oxygen
P. spp	Pseudomonas spp.
P3HX, PHX	Polyhydroxy x where
	X= butyrate (b), valerate (v), hexanoate (hx), octanoate (o)
	Decanoate, dodecanoate, tetradecanoate.
PCR	Polymerase chain reaction
PE	Polyethylene
PET	Polyethylene terephthalate
PHA, P3HA	Polyhydroxyalkanoates
PhaC	Polyhydroxyalkanoate polymerase
PhaCAB	Pha operon from *c. Necator*
PhaG	3-hydroxydecanoyl-acp:
phaZ	Polyhydroxyalkanoate depolymerase
Phe	Phenylalanine
PmePhaC	Pha synthase from *pseudomonas mendocina* nk-01
PMMA	Poly(methylmethacrylate)
pN	Petanewton
pNPA	Para-nitrophenylalkanoate
PP	Polypropylene
PpuPhaC	Pha synthase from *pseudomonas putida* kt2440
PS	Polystyrene
PstPhaC	Pha synthase from *pseudomonas stutzeri* 1317
Ptac	Tac promoter
PVC	Polyvinyl chloride
RT	Retention time
S, Ser	Serine
SBD	Substrate binding domain
SDR	Short-chain alcohol dehydrogenase/reductase
SCFA	Short carbon chain length fatty acids(c4-c6)

scl	Short chain length
thr	Threonine
Trp	Tryptophan
Tyr	Tyrosine
Vmax	Maximum velocity

DEDICATION

I want to dedicate this thesis work to **mom**, my biggest emotional supporter and cheerleader, because you were always there and never stopped believing in me.

Quiero dedicar este trabajo de tesis a mi **Mamá**, quien es mi más grande apoyo emocional y porrista, porque siempre ha estado ahí y nunca ha dejado de creer en mí. Te amo mami.

ACKNOWLEDGEMENTS

I came from Mexico to England with great hope and a big dream: to prepare myself for becoming a scientist in one of the best universities in the world.

My journey in Sheffield, although interesting and exciting, it also turned out to be much more difficult than originally expected. I faced all types of challenges both professionally and personally and I would have not been able to overcome all the hardships alone. Many people accompanied me through this journey.

I would like to thank my supervisor Esther Karunakaran for believing in me and giving me a second chance. Esther's lab feels like home to me.

I feel deep gratitude towards my family: mom Ileana, dad Ignacio, sister Maria Elena and Grandma Maria Elena. For all the virtual talks and experiences that we shared together and for always putting a smile on my face. For always staying in touch and for proving that love is bigger than distance.

I would also like to thank Jyoti for always being there when I needed it and for being the light of all the rainy, cold days in Sheffield. This experience would have never been the same without you!

Lastly, I would like to extend my deepest gratitude to CONACyT and my country Mexico for enabling this journey and granting me a scholarship.

COVID-19 AND UNFORSEEN CIRCUMSTANCES IMPACT STATEMENT

Important as well as unforeseen circumstances affected the present PhD investigation. I started my PhD on September of 2019 and my supervisor at that time was working abroad, therefore I decided to spend the first 3 months of my degree reading papers and studying before going to the lab. My first week on the lab was on mid-January 2020. Unfortunately, on March 10th University of Sheffield went on complete lockdown and I lost 6 complete months of activity (returned 12th of August 2020). After I returned to the lab, my work continued to be impacted by the pandemic due to social distancing and less access to resources. Example: a supplier took 2 months to deliver sodium tetradecanoate, sodium dodecanoate and other reactants that were crucial to grow my cells.

On top of this, my relationship and communication with my supervisor at that time was so very poor that on April, 2022 I decided to apply for a change of lab and supervisory team (30 months after the start of my PhD). I was reincorporated into a new lab work until July of that year. This change brought also extra challenges to my project as some of my methods changed and were adapted to fit my new circumstances.

On September 2022 (end of tuition period 36 months) I decided to extend my PhD work period for an extra 12 months to meet the necessary criteria for a successful thesis work.

The work presented in this thesis is the direct result of my circumstances, resources, perseverance, and hard work.

ABSTRACT

Polyhydroxyalkanoates (PHAs) are sustainable microbial biopolymers that, due to their biodegradability and biocompatibility, could potentially replace petroleum-based plastic. Medium chain length polyhydroxyalkanoates (mcl-PHAs) are a type of PHA that consist of monomers that are between 6 and 14 carbons long. They are elastic and flexible and can be used for a range of applications where these properties are advantageous such as soft tissue implants, heart valves, nerve tissue scaffolds etc.

In all microbial cells, mcl-PHA is synthesized by the PHA synthase enzyme (PhaC) from 3-hydroxyacyl-CoA which is an intermediate metabolite of the β-oxidation pathway. The main objective of this project was to optimize the β-oxidation pathway to channel more precursors into biosynthesis of a novel mcl-PHA with high hydroxydodecanoate (C12) and/or hydroxytetradecanoate (C14) monomer composition (≥ 30%) using sodium dodecanoate or tetradecanoate as substrates. *Escherichia coli* was chosen as a chassis to compare enzymes activity related to this pathway and to compare the biosynthesized PHAs.

A method for digestion and quantification of PHA using gas chromatography (GC) was first validated and standard curves were successfully constructed for PHAs of different chain lengths and for identification of residual substrates in the samples. Subsequently, a metabolic engineering strategy was followed using techniques in molecular microbiology to biosynthesise PHAs in *E. coli*. Firstly, 3 different *phaCs* from different *Pseudomonas (Pseudomonas mendocina,* NK-01*, P. putida* KT2440 *and P. stutzeri* 1317) were cloned in 2 different plasmid backbones each and the production of the target mcl-PHA inside *Escherichia coli* DH5α and inside the Δ*fad*A knockout *E.coli*- K-12 was compared using sodium dodecanoate (C12) and/or sodium tetradecanoate (C14) as substrates. The β-oxidation inhibitor sodium acrylate was also tested for its ability to channel more intermediate metabolites towards PHA production. Secondly, 2 different FabG enzymes (3-ketoacyl-acyl carrier protein (ACP) reductases) from *E. coli* -K-12 (EcolifabG) and *M. tuberculosis* (MtubfabG) were expressed in *E. coli* and compared for their ability to channel

more intermediate metabolites towards PHA production. Lastly, the gene encoding the FadR protein (β-oxidation repressor) was knocked out from the Δ*fad*A *E. coli* K-12 strain to test the constitutive expression of β-oxidation pathway for the same purpose.

All the dry biomass collected from the recombinant strains cultures was digested and analyzed using GC-FID for PHA content. Results showed that further optimization needs to be undertaken for production to reach levels that are detectable and quantifiable.

CHAPTER 1

Literature review

An overview to the future of bioplastics: Polyhydroxyalkanoates

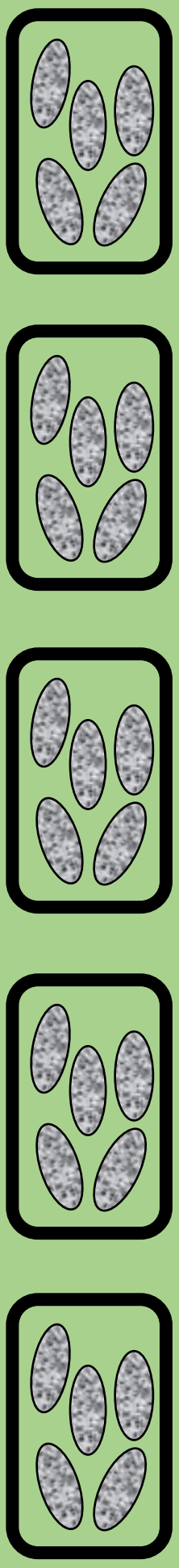

CHAPTER 1. LITERATURE REVIEW: An overview to the future of bioplastics: Polyhydroxyalkanoates.

1.1 Petroleum-based plastic contamination

According to Geyer, Jambeck and Law [23] 8300 million metric tons of virgin plastics had been produced by 2017 from non-renewable petrochemical feedstocks and only a few proportion had been recycled or incinerated. They estimated that if current trends continue, approximately 1200 metric tons of plastic waste will be accumulated in landfills or in the natural environment by 2050. This analysis included thermoplastics, thermosets, polyurethanes (PURs), elastomers, coatings, and sealants but focused on the most abundant resins and fibers: high-density polyethylene (HPE), low-density and linear low-density PE (LPE), polypropylene (PP), polystyrene (PS), polyvinylchloride (PVC), poly-ethylene terephthalate (PET), and PUR resins; and polyester, poly-amide, and acrylic (PP&A) fibers.

The ubiquitous distribution of the plastic contamination in both terrestrial (all land) and marine environments (lakes, rivers, nearshore marine and offshore marine) has identified the phenomenon as a key geological indicator of the Anthropocene [24] which is an epoch of time defined by the domination of humanity over surface geological processes [25]

Plastic pollution is a serious issue that affects animal and human life. In the sea, for example, it has been reported that over 260 of marine species including mammals, seabirds, turtles and invertebrates become entangled or ingest plastic waste which impair their movement, feeding and reproductive capabilities or cause internal lacerations and ulcers ultimately resulting in death. [26] Whereas in humans it has been proven that ingestion of nano-plastics and micro-plastics are neurotoxic, genotoxic and cytotoxic and can produce

metabolic disorders, induce DNA damage and oxidative stress which in turn leads to carcinogenesis. [27]

1.2 Bioplastics

Bioplastics are a growing class of materials that can be used as an alternative to petroleum-based plastic. [28] They can be biodegradable but they can also be not degradable but produced from biological material or renewable feedstock. [28] Main types of bioplastics are illustrated in **Figure 1 .** Bioplastics have been studied for more than a century and yet, their industrialization is still embryonic. [29] According to the report of the European Bioplastics, bioplastics currently (2023) represent roughly 0.5% percent of the over 400 million tonnes of plastic produced annually [30]

The main advantage of most bioplastics is that they have a faster biodegradation rate than petroleum-based plastics in a wide range of environments and that, unlike fossil resources, they are an inexhaustible resource that produces less carbon footprint.[31, 32]

On the other hand, one of the main roadblocks to produce bioplastics is their higher costs. Other additional disadvantages include the use of land to grow feedstock, and thermophysical properties of some types of these plastics such as thermal instability, brittleness, low melt strength et cetera.[33]

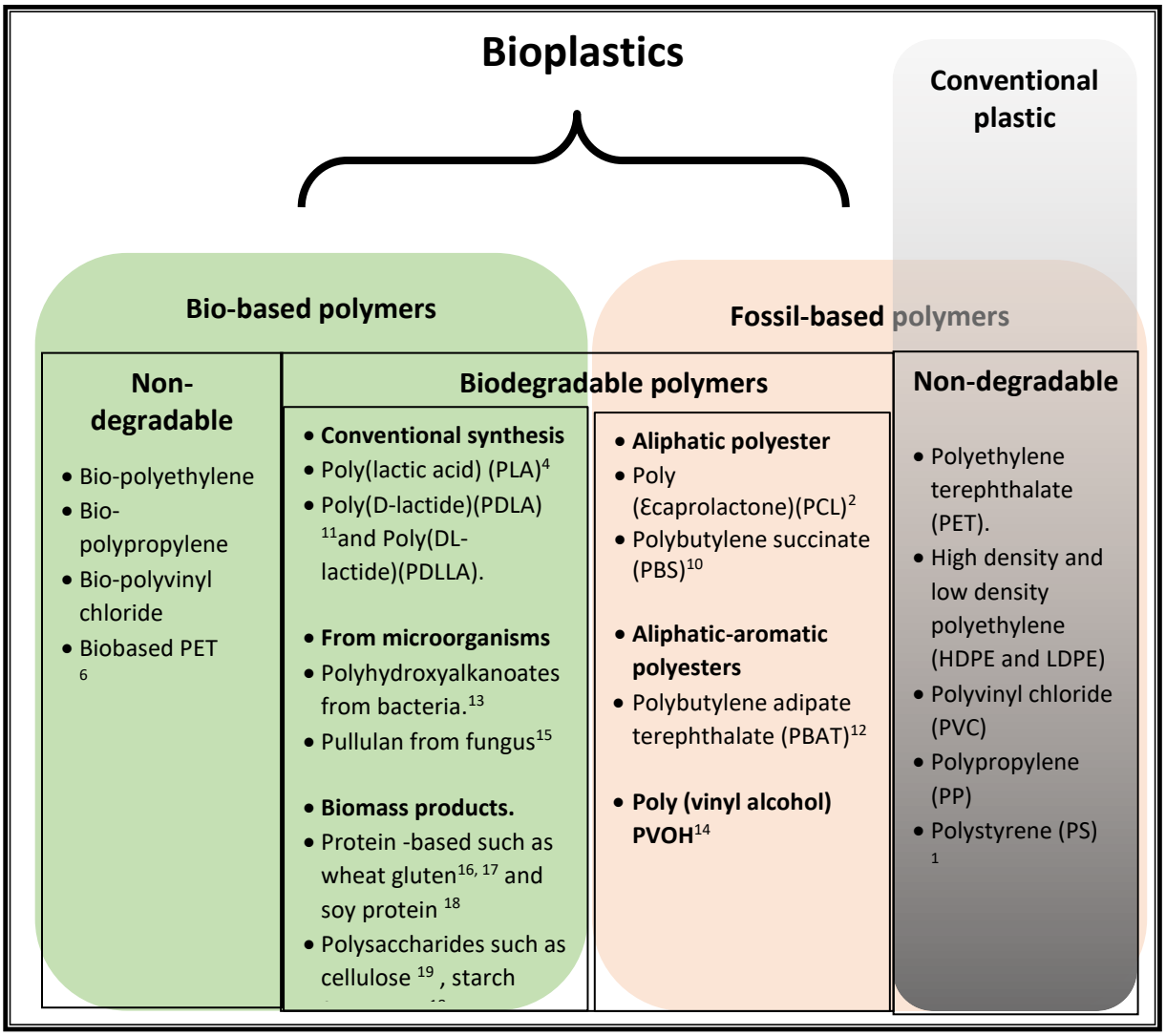

***Figure 1**. Types of bioplastics modified from [5]*

1.3 PHA

Microorganisms produce a wide variety of biopolymers.[34-36] Polyhydroxyalkanoates (PHA) are biopolymers classified as polyesters which many bacteria accumulate in the form

of intracellular granules as a reservoir of energy and carbon in response to stress conditions, especially when nitrogen is limited. [37-39] Maurice Lemoigne was the first scientist to isolate and characterize poly-3-hydroxybutyrate (P3HB) , the simplest type of PHA, as a storage compound from *Bacillus megaterium* in 1926. [38, 40] P3HB is a polymer composed of 4 carbon-chain-length repeating monomers, and it is the most common and abundant PHA in bacteria. [41, 42] However, many other PHAs have also been characterized and studied especially due to their biodegradability and biocompatibility, which makes them good candidates to substitute petroleum-based plastic. [43]

1.4 Types of PHA.

PHA polymers are classified by their monomer length as short chain length (scl), which normally contain less than 5 carbons (≤C5), for example poly-3-hydroxyvalerate (P3HV) (P3HB falls in this category as well) and as medium chain length (mcl) which contain in between 6 and 14 carbons (≥C6, ≤C14), for example: poly-3-hydroxyoctanoate (P3HO) and poly-3-hydroxyhexanoate (P3HHX). [44-46] PHA polymers are composed of a backbone and a lateral chain (R) which is normally an alkane chain (Refer **Figure 2**). [47]

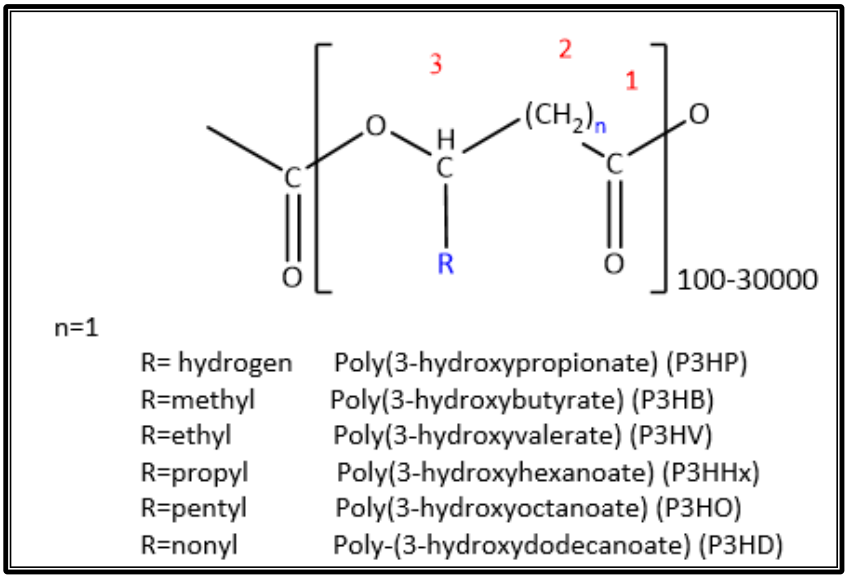

Figure 2. *PHA general formula.* [47] *Structure modelled using ChemDraw.* [7]

Aside from alkanes, PHAs can have lateral chains containing double or triple bonds and /or include different functional groups such as halogen atoms, methoxy, benzoyl, ethoxy, cyanophenoxy, acetoxy, phenoxy, hydroxyl, nitrophenyl, epoxy, carbonyl, cyano and others. [48]

There are PHAs in which the length of the backbone is longer, so the hydroxyl group to be esterified is not in carbon C3. Other PHAs have a thioester group in the place of the oxoester linkage. Some of these PHAs are uncommon and can only be obtained by chemical or physical modification of naturally occurring ones. [42, 48, 49]

PHAs can also be classified as homopolymers and copolymers, for example poly(3HB-co-3HV) is a copolymer made up from 3-hydroxybutyrate and 3-hydroxyvalerate monomers. This process depends on the carbon substrate, metabolic pathways available and the specificity of the enzymes involved. [50] For example, *Klebsiella* spp. can produce poly(3HB-co-3HV) with a higher portion of 3HV using soy waste and with a lower portion of 3HV using malt wastes as carbon feedstock, while *Alcaligenes latus* and *Staphylococcus* spp. can only produce homopolymers of hydroxybutyrate using these same substrates.[51] In contrast, *Cupriavidus necator* (*Alcaligenes eutrophus)* is capable of increasing the proportion of HV inside poly(3HB-co-3HV) when NH_4OH is present in the medium. [52]

In addition to the above classifications, PHAs can be classified as block copolymers. Block copolymers are macromolecules composed of sequences, or blocks, of chemically distinct repeat units. Hence, PHAs block copolymers are composed of different sets of PHA homopolymers linked together. Possible block copolymer structures include A-B diblock, A-B-A, A-B-C triblock, or (AB)n repeating multiblock . [53] It has been demonstrated that alternating between different carbon feedstocks leads to the formation of block copolymers; For instance *Cupriavidus necator* can synthetize poly(3-hydroxybutyrate)-block-poly(3-hydroxybutyrate-co-3-hydroxyvalerate) (P3HB-b-P3HBV) when valeric acid containing substrate is alternated with non-valeric acid substrate. [54]

1.5 Observation of PHA granules.

PHA is stored in the cytoplasm as body inclusions as shown in **Figure 3B**. These granules are PHA cores surrounded by a monolayer of phospholipids and proteins which include PHA synthase, phasins, PHA depolymerases for remobilisation of the carbon supply and a regulator protein (**Figure 3A**). [55, 56]

Granules can be observed using diverse microscopic techniques, for example, phase contrast microscopy can detect brightly refractile cytoplasmic inclusions (RCI). Another option would be to dye the colony with Nile blue or Nile red to observe granules in Gram-negative bacteria such as *Azotobacter vinelandii*, *E. coli*, *P. putida* and *C. necator* whereas the stain Sudan Black can be used for both, Gram-negative and Gram-positive bacteria under bright field microscope. [57-60]

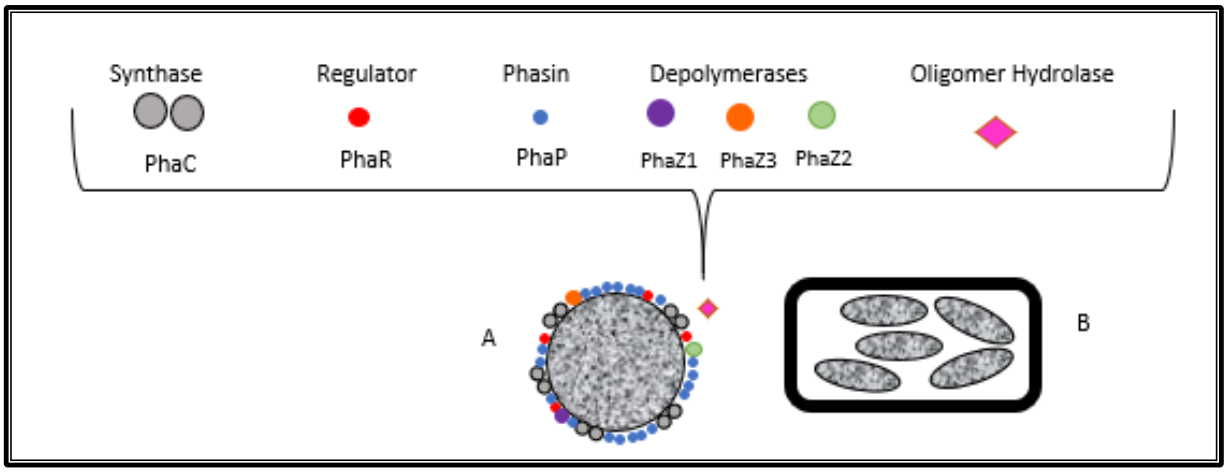

***Figure 3**. A) Proteins involved in PHA homeostasis surrounding a PHA granule. B) Representation of PHA granules accumulated in C. necator (Taken from Stubbe and Tian, 2003)*[55]

1.6 Commercial value, industrial production, and applications of PHAs.

The global bioplastic polyhydroxyalkanoate (PHA) market was estimated to be 57 million dollars in 2019 and ,it is predicted to grow to 98 million dollar by 2024. [61] This boost will be, partly, due to the increasing number of policies to reduce single-use plastic such as plastic bags and microbeads all around the world but mostly in Europe. [62, 63]

In the history of PHAs, 24 companies are known to have engaged in PHA production and more than 10,000 PHA products have been available on the market. [64, 65] These are mainly made from P3HB, poly(3HB-co-3HV), poly(3HB-co-4HB), poly(3HB-co-3HHx) and on less scale medium-chain-length (mcl) PHAs. [46, 64]

However, the 6 most important companies nowadays are : BioMatera (Canada), Bio-on (Italy), Danimer Scientific (USA) , TianAn Biologic Materials (China) , Tianjin GreenBio Materials (China) and Yield10 Bioscience (USA). [66] (**Table 1**) followed by Kaneka Corporation (Japan), Shenzhen Ecomann Biotechnology Co., Ltd (China), Newlight Technologies, LLC (U.S) and others.

Different types of PHAs could potentially replace poly(methylmethacrylate) PMMA, low density polyethylene (LDPE), polyethylene terephthalate (PET), high density polyethylene (HDPE), polyethylene (PE), polypropylene (PP), polystyrene (PS) and/or polyvinyl chloride (PVC). [67] Danimer Scientific (U.S.), for example, partnered with Nestle to replace PET and produce PHA-made biodegradable water bottles. [61] PHAs could replace food packaging (originally from polypropylene) [68, 69] and microbeads in cosmetics such as lipstick, lip gloss, mascara, eye-liner, creams and shampoo. [67] It can also replace shopping plastic bags or plastic bags to produce agricultural seedlings.

Table 1. Main PHA producing companies.

Company	Substrate	Main product	Brand name	Main uses	Organism used	Capacity
BioMatera(Canada),	Renewable raw materials	PHA resins	Biomatera	Food packaging, agricultural products, inks, cosmetics and biomedical	Non-transgenic, non-pathogenic bacteria isolated from soil	Not specified
Bio-on (Italy)	Sugar beet, sugar cane bioproduct, agricultural waste	PHA P3HB, poly(3HB -co-3HV)	Minerv®	Medical, cosmetics and bioremediation	*Cupravidus necator*	10,000 tons annually
Danimer Scientific (USA)	Canola oil, plant-based oils	mcl-P3HB	Nodax™	Pure resin for food packaging, agriculture etc.	Not specified	Not specified
TianAn Biologic Materials (China)	Corn or cassava grown in China	poly(3HB -co-3HV) P3HB	Enmat™	Thermoplastic resins, fibers, water treatment	*Cupravidus necator*	2,204 tons per year
Tianjin GreenBio Materials (China)	Sucrose	P(3,4 HB)	Sogreen™	Pure resin, films, injection moulding and foam	*Escherichia coli*.	10,000 tons per year
Yield10 Bioscience (Metabolix before) (USA)	Corn	P3HB	Mirel	Injection moulding, packaging	*Cupriavidus necator*	50,000 tons per year

mcl-PHA: medium chain length PHA, poly(3HB): poly(3-hydroxybutyrate), poly(3HB-co-HV): poly(3-hydroxybutyrate-co-3-hydroxyvalerate), P(3,4 HB): poly (3-hydroxybutyrate-co-4-hydroxybutyrate). [65-67, 70-74]

Moreover, PHAs have a wide range of medical applications, for instance, sutures threads, skin substitutes, bone plates, surgical mesh, staples, orthopaedic pins and many others. [75]

1.7 Advantages and disadvantages of PHAs

One of the main advantages of PHAs is its high biodegradability compared to petroleum-based plastic. For example, a PHA-made water bottle would be expected to completely degrade in 1.5 to 3.5 years in marine environment [76] while a high-density polyethylene bottle has a marine half-life of 58 years.[77] However they also present some disadvantages such as the high cost of production. [78] Other advantages and disadvantages are listed below:

Advantages

- Less $C0_2$ emissions and sustainability.[79]
- The industrial production has a low safety risk compared to petroleum-based plastic production which includes flammable and toxic by-products.[79]
- Waste water is non-toxic.[79]

Disadvantages

- Not economically competitive compared to petroleum-based plastic [79]
- The monomer composition of the polymer is difficult to control [79]
- Difficulties in processing due to their low crystallization process.[79]
- Heavy water consumption. [79]
- Substrate to product conversion is low[79]

1.8 Characteristics and uses of medium-chain-length polyhydroxyalkanoates.

Comparison of the thermophysical characteristics between short-chain-length and medium-chain-length polyhydroxyalkanoates are illustrated in **Table 2.**

Table 2. Comparison of the thermophysical characteristics between short-chain-length and medium-chain-length PHAs.

Short-chain-length PHAs	Medium-chain-length PHAs
Highly crystalline[80, 81]	Low crystallinity[80, 81]
Hard [80, 81]	Soft[80, 81]
Brittle[80, 81]	Flexible[80, 81]
	Thermo-elastomeric polyesters[80, 81]
	Low glass transition and melting temperature[80, 82]
	Low tensile strength and modulus[80, 82]
	Higher elongation at break[80, 82]

PHAs, in general, can be used in medical devices such as suture threads, patches, meshes, implants, tissue engineering scaffolds and controlled drug delivery systems. In particular, due to their elasticity, medium chain length PHAs have been reported to be used for soft tissue implants. [83] Moreover, there is evidence showing that the cytotoxicity of polyhydroxyalkanoates is inversely proportional with the length of the side chain of the monomer (longer side chains are less cytotoxic) making medium-chain- length PHAs better candidates for medical applications. [84]

Mcl-PHA are specially utilized for cardiac tissue engineering applications and heart valves because elastic materials are more suitable to be used as leaflets inside the tri-leaflet valve. [84] They also mimic better the mechanical properties of soft nerve tissue. [85] Scaffolds of the co-polymer poly(3HB-co-3HHx) compared against scaffolds with scl-PHA monomers showed stronger potential to promote differentiation of neural stem cells into neurons and therefore showed biomedical potential for repairing the central nervous system. [86]

However, studies remain limited mainly to PHO and the co-polymer poly(3HB-co-3HHx) which are the only mcl-PHAs in large quantities. [85]

1.9 Quantification of PHA content.

The conventional method for determining polymer content is through gas chromatography after methanolysis.[87-90] Similarly, HPLC can be used after acid pretreatment to quantify PHB or after alkaline pretreatment to quantify PHAs with longer chains. [91]

Apart from these, there are other methods, for instance, Fourier Transform Infrared Spectroscopy (FT-IR). The technique is based on the comparison of the absorbance of the ester band of PHAs and the absorbance of the amide group of bacteria to make a calibration curve and determine polymer content. It is non-destructive, rapid and it can also determine the composition of the PHA by examining the wavenumber band. [92] Differential scanning calorimetry (DSC) is another proven method to quantify mcl-PHA and can also be used to obtain structural information on PHA inclusion bodies in cells without the need to isolate them. [93]

PHAs can, as well, be quantified directly by measuring the absorbance of the Nile blue dye fixed by PHA granules or indirectly by measuring the absorbance of the residual supernatant obtained after staining these cells. [60]

1.10 Strains used for PHA production.

More than 5000 species of bacteria distributed in more than 14 bacterial groups including *Firmicutes*, *Bacilli*, *Clostridia*, *Actinobacteria*, *Micrococcal*, *Streptomycetales*, *Corynebacterial*, *Cyanobacteria*/*Melainabacteria* group, *Proteobacteria*, *Alpha proteobacteria*, *Gamma proteobacteria*, *Betaproteobacteria*, *Delta*/*Epsilon* subdivisions and other groups have the capacity of synthetizing PHA. [50, 94] Even some microalgae (phylum *Cyanobacteria*) and halophilic archaea can accumulate it. [95, 96]

However, although a wide variety of microorganisms accumulate PHA only a few of them produce enough quantity to be used for industrial-scale production (1 g L^{-1} h^{-1} to 2 g L^{-1} h^{-1}).[97] Example of these microorganisms are *Cupriavidus necator*, *Azohydromonas lata* (previously *Alcaligenes latus* [98]) *Azotobacter vinelandi , Pseudomonas oleovorans,* and recombinant *E. coli.* [47, 99, 100] *Pseudomonas putida, Bacillus* spp. and *Aeromonas hydrophila* are other examples. [65] (see **Table 3**)

Table 3. Most common strains used for PHA production.

Strain	PHA type	Company
Cupriavidus necator	P3HB poly(3HB-co-3HV) poly(3HB-co-3HV-co-3HV) P(3,4HB) poly(3HB-co-3HHx)(recombinant)	Tianjin North. Food (China), Bio-on (Italy), TianAn Biological materials (China), Yield 10 Bioscience (USA) ICI Chemicals (UK), Bio-on (Italy), TianAn Biological materials (China). Bio-on (Italy) Yield 10 Bioscience (USA) P & G, Kaneka (Japan)
Alcaligenes latus	P3HB	Chemie Linz (Austria)
Escherichia coli	P3HB, P(3,4 HB)	Jiang Su Nan Tian (China) Tianjin Greenbio (China)
Aeromonas hydrophila	poly(3HB-co-3HHx) poly(3HB-co-3HHx)(recombinant)	P & G,Jiangmen Biotech (China) Shandong Lukang (China)
Pseudomonas putida and *P. oleovorans*	mcl-PHA	ETH (Switzerland)
Bacillus spp.	P3HB	Biocycles, Brazil

mcl-PHA: medium chain length polyhydroxyalkanoate, P3HB: poly(3-hydroxybutyrate), poly(3HB-co-3HV-co-3HV): poly(3-hydroxybutyrate-co-3-hydroxyvalerate-co-3-hydroxyvalerate), poly(3HB-co-3HV): poly(3-hydroxybutyrate-co-3-hydroxyvalerate), P(3,4 HB): poly (3-hydroxybutyrate-co-4-hydroxybutyrate), poly(3HB-co-HHx): poly(3-hydroxybutyrate-co-3-hydroxyhexanoate)(Adapted from Chen, 2009). [65]

1.10.1 Cupriavidus necator.

From all microorganisms mentioned above, by far, the most common and studied for industrial production of PHAs is *Cupriavidus necator* [101] (also known as *Alcaligenes eutrophus, Wautersia eutropha, or Ralstonia eutropha*[102]). *C. necator* was first isolated in 1961 [103] and it is a β-proteobacterium capable of utilizing either H_2 or organic compounds

as sources of energy and CO_2 or organic compounds as carbon sources. It can also perform aerobic (use of O_2) or anaerobic respiration by denitrification (conversion of nitrate and/or nitrite to nitrogen gas)[104, 105]. Due to its remarkable metabolic versatility, it can produce PHAs from a wide range of substrates. A glucose-utilizing mutant of this bacteria was used for the first industrial production of PHA by Imperial Chemical Industries (London) in 1980. [106]

In 2006, the complete genome of *C. necator* was sequenced, allowing the biotechnological exploitation of the bacteria [105] and although, the bacteria is a representative producer of short chain length PHAs, efforts have also been made to produce medium chain length PHAs, such as poly(3HB-co-3HHx) which is a polymer with high biodegradability, even in marine environments. [107-109] Procter & Gamble Co., Ltd. (Cincinnati, OH, USA) produces this polymer commercially. [65]

Apart from the above ,novel biopolymers, polythioesters and other interesting value added chemicals such as alkanes, alcohols, alkenes, cyanophycins and others products can also be synthesized by *C. necator.* [110]

1.10.2 Recombinant *Escherichia coli.*

PHA synthesis, from acetyl-CoA, is controlled by one operon containing 3 genes: β-ketothiolase, acetoacetyl-CoA reductase and PHA synthase (**Figure 4**). [47, 111] Slater, Voige and Dennis [112] cloned all three genes from *C. necator* H16 and inserted them into *Escherichia coli* which was able to synthetize P3HB to, nearly, 80% of the bacterial cell dry weight.

Since then, *E. coli* has been further engineered to synthetize poly(3-hydroxyvalerate), poly(3-hydroxybutyrate-co-3-hydroxyvalerate)[113], poly(3-hydroxypropionate)[114] and various mcl-PHAs [115, 116] in between other PHAs.

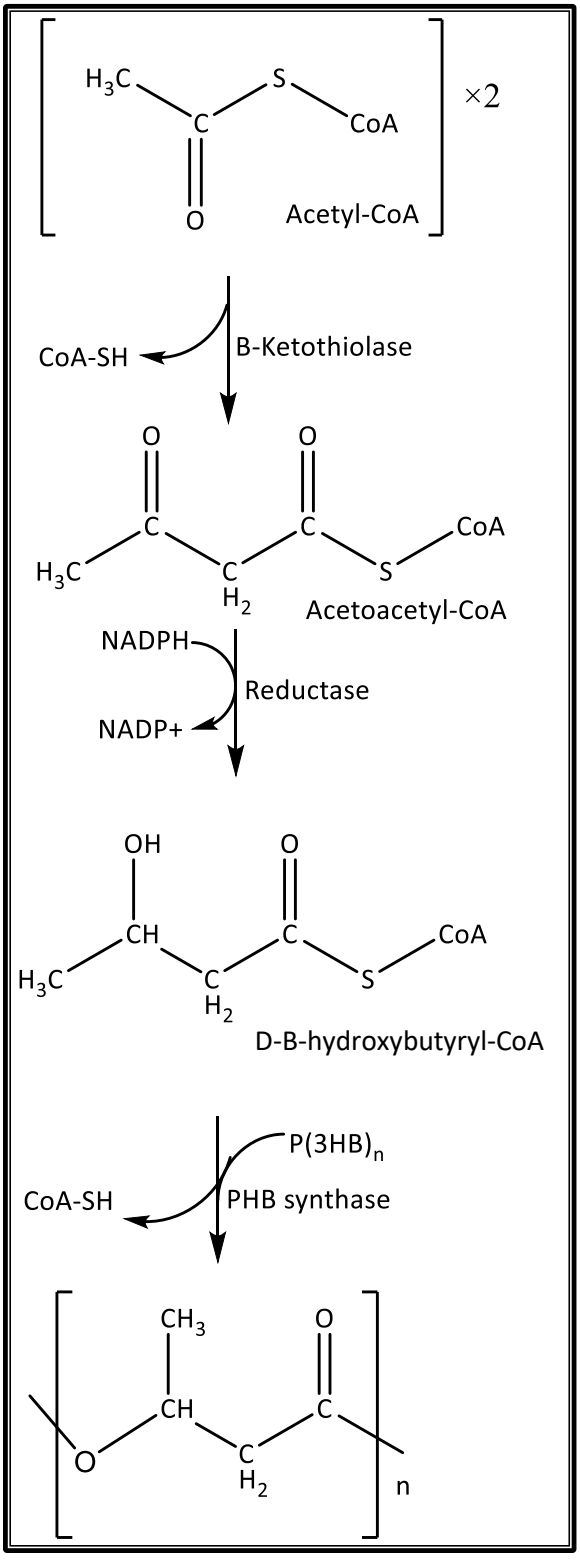

***Figure 4**. Metabolic pathway for the synthesis of PHB in C. necator. Metabolic pathway modelled using ChemDraw*[7]

1.10.3 *Pseudomonas* to produce medium-chain-length PHAs.

As discussed in **section 1.8,** P3HB is crystalline, stiff and easy to break. [69] Mcl-PHAs with longer monomer chains lengths will be less crystalline, more elastic, and more flexible, and therefore they can be used for a bigger range of applications were these properties are advantageous. [85]

The representative genus for mcl-PHA production is *Pseudomonas*, for instance, *P. mosselii* T07, *P. corrugata*, *P. mediterranea*, *P. putida* and *P mendocina*, from which one of the most promising ones is *Pseudomonas putida* KT2440 due to its capacity to hyperaccumulate PHA from cheap substrates (example: glucose) .[117] (**Table 4**)

Table 4. Different *Pseudomonas* to industrially produce mcl-PHA.

Strain	DNA manipulation	PHA type	C-source	final CDW (g/l)	Final PHA (%CDW)	
P. putida mt-2	No	P3HO	Glycerol/ octanoate		57%	[118]
P. putida KT2440	Xylose isomerase, xylulokinase	mcl-PHA	Xylose, octanoic acid	2.5	20%	[119]
• *P. putida* W619	No	mcl-PHA	Glucose	0.85	25%	[120]
• *P. putida* KT2440	No	mcl-PHA	Glucose	0.93	32.1%	
• *P. fluorescens* 555	No	mcl-PHA	Glucose	0.86	37.2%	
• *P. putida* KT2440	No	mcl-PHA	Glycerol	4.23	34.5%	[121]
• *P. putida* KT2442	No	mcl-PHA	Glycerol	3.45	26.5%	
• *P. putida* F1	No	mcl-PHA	Glycerol	3.50	10.3%	
• *P. putida* S12	No	mcl-PHA	Glycerol	3.20	12.6%	
P. putida LS46	No	(P3HO) (P3HD)	Biodiesel-derived "waste" fatty-acids		29%	[122]
P. putida KT2440	Δ*phaZ* Δ*fadB*A1 Δ*fadBAE2* Δ*aldB::Ptac-phaG-alkK-phaC1-phaC2*	mcl-PHA	P-coumaric acid (lignin derived)	1.758	54.2	[123]
			Corn stover (lignin-containing)	0.657	17.7	

1.11 Carbon feedstock.

Microorganisms can produce PHA from a wide range of substrates. They can use simple sugars, such as glucose or lactose and complex ones such as starch or lignocellulose. They can use lipids such as triacylglycerols from animal fats, plant oils, fatty acids and glycerol and they can even use hydrocarbons such as methane (Refer **Figure 5** for the main PHA metabolic pathways). The type of feedstock used depends highly on the strain of microorganism chosen for PHA production. [45, 71, 124, 125]

Companies like Kaneka and Danimer Scientific use vegetable oil from canola, soy, and palm while sugars from corn and sucrose are used as main feedstock by other big companies like Tianjin, TianAn and Yield10 (**Table 1**). [65-67, 70-74]

PHA production is still more expensive than conventional plastic production and some of the main carbon feedstocks used compete directly with the agricultural cultivation of the feedstock for human consumption, therefore researchers are trying to take advantage of substrates like methane, methanol (Mitsubishi Gas Chemicals in Japan produce P(3HB) Biogreen ™ from methanol [43]) and CO_2 (Bio-on is making research on *C. necator's* capability to feed autotrophically [67]) to solve this problem .[126]

In addition, extensive research has been conducted in the conversion of industrial and domestic wastes such as mixed food waste [127, 128], waste lipids, waste from sugar industry, crop residues, petrochemical plastic waste, syngas (CO, CO_2, H_2), waste glycerol, woody residuals [129] and other wide range of industrial wastes such as malt wastes from beer production [130], palm oil mill, paper mill, molasses and others[131] into PHA. Other non-food grade oils like jatropha oil could also be used. [132]

Hemicellulose hydrolysates and crude glycerol could also be considered as potential carbon sources for sustainable production of PHA given that they are produced during biofuel production, making it possible to make bioplastics and biofuel simultaneously. [71]

When PHA is produced out of wastes , it is recommended to use mixed cultures of microorganisms so that most of the carbon sources in the substrate can be used [131, 133], for example, when using activated sludge from municipal wastewater. [134]

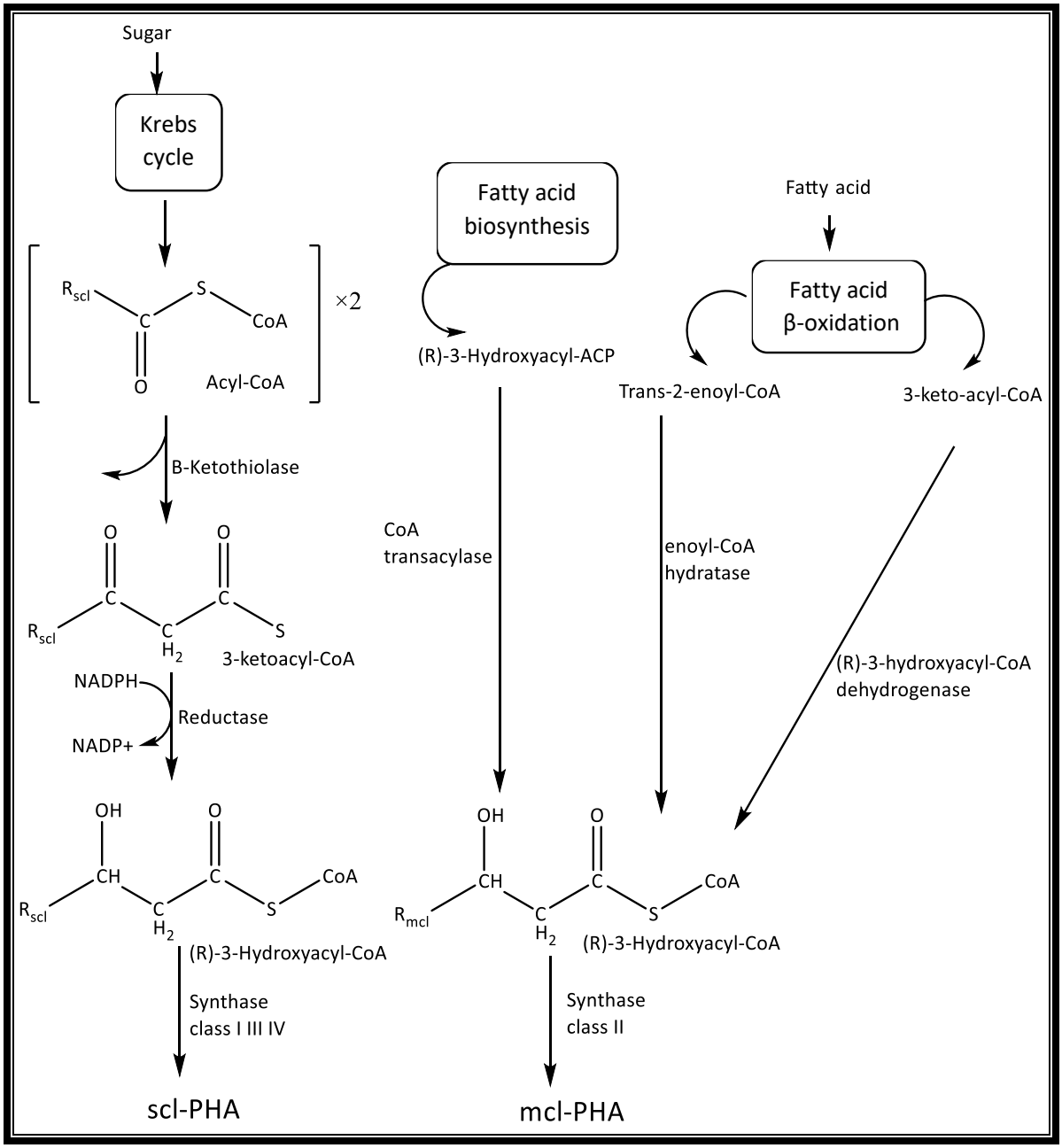

***Figure 5**. Main metabolic pathways for the production of short chain length (scl-PHA) and medium chain length (mcl-PHA) polyhydroxyalkanoates (Adapted from Thomson et al., 2010).[50, 135] Modelled using ChemDraw. [7]*

1.12 Metabolic engineering to optimize mcl-PHA cell production.

The monomer carbon length composition of medium-chain-length PHAs is directly influenced by the carbon length of the fatty acid provided as β-oxidation substrate. [136] In each complete β-oxidation cycle, 2 carbons are removed from the fatty acid chain provided [137], giving as a result a heteropolymers containing several monomers of different chain lengths. Weakening the β-oxidation pathway will increase the carbon flux towards enoyl CoA (mcl-PHA precursor) and avoid the degradation of the fatty acid substrate, which will enhance PHA accumulation inside the cell [138, 139] and result in a more homogenous PHA in terms of monomer composition [139, 140]

The most common method to weaken the β-oxidation pathway is through knockout of *fadB* and *fadA* genes (See **Figure 6**, **Table 5**). [3] However, similar results have been achieved when using the β-oxidation pathway inhibitor acrylic acid (See **Figure 6, Table 5**). [88]

On the other hand, mcl-PHA accumulation can also be enhanced by overexpressing genes that are related to the β-oxidation pathway such as *phaJ*, *phaG*, *fabG* and *alKk* (See **Figure 6, Table 5**) [141, 142]

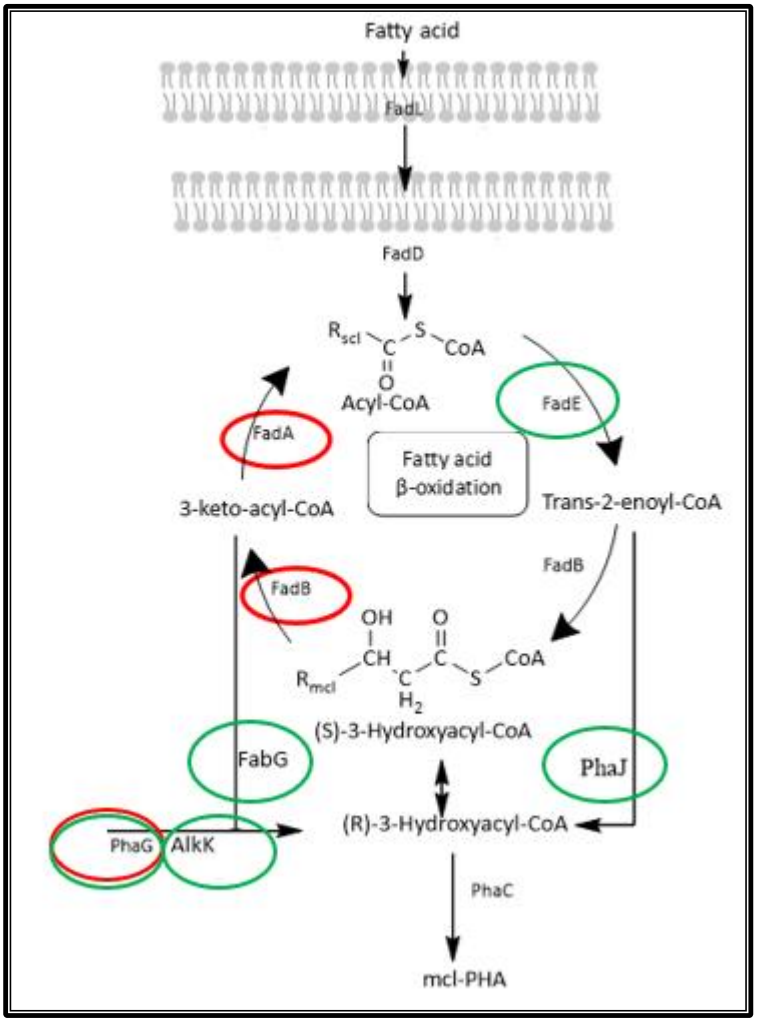

Figure 6. *Representation of the β-oxidation pathway and β-oxidation pathway-related genes. Genes circled in red have promoted PHA accumulation when inactivated in several studies (Refer to* ***Table 5****). Genes circled in green have promoted PHA accumulation when overexpressed (Refer to* ***Table 5****).*

Table 5. mcl-PHA accumulation enhanced by metabolic engineering of the β-oxidation pathway and the β-oxidation pathway-related enzymes. Inactivated genes are presented in red, overexpressed genes are presented in green.

Organism used	B-oxidation pathway modification	PHA yield	% of mcl-monomer	Substrate used	
***P. putida* KT2442**	Deletion of: *fadB2x*, *fadAx*, *fadB*, *fadA*, 3-hydroxyacyl-CoA deshydrogenase, acyl-CoA dehydrogenase and *phaG*.	9.19 wt% 1.03 g/L CDW	P(3HD-co-84%-3HDD)	Decanoic acid Dodecanoic acid	[139]
Ralstonia eutropha	Heterologous expression of *phaC* from, *Rhodococcus aetherivorans* I24, Expression of *phaJ* from *P. aeruginosa* to increase PHA accumulation, varying the activity of PHAB for HHx composition.	71 wt% 66 wt%	P(HB-co-17%-HHx) P(HB-co-30%-HHx)	Palm oil	[143]
***Cupriavidus necator* (*Ralstonia eutropha*)**	*phaC* from *R. aetherivorans* I24 and *phaJ* from *P. aeruginosa* expressed in plasmid pCB113	45 wt% 1.3 g/l PHA	P(HB-co-70%HHx)	Crude palm kernel oil	[144]
Ralstonia eutropha	Introduction of crotonyl-CoA reductase from *Streptomyces cinnamonensis*, *phaC* and *phaJ* from *A. caviae*	48 wt% 1.48 g/l DCW	P(HB-co-1.5%HHx)	Fructose	[145]
Ralstonia eutropha	Overexpression of enoyl coenzyme-A hydratase (*phaJ*) and *phaC2*. Deletion of acetoacetyl Co-A reductases (*pHaB1*, *phaB2* and *phaB3*)	69 wt%	P(78%HB-co-22%HHx)	Coffee waste oil	[90]
***P. putida* KT2442**	Deletion of *fadB* and *fadA*, Deletion of *phaC* and replacement with *phaPCJAC* operon (KTOYO6ΔC (*phaPCJAc*) strain)	5.82 g/l CDW 57.80 wt%	58%PHB-block-42%PHHx	sodium butyrate, sodium hexanoate (1:2) alternating times	[146]
***Pseudomonas entomophila* LAC32**	Weakening of β-oxidation pathway (Deletion of *fadA(x)*, *fadB(x)* and *phaG*)	Not reported	different rations with mcl from 0 to 100%	Glucose and related fatty acids	[147]

	Insertion of *phaA* and *phaB* from *C. necator.* PhaC mutated from *P. putida* 61-3. Block of some genes in *de novo* fatty acid synthesis pathway				
***Pseudomonas putida* KT2442**	*fadA* and *fadB* knockout mutant	84 wt%	P(41%HDD-co-59%HA)	Dodecanoate	[148]
***Pseudomonas putida* KCTC1639**	Overexpression of *phaJ* Overexpression of *fabG*	27%wt 0.51 g/l PHA (FabG overexpression depressed PHA production)	NI	Octanoic acid	[141]
***Pseudomonas mendocina* NK-01**	*fadA* and *fadB* knockout mutant (NKU-Δβ5) *fadA*, *fadB*, *phaG*, *phaZ* knockout mutant (NKU-Δ8) NKU-Δ8.	38 wt%, 1.7 g/l CDW 44 wt%, 2.3 g/l CDW 32 wt%, 1.3 g/l CDW	P(5.57%HHx-co-93.3%HO-co-1.05%HD) P(5.29%HO-co-94%HD) P(2.99%HO-co-28%HD-co-68%HDD)	Sodium octanoate Sodium decanoate Dodecanoic acid	[149]
Cupriavidus necator	Expression of *fadE* from *E. coli* and *phaJ1* from *P. putida* KT2440, in plasmid pMPJAS03	46.1wt%, 4.1 g/l CDW 38.3 wt%, 3.28 g/l CDW	P(99%HB-co-0.37%HV-co-0.27%HHx-co-0.21%HO-co-0.08%HD) P(99.39%HB-co-0.33%HV-co-0.18%HHx-co-0.10%HO)	Canola oil Avocado oil	[142]
***Pseudomonas putida* KT2442**	Deletion of *fadA*, *fadB* (*P. putida* KTOY06)	2.86 g/l CDW 45.99 wt%	P(2.2%HHx-co-11%HO-co-21.6%HD-co-16.1%HDD-co-49%HTD)	Tetradecanoic acid	[150]
DH5α *Escherichia coli*	Deletion of key genes in β-oxidation pathway overexpression of BTE, *phaJ3* and *phaC2* from PAO1 and *PP_0763* from *P. putida* KT2440 strain (*fadRABIJ*)	0.93 g/L CDW 0.75 wt%	P(100%HDD)	Decanoic acid	[151]
***Escherichia coli* W3110**	Expression of *fabG* from *E. coli* and *phaC2* from *Pseudomonas* sp 61-3	4.8 wt%, 1.73g/l	P(11%HHx-co-39%HO-co-50%HD)	Sodium decanoate	[152]

***Escherichia coli* WA101(*fadA* mutant)**	Expression of *rhlG* from *P. aeruginosa* and PhaC2 from *Pseudomonas*. sp 61-3 Expression of *fabG* from *E. coli* and *phaC2* from *Pseudomonas* .sp 61-3	CDW, 0.08g/l PHA 3.2wt%, 1.20g/l CDW, 0.04g/l PHA 22.1wt%, 0.98g/l CDW, 0.22g/l PHA	poly(47%HO-co-53%HD) poly(7%HO-co-93%HD)		
Cupriavidus necator	5 different transformants harboring *phaC* BP-M-CPF4 gene. (*phaJ* from *P. aeruginosa* expression increased HHx proportion). (*phaB* and *phaA* genes expression modify composition)	(48.9-83.7)wt% (3.6-6.2)CDW (2.1-1.4)g/l PHA	HHx(1-18%)	Palm olein Palm kernel oil	[153]
***Pseudomonas putida* KT2440**	Deletion of *phaZ*, *fadBA1* and *fadBA2* and overexpression of *phaG, alkK, phaC1* and *phaC2* (strain AG2162)	1.758 g/l CDW 54wt% 0.657g/l CDW, 17.7wt%	No information	P-coumaric acid Lignin(corn stover)	[123]
***Pseudomonas putida* KT2440**	No (acrylic acid inhibits β-oxidation pathway)	75.5wt% 1.8 g/lh PHA	poly(89%HHp-co-11%HN)	nonanoic acid: glucose: acrylic acid (1.25:1:0.05)	[88]

To recapitulate, reasonably high productivities, for pilot or industrial scale production, of PHA using fed-batch fermentation should exist in a range of (1 g L^{-1} h^{-1} to 2 g L^{-1} h^{-1}) according to Blunt, Levin and Cicek [97]. Even so, most of the studies presented on the table above (**Table 5**) were run on batch cultures and have a lower productivity. For example, PHA production in the study in which *Ralstonia eutropha* accumulated 71% of its dry weight of the copolymer P(HB-co-17%-HHx) equivalates to a final ≈2 g/l after 72 hours of cultivation. [144] This information leads us to believe that some of the studies that already exist could be candidates for industrial production but experimental work for scale up is needed.

1.13 PHA synthase PhaC

1.13.1 Classification

PHA synthases are divided into four classes based on their substrate specificity and on their subunit composition. Classes I, III and IV prefer to synthesize scl-PHA while class II PhaC synthesize mcl-PHA .[154, 155] (see **Table 6**) Only in few cases microorganisms such as *Pseudomonas stutzeri* strain 1317, the PhaC2 (type II PHA synthase) can incorporate both short-chain-length and medium-chain-length hydroxyalkanoates into PHA. [156] *Chromobacterium* sp. USM2, which, utilizes 3-hydroxybutyrate (3HB), 3-hydroxyvalerate (3HV), and 3-hydroxyhexanoate (3HHx) monomers in PHA biosynthesis is another exception.[157]

Table 6. Polyester synthases can be divided into four classes.

Class	Active state	Subunits	Species	Substrate	% identity from PhaC1(*C. necator*)
I	homodimer	60-73 kDa PhaC1 PhaC1	*Cupriavidus necator* *Chromobacterium* *Azohydromonas lata* *Aeromonas hydrophila*	Scl	100 46.88 61.64 40.41
II	monomer	60-65 kDa PhaC1 or PhaC2	*Pseudomonas aeruginosa* *P. putida, P. oleovorans, P.spp*	Mcl	38.21 39.43
III	heterodimer	40 kDa 40kD PhaC3 PhaE	*Allochromatium vinosum*	Scl	26.44 – 66.67

IV	heterodimer	40kDa 20kDa 	*Bacillus megaterium* *Bacillus cereus.*	Scl	28.25 -50 27.67 - 50

94, 154, 158-160

1.13.2 Structure and sequence.

PHA synthases belong to the *α/β*-hydrolase superfamily and have only 8 strictly conserved amino acid residues. This so-called *α/β*-hydrolase fold consists of a characteristic succession of alpha helices and beta strands, usually found in lipases, where the catalytic residues aspartate, histidine and cysteine are**.** Out of the catalytic triad, the conserved cysteine residue is used as catalytic nucleophile. [154, 161]

This cysteine is embedded in the PhaC box sequence (GS)-X-C-X-(GA)-G (X is an arbitrary amino acid), which is similar to the lipase box G-X-S-X-G proper of lipases, in the active site of the catalytic domain of the protein . [161, 162] Point mutagenesis revealed that PhaC box sequences ([GAST]-X-C-X-[GASV]-[GA]) are functional PHA synthases, which shows the low mutational robustness of the last glycine residue as well as that of the cysteine. [155, 162]

In *C. necator*, the PhaC class I active enzyme is a homodimer with only one active catalytic site. [161, 163] Each monomer is composed of a single polypeptide chain of 65 kDa which contains an N-terminal domain of unknown function (residues 1–200) and a C-terminal catalytic domain (residues 201–589) (**Figure 7**). The active site of each monomer is separated from the other by 33 Å across an extensive dimer interface. The opening in the substrate access channel of the enzyme is near two arginine residues (one from each chain of the dimer), from which Arg_{398} is strictly conserved in class I PhaCs. This arginine along with the His_{481} are believed to be important for substrate HB-CoA binding and stabilizing while Arg_{421} may be involved in chain termination. [161]

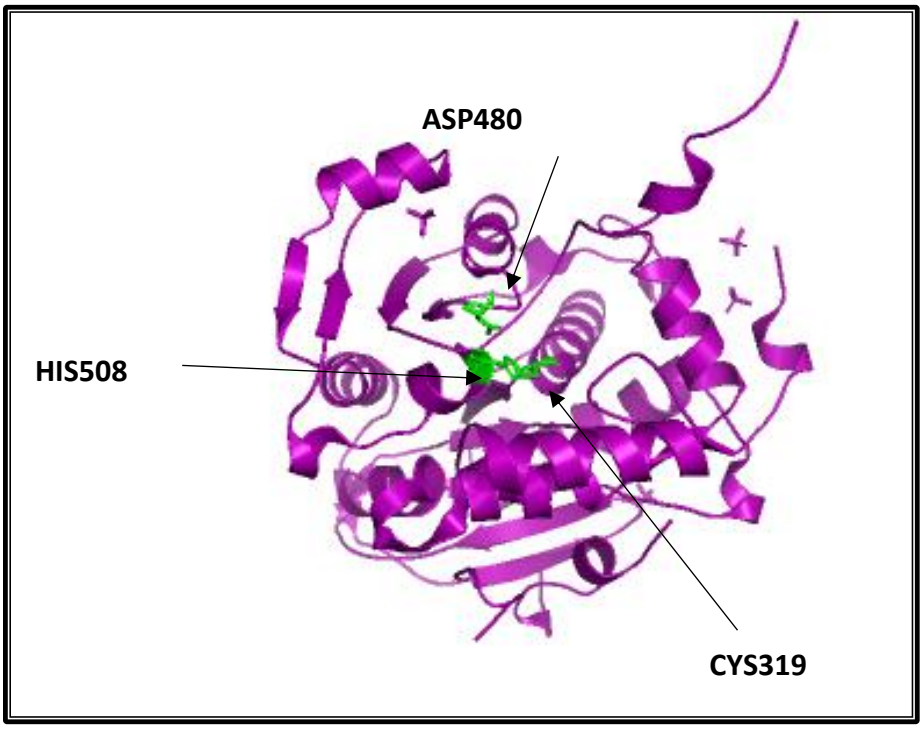

***Figure 7**. The catalytic domain of PHA synthase from C. necator. Catalytic triad is presented in green.* [161] Molecule modelled in PyMOL for this work [164].

The catalytic domain of PHA synthase from *Cupriavidus necator* shares 29% sequence identity with the class III PhaC from *Allochromatium vinosum*, which suggests structural similarity with class III synthases. The catalytic domains of class II and IV phaCs, despite of have being a lot less characterized, are also likely to be homologous, sharing 40 and 30% identity respectively. [161]

1.13.3 Molecular mechanism

PhaC has a transferase activity transferring acyl groups. 3 molecular mechanisms for PHB formation have been proposed to date. [55, 161, 165] Being the newest one proposed by Wittenborn, Jost, Wei, Stubbe and Drennan [161] whom described the mechanism as follows:

"His_{508} deprotonates Cys_{319}, allowing for nucleophilic attack on the HB-CoA thioester; the histidine base is regenerated by transfer of the proton to the CoASH leaving group. A second HB-CoA substrate binds, and the HB hydroxyl group is deprotonated by His_{508}, facilitated through modulation of the histidine basicity by Asp_{480}. The newly formed HB alkoxide attacks the Cys-HB thioester, generating a noncovalent, Co-A bound intermediate. The growing PHB chains is then transferred back to Cys_{319}." (**Figure 8**).

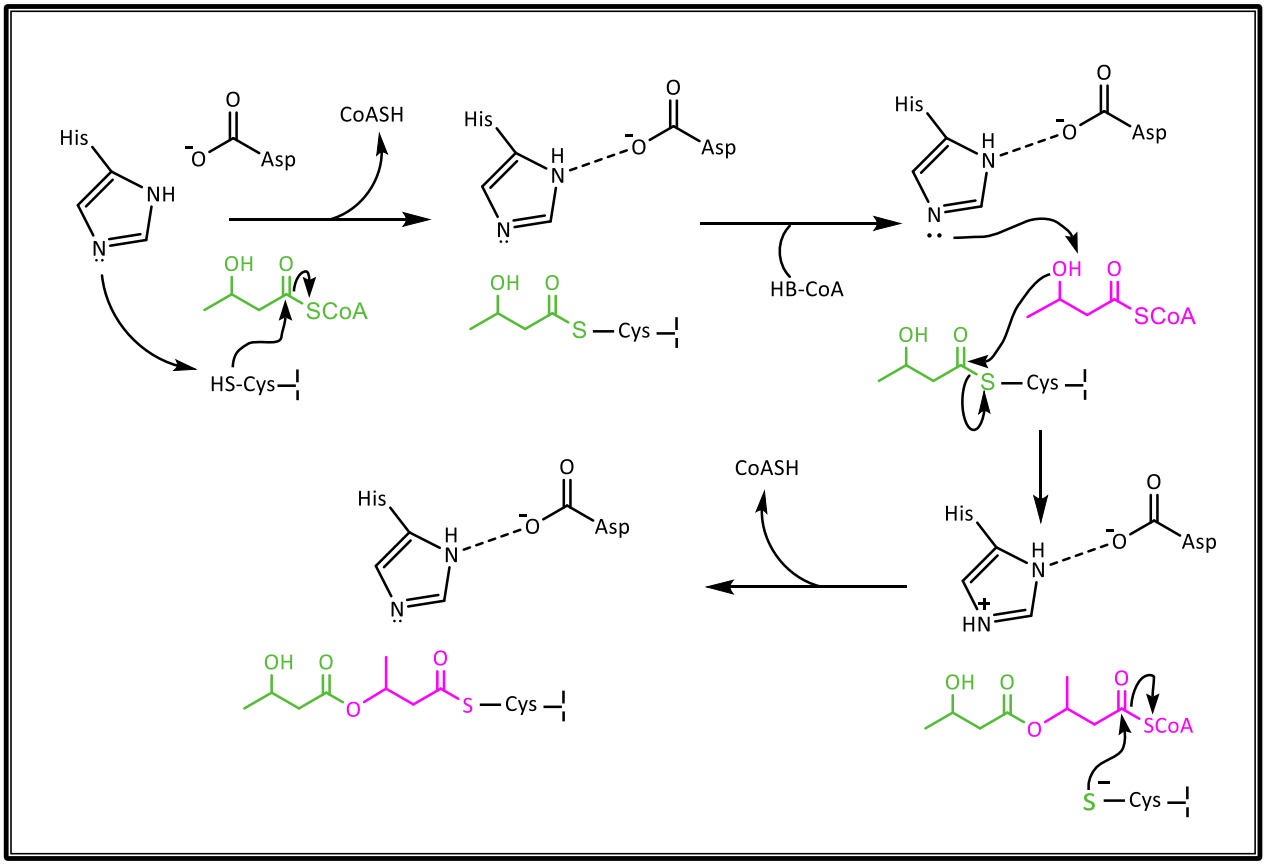

Figure 8. *Proposed mechanism for polyhydroxybutyrate formation in C. necator as proposed by Wittenborn, Jost, Wei, Stubbe and Drennan [161]. Modelled using ChemDraw [7]*

1.13.4 Substrate specificity and kinetics

Comparing K_m of different substrates gives some clues to the specificity of an enzyme. In the study of Zhang, Yasuo, Lenz and Goodwin [163] the much larger K_m value for 4HB-CoA compared with 3HB-CoA and 3HV-CoA indicates the importance of the distance between the hydroxyl group and the CoA moiety for substrate binding in the PhaC of *C. necator*, however, a longer side chain does not seem to strongly affect the substrate binding to PHA synthase of *C. necator*. (for comparison of more substrates and its K_m read Table II from Yuan, Jia, Tian, Snell, Müh, Sinskey, Lambalot, Walsh and Stubbe [166]) It is also important to mention that, while the natural substrate of PhaC in *C. necator* is 3HB-CoA, it has been able to accept 3-hydroxyoctanoate-CoA and 3-hydroxydodecanoate-CoA to produce medium chain PHA when expressed in *E. coli* suggesting that it might have a broader substrate specificity than previously found. [167]

Substrate specificity can rely in as much as one amino acid. The substitution of Leu484 in PhaC from *Pseudomonas putida* for valine shifts the substrate specificity from 8C to 4C; 484 is an amino acid adjacent to the catalytic triad that is conserved as leucine in class II synthases, as valine in class III and as valine or isoleucine in class I (*C. necator*) and is critical in determining substrate specificity. [168] Also, amino acids Ser326 and Gln482 in *Pseudomonas spp.* are conserved residues that when substituted for other residues (thr326, cys326 and lys482, arg482 respectively) increases the enzyme preference for producing PHB over mcl-polymers. [169]

1.13.5 Protein engineering for catalytic enhancement

PHA synthase engineering is being performed for a variety of purposes that include improved PHA accumulation yield, substrate specificity modification and/or higher molecular weight. [170, 171]

The engineering strategies for these purposes include random mutagenesis, error-prone PCR mutagenesis, site-specific saturation mutagenesis, localized semi-random mutagenesis, gene shuffling, recombination of beneficial mutations and engineering of chimeric PHA synthases between others. [171, 172] Examples of enhanced PhaCs by enzyme evolution are shown in **Table 7.**

Table 7. Studies of PhaC enhancement through synthetic PHA synthase evolution.

Method	PhaC source	Changed enzyme property	Polyester	
Diversify PCR random mutagenesis	*Pseudomonas putida* KT2440	Higher yield with higher molecular weight	P3HDD	[89]
Error-prone PCR mutagenesis, saturation mutagenesis, in vitro recombination	*Pseudomonas* sp. 61-3	Higher yield	P3HB	[173]
Site-specific mutagenesis	*Pseudomonas* sp. SG4502	Substrate specificity	poly(LA-co-3HB)	[174]
Localized semi-random mutagenesis	*Pseudomonas oleovorans* GPo1	Substrate specificity	P3HB, P3HA	[175]
Gene shuffling	*C. necator*	Higher yield, substrate specificity	P3HA	[176]
PCR-mediated random mutagenesis, intragenic suppression-mutagenesis	*Ralstonia eutropha*	Yield	P3HB	[177]
Chimeric PHA synthase	*P. oleovorans* *P. fluorescens* *P. aureofaciens*	Higher yield, substrate specificity	scl/mcl	[178]
Recombination of beneficial mutations	*Aeromonas caviae*	Molecular weight, fraction composition	poly(3HB-co-3HHx)	[179]
Chimeric PHA synthase	*Aeromonas caviae* *C. necator*	Substrate specificity	poly(3HB-co-3HHx-co-3HO)	[180]
Chimeric PHA synthase	*A. caviae* *C. necator*	Substrate specificity	3HHx / 3HB	[181]

Site specific mutagenesis	*Pseudomonas sp.* S64502	Substrate specificity	poly(LA-co-3HB)	[174]
Site specific mutagenesis	*P. chlororaphis* P.sp.61-3 *P.putida* KT2440 *P.resinovorans* *P.aeruginosa* PAC1	Substrate specificity	poly(3HB-co-LA)	[182]
Site specific mutagenesis Saturation mutagenesis	*Pseudomonas sp. MBEL 6-19*	Substrate specificity	poly(3HB-co-LA)	[183]
Site specific mutagenesis, saturation mutagenesis	*Pseudomonas putida* GPo	Yield, substrate specificity	Copolymers with 3HB, 3HHx, 3HO, 3HD	[184]
None (natural mutation)	*Pseudomonas MBEL 6-19*	Substrate specificity	poly(LA-co-GA-co-3HB) poly(LA-co-GA-co-4HB), poly(LA-co-GA-2HB)	[185]
Site specific mutagenesis	*Pseudomonas stutzeri*	Substrate specificity	poly(LA-co-3HB-co-3HP)	[186]
PCR- mediated random mutagenesis Recombination of beneficial mutations.	*Pseudomonas sp.*61-3	Yield	P3HB	[187]

Scl: small-chain-length, mcl: medium-chain- length, P3HA: poly(3-hydroxyalkanoate), PLA: polylactate, PGA: polyglycolate, P3HB: poly(3-hydroxybutyrate), P3HP: poly(3-hydroxypentanoate), P3HHx: poly(3-hydroxyhexanoate), P3HO: poly(3-hydroxyoctanoate), P3HD: poly(3-hydroxydecanoate), P3HDD: poly(3-hydroxydodecanoate).

In addition to the above, PhaC catalytic activity can also be enhanced and/or modified indirectly by modifying metabolic routes, for instance, the *β*-oxidation pathway to produce mcl-PHA [50, 140], by recycling the CoA released from the transformation of 3-hydroxyacyl-CoA into PHA (CoA inhibits PhaC) [188] or by the co-expression of molecular chaperones, which results in the synthesis of larger quantities of enzyme. [189]

Another approach would be to use thermo-tolerant PHA synthases in order to enhance the bioconversion process and decrease the energy costs related with managing the exothermic fermentation process .[171]

1.13.6 Methods to evaluate the enzymatic activity of PhaC.

The activity of PHA synthase can be determined by measuring the amount of CoA released from thioester-CoA during polymerization. The CoA in the medium is detected spectroscopically at 412 nm by reduction of 5,5-dithio-bis (2 nitrobenzoic acid) (DTNB), a compound which specifically reacts with thiol groups. One unit of enzyme activity is defined as the amount of enzyme that catalyses the release of 1 mol CoA/min. This technique, originally developed for short chain PHA synthases was then modified for medium chain synthases. [190, 191] It is the most common technique and it is quick to perform, unfortunately, hydrolysis reactions can lead to the release of CoA independently of polymerisation which can give false results. [135]

Another way to measure PHA synthase activity is by measuring , spectrophotometrically at 236 nm, the hydrolysis of thioesters in substrates as described by Fukui, Yoshimoto, Matsumoto, Hosokawa, Saito, Nishikawa and Tomita [192]. In this technique one unit of enzyme activity is defined as the amount of enzyme necessary to convert 1 µmol of substrate to PHA in one minute. It is a convenient technique but less accurate than measuring CoA release. [135] Later on, Gerngross, Snell, Peoples, Sinskey, Csuhai, Masamune and Stubbe [193] modified the technique and used a labelled substrate ([3-^{3}H]-hydroxyacyl-CoAs). [135, 193]

In the other hand, the enzyme activity essay developed by Kraak, Kessler and Witholt [194] is based on the analysis of substrate depletion by HPLC and production formation by gas chromatography and has proven to be highly accurate to measure the enzyme activity of medium size chain PHA synthases, but ,the method is very time consuming.

The reliance on spectrophotometric assays has the drawback of hindering the simultaneous measurement of more than one enzyme activity.[135] Burns, Oldham, Thompson, Lubarsky and May [195] developed a HPLC methodology to measure fluctuations in the concentration of CoA, acetyl-CoA, acetoacetyl-CoA, and β-hydroxybutyryl-CoA metabolites and to associate these fluctuations to the activity of an enzyme on the overall system.

A summary of the methods discussed in this section is shown in **Table 8.**

Table 8. Different methods to analyse PhaC activity.

Method	Advantages	Disadvantages	Reference
CoA detection 412 nm	Quick	False positives due to other hydrolysis reactions that release CoA.	135, 190, 191
Thioesters hydrolysis detection 236 nm	Quick	Less accurate than CoA detection.	135, 192, 193
Substrate depletion and product formation analysis with HPLC and GC	Highly accurate	More time consuming	194
Co-A, acetyl-CoA and β-hydroxybutyryl-CoA analysis with HPLC	Is accurate and measures fluctuation in the overall system	Costly and time consuming	195

1.14 PHA depolymerase (PhaZ)

The PHA depolymerase, as indicated by its name, is an enzyme in charge of catabolizing intracellular and extracellular PHA. [196] Most of the existing knowledge about this enzyme comes from the analysis of scl-PHAs [196], however, there is proof that *Pseudomonas putida* KT2442 codes for a mcl-PHA-specific depolymerase. [197] Therefore, it comes as no surprise that PhaZ mutants, where this gene has been deleted, are better hosts for PHA

production.[198, 199] On the other hand, the study of this enzyme is going to be important in the near future to make PHA production sustainable and ensure its biodegradation. [200, 201]

1.14.1 Classification

PHA depolymerases are carboxylesterases classified in 3 superfamilies according to the place where they are found in the cell (intracellular, extracellular, periplasmic) which at the same time are divided according to their substrate specificity (short or medium chain length) and according to their sequence similarities (presence of the lipase box and catalytic domain type).

They can also be classified according to the type of PHA they degrade which are, either native intracellular granules (amorphous)(nPHA) or denatured extracellular granules (crystalline)(dPHA) as shown in **Figure 9.** [41, 202]

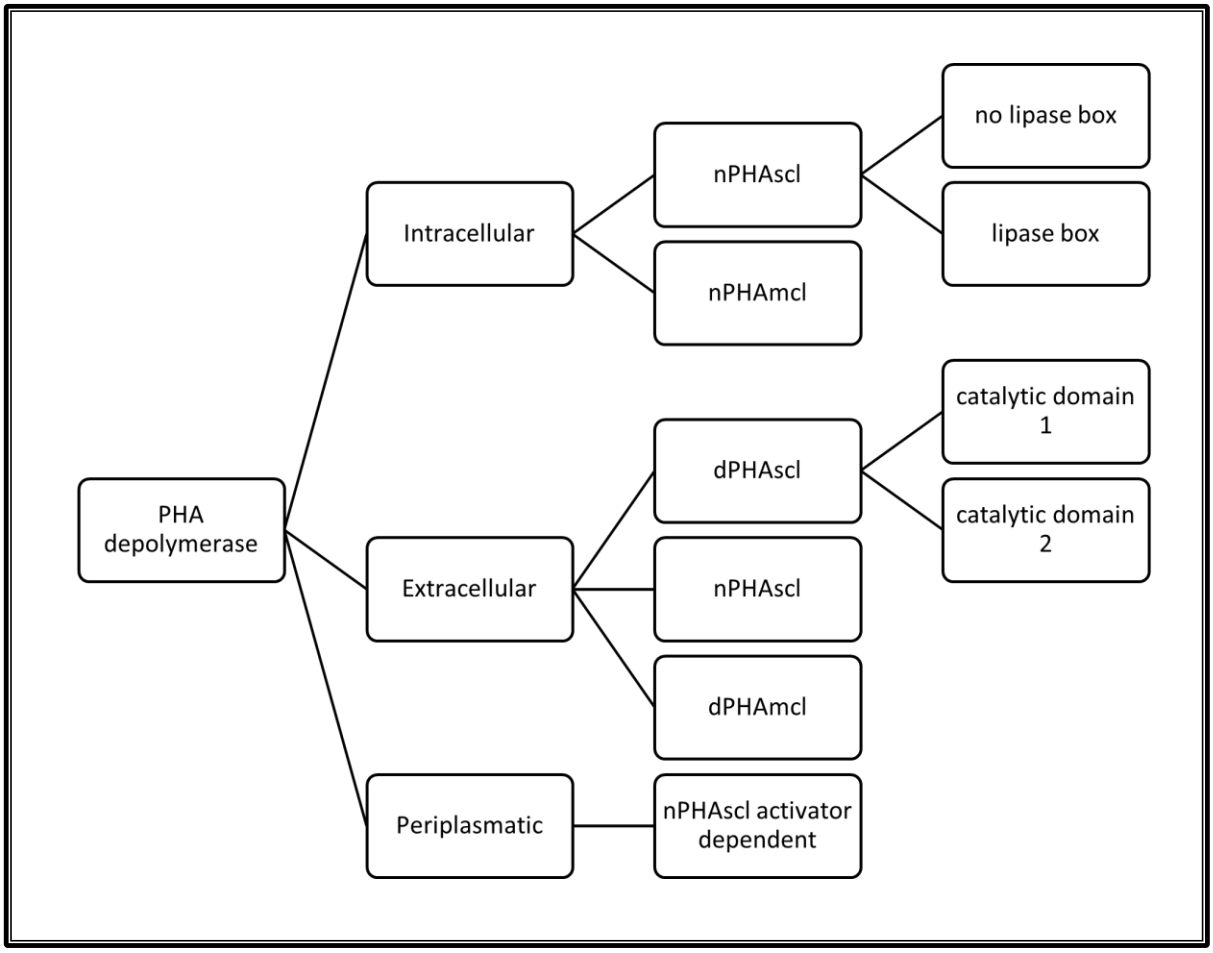

***Figure 9**. Classification of PHA depolymerases*

1.14.2 Structure and sequence.

PHA depolymerases have a catalytic triad (serine – histidine – aspartic acid) as active site. Similarly to PhaC, the catalytic serine is located in a G-X-S-X-G lipase box that is present in other α/β-hydrolases. Apart from this, a conserved non-catalytic histidine near the oxyanion hole, also present in lipases, can be found in PhaZ. It is important to note that there are also non-lipase box depolymerases. [41, 202, 203]

The best studied PHA depolymerases are dPHAscl depolymerases which contain a short signal peptide, a catalytic domain (containing the oxyanion hole and the lipase box), a short linker domain, and a substrate binding domain. [202, 204] In dPHAscl with catalytic

domain 1 the oxyanion hole can be found in the N-terminal to the lipase box, like lipases, whereas in dPHAscl with catalytic domain 2 the oxyanion hole is found C-terminal to the catalytic triad. Example of microorganisms harbouring dPHAscl with catalytic domain 1 are *Sorangium cellulosum, Paracoccus denitrificans, Alcaligenes faecalis and Burkholderia mallei;* whereas examples of microorganisms with catalytic domain type 2 are *Alteromonas macleodii, Pseudoalteromonas atlantica, Cupriavidus pinatubonensis* and others. [41, 202]

Similarly, there are three types of short linker domain: fibronectin type (i.e. *Alcaligenes faecalis* [205]), cadherin-like domain (i.e *Pseudomonas stutzeri* [206]) and 2 types of substrate binding domain (i.e. *Pseudomonas stutzeri* has both of these domains [206]) as shown in **Figure 10.** [205, 207]

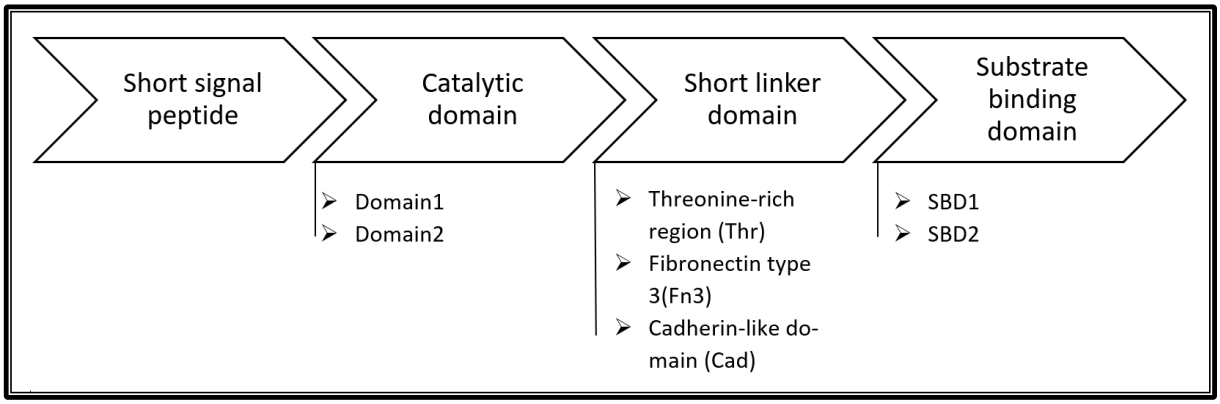

Figure 10. *Regions of a PHA depolymerase and their classifications.*

The dPHAscl catalytic domain Type II from *Penicillium funiculosum*, shown in **Figure 11,** is comprised of a single domain. The catalytic triad residues are Ser39, Asp121 and His155 and the amide groups of Ser40 and Cys250 form the oxyanion hole. A mutant revealed that Trp307 plays a role in the recognition of the ester group adjacent to the scissile group. [8]

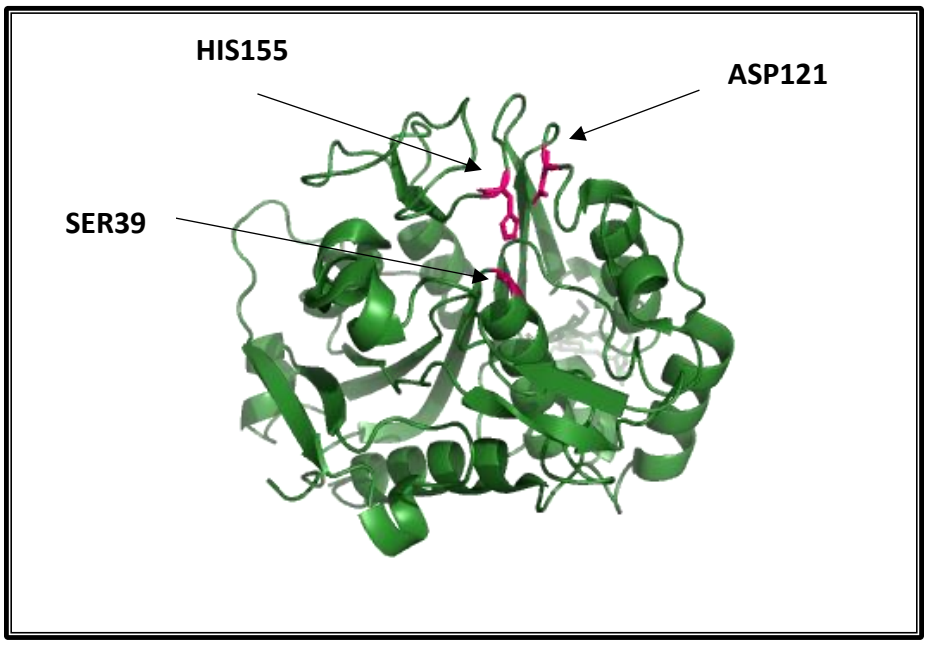

***Figure 11**. dPHAscl type II from Penicillium funiculosum. The enzyme has 319 amino acid residues with a molecular mass of 33569 Da. The enzyme has a α/β hydrolase fold where the catalytic residues are (marked in pink).[8] Molecule modelled in PyMOL for this work.[164]*

Crystallization of PHA depolymerase from *Paucimonas lemoignei*, whose catalytic triad special arrangement is similar to that one from *P. funiculosum* [208, 209] and from *Bacillus thuringiensis* [210] have also being achieved.

1.14.3 Molecular mechanism

Hisano, Kasuya, Tezuka, Ishii, Kobayashi, Shiraki, Oroudjev, Hansma, Iwata, Doi, Saito and Miki [8] proposed, the following mechanism (**Figure 12**) for the action of PHB depolymerase from *P. funiculosum* over PHB: "In this model Ser39 changes its conformation to form a hydrogen bond with His155. Contiguous monomer units are bound to the subsites, making predominantly hydrophobic interactions with the enzyme with concomitant hydrophilic interactions. The carbonyl oxygen of unit 2 is hydrogen bonded to Trp307, and that of unit 3 is hydrogen bonded to Asn300 and to Asn302 via a water molecule. The methyl groups of

units 1 and 2 are specifically bound to the hydrophobic pockets of the enzyme. The scissile bond is located between units -1 and 1. Nucleophilic attack on the carbonyl carbon involved in the scissile bond by Ser39 results in the formation of a covalent acyl-enzyme intermediate via tetrahedral transition state, which is stabilized by two main chain amide groups of Ser40 and Cys250. The acyl-enzyme intermediate is subsequently hydrolyzed by a water molecule activated by His135 via formation of a similar tetrahedral transition state. After regeneration of Ser39, or liberation of the remaining product, Ser39 suffers a conformational change, which disrupts a hydrogen bond with His155 and forms one with the amide group Ser40".

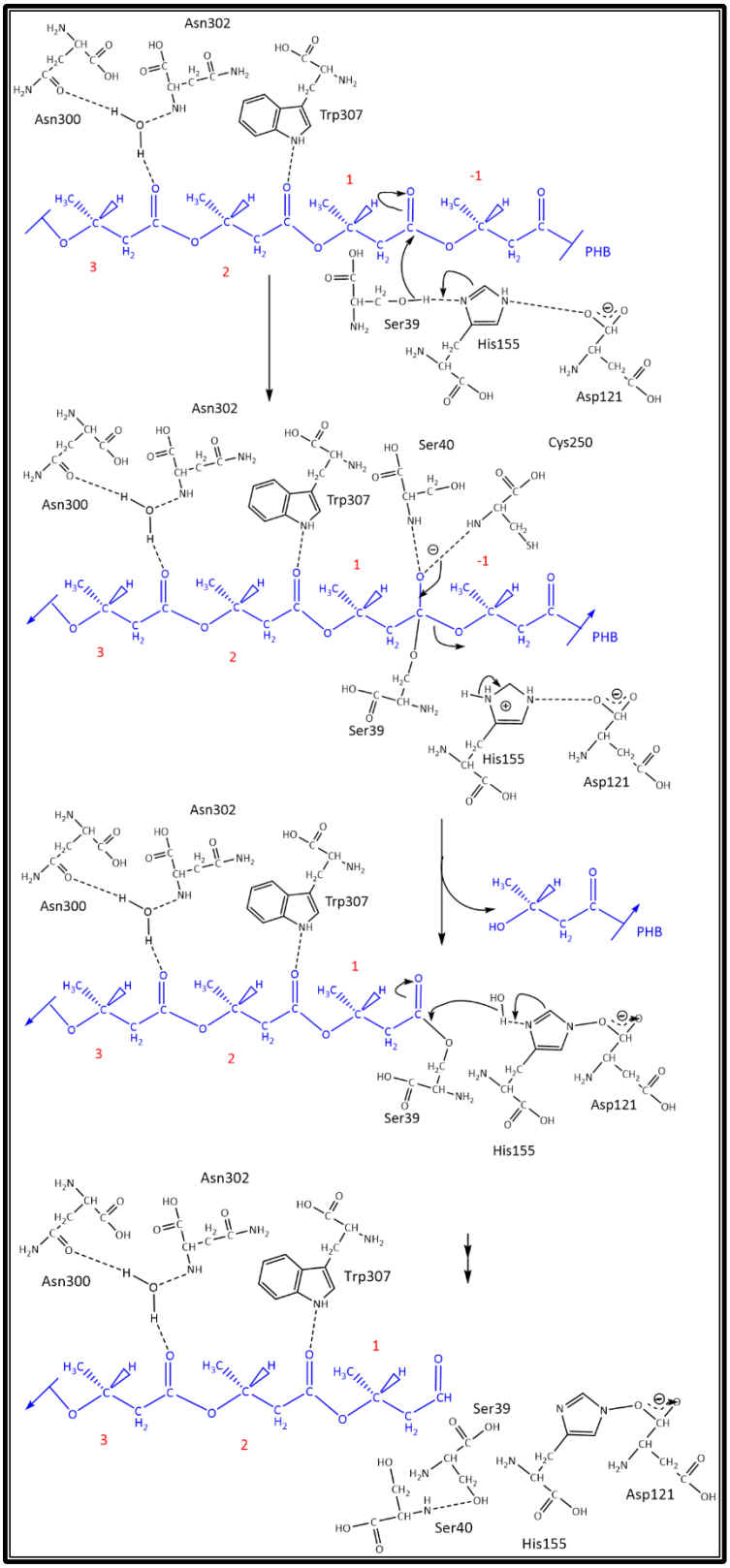

Figure 12. *Molecular mechanism of PHB depolymerase from P. funiculosum [8]. Modelled using ChemDraw [7]*

1.14.4 Substrate specificity and kinetics

PHA depolymerase catalyzes the reaction in **Figure 13.**

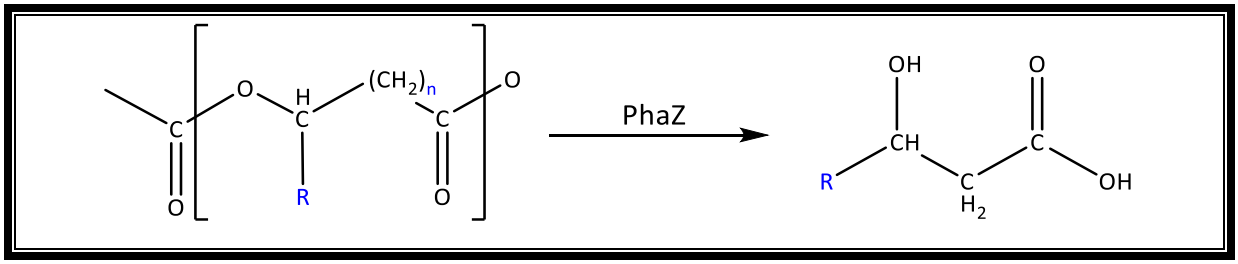

Figure 13. *Polyhydroxyalkanoate polymers are degraded to hydroxyalkanoic acid monomers. Modelled using ChemDraw.* [7]

PHA depolymerization occurs in two steps: adsorption by the substrate binding domain and then hydrolysis by the catalytic domain. [211, 212] The C-terminal amino acids of dPHAscl depolymerases represent the PHA-specific binding domain to the substrate (SBD). [204] SBD has an interaction of 100 pN with the substrate [213] and such interaction consists of hydrogen bonds between hydrophilic residues in the enzyme and ester bonds in the polymer and between the hydrophobic residues in the enzyme and the methyl groups in the polymer. Check **Figure 14** . [214]

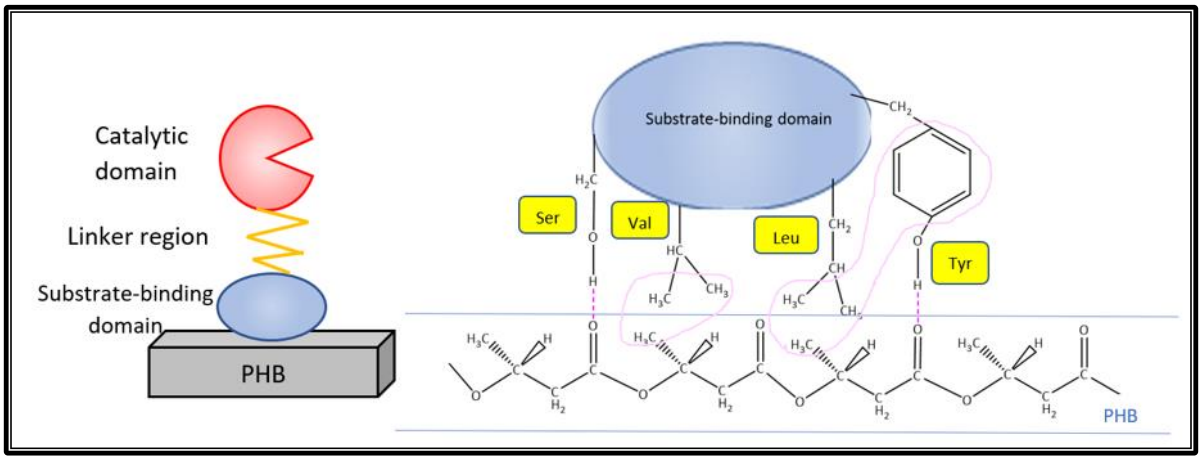

Figure 14. *Schematic model of the interaction of the substrate-binding domain with the PHB (Taken from Hiraishi, 2006* [214]*). Dashed bonds are used to represent hydrogen bonds whereas hydrophobic interactions are circled.*

Using *Alcaligenes faecalis*, in a study with 5 substrates the SBD was capable of adsorbing on the surface of all films (PHB, PHP, P4HB, P(2HP) and P(6Hx)); However, the enzyme, only hydrolysed 3 films (PHB, PHP and P(4HB) out of the 5, demonstrating that the binding domain works independently of the catalytic domain and that it is less specific. [212]

In the other hand, dPHAmcl depolymerases do not contain a substrate binding domain. In these enzymes, the N-terminal region of the catalytic domain is thought to function as substrate binding site [41, 202]

As mentioned before, there are two types of catalytic domains in PHA depolymerase depending on the position of the lipase box and oxyanion hole. Nevertheless, comparisons of substrate specificities between *Alcaligenes faecalis* (domain type 1), *Pseudomonas stutzeri* (type 1), and *Comamonas acidovorans* (type 2) using 12 different aliphatic polyesters showed that active sites of PHA depolymerases have a similar conformational structure, independently of a difference in the sequence structure of the catalytic domains given that they were able to degrade the same 5 substrates (PHB, PHP, P(4HB), poly(ethylene-succinate) and poly(ethylene-adipate)) and unable to degrade the other seven. [215]

The maximum rate of PHA depolymerase catalysed reaction (Vmax) as well as the Km constant for the degradation of PHB at optimal conditions have been measured for several organisms as shown in **Table 9.** A low Km represents a very big affinity for the substrate.

Table 9. PHA depolymerases and their kinetic parameters using PHB as a substrate.

Organism	Type	Apparent Km(µg/ml)	Apparent Vmax(µg/min)	
Penicillium expansum	ePHAscl	1.04	4.5	[216]
Thermus thermophilus	edPHAscl-typeI	53	N/A	[207]
Fusarium solani	ePHAscl	100	50	[217]
Penicillium citrinum	ePHAscl	1250	12.5	[218]
Alcaligenes faecalis	edPHAscl-typeI	13.3	N/A	[219]

1.14.5 Protein engineering for catalytic enhancement.

Engineering of PHA depolymerases can be achieved using the same techniques described for PHA synthase engineering but a lot less research has been made over PhaZ.

The degradation rate of a piece of PHB is usually on the order of a few months (in anaerobic sewage) or years (in seawater) [220] but genetical engineering can be applied to make the process more efficient, for example, Hiraishi, Komiya and Maeda [221] made an amino acid substitution of the residue Tyr443 for a more highly hydrophobic amino acid (Phe) in PhaZ from *Ralstonia pickettii* which resulted in a higher PHB degradation activity while Tan, Hiraishi, Sudesh and Maeda [222] performed directed evolution over the catalytic domain through error- prone PCR to achieve a tenfold increase of the PHB depolymerase activity.

1.14.6 Methods to evaluate enzymatic activity of PhaZ.

As mentioned before, one of the most common and simple techniques to identify PHA-producing colonies is staining them with the hydrophobic dye Sudan Black and observing under the microscope. When PHA consumption conditions are present, colonies expressing intracellular PHA depolymerase will look less stained than before, [223] whereas, a simple way to observe extracellular depolymerase activity is using an agar plate assay (halo formation) as indicated by Schirmer, Jendrossek and Schlegel [224] The diameter of the resulting clear zone semi-quantitatively indicates the activity of the enzyme. The technique can also be used to screen microorganisms that utilize extracellular PHA. [41, 225]

In the other hand, quantitative methods include the measurement of the 3HB released by, either using 3HB dehydrogenase and hydrazine and measuring spectrophotometrically [226, 227] or by directly monitoring absorption at 210 nm of carbonyl groups of 3HB monomer and dimers. [228, 229] Another approach to determine PHA depolymerase activity is to take advantage of the esterase activity of the enzyme and use *para*-nitrophenylalkanoate (pNPA) as substrate. The concentrated p-nitrophenol released by the hydrolysis of pNPB is measured spectrophotometrically at 410 nm.[207, 224]

Alternatively, there are weight loss measurements in which a PHA loses weight, over time, as consequence of depolymerization. However, this technique is not practical for rapid routine assays. [230, 231]

Finally, non-common methods for recording degradation of polyesters include electron microscopy [232], 1H-NMR (hydrogen-nuclear magnetic resonance) imaging [233], ^{13}C-NMR (carbon nuclear magnetic resonance) [234] and tracking radiolabelled polymers (this technique can be used to measure both polymerization and depolymerization of PHA). [235, 236]

Summary of the methods discussed in this section are shown in **Table 10.**

Table 10. Comparison of common methods to evaluate PhaZ activity.

Method	Advantages	Disadvantages	Reference
Sudan Black observation	Easy and quick	Not quantitative result	223
Halo formation in plate assay	Easy and quick, for extracellular PhaZ only.	Semi-quantitative result	41, 224, 225
Measurement of 3HB release	Quantitative method	No information	226-229
Measure esterase activity at 410 nm	Quantitative method	No information	207, 224
Measurement of PHA weight lost	Easy	Not practical for rapid routine assays	230, 231

1.14.7 Lipases capable of degrading PHA

It has been proven that several lipases can degrade PHAs. [203, 237, 238] A comparison study of PhaZ from *P. lemoignei* and T1 lipase (isolated from the palm *Geobacillus zalihae*, capable of degrading amorphous P3HB) showed that their active site residues are very well aligned. The enzymes have 21.4% sequence identity and 53.8% sequence similarity only and ,yet, their structures are very similar and they both contain the oxyanion pocket and the lipase box pentapeptide (GXSXG)[239], which can explain this phenomenon.

Most bacterial lipases are capable of hydrolyzing polyesters consisting of an ω-hydroxyalkanoic acid such as poly(6-hydroxyhexanoate) or poly(4-hydroxybutyrate), whereas polyesters containing side chains in the polymer backbone such as poly(3-hydroxybutyrate) and other poly(3-hydroxyalkanoates) are not or only somewhat hydrolyzed. [203, 238] Great diversity of commercial lipases going from yeast (*Candida antartica* and *C. rugosa*), bacteria (*Pseudomonas cepacia* , *P. fluorescens, Chromobacterium viscosum*), fungus (*Rhizopus arrhizus* and *R. oryzae*), insect (*Myagrus javanicus*), shrub

(*Rubus niveus*) and animals (porcine pancreas) are capable of degrading P(3HB-*co*-4HB). [240-242]

No efforts have been made to enhance the catalytic activity of lipases to degrade PHAs but they have been immobilized on the surface of intracellular polyhydroxybutyrate (PHB) granules by fusion of the lipase gene with the phaC operon to produce fatty acid alkyl esters such as biodiesel. [243, 244]

PROJECT OVERVIEW

PHAs will potentially replace petrochemical plastics due to their similar characteristics and biodegradability. Due to this, a lot of research has been done to characterize different PHAs, produce new ones and to improve their production yield. In future, research should continue focusing on reducing the cost of PHA production and on the industrial production of mcl-PHAs with novel characteristics.

PROJECT AIMS AND OBJECTIVES

PROJECT AIM

- To engineer the metabolism of *Escherichia coli* for production of a novel, flexible and elastic, medium-chain-length polyhydroxyalkanoate bioplastic with high hydroxydodecanoate and/or hydroxytetradecanoate monomer composition that could potentially be used in the medical field and/or packaging.

OBJECTIVES

- **CHAPTER 2**

  To express 3 different PhaC enzymes from different *Pseudomonas* and to validate a method for PHA quantification using Gas Chromatography- FID.

- **CHAPTER 3**

  To codon-optimize the 3 *phaC* for expression in *E. coli* and to re-do the cloning using a new plasmid backbone for production and quantification of PHA.

- **CHAPTER 4**

  To clone 2 different ketoacyl reductases (*fabG*) genes from *Escherichia coli* K-12 BW25113 and *Mycobacterium tuberculosis* H37Rv respectively inside our plasmids and to quantify of the PHA produced.

- **CHAPTER 5**

  To knockout the β-oxidation repressor (*fadR*) gene using Δ*fadA Escherichia coli* K-12 BW25113 as a host and to express our plasmids expressing PhaC-FabG enzymes inside the engineered host.

- **CHAPTER 6**:

  To clone, once more, 3 *phaC*s and *fabG* from *M. tuberculosis* into a new plasmid backbone and to validate protein expression through SDS-PAGE.

A schematic representation of the project can be observed in **Figure 15.**

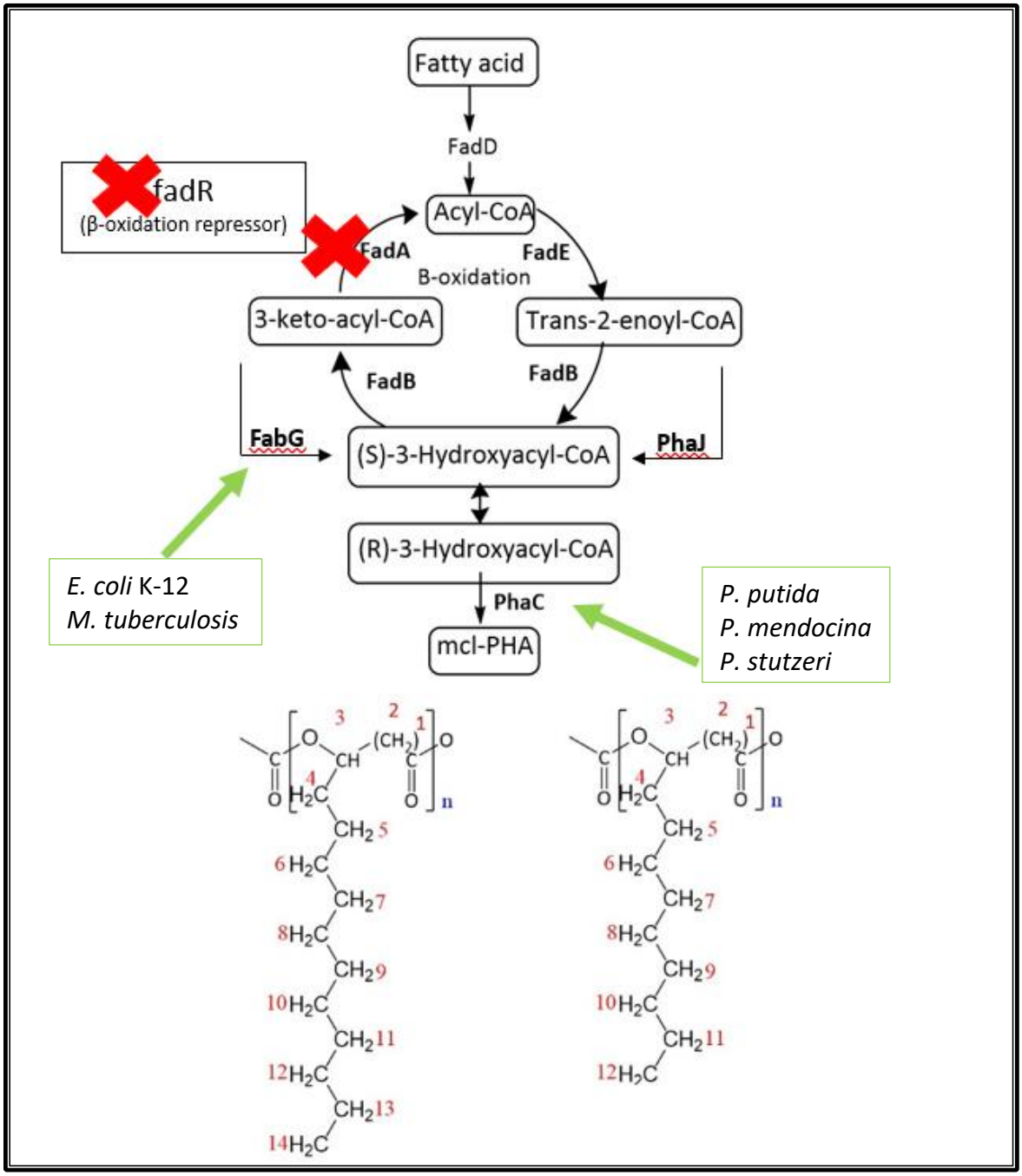

Figure 15. *Representation of the β-oxidation pathway and β-oxidation pathway-related genes. Genes that are crossed out with red represent the knockouts studied in this work: FadR: β-oxidation repressor and FadA: β-ketoacyl-CoA thiolase. Green arrows point out the genes that were upregulated: FabG: ketoacyl reductase and PhaC: PHA synthase. At the bottom there is a representation of the polymers of 14 and 12 carbons each. Metabolic pathway modelled using ChemDraw* [7]

CHAPTER 2

PhaC evaluation:

Comparison of different PhaCs from *Pseudomonas* to produce PHA with high hydroxydodecanoate (HDD) and hydroxytetradecanoate (HTD) monomer composition.

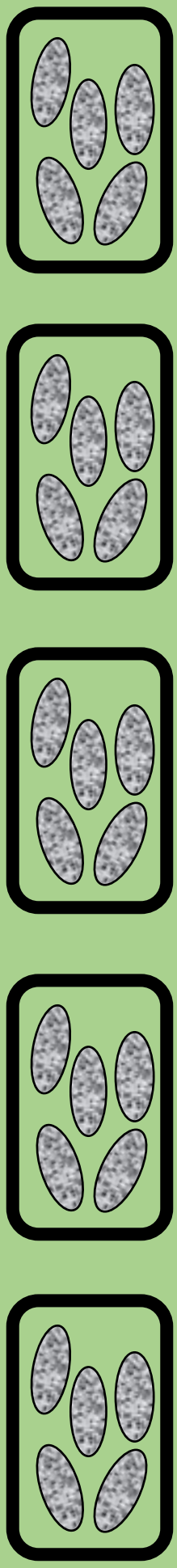

CHAPTER 2. PhaC EVALUATION: Comparison of different PhaCs from *Pseudomonas* to produce PHA with high hydroxydodecanoate and hydroxytetradecanoate monomer composition.

2.1 Introduction

Polyhydroxybutyrate (PHB) is a polyhydroxyalkanoate polymer of 4 carbons that is known to be hard and brittle and, as a consequence, it is difficult to process industrially . [80, 81, 245] However, it has been long proven that co-polymers of PHB with medium chain length PHA decrease the crystallinity of the material, making it less brittle and more elastic. [246] Medium chain length polyhydroxyalkanoates alone and/or copolymers with short-chain-length PHAs are suitable for a wide range of industrial and even biomedical applications where flexible materials are needed such as heart valves and controlled matrices for drug delivery. However, industrial production is still limited to the copolymer poly(hydroxybutyrate-co-hydroxyhexanoate) .[65, 85]

As mentioned before in this project, PHA synthases are divided in Class I, II, III and IV based on their substrate specificity and on their domain composition .[154, 155] The representative genus for class II polyhydroxyalkanoate synthase (PhaC) ,and therefore for mcl-PHA production, is *Pseudomonas.* [154] Species of this genus that have been studied for PHA production include *P. mosselii* T07, *P. corrugata*, *P. mediterranea*, *P. putida* and *P. mendocina* [117] as well as *Pseudomonas stutzeri* strain 1317, whose PhaC can incorporate both short-chain-length and medium-chain-length hydroxyalkanoates into PHA. [156]

Liu and Chen [150] produced mcl-PHA consisting of 3-hydroxyhexanoate (HHx), 3-hydroxyoctanoate (HO), 3-hydroxydecanoate (HD), 3-hydroxydodecanoate (HDD), and high-content of 3-hydroxytetradecanoate (HTD) (≥30% monomer composition) for the first time in 2007 using tetradecanoic acid as the single substrate and using *Pseudomonas putida*

KT2442 as a host. The authors found that higher contents of HTD portion led to an increase of melting temperature and that copolymers containing more than 30% HDD or HTD show a remarkable change in mechanical properties from normal mcl, as they become normal elastic materials that are not sticky. Liu and Chen [150] also observed that PHA containing high HTD monomer content (between 31% to 49% monomer composition) has higher crystallinity and improved tensile strength compared with typical PHA. However, these polymers have not been explored further and more studies are needed to find whether other PhaCs from *Pseudomonas* can produce them.

Based on this reasoning, the objective of this **Chapter 2** was to compare 3 different PhaCs , in terms of PHA production and monomer composition analysis, from different *Pseudomonas: Pseudomonas stutzeri* 1317, *P. putida* KT2440 and *P. mendocina* NK-01 using sodium dodecanoate and sodium tetradecanoate as substrates. *Escherichia coli* was used as a host to provide uniform metabolic background for the enzymes as suggested by Chen, Liu, Zheng, Chen and Chen [156] and by Hiroe, Ushimaru and Tsuge [247]

Initially, *Escherichia coli* DH5α was used as a chassis, however, with the purpose of enhancing the supply of substrate to our PhaC enzymes, it was decided to compare them using the β-oxidation pathway weakened strain Δ*fadA E. coli* K-12 as a host as well. FadA catalyzes the final step in the β-oxidation pathway [248, 249] and by knocking out this enzyme, there is accumulation of the intermediate metabolite 3-keto-acyl-CoA (FadA's subtrate) that can be converted into 3-hydroxyacyl-CoA, which in turn will serve as a substrate for our PhaC enzymes, thus increasing PHA yield [250] (Refer to the metabolic pathway for mcl-PHA production shown in **Figure 15,** which is based on *Escherichia coli's* metabolism).

Furthermore , we also experimented with the β-oxidation weakening agent acrylic acid, which also inhibits the 3-ketoacyl-CoA thiolase (FadA) enzyme and channels β-oxidation intermediates to mcl-PHA production in several organisms including *E. coli* . [138, 248, 251, 252] PHA increase has also been observed when the sodium salt version of acrylic

acid (sodium acrylate) is used in *Ralstonia eutropha* (*Cupriavidus necator*) .[253] In this work, it was hypothesized that sodium acrylate would increase mcl-PHA accumulation inside *Escherichia coli* using sodium dodecanoate and tetradecanoate as substrate.

PHA accumulation from our biomass was evaluated using Gas Chromatography (GC) which is considered the most conventional and widely spread method used for PHA quantification [254]. It has the advantage of being quantitative and it is able to distinguish different types of polymer monomers. [255] [88, 113, 116, 143, 150, 157, 181, 182, 256] Qualitative methods such as microscopy after staining could also be useful for rapid qualitative screening. [255]

GC was first proposed by Braunegg, Sonnleitner and Lafferty [87] in 1978 and consisted in the digestion of polyhydroxybutyrate (4 carbons) into its volatile monomer , methyl (R)-3-hydroxybutyrate, through acid methanolysis (Reaction is shown below in **Figure 16**) which can then be processed and detected.

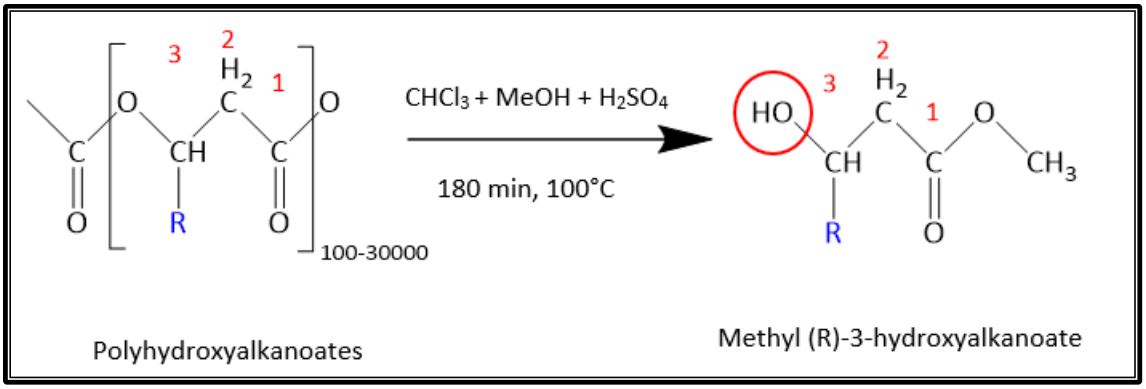

Figure 16. *Conversion of polyhydroxyalkanoates into their volatile monomer form methyl-3-hydroxyalkanoates through acid methanolysis. Conditions were modified from Braunegg, Sonnleitner and Lafferty 1978. Modelled using ChemDraw*[7]

Additionally, the acid methanolysis digestion not only converts the PHA monomer but also converts the fatty acids present in the sample into volatile methyl esters that are also easily identified by the GC [257-259] (Reaction shown in **Figure 17**). This reaction is relevant for the present study given that the bacterial cultures will be fed with sodium dodecanoate

(C12) and sodium tetradecanoate (C14) as carbon sources and therefore, it is expected to take place in every sample.

It is important to note that the fatty acid methyl esters (FAMES) and the PHA methyl esters only differentiate from one another by one hydroxy group in the third carbon of the molecule that is absent on FAMES and present in methyl esters (Shown in **Figure 16** and **Figure 17**) .It is expected and desired for GC analysis to be sensitive enough to allow us to identify residual fatty acid substrate in the cell pellet and to, due to the molecular difference, be able to segregate these values from the actual PHA measurements.

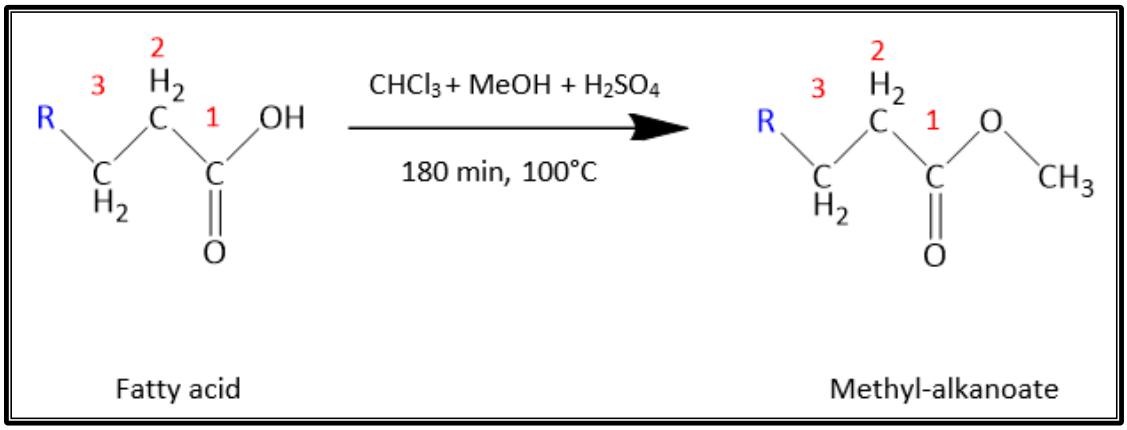

***Figure 17**. Conversion of fatty acids into their volatile monomer form methyl-alkanoates through acid methanolysis. Modelled using ChemDraw* [7]

Based on this information, it was considered indispensable for this work to include an experiment where a GC method is validated for the accurate identification and quantification of polyhydroxyalkanoates with monomer-chain- lengths from C4 to C14 and for the accurate identification of fatty acids with C12 and C14 carbons in our samples.

2.2 Materials and Methods.

List of detailed information on the materials used (reagents, kits, equipment, software, media preparation and miscellaneous) can be found in **Appendix 1-5.** Strains and plasmids are shown in **Table 11**

Table 11. Strains and plasmids used for this study.

Strains	Relevant genotype	Source or reference
DH5α	F-, Δ(argF-lac)169, ϕ80dlacZ58(M15), ΔphoA8, glnX44(AS), λ-, deoR481, rfbC1?, gyrA96(NalR), recA1, endA1, thiE1, hsdR17	Lab collection
E. coli K-12 BW25113 Δ*fadA*	F-, *Δ(araD-araB)567*, *ΔlacZ4787*(::rrnB-3), λ^-, *rph-1*, *Δ(rhaD-rhaB)568*, *hsdR514, ⊿fadA, Kan^R*	[260]
Plasmids		
pBBR1c-*PmePhaC*	P_{BAD} promoter, PhaC from *P. mendocina*, Cam^R	This study
pBBR1c-*PstzPhaC*	P_{BAD} promoter, PhaC from *P. stutzeri*, Cam^R	This study
pBBR1c-*PpuPhaC*	P_{BAD} promoter, PhaC from *P. putida*, Cam^R	This study

Abbreviations: Cam^R, chloramphenicol resistance; Kan^R, kanamycin resistance

Plasmids used in this chapter are inducible with arabinose (0.2% (w/v) was used). *Escherichia coli* is naturally capable of metabolising arabinose [261] and while this capability is still present in DH5α, *Escherichia coli*-K12 had those genes deleted.

2.2.1 *phaC* gene selection for alignment and comparison of sequences.

Using the research engine PubMed (8th of April 2020), and the input term "synthesis of medium chain length polyhydroxyalkanoates by *Pseudomonas*" 264 results were displayed . Out of all the studies, the names of the following strains stood out: Pseudomonas mosselii,[262, 263] *Pseudomonas corrugata,* [264-266] *Pseudomonas mediterranea,* [264, 265]

Pseudomonas putida, [266-268]*Pseudomonas mendocina*,[269, 270] *Pseudomonas chlororaphis*,[271, 272] *Pseudomonas stutzeri* 1317 [136, 169] and *Pseudomonas entomophila*. [147, 273]

Based on these findings, 10 protein sequences were searched from NCBI to build a phylogenetic tree. These sequences correspond to the following strains: *Pseudomonas entomophila* L48*, Pseudomnas putida* KT2440*, Pseudomonas mediterranea* DSM 16733*, Pseudomonas oleovorans, Pseudomonas putida* LS46*, Pseudomonas stutzeri 1317, Pseudomonas mendocina NK-01, Pseudomonas corrugate RM1-1-4* and *Pseudomonas chlororaphis qlu-1*. The PhaC protein sequence from *Cupriavidus necator* H16 was added to the tree as well.

Specifically, the strain *Pseudomonas putida* KT2440 stood out for being the most reported strain found for mcl-PHA production [89, 123, 267, 268, 274-281] and because, when compared against other *Pseudomonas* strains, it produces higher mcl-PHA yields. [120, 282] PhaC2 from *Pseudomonas stutzeri* 1317 is also an interesting enzyme because, unlike the rest of the *Pseudomonas*' PhaC enzymes, this PhaC has proven to have a wider substrate specificity and can polymerize both short-chain-length and medium-chain-length PHAs.[136] Both of these PhaCs were chosen for laboratory experimentation plus the PhaC from *Pseudomonas mendocina* NK-01 which is a less studied strain than *P. putida* KT2440 but that has shown the capability of co-producing mcl-PHA and alginate oligosaccharides using glucose as a substrate. [283] The entire genome of this strain is available and strong promoters have been identified which is advantageous for genetic engineering in the future [269, 283]

2.2.2 Nucleotide sequence accession numbers for the laboratory experiments.

The PhaC sequences from *Pseudomonas mendocina* NK-01 and from *Pseudomonas putida* KT2440 were both taken from the database KEGG: Kyoto Encyclopedia of Genes and Genomes. [284] using the entries MDS_0566 and PP_5003 respectively, whereas the PhaC sequences for *Pseudomonas stutzeri* 1317 and for *Cupriavidus necator* H16 were retrieved

from The National Center for Biotechnology Information (NCBI) using the protein accession numbers (*P. stutzeri* PhaC) AAO59384.1 and P23608.1 (*C. necator* PhaC).[285]

The 3 PhaC sequences from *Pseudomonas* were codon optimized to be expressed in *Escherichia coli* K-12 using the bioinformatic Codon Optimization Tool from Integrated DNA Technologies and then purchased as synthetic genes using this same company. https://www.idtdna.com/pages.

2.2.3 Plasmid construction and bacteria transformation.

All plasmids were derived from pBBR1c-*RFP* constructed by Johnson, Gonzalez-Villanueva, Tee and Wong [286] which contains P_{BAD} promoter (induced in the presence of arabinose) and chloramphenicol resistance gene (25 µg/ml). Three synthetic genes that code for polyhydroxyalkanoate synthase (PhaC) from *Pseudomonas stutzeri* 1317, *P. putida* KT2440 and *P. mendocina* NK-01 respectively were purchased from Eurofins (Ebersberg, Germany). Digestion of plasmid and genes was done using NdeI and BamHI enzymes to then, recirculate the plasmids using T4 ligase from New England Biolabs (Hitchin, UK). (see **Figure 18**).

Each of the three plasmids constructed was used to transform *E. coli* DH5α and *E. coli* K-12 (*fadA* knockout mutant) using the standard $CaCl_2$ method [287] and plated on TYE agar (10 g/L tryptone, 5 g/L yeast extract, 8 g/L NaCl, 15 g/L agar) supplemented with 25 µg/mL of chloramphenicol, and incubated overnight at 37 °C.

Figure 18. *Plasmid maps. A) pBBR1c-PmePhaC (harbouring PhaC from P. mendocina); B) pBBR1c-PstPhaC (harbouring PhaC from P. stutzeri and C) pBBR1c-PpuPhaC (harbouring PhaC from P. putida). Maps were built using SnapGene.*

2.2.4 Bacteria growth kinetics

Both *E. coli* strains (DH5α and ΔfadA) with and without plasmid (pBAD-*PmePhaC*) were grown overnight in 2×YT media (tryptone 16 g/l, yeast 10 g/l, NaCl 5 g/l) (37°C, 250 rpm) and chloramphenicol (25 µg/ml) when needed . The next day the culture was adjusted to an OD600≈0.03 in 50 ml of fresh media and grown in the same conditions. Absorbance of cells was measured using optical density every hour for 24 hours at 600 nm and these values were used to estimate the number of cells using the polynomial degree equation from Mira, Yeh and Hall 356. Protein expression was not induced therefore growth differences are only attributed to the metabolic burden of the presence of the plasmid inside the cell and not to PhaC expression or PHA production.

2.2.5 Bacteria cultivation and PHA production

The six strains obtained from the transformation of *E. coli* DH5α and the Δ*fadA* knockout mutant of *E. coli* K-12 BW25113 with the plasmids pBBR1c-*PmePhaC*, pBBR1c-*PstPhaC* and pBBR1c-*PpuPhaC* were used for the analysis of PHA production. One colony of each transformant was grown in 5 ml of medium 2×YT (tryptone 16 g/l, yeast extract 10 g/l and NaCl 5 g/l) and chloramphenicol (25 µg/ml) overnight. Subsequently, optical density at 600 nm was measured and adjusted to ~8. Flasks with 50 ml of medium 2×YT and chloramphenicol (25 µg/ml) were inoculated with 1 ml of the correspondent overnight culture and left to grow (37℃, 250 rpm) in a shaker till OD_{600} reached ~0.3-0.5. At this point PHA production was induced by adding arabinose (0.2% (w/v)) and prewarmed substrate in 50% ethanol (final concentration 0.5% (w/v)), the β-oxidation pathway inhibitor sodium acrylate was also added in this stage when indicated (0.05% (w/v)). For this work sodium dodecanoate and sodium tetradecanoate were used as substrates. The culture was left to grow for 48 hours after induction. Biomass was collected by centrifugation (8000 rpm, 10 min) then washed with 10 ml of prewarmed ethanol (50℃) (centrifuged 8000 rpm, 10 min)

to eliminate the residual substrate and then with 10 ml of distilled water (centrifuged 8000 rpm, 10 min). After this, biomass was left to oven-dry overnight at 50℃.

The total number of cultivations needed for this **Chapter 2** was calculated as follows:

$$2strains \times (3PhaC + 1control) \times 2\ substrates \times 2\ acrylate = 32$$

Each of the 32 different cultures were cultivated by triplicate (96 cultivations in total) in completely different batches.

The red fluorescent protein (mRFP1) was successfully expressed (positive control of protein expression) using the vector pBBR1c and shown in **Figure 19 A).** It was considered important the use of mRFP1 as a reporter gene because it is a validated method to easily monitor protein expression in *E. coli.* [288]

DH5α and the knockout Δ*fadA*- *E. coli*- K-12 were grown and analysed as negative controls for PHA expression (**Figure 19 B,C**)

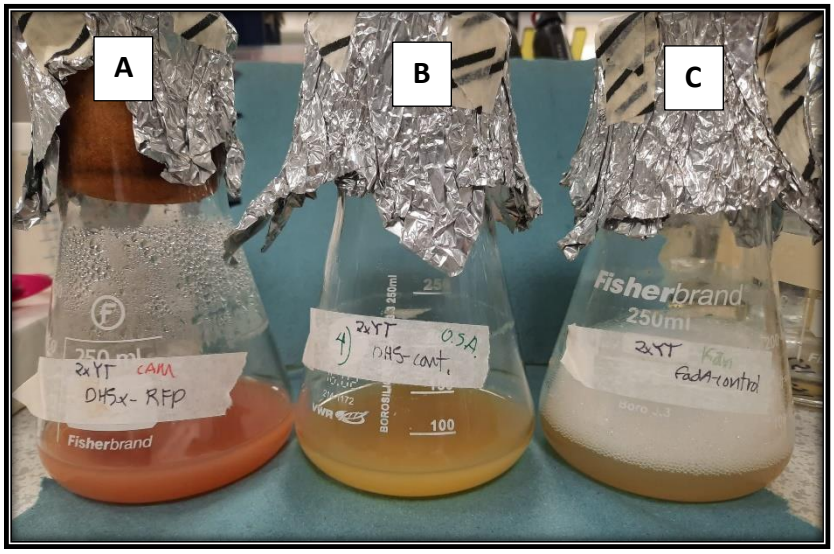

***Figure 19**. Cultivation of controls using sodium tetradecanoate as substrate were A) is DH5α transformed with pBBR1c-FRP, B) is DH5α with no plasmid and C) is the knockout ΔfadA-E. coli -K12 with no plasmid.*

2.2.6 Gas chromatography analysis

Gas Chromatography (GC) is a common technique to determine both, monomer composition and total PHA yield inside the cell. [88, 113, 116, 143, 150, 157, 181, 182, 256] GC equipment used was PERKIN ELMER AutoSystem XL (Serial No.610N1092802) and the stationary phase column was the Zebron ZB-5 plus column, 30 meters long, 0.25 mm I.D. and 0.25 µm film thickness (serial No. 583604).

Conditions used were the following : the oven was held at 80°C for 5 min then heated to 220 °C at 20 °C min− 1 , then held at 220 °C for 5 min. Peak detection was performed by a flame ionization detector, which was maintained at 300 °C. H_2 was used as carrier gas as suggested by Bhatia, Kim, Kim, Kim, Hong, Hong, Kim, Jeon, Kim, Ahn, Lee and Yang [90]

Reactants for all the standards and PHB for validation of the digestion were commercially bought and are described in more detail in **Appendix 1.** Benzoic acid was

used as internal standard (1 mg/ml). All the samples were diluted in chloroform and the volume of injection was 0.2 µl.

The method for the digestion of samples was taken and modified from Juengert, Bresan and Jendrossek [289] and was performed as follows: Three milligrams of commercial PHB was transferred into a glass culture tube with screw cap and dissolved with 1 ml of chloroform containing 1 mg/ml of benzoic acid (used as internal standard) and 1 ml of acidified methanol [15% (v/v) H_2SO_4]. To mix well, the sample was vortexed for 3 seconds and then the digestion took place for 3 hours at 100 °C. The sample was cooled on ice before adding 0.5 ml of double distilled water and then vortexed for 30 seconds. The tube was left to stand at room temperature to allow phase separation and ≈250 µl from the organic layer was recovered (bottom layer) and analysed using GC. This sample was prepared 15 times.

After the GC analysis the following parameters were recorded per sample: Area under the peak for methyl-3-hydroxybutyrate (µV*s), Area under the peak for methyl benzoate (internal standard) (µV*s) and retention time (RT) (min) for both compounds.
Using this data, the Area (µV*s) for methyl-3-hydroxybutyrate was adjusted to correct injection errors as shown in the equation below. The new Area was labelled and Normalized area:

$$Normalized\ C4\ area\ value\ (\mu V * s) = \frac{\text{Average internal standard area}}{\text{internal standard area value}} \times \text{C4 area value}$$

For cell analysis, biomass was collected from 50 ml of culture by centrifugation, dried overnight at 50°C and digested using the same method.

2.2.7 Statistical Analysis

All the statistical analysis was calculated with 95% confidence level using the software STATGRAPHICS Centurion XV.11[290] using at least 3 replicates of completely different cultivations. The Tukey HSD test was used to evaluate the significant difference between cultivations. Homogeneity of variances was confirmed in each case using the Bartlett's test.

One-way analysis of variance (ANOVA) and Multifactor ANOVA were also performed when necessary.

2.3 Results

2.3.1. PhaC alignment and comparison of sequences.

The nine PhaC enzymes selected were aligned and analysed using Jalview[291] and compared against the PhaC from *C. necator* which is the representative strain for short-chain-length PHA production. [101] The alignment and colouring was done using Clustal OWS.[292] The colouring criteria was ≥75% identity threshold and ≥75% conservation threshold using the colour code (Clustal X) [292] which is shown in **Figure 20.**

Category	Colour	Residue at position
Hydrophobic	BLUE	A,I,L,M,F,W,V
		C
Positive charge	RED	K,R
Negative charge	MAGENTA	E
		D
Polar	GREEN	N
		Q
		S,T
Cysteines	PINK	C
Glycines	ORANGE	G
Prolines	YELLOW	P
Aromatic	CYAN	H,Y
Unconserved	WHITE	any / gap

***Figure 20**. Clustal X colour scheme for amino acids.*

A phylogenetic tree was also constructed (**Figure 22**) to investigate the evolutionary relationship between the 10 PhaC sequences mentioned above. Sequences were compared using the neighbour joining method [3] and the BLOSUM62 alignment score matrix [9]

PhaC alignment is shown in **Figure 21.** The amino acid sequence of the PhaC from *Cupriavidus necator* H16 was added to both the alignment and the phylogenetic tree since this enzyme is by far the most studied for PHA production both in lab and industrial scale.[65, 101] This PhaC has high activity and is representative of class I synthases for short-chain-length production [154, 293] Therefore, sequence differences between *C. necator* PhaC and the other 9 PhaCs from *Pseudomonas* used in this study would provide a hint of the amino acids responsible for substrate preference and activity.

The phylogenetic tree (**Figure 22**) displays, as expected, the *C. necator* PhaC as the most distantly related PhaC from all the 10 enzymes compared. From the 3 PhaCs selected

to evaluate *in vivo* (*P. mendocina* NK-01, *P. stutzeri* 1317 and *P. putida* KT2440) *PmePhaC* and *PstzPhaC* are the most closely related.

As mentioned in **Chapter 1**, section **1.12.2**, the PhaC enzymes contain the so-called lipase box G-X-S-X-G (X is an arbitrary amino acid) and a secondary structure containing the α/β hydrolase fold which is a characteristic succession of alpha helices and beta strands also present in lipases. In PhaC, the box sequence was found to be ([GAST]-X-C-X-[GASV]-[GA]) and was renamed as the PhaC box consensus sequence from which the central cysteine is the catalytic nucleophile. [161, 162] [155, 162]

In addition to this cysteine, other 2 amino acids make up the catalytic triad. **Figure 21** shows the alignment of the 10 enzymes sharing the same catalytic triad: cysteine, aspartic acid, and histidine [161] (**Figure 21 ;** black squares) Squared in red is the PhaC box sequence. [162] However, and consistently with the phylogenetic tree, It can be observed that inside the PhaC box (one position before the catalytic cysteine) a phenylalanine is present in the PhaC of *C. necator* instead of the alanine conserved in all 3 *Pseudomonas* presented, whereas one position after the cysteine PpuPhaC presents a glycine, *C. necator* PhaC a valine and PstzPhaC and PmePhaC (which are more related to each other) have an alanine.

PhaCs are classified into classes according to their sequence and monomer preferences: classes I, III and IV prefer to synthesize scl-PHA while class II PhaC synthesize mcl-PHA .[154, 155] Nonetheless, it has been proven that substrate specificity can rely in as much as one amino acid difference. For example, the substitution of Leu484 in PhaC from *Pseudomonas putida* for valine shifts the substrate specificity from PHO to PHB (C8 to C4). Aminoacid at position 484 is adjacent to the catalytic triad that is conserved as leucine in class II synthases, as valine in class III and as valine or isoleucine in class I (*C. necator*) and is critical in determining substrate specificity. [168] This amino acid is squared in blue and shown in **Figure 21.**

Based on the above information, it was expected for this work to find similar results, in terms of monomer composition and yield between PmePhaC and PstzPhaC while results from PpuPhaC were expected to differ more from the other two. However, more experiments are needed to elucidate the specific mutations in the sequence that are responsible for this difference. A plausible hypothesis would be that the mutations inside and around the PhaC box and surrounding the catalytic triad could be responsible.

The amino acid sequence alignment of the 3 enzymes evaluated *in vivo* (PmePhaC, PstzPahC, PpuPhaC) and the identification of the catalytic triad in the 3D structure is shown in **Figure 23**.

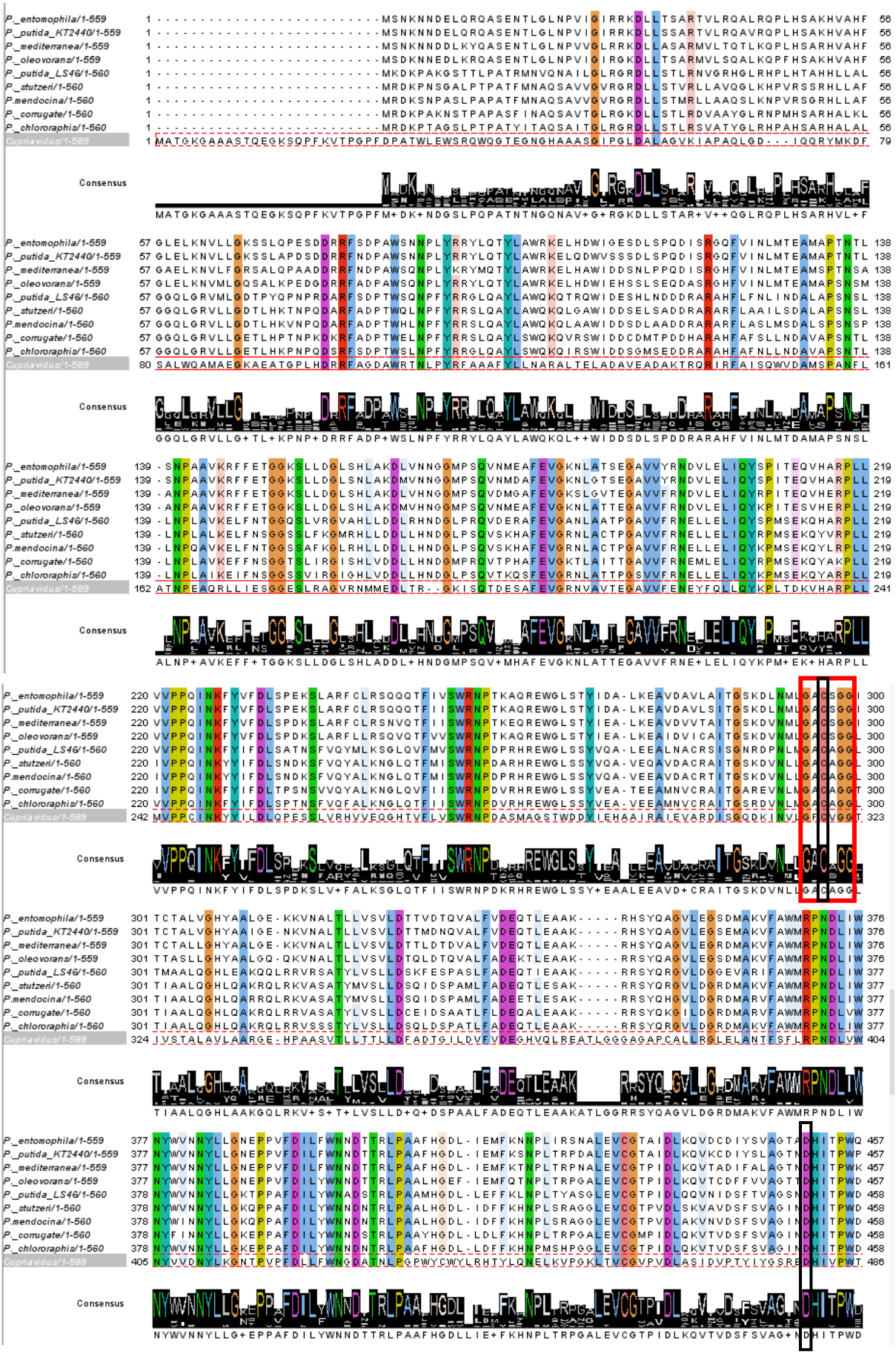
P._entomophila/1-559
P._putida_KT2440/1-559
P._mediterranea/1-559
P._oleovorans/1-559
P._putida_LS46/1-560
P._stutzeri/1-560
P.mendocina/1-560
P._corrugate/1-560
P._chlororaphis/1-560
Cupriavidus/1-589
Consensus

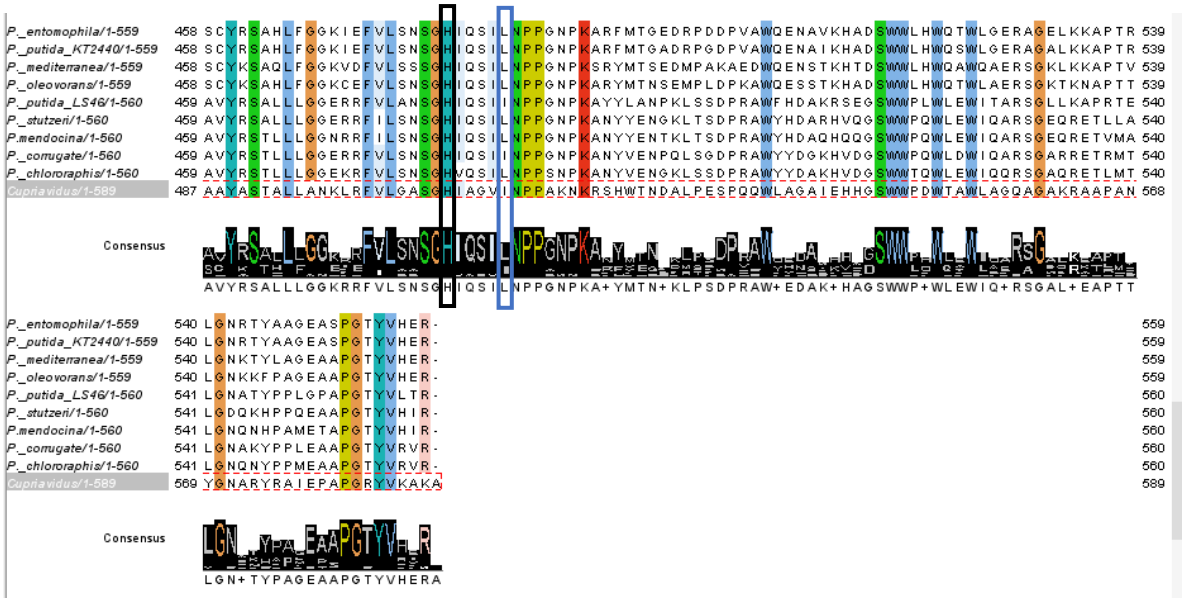

Figure 21. *Alignment of 10 different PhaCs from different Pseudomonas and from Cupriavidus necator respectively. Squared in red is the PhaC box sequence containing the catalytic nucleophile cysteine.*[162] *Squared in black are the catalytic triad: cysteine, aspartic acid, and histidine. The alignment and colouring was done using Clustal OWS. The colouring criteria was ≥75% identity threshold and ≥75% conservation threshold using the color code (Clustal X).*

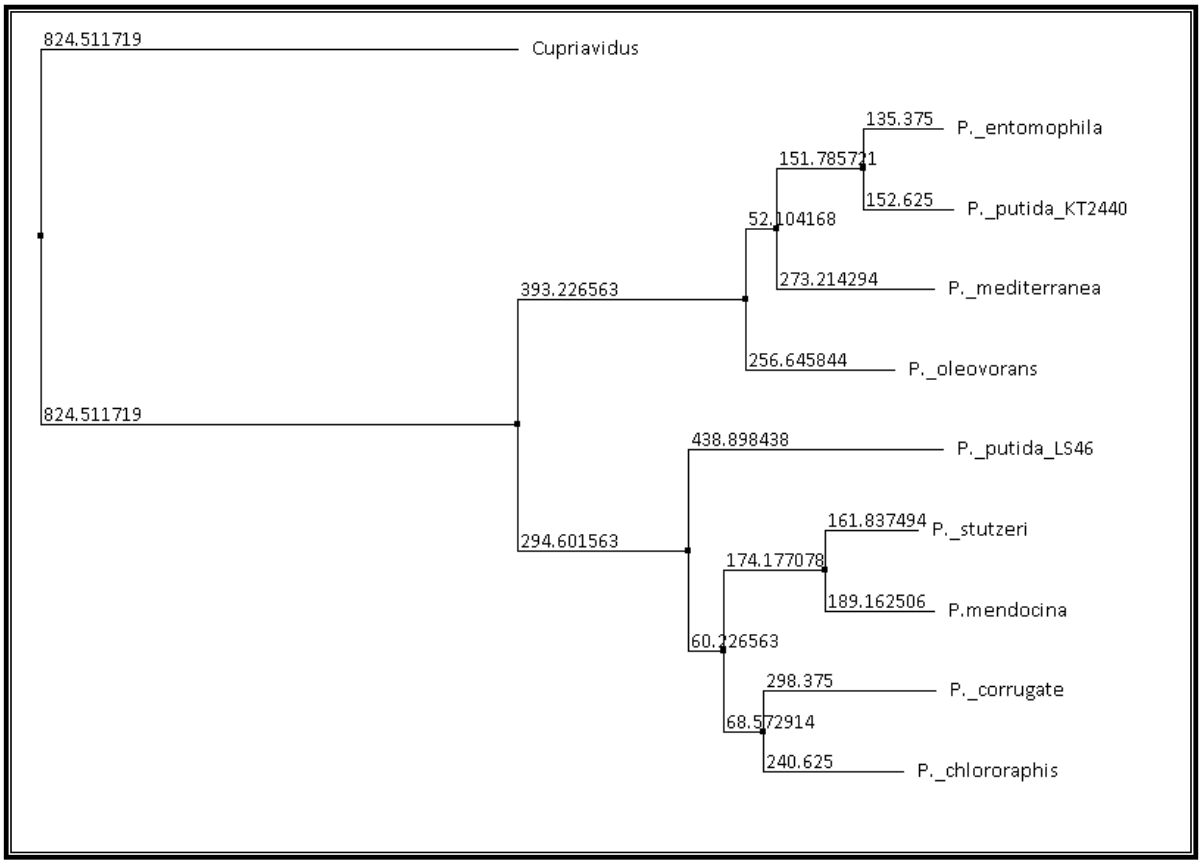

Figure 22. *Phylogenetic tree based on the PhaC sequences of 10 different organisms. Sequences were compared using the neighbor joining method[3] 3 and the BLOSUM62 alignment score matrix.* [9]

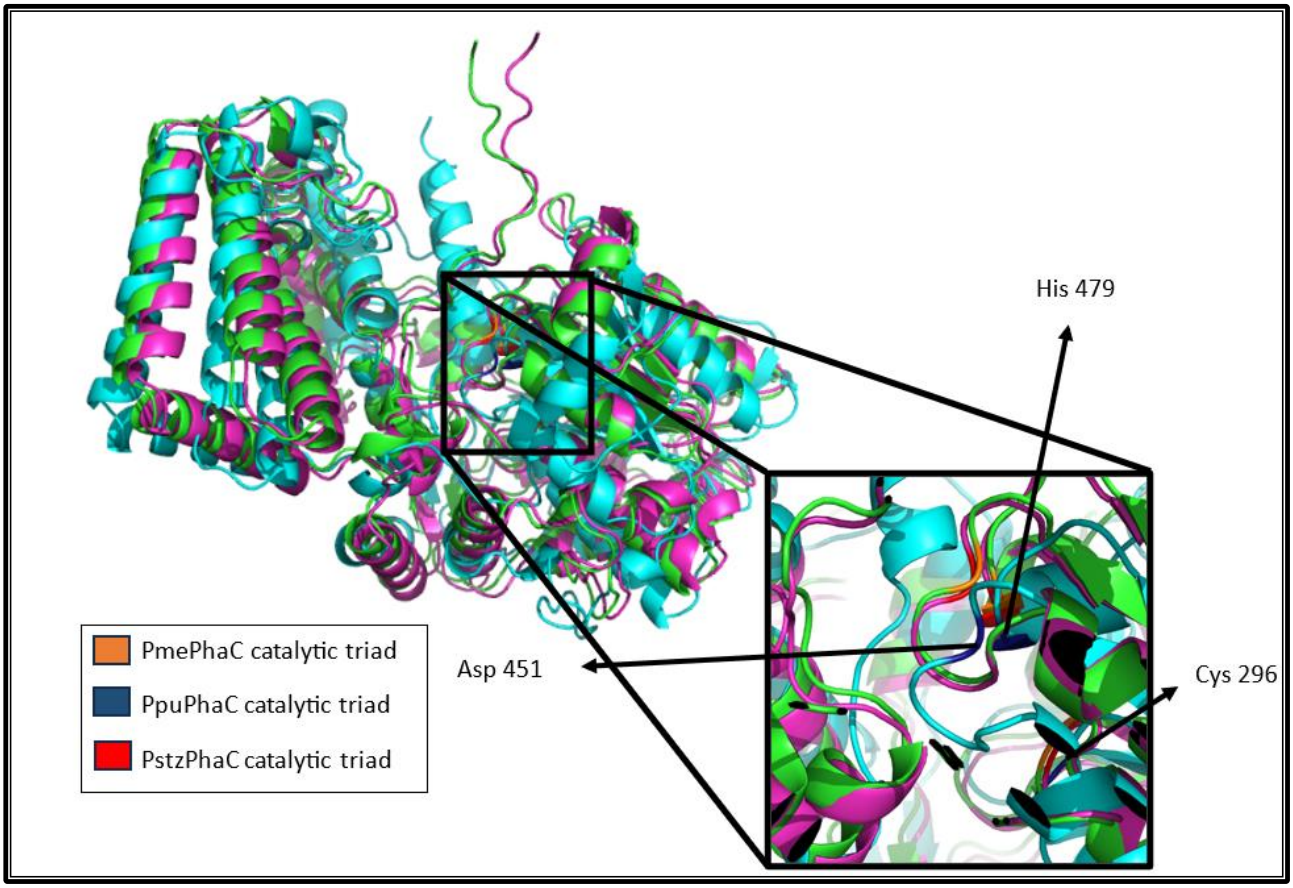

***Figure 23**. Pymol structure of 3 aligned PhaCs (PmePhaC, PpuPhaC and PstzPhaC) from P. mendocina NK-01, P. putida KT2440 and P.stutzeri 1317 respectively. The catalytic triads Cys, Asp and His are coloured.*

2.3.2. Validation of the acid methanolysis digestion of polyhydroxybutyrate (PHB) into methyl-3-hydroxybutyrate.

The standard curve for methyl-3-hydroxybutyrate was prepared and then analyzed in three totally independent replicates and the linear regression equation was elucidated from the average of these replicates with a R^2 of 0.98. The standard curve was also graphed and shown in **Figure 24** were concentration of methyl ester in chloroform (µg/µl) was chosen for the "x" axis and area under the peak of the chromatogram (µV*s) for "y".

The retention time observed for C4 was 1.91 ± 0.01 minutes.

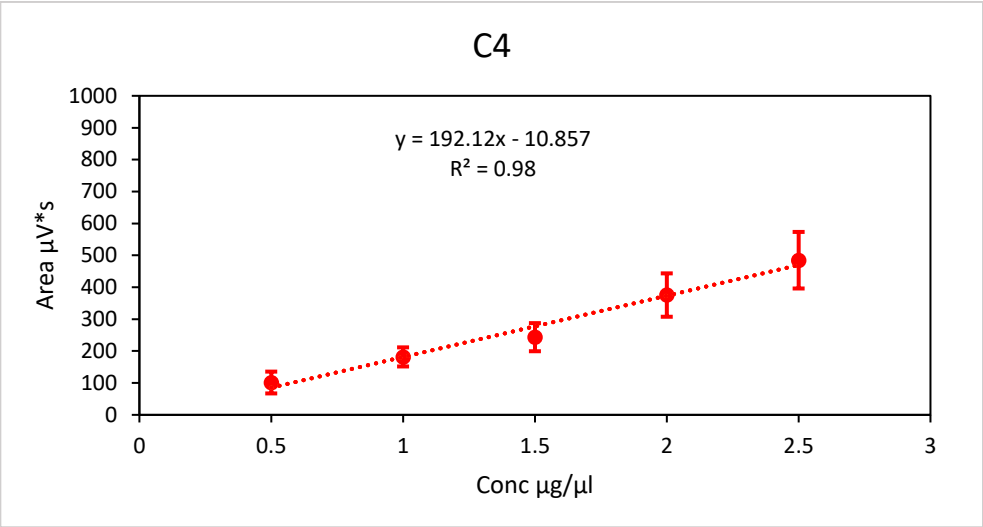

***Figure 24**. Standard curve of the monomer methyl-3-hydroxybutyrate. Retention time: 1.91 ± 0.013 min.*

Standard curves for the methyl-3-hydroxyalkanoates of C6, C8, C10 , C12 and C14 carbon-chain- lengths and their retention time (RT) were also recorded, and the data is shown in **Annex 4.** Standard curve for methyl alkanoates of C12 and C14 carbons and their retention time (RT) are shown in **Annex 5**.

The digestion of 3 mg of commercial PHB (polyhydroxybutyrate) polymer resulted in the successful conversion of PHB into methyl-3-hydroxybutyrate throughout the 15 wells present in the heat block used, (see **Figure 25 and Figure 26**). The average retention time (RT) recorded for the 15 wells of this compound was 1.89 ±0.003 min which was consistent with the retention time recorded in the standard curve for the same monomer (1.91 ± 0.013 min) .

Similarly, the average of the area under the peak (µV*s) recorded for the 15 samples was 358.88 ± 34.37 µV*s which is consistent with the Area (375 .45 µV*s) corresponding to the concentration (2 µg/µl) shown in the standard curve in **Figure 24 .** (3000 µg of

methyl-3-hydroxybutyrate were suspended in 1500 µl of organic phase from the digestion which equals to 2 µg/µl).

Aside from the information above, benzoic acid, which was used as internal standard in every sample (1 mg per sample), was also successfully converted to methyl-benzoate. The retention time for this compound was 5.87 ±0.006 min. There was no benzoic acid detected in the GC for any of the samples indicating that the conversion to methyl benzoate was completed and the average area under the peak was 434.84± 41.25 (µV*s) which was assumed to correspond to the concentration 0.7 µg/µl (calculated as 1000 µg of methyl benzoate in 1500 µl of organic phase in the digestion).

Average value of the area (µV*s) recorded through GC, standard deviation and coefficient variation for both compounds are recorded on **Table 12** and shown in **Figure 25.** The complete peak chromatogram report showing the Area (µV*s) and retention times for all the peaks detected in each of the 15 samples are reported in this work in **Annex 1**.

The variation (±SD) of the methyl-benzoate represents the variation observed in the digestion procedure itself plus the gas chromatography equipment analysis, while the methyl-3-hydroxybutyrate variation (±SD) represents the variation of all the process from analytical weight of the polymer, digestion, and GC analysis.

Table 12. Gas chromatography results of the acid methanolysis digestion of PHB and benzoic acid into methyl-3-hydroxybutyrate and methyl benzoate respectively. Error is expressed as ± the standard deviation.

	Area µV*s	Error	Coefficient variation	RT (min)	Error
Methyl-3-hydroxybutyrate	360.68	±63.63	17.641	1.89	±0.003
Methyl-benzoate	434.84	±41.25	9.487	5.88	±0.006

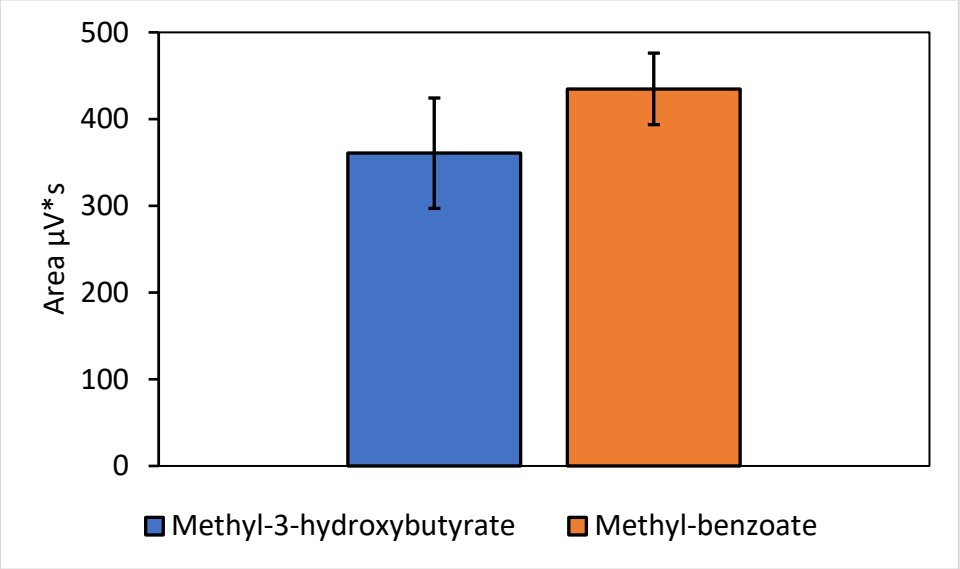

***Figure 25**. Gas chromatography results of the acid methanolysis digestion of 15 samples from the 15 wells present in the heat block used. The samples contained PHB polymer and benzoic acid as internal standard, which converted into methyl-3-hydroxybutyrate and methyl benzoate respectively. (vol of injection was 0.2 µl) .*

The normalized concentrations of C4 methyl esters for each of the 15 wells were calculated using the linear regression from the standard curve and the values for normalized area under the peak (µV*s) (See the equation in the Methods section to normalize the Area under the peak) and shown in the figure below (**Figure 26**).

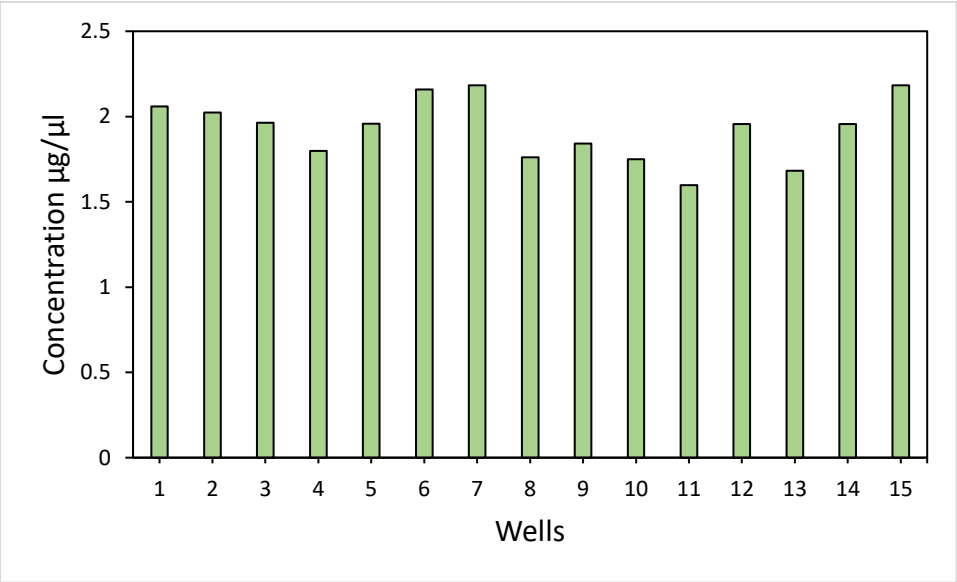

***Figure 26**. The C4 methyl ester normalized concentration (µg/µl) present in the organic phase (bottom layer) as a result of the PHB acid methanolysis digestion for each of the wells present in the equipment.*

2.3.3. Plasmid construction

The plasmids used for this **Chapter 2** were constructed by Johnson, Gonzalez-Villanueva, Tee and Wong [286]. This plasmid has the strong inducible pBAD promoter which is being widely used for expression in *Escherichia coli* strains. [294]

It also has the broad host range origin of replication pBBR1 which can replicate is a variety of PHA-producing, Gram-negative hosts such as *E. coli*, *Pseudomonas* and *C. necator* [295] which might me convenient for future experimentation in different hosts.

2.3.4. Bacteria kinetics

Growth kinetics of both *E. coli* DH5α and ΔfadA-*E. coli* with and without plasmid using 2×YT medium was recorded and shown in **Figure 27** where ΔfadA-*E. coli* shows higher growth rate than DH5α.

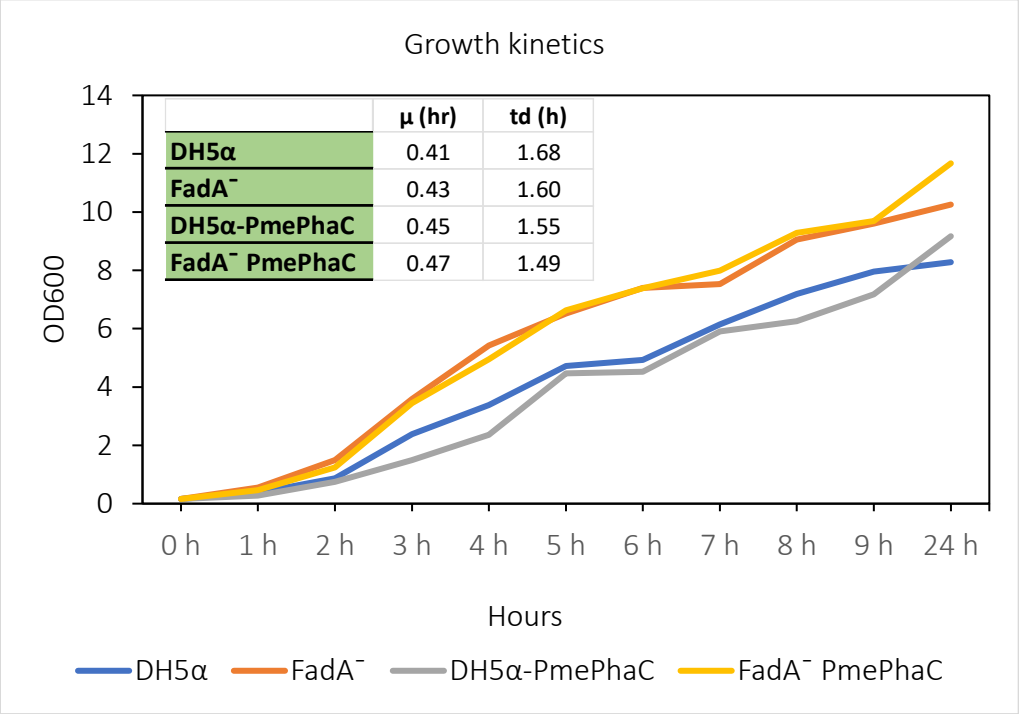

Figure 27. *Growth rate comparison between the knockout fadA Escherichia coli K-12 strain and DH5α E. coli strain with and without the pBBR1c-PmePhaC plasmid (no expression with arabinose). The medium used was 2xYT with NO fatty acid substrate added.*

2.3.5. Comparison of PhaCs using sodium dodecanoate (C12) as the substrate for reaction.

There was no significant difference between the dry cell biomass of different *E. coli* transformants expressing different PhaCs from *Pseudomonas* in the presence of sodium dodecanoate (C12) as substrate (Tukey (P≤0.05)). This statement was true for both strains tested: DH5α and Δ*fadA*. (**Table 13**, **Figure 28 A and B**). However, the *fadA* knockout mutant strain accumulated less biomass than *E. coli* DH5α (**Table 13**, **Figure 28 A and B**).

All the biomass was digested and analysed using GC-FID but there was no PHA found in detectable levels in any of the strains.

Table 13. Comparison of different PhaCs using sodium dodecanoate as substrate. Cultures were incubated 37°C, 250 rpm for 48 hours after arabinose induction (0.2% (w/v))

Host	PhaC source	Substrate 0.5% (w/v)	CDW (g/l)	wt%
DH5α	*P. putida*	C12	0.916 ± 0.058 **a**	Non-detectable levels
	P. stutzeri	C12	0.915 ± 0.168 **a**	Non-detectable levels
	P. mendocina	C12	0.860 ± 0.270 **a**	Non-detectable levels
	control	C12	0.760 ± 0.091 **a**	Non-detectable levels
FadA Knockout	*P. putida*	C12	0.604 ± 0.140 **a**	Non-detectable levels
	P. stutzeri	C12	0.567 ± 0.097 **a**	Non-detectable levels
	P. mendocina	C12	0.600 ± 0.127 **a**	Non-detectable levels
	control	C12	0.526 ± 0.030 **a**	Non-detectable levels

Each culture was grown in triplicate and the value presented is the mean ± the standard deviation. Means with different letters are significantly different Tukey (P≤0.05). Abbreviation: CDW, cell dried weight; wt%, percentage of cell dried weight that corresponds to PHA analysed by GC-FID.

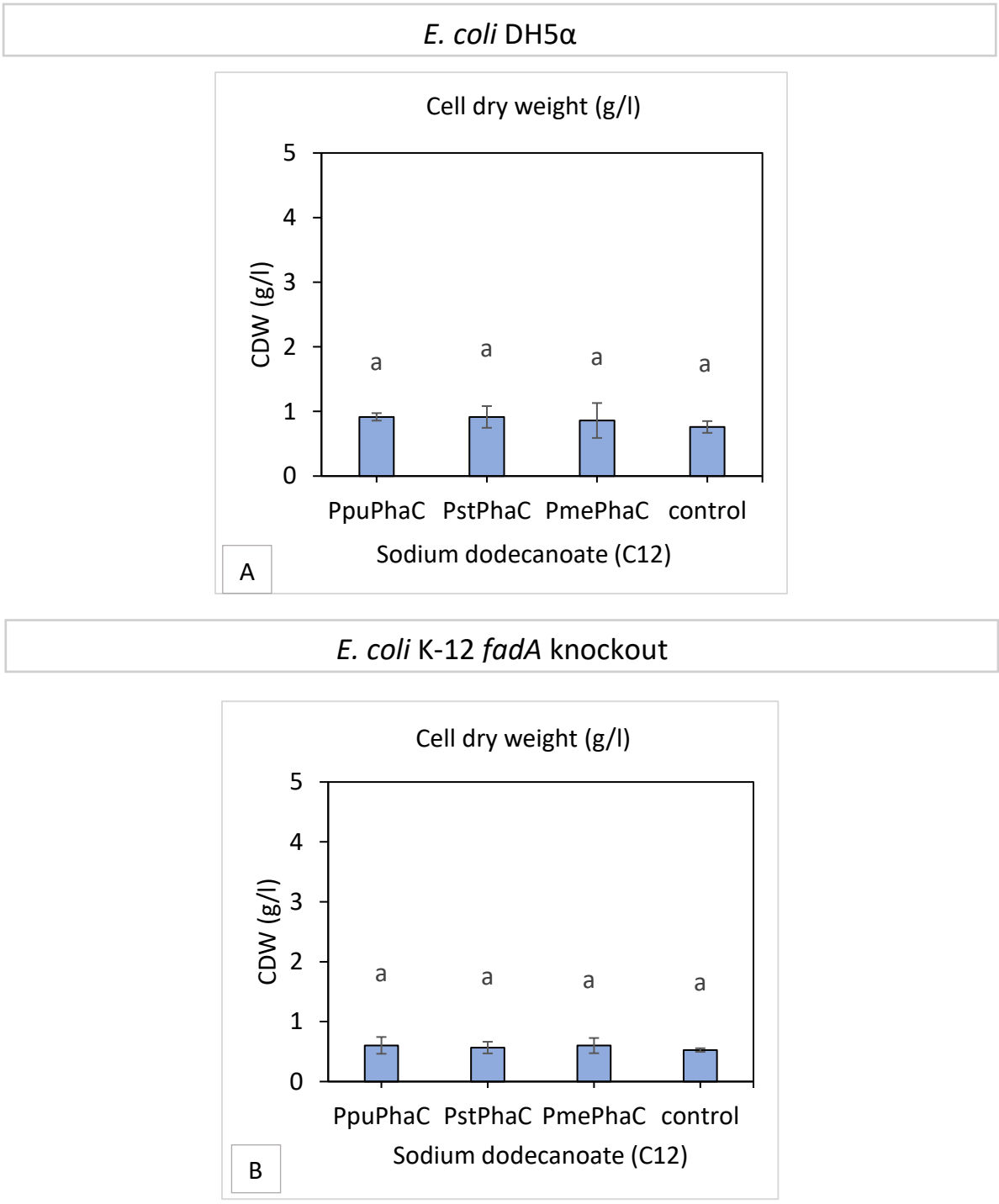

***Figure 28**. Bars with the same letter are statistically equal according to Tukey (P≤0.05). A) shows the comparison of cell dry weight between E. coli DH5α transformed with different PhaCs from Pseudomonas. B) Shows the comparison of cell dry weight between the knockout ΔfadA transformed with different PhaCs from Pseudomonas. Data was taken from 3 parallel experiments.*

2.3.6. Comparison of PhaCs using sodium tetradecanoate as the substrate for reaction.

Dry cell biomass collected from *E. coli* DH5α expressing PhaC from *Pseudomonas putida* , in the presence of sodium tetradecanoate (C14) as carbon source, was statistically higher (Tukey (P≤0.05)) than the dry biomass from the same strain expressing PhaCs from the other 2 *Pseudomonas* (**Table 14, Figure 29 A**). This could suggest that the activity of the PhaC from *Pseudomonas putida* is different from the activity of the other two enzymes in this strain and under these conditions. On the contrary, *E. coli* DH5α-*PpuPhaC* was statistically equal to the *E. coli* DH5α-control which means that there could be another unexplored reason besides the expression of PhaC. Nevertheless, this observation was not true for the Δ*fadA E.coli* strain where all the recombinant cultures are statistically equal (**Table 14**, **Figure 28 B**). DH5α accumulates higher biomass than Δ*fadA* in the presence of sodium tetradecaonate as substrate(**Table 14, Figure 29 A and B**). All the biomass was digested and analysed using GC but there was no PHA found in detectable levels.

Table 14. Comparison of different PhaCs using sodium tetradecanoate as carbon source. Cultures were incubated 37℃, 250 rpm for 48 hours after arabinose induction (0.2% (w/v))

Host	PhaC source	Substrate 0.5% (w/v)	CDW (g/l)	wt%
DH5α	*P. putida*	C14	3.993±0.221 **b**	Non-detectable levels
	P. stutzeri	C14	2.480±0.417 **a**	Non-detectable levels
	P. mendocina	C14	2.640± 0.711 **a**	Non-detectable levels
	control	C14	3.393± 0.764 **ab**	Non-detectable levels
FadA Knockout	*P. putida*	C14	0.913±0.080 **a**	Non-detectable levels
	P. stutzeri	C14	1.173±0.302 **a**	Non-detectable levels
	P. mendocina	C14	1.193±0.598 **a**	Non-detectable levels
	control	C14	1.253±0.133 **a**	Non-detectable levels

Each culture was grown three times and the value presented is the mean ± the standard deviation. . Means with different letters are significantly different according to Tukey (P≤0.05). Abbreviation: CDW, cell dried weight; wt%, percentage of cell dried weight that corresponds to PHA analysed by GC.

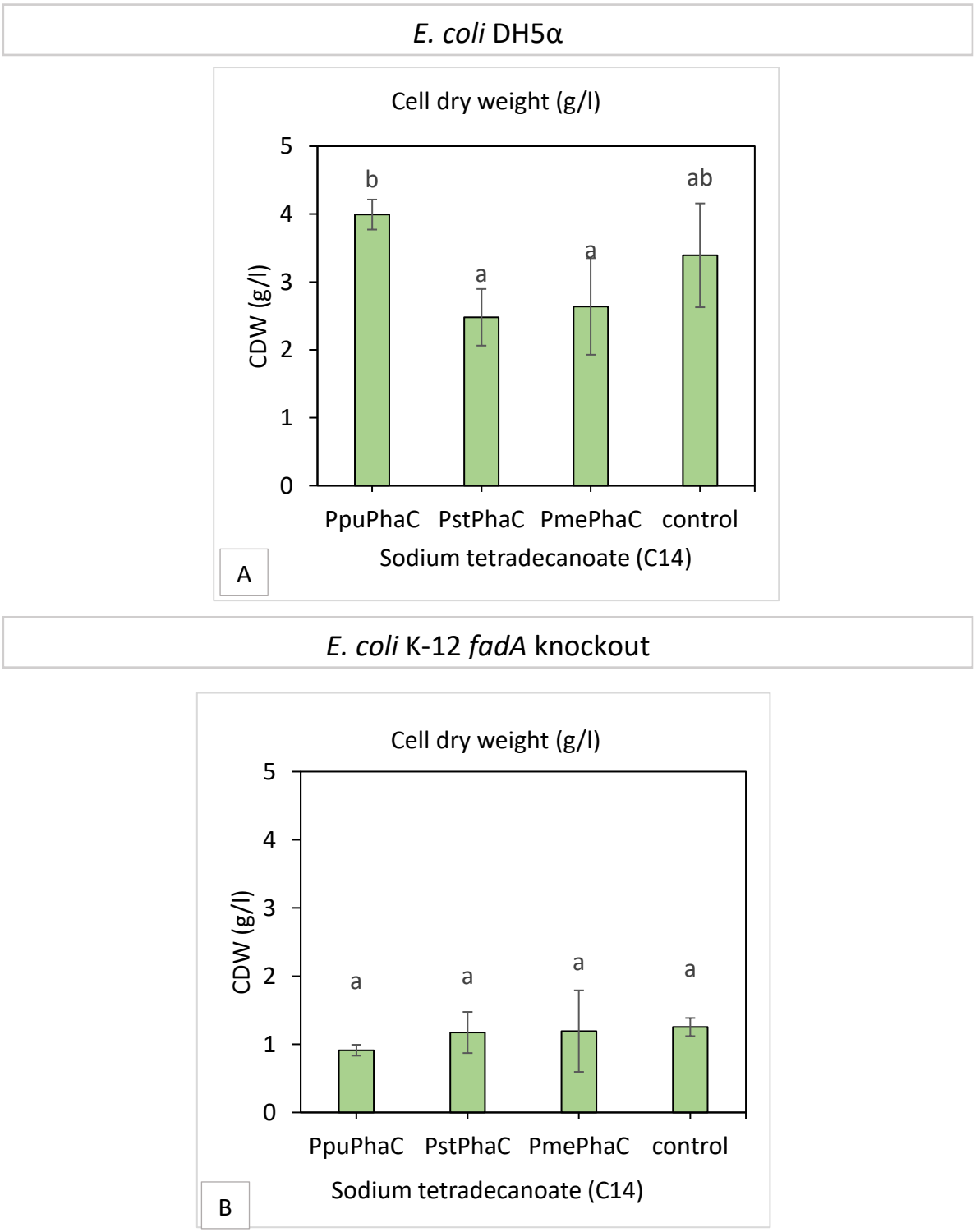

Figure 29. *Bars with the same letter are statistically equal according to Tukey (P≤0.05). A) shows the comparison of cell dry weight between E. coli DH5α transformed with different PhaCs from Pseudomonas B) Shows the comparison of cell dry weight between the knockout ΔfadA transformed with different PhaCs from Pseudomonas. Data was taken from 3 parallel experiments.*

2.3.7. Comparison of PhaCs using sodium dodecanoate as substrate and using sodium acrylate as β-oxidation inhibitor.

Dry cell biomass collected from *E. coli* DH5α expressing PhaC from *Pseudomonas putida* was statistically higher (Tukey (P≤0.05)), in the presence of sodium dodecanoate as substrate and sodium acrylate as β-oxidation inhibitor, than the dry biomass from the control with no plasmid. (**Table 15, Figure 30 A**). This may suggest that the activity of the PhaC from *Pseudomonas putida* has an impact over the biomass accumulation in this strain, whereas the biomass from the *fadA* knockout strain remains statistically equal in all 4 cultivations (**Table 15, Figure 30 B**). DH5α accumulates higher biomass than Δ*fadA* in the presence of sodium dodecanoate and sodium acrylate (**Table 15, Figure 30 A and B**).

All the biomass was digested and analysed using GC-FID but there was no PHA found in detectable levels.

Table 15. Comparison of different PhaCs using sodium dodecanoate as substrate and sodium acrylate (0.50 mg/ml) as β-oxidation inhibitor. Cultures were incubated 37°C, 250 rpm for 48 hours after arabinose induction (0.2% (w/v)).

Host	PhaC source	Substrate 0.5% (w/v)	CDW (g/l)	wt%
DH5α	*P. putida*	C12	1 ±0.121 **b**	Non-detectable levels
	P. stutzeri	C12	0.893 ±0.140 **ab**	Non-detectable levels
	P. mendocina	C12	0.786 ±0.172 **ab**	Non-detectable levels
	control	C12	0.626±0.030 **a**	Non-detectable levels
FadA Knockout	*P. putida*	C12	0.613 ±0.030 **a**	Non-detectable levels
	P. stutzeri	C12	0.586 ±0.050 **a**	Non-detectable levels
	P. mendocina	C12	0.513 ±0.204 **a**	Non-detectable levels
	control	C12	0.500±0.080 **a**	Non-detectable levels

Each culture was grown three times and the value presented is the mean ± the standard deviation. . Means with different letters are significantly different according to Tukey (P≤0.05). Abbreviation: CDW, cell dried weight; wt%, percentage of cell dried weight that corresponds to PHA analysed by GC-FID.

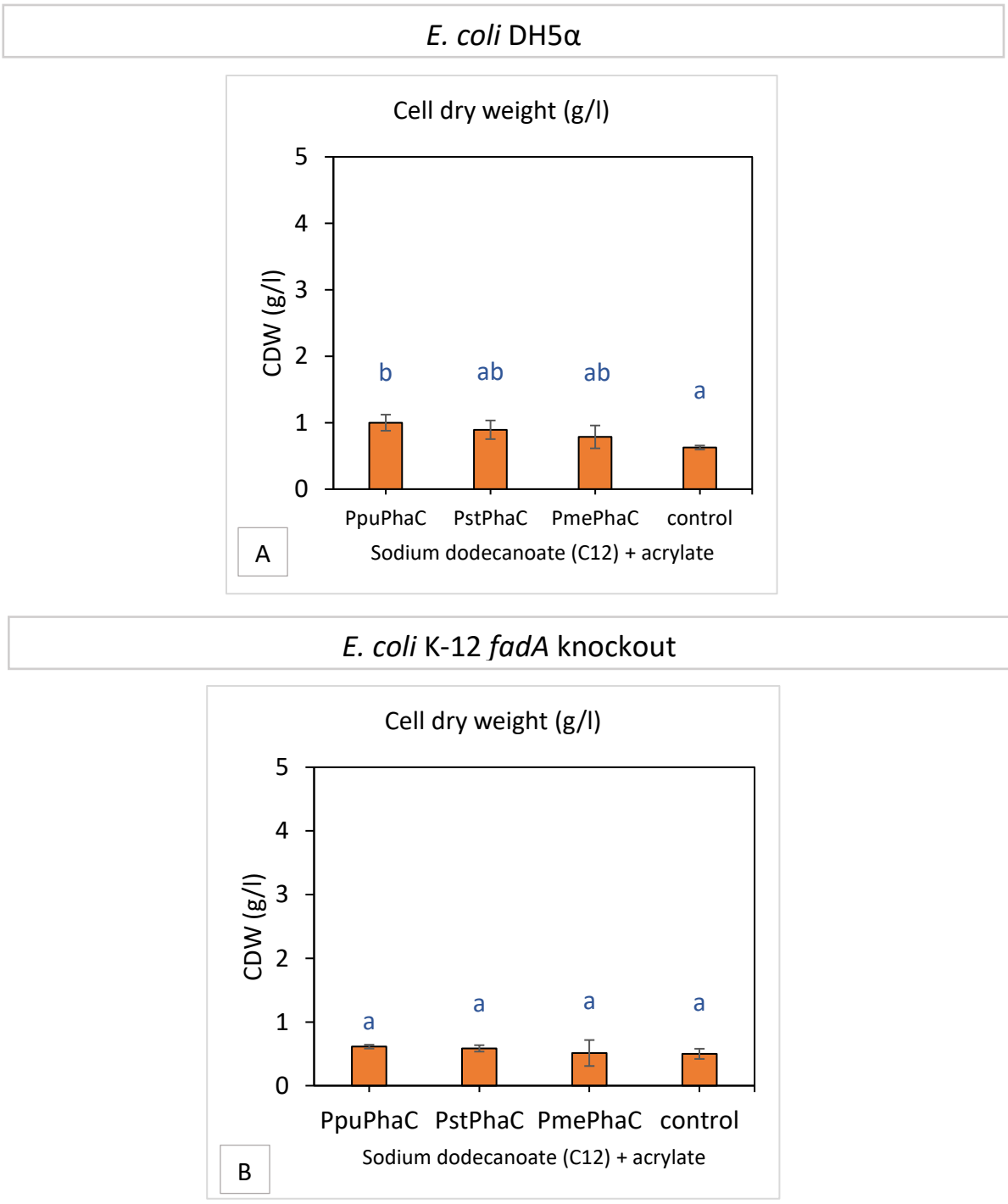

***Figure 30**. Bars with the same letter are statistically equal according to Tukey (P≤0.05). A) shows the comparison of cell dry weight between E. coli DH5α transformed with different PhaCs from Pseudomonas B) Shows the comparison of cell dry weight between the knockout ΔfadA transformed with different PhaCs from Pseudomonas. Data was taken from 3 parallel experiments.*

2.3.8. Comparison of PhaCs using sodium tetradecanoate as substrate and using sodium acrylate as β-oxidation inhibitor.

Dry cell biomass collected from *E. coli* DH5α and from the *fadA* knockout expressing every PhaC from *Pseudomonas* are statistically equal according to Tukey (P≤0.05) in the presence of sodium tetradecanoate (C14) as substrate and the β-oxidation inhibitor sodium acrylate. (**Table 16, Figure 31**). DH5α accumulates higher biomass than Δ*fadA* in the presence of sodium tetradecaonate and sodium acrylate (**Table 16, Figure 31 A and B**).

All the biomass was digested and analysed using GC but there was no PHA found in detectable levels.

Table 16. Comparison of different PhaCs using sodium tetradecanoate as substrate and sodium acrylate (0.50 mg/ml) as β-oxidation inhibitor. Cultures were incubated 37°C, 250 rpm for 48 hours after arabinose induction (0.2% (w/v)).

Host	PhaC source	Substrate 0.5% (w/v)	CDW (g/l)	wt%
DH5α	*P. putida*	C14	2.58 ±0.846 **a**	Non-detectable levels
	P. stutzeri	C14	2.173 ±0.192 **a**	Non-detectable levels
	P. mendocina	C14	3.760 ±1.910 **a**	Non-detectable levels
	control	C14	3.606±0.597 **a**	Non-detectable levels
FadA Knockout	*P. putida*	C14	1.473 ±0.553 **a**	Non-detectable levels
	P. stutzeri	C14	1.480 ±1.090 **a**	Non-detectable levels
	P. mendocina	C14	2.526 ±0.841 **a**	Non-detectable levels
	control	C14	1.500 ±0.393 **a**	Non-detectable levels

Each culture was grown three times and the value presented is the mean ± the standard deviation. . Means with different letters are significantly different according to Tukey (P≤0.05). Abbreviation: CDW, cell dried weight; wt%, percentage of cell dried weight that corresponds to PHA analysed by Gas chromatography.

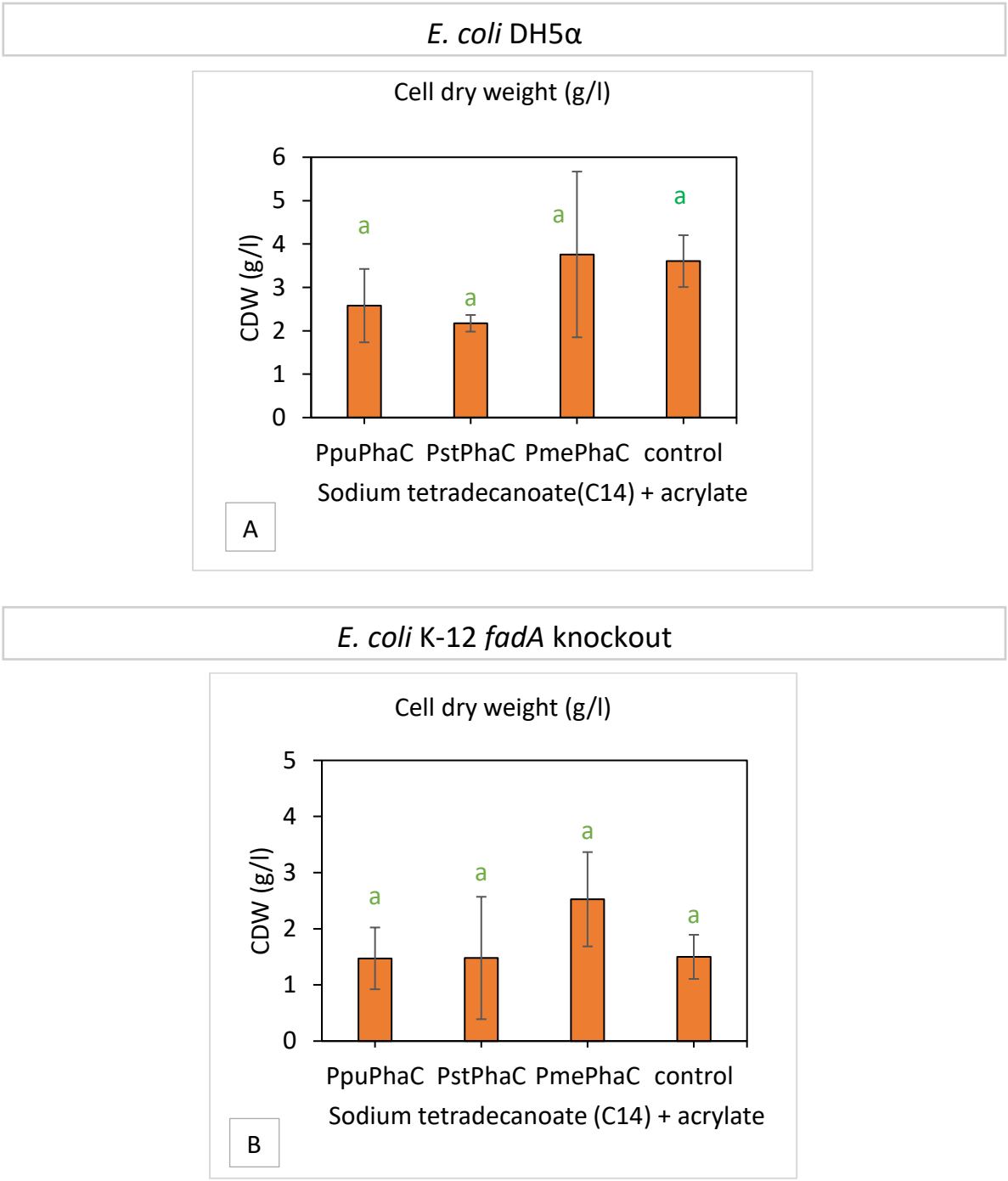

Figure 31. *Bars with the same letter are statistically equal according to Tukey (P≤0.05). A) shows the comparison of cell dry weight between E. coli DH5α transformed with different PhaCs from Pseudomonas B) Shows the comparison of cell dry weight between the knockout ΔfadA transformed with different PhaCs from Pseudomonas. Data was taken from 3 parallel experiments.*

2.3.9. Comparison of cultures with and without the β-oxidation inhibitor sodium acrylate.

A multifactorial ANOVA (95% confidence) was constructed to compare the CDW (g/l) collected from both recombinant strains (DH5α and Δ*fadA* K-12) expressing 3 different PhaCs from *Pseudomonas* in the presence of C12 and C14 as substrate and in the presence and absence of sodium acrylate. The factors used for the ANOVA were PhaC *(PpuPhaC, PmePhaC, PstzPhaC* and control) and sodium acrylate (presence and absence).

In this section, the ANOVA from **Table 17** supports the results from **section 2.3.7** of this **Chapter 2** where it is shown that DH5α-*PpuPhaC* accumulated more biomass than the same strain harbouring either of the other 2 PhaC enzymes when grown in the presence of C12 and sodium acrylate and that this difference is statistically significant. On the other hand, sodium acrylate does not influence the accumulation of biomass in this strain (**Table 17, Figure 32**). There was also no significant difference in biomass production for the strain ΔfadA under the same culture conditions (**Table 18, Figure 33**).

Similarly, no significant differences were found between PhaCs or between presence/absence of sodium acrylate when using C14 as substrate in DH5α (**Table 19, Figure 34)** Yet, the multifactorial ANOVA shows that the presence of sodium acrylate significantly favours the production of biomass in the *fadA* knockout *E. coli* strain (**Table 20**, **Figure 35**).

Table 17. *Multifactorial ANOVA (95% confidence) results for cell dry biomass. The factors analysed were presence/absence of acrylate and different PhaCs from Pseudomonas. Values that show significant difference are shown in red.*

A	CDW	
	DH5α C12	
	Factors	**P-Value**
A	PhaC	0.0367
B	Acrylate	0.5605
	Interactions	**P-Value**
	AB	0.6405

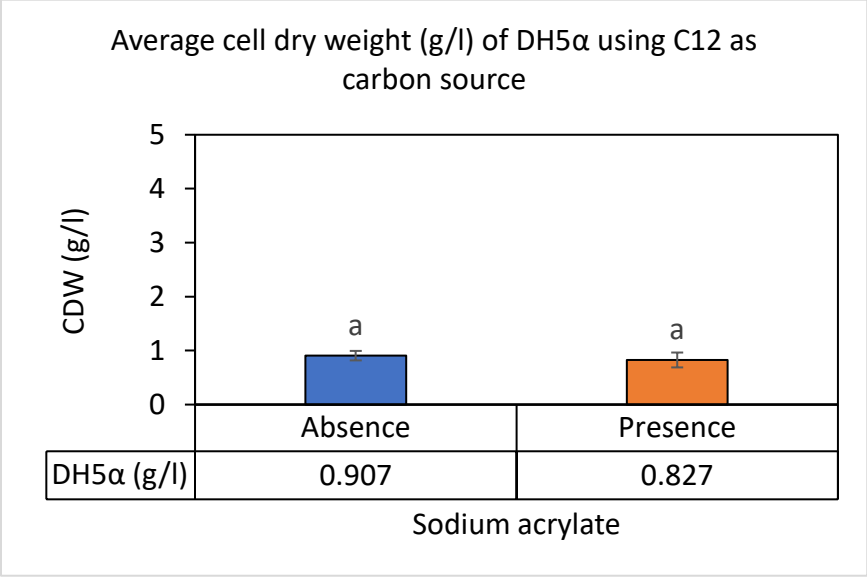

Figure 32*. Comparison of CDW (g/l) accumulation (across all the recombinant cells with the 3 different PhaCs plus the control) in the absence and presence of sodium acrylate using DH5a as a strain and C12 as substrate. Data was taken from 3 parallel experiments.*

Table 18. *Multifactorial ANOVA (95% confidence) results for cell dry biomass. The factors analysed were presence/absence of acrylate and different PhaCs from Pseudomonas. Values that show significant difference are shown in red.*

B	CDW	
	FadA knockout C12	
	Factors	**P-Value**
A	PhaC	0.5025
B	Acrylate	0.6406
	Interactions	**P-Value**
	AB	0.7940

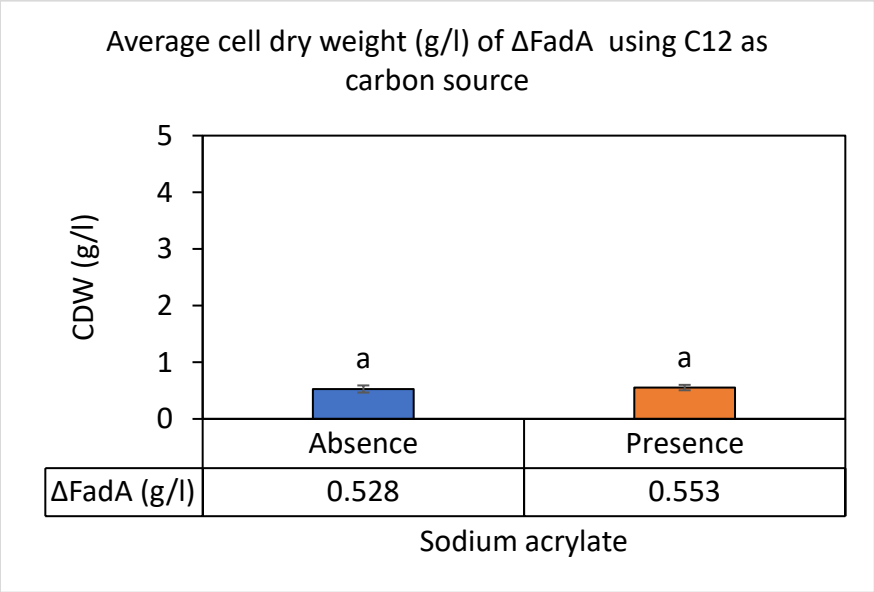

Figure 33. *Comparison of CDW (g/l) accumulation (across all the recombinant cells with the 3 different PhaCs plus the control) in the absence and presence of sodium acrylate using fadA knockout as a strain and C12 as substrate. Data was taken from 3 parallel experiments.*

Table 19.*Multifactorial ANOVA (95% confidence) results for cell dry biomass. The factors analysed were presence/absence of acrylate and different PhaCs from Pseudomonas. Values that show significant difference are shown in red.*

CDW (g/l)		
DH5α C14		
	Factors	**P-Value**
A	PhaC	0.1247
B	Acrylate	0.7838
	Interactions	**P-Value**
	AB	0.1131

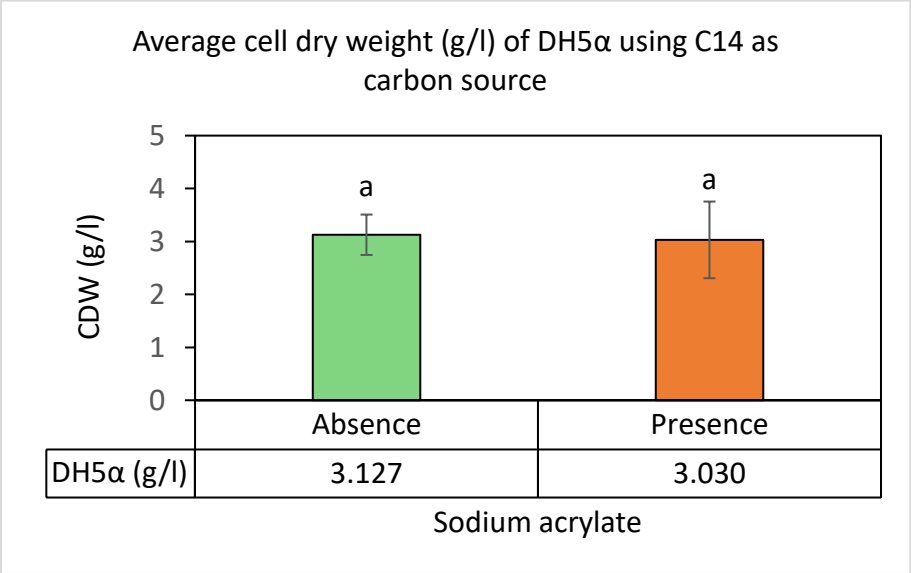

Figure 34. *Comparison of CDW (g/l) accumulation (across all the recombinant cells with the 3 different PhaCs plus the control) in the absence and presence of sodium acrylate using DH5α as a strain and C14 as substrate. Bars with the same letter are statistically equal according to Tukey (P≤0.05). Data was taken from 3 parallel experiments.*

***Table 20**. Multifactorial ANOVA (95% confidence) results for cell dry biomass. The factors analysed were presence/absence of acrylate and different PhaCs from Pseudomonas. Values that show significant difference are shown in red.*

CDW (g/l)		
FadA knockout C14		
	Factors	**P-Value**
A	PhaC	0.2697
B	Acrylate	0.0229
	Interactions	**P-Value**
	AB	0.3943

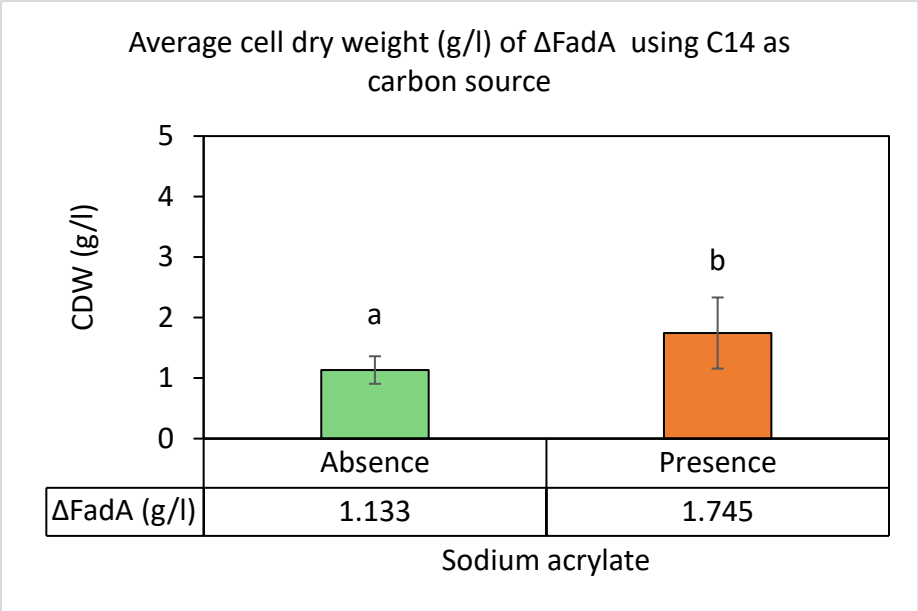

***Figure 35.** Comparison of CDW (g/l) accumulation (across all the recombinant cells with the 3 different PhaCs plus the control) in the absence and presence of sodium acrylate using fadA knockout as a strain and C14 as substrate. Bars with the same letter are statistically equal according to Tukey (P≤0.05). Data was taken from 3 parallel experiments.*

2.4 Discussion and future perspective.

The acid methanolysis method followed by GC is a widely used and reported method to identify and quantify polyhydroxyalkanoates of different monomer chain-lengths and the majority of methods reported so far focus mainly on the study of the short-chain-length PHB polymer. [289] In this work, we demonstrated that the conversion of PHB into C4 methyl esters through acid methanolysis is successful and that it accurately relates to the concentration values of the standard curve constructed using the commercial methyl-3-hydroxybutyrate.

Once the GC method was validated, in this chapter, 3 different PHA synthases (PhaCs) from *Pseudomonas stutzeri* 1317, *P. putida* KT2440 and *P. mendocina* NK-01 (named *PstzPhaC, PpuPhaC* and *PmePhaC* respectively) were compared using *E. coli* DH5α and Δ*fadA E.coli* K-12 BW25113 as hosts and using sodium dodecanoate (C12) and sodium tetradecanoate (C14) as substrates to produce polyhydroxyalkanoates. Furthermore, the impact of the β-oxidation inhibitor sodium acrylate on polyhydroxyalkanoate production was studied as well.

As mentioned before, PHAs with high (≥30%) C12 and/or C14 monomer composition have improved properties and the most straightforward method to obtain these lengths is feeding the cell with the related fatty acid. [150, 151] In *Escherichia coli* K-12, the uptake of long-chain-length fatty acids (LCFA) (C11 to C18) by the cell is mediated by the FadL protein [296, 297] while medium-chain length fatty acids (MCFA) can enter by simple diffusion (C7 to C10).[296] Once inside the cell, both, medium and long fatty acids require the activation of the fatty acid degradation (fad) regulon to be metabolised [249] . In this study, both substrates used are classified as MCFA (C12 and C14) which means that they both use the same transport system to enter the cell and the same pathway to be metabolized but , in spite of this, in our study, cells fed with tetradecanoate (C14) accumulate more biomass than those

fed with sodium dodecanoate (C12), in other words, *Escherichia coli* seems to metabolize in a more efficient manner the C14 fatty acid substrate than the C12 one. This observation seems true for both strains: DH5α and Δ*fadA* K-12.

Sodium dodecanoate and sodium tetradecanoate have never been, to the best of my knowledge, compared for biomass accumulation and PHA production in *Escherichia coli* before, but a study by Kim, Lee, Park, Kim and Lee [298] compared the effects of dodecanoic acid and tetradecanoic acid on the expression of biofilm-related genes, fimbria genes, motility genes and quorum-sensing genes and found out that both substrates repressed to some extent all the genes studied and that the repression was stronger in the presence of dodecanoic acid than in the presence of tetradecanoic acid.

Also, in regards of biomass accumulation, Δ*fadA* knockout accumulates less biomass than DH5α in the presence of either substrates C12 or C14. The main reason for this phenomenon might be the fact that the Δ*fadA*-K-12 has an incomplete β-oxidation pathway (3-β-ketoacyl-CoA thiolase (FadA) from this pathway [249] has been knocked out[260]) and therefore is incapable of transforming the fatty acid substrate to biomass. However, these 2 strains come from different parental strains [299] (parental strain for Δ*fadA* knockout is *E.coli* - K12 BW25113[260] while the parental strain for DH5α is DH1[300, 301]) and therefore there are other genomic differences between them that might also play a role in growth rate and total biomass accumulation. [299] In fact, we observed a higher growth rate in the Δ*fadA E.coli* K-12 strain than in DH5α when cultured in the absence of a fatty acid substrate with and without plasmid. (Refer to **Figure 27** to see these results) which is consistent with other studies describing different growth rates between *E. coli* strains [302, 303]

Interestingly, the addition of the β-oxidation pathway inhibitor sodium acrylate did not inhibit DH5α growth as originally expected and as observed in other studies . [253, 304] For example, CDW (g/l) was reduced from 2.2 to 1.5 in *R. eutropha* H16 when using 2.65 mM of acrylate. [253] while CDW (g/l) from A. *hydrophila* 4AK4 was reduced from 2.5 to 0.8 with 0.75

mM [305] The concentration for this study was 0.50 mg/ml or 5mM. Moreover, in the Δ*fadA*-K12 strain using C14 as substrate, there was a statistically significant increase in biomass accumulation which might indicate that sodium acrylates interact with the cell in other ways besides the inhibition of FadA enzyme, however more studies would need to be done to confirm this theory.

The *RFP* gene in pBBR1c was constructed and RFP expression was validated in a previous study. [286] It was communicated by the authors that the *phaC* genes in pBBR1c shared at the start of this study were constructed using the same techniques and believed to express PhaC. Whilst the engineered organism was shared, the constructed plasmid was deemed to be commercially sensitive, and the transfer agreement prevented sequence and expression analysis; thereby preventing further exploration of the genetically modified strains. It is likely that the plasmid construction was faulty, or the clones shared had accumulated mutations that prevented PhaC expression and subsequent PHA accumulation.

It is unlikely that the lack of PHA accumulation is due to the choice of *E. coli* as the chassis for this study because several studies have produced PHA in *E. coli*. For example, Lu, Zhang, Wu and Chen [138] managed to produce the co-polymer P(HB-co-HHx) (C4-co-C6) in a concentration range of in between 1.47 wt% and 15.94% using the recombinant strains *E. coli* JM109 *E. coli* DH5α and *E. coli* XL1-blue co-expressing the PhaC and (R)-enoyl-CoA hydratase gene (phaJ) from *Aeromonas caviae* and Acyl-CoA dehydrogenase gene (yafH) from *Escherichia coli*. In another study, Qi, Steinbüchel and Rehm [250] accumulated 2.8 wt% of PHA in the strain K-12 expressing the PhaC from *P. aeruginosa* and using decanoate as carbon source.

Having said that, the biomass accumulation in DH5α-pBBR1c-*PpuPhaC* is statistically higher than the control when using C14 as substrate and when using C12 with sodium acrylate , which may suggest that PHA could be present below detectable levels. It is

hypothesized that inside the control, there is an hyperaccumulation of β-oxidation intermediate metabolites that lead to the overall repression of the β-oxidation pathway and cell death through several mechanisms such as cell disruption [306] while in the presence of the PpuPhaC these metabolites are channelled into PHA production and therefore there is less toxicity inside the cell that results in more biomass production. More studies are needed to test this hypothesis.

In future, work should focus on strategies to optimize PHA production inside *Escherichia coli* with high hydroxydodecanoate and high hydroxytetradecanoate above the limits of detection for the proper study of this polymer and the enzymes related to it. One way of achieving this is to optimize the heterologous expression of PhaC inside *Escherichia coli.* Factors that influence heterologous expression of proteins include: the specific strain used, the promoter, the plasmid copy number, codon usage, temperature, growth conditions/media, provision of cofactors, specific mutations etc. [307]

CHAPTER 3

PhaC evaluation

Comparison of different PhaCs from *Pseudomonas* using a different plasmid backbone to produce PHA with high hydroxytetradecanoate (HTD) monomer composition

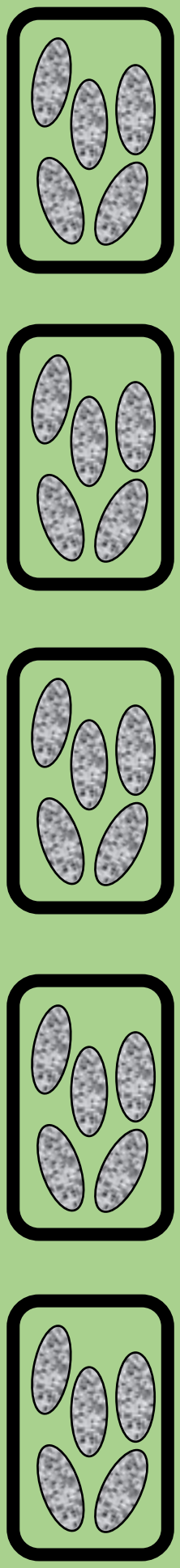

CHAPTER 3: PhaC EVALUATION. Comparison of different PhaCs using a different plasmid to produce PHA with high hydroxytetradecanoate monomer composition.

3.1 Introduction

As mentioned before in this work, polyhydroxyalkanoates (PHAs) are biopolymers that, due to their biodegradability and biocompatibility, could potentially substitute petroleum-based plastic. [43] Medium-chain-length PHAs (mcl-PHA) are a type of PHAs that contain in between 6 and 14 carbons (≥C6, ≤C14). [44-46] and that are less crystalline, more elastic and more flexible than the commercial 4C polyhydroxybutyrate . [85] [69]

The main objective of this thesis was to produce a new mcl-PHA polymer with high hydroxytetradecanoate (C14) and/or hydroxydodecanoate (C12) monomer composition. With this objective in mind, in the previous chapter (**Chapter 2**) we compared 3 different PhaCs in the presence of sodium tetradecanoate and sodium dodecanoate to produce the desired PHA polymer. Unfortunately, GC-FID results showed no defined peak that could indicate with certainty the presence of the target mcl-PHA. In **Chapter 2** also, all 3 PhaCs were expressed in the plasmid pBBR1c derived from the work of Johnson, Gonzalez-Villanueva, Tee and Wong [286] and Gruber, Hagen, Schwab and Koefinger [308] . This vector has a broad-host-range origin of replication and has been validated by both authors for efficient gene expression in *Ralstonia eutropha* H16.

Escherichia coli is probably the most studied microorganism there has ever been. It is easy to grow and easy to genetically modified.[309] It has also been used extensively for heterologous expression of enzymes and it has proven to be a good host for PHA production at laboratory and large scale. [310] One of the several strategies to increase heterologous

protein expression in *E. coli* and ,as a consequence, to increase the accumulation of mcl-PHA inside the cell is to codon-optimize the gene sequences for this specific host.[311, 312] Therefore for this **Chapter 3** it was decided to codon optimize the sequences and to re-do the cloning in a new cloning vector for protein expression of , once again, 3 PhaCs from different *Pseudomonas* strains: *P. stutzeri* 1317, *P. putida* KT2440 and *P. mendocina* NK-01 (named *PstzPhaC*, *PpuPhaC* and *PmePhaC* respectively) to produce mcl-PHAs.

Both plasmids pBAD and pBBR1c contain the PBAD promoter of the araBAD (arabinose) operon, and its regulatory element AraC. Therefore, recombinant protein expression is induced in the presence of arabinose in both cases. [313, 314] pBAD is a well-studied strong promoter that increases 300- fold the expression of genes above the basal state in *Escherichia coli.* [314-317] A representation of both plasmids is presented in **Figure 36**.

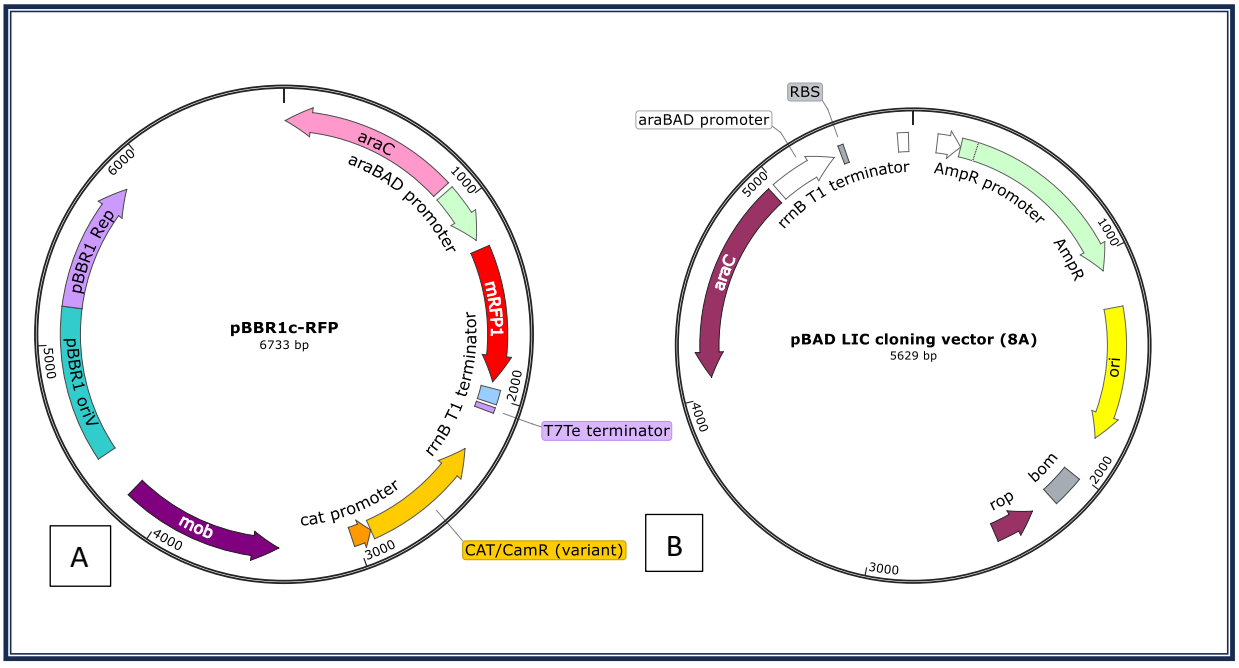

Figure 36. *Plasmids used for this thesis project where A) pBBR1c is a broad-range-host vector used for* ***Chapter 2*** *and B) pBAD is an E. coli vector used for* ***Chapter 3****.*

Aditionally, it was also decided to focus on the study of PHA with high hydroxytetradecanoate (C14) monomer composition and use sodium tetradecanoate as a sole substrate for this chapter. This decision was made from the evidence from **Chapter 2** indicating that tetradecanoate (C14) can be better metabolized (more biomass accumulation) by the cell than dodecanoate (C12).

3.2 Materials and Methods

3.2.1. Materials

List of detailed information on the materials used (reagents, kits, equipment, software, media preparation and miscellaneous) can be found in **Appendix 1-5.** Strains, plasmids, and primers are shown in **Table 21.**

Table 21. Strains and plasmids used for this study.

Strains	**Relevant genotype**	**Source or reference**
Escherichia coli DH5α	F-, Δ(argF-lac)169, ϕ80dlacZ58(M15), ΔphoA8, glnX44(AS), λ-, deoR481, rfbC1?, gyrA96(NalR), recA1, endA1, thiE1, hsdR17	Thermofisher 18265017
Escherichia coli K-12 Δ*fadA*	F-, *Δ(araD-araB)567*, *ΔlacZ4787*(::rrnB-3), λ^-, *rph-1*, *Δ(rhaD-rhaB)568*, *hsdR514, ⊿fadA, Kan^R*	[260]
Plasmids		
pBAD-*PmePhaC*	P_{BAD} promoter, *phaC* from *P. mendocina*, Amp^R	This study
pBAD-*PstzPhaC*	P_{BAD} promoter, *phaC* from *P. stutzeri*, Amp^R	This study
pBAD-*PpuPhaC*	P_{BAD} promoter, *phaC* from *P. putida*, Amp^R	This study
Primers		
pBAD forward and reverse	ATGCCATAGCATTTTTATCC GATTTAATCTGTATCAGG	

Abbreviations: Amp^R, ampicillin resistance ; Kan^R, kanamycin resistance

3.2.2. Plasmid construction, bacteria transformation, and clone check.

All plasmids were derived from the commercial pBAD LIC cloning vector (pBAD LIC cloning vector (8A) was a gift from Scott Gradia (Addgene plasmid # 37501)) which contains the inducible P_{BAD} promoter and ampicillin resistance gene. Three synthetic genes that code for polyhydroxyalkanoate synthase (PhaC) from *Pseudomonas stutzeri* 1317, *P. putida* KT2440 and *P. mendocina* NK-01 respectively were purchased from Integrated DNA technologies (Iowa, United States). Synthetic genes were delivered inside the pUC19 plasmid.

Digestion of plasmids and genes was done using EcoRV-HF (New Englands Biolabs) and BamHI-HF (New Englands Biolabs) to then re-circularized using T4 ligase (New Englands Biolabs). (**Figure 37**)

Each of the three plasmids constructed was used to transform *E. coli* DH5α using the standard $CaCl_2$ and heat shock method [318] and plated on TYE agar (10 g/L tryptone, 5 g/L yeast extract, 8 g/L NaCl, 15 g/L agar) supplemented with 100 µg/mL of ampicillin for clone selection, and incubated overnight at 37 °C.

Subsequently, clones were confirmed using colony PCR: one colony was suspended in 25 µl of distilled water and heated to 98 °C for 10 min, then centrifuged at 4,000 g for 5 min. 3 µl of the supernatant was used as DNA template for PCR reaction. Commercial default Addgene pBAD primers (shown in **Table 21**) were used.

Clones were stored at -80°C in 25% v/v glycerol.

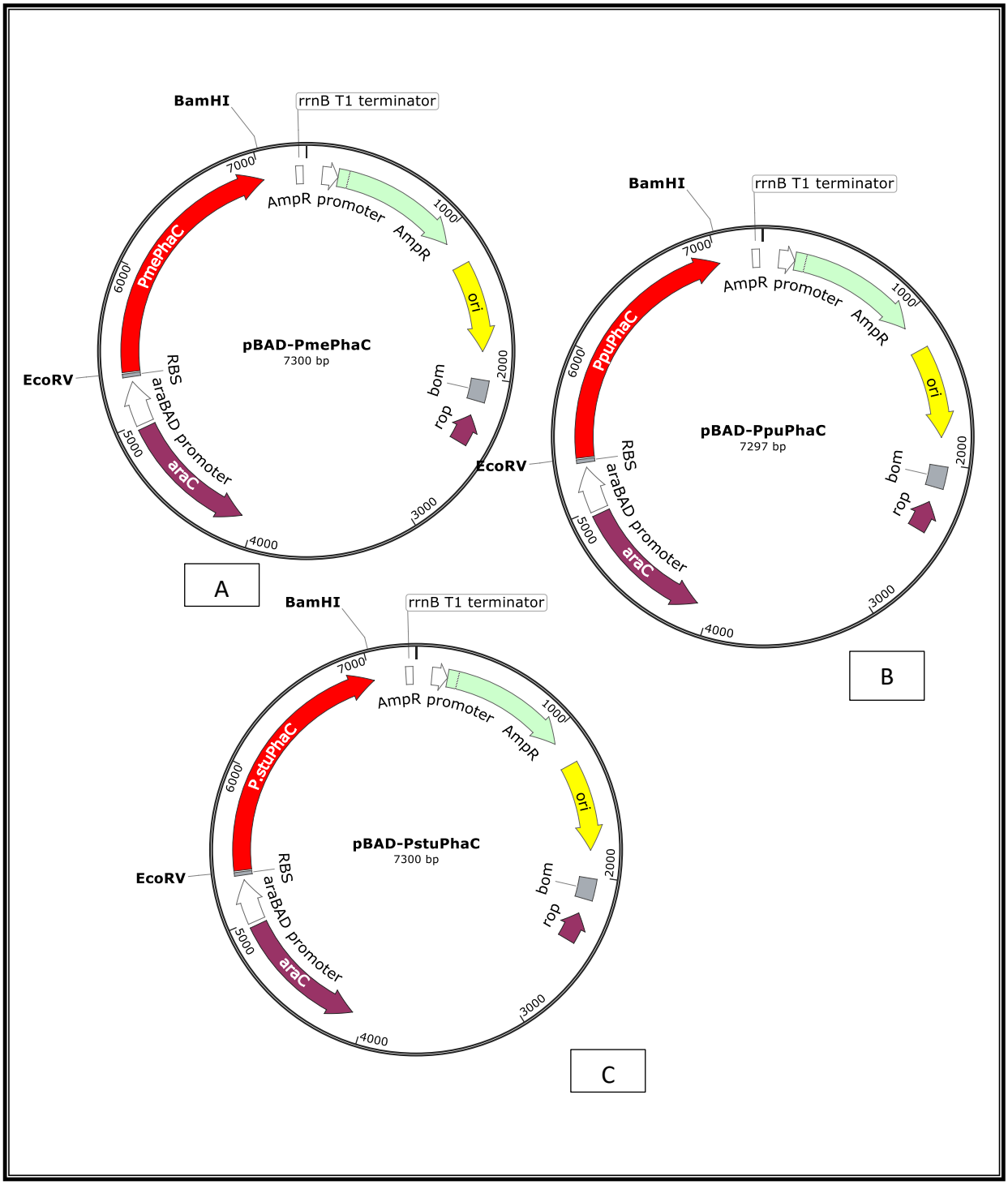

Figure 37. *Plasmids constructed in* ***Chapter 3*** *where the PhaC from 3 different Pseudomonas are expressed in the backbone pBAD. A)pBAD-PmePhaC, B) pBAD-PpuPhaC, C) pBAD-PstzPhaC. The promoter is inducible with arabinose.*

3.2.3. Proteomic profile of transformants in *Escherichia coli* .

With the purpose of knowing whether the 3 PhaC enzymes were being expressed inside *Escherichia coli* DH5α a proteomic profile was built for each one of them using the following procedure: firstly, 5 ml overnight cultures of the recombinant *E. coli* were grown plus a control with no plasmid. The cultures were induced with a final concentration of arabinose 0.2% w/v at the time of inoculation. The next morning cells were centrifuged (8000 rpm, 10 min) and resuspended in 1 ml of PBS buffer (phosphate buffered saline) (137 mM NaCl, 2.7 mM KCl, 8 mM Na2HPO4, and 2 mM KH2PO4) and 200 µl of zirconium beads. The tube was vortexed at maximum speed for 1 min and incubated on ice for 1 min. This process was repeated 5 times to lyse the cells. Samples were centrifuged at (17, 000 g, 3 min) and the supernatant was used for protein quantification. Protein samples were diluted 1:100 and then were quantified using Folin's phenol method. [319] Once the protein had been quantified, equal volume of loading buffer was added to the sample, and it was heated at 95°C for 5 min for protein denaturalization. Samples were centrifuged and 5 µg of the protein was used for SDS-PAGE gel separation.[320] Protein bands on the gel were revealed using a modified silver staining protocol from Couto, Barber and Gaskell [321]

3.2.4. Sanger sequencing

All the newly constructed plasmids were sent for sequencing , using the Sanger sequencing[322] service from GENEWIZ Azenta, to verify the integrity of the *phaC* gene sequence .

3.2.5. Bacteria cultivation and PHA production

The six strains obtained from the transformation of *E. coli* DH5α and the Δ*fadA* knockout mutant of *E. coli* K-12 BW25113 with the newly constructed plasmids pBAD-*PmePhaC*, pBAD-*PstPhaC* and pBAD-*PpuPhaC* were used for PHA production. One colony of each transformant was grown in 5 ml of medium 2×YT (tryptone 16 g/l, yeast extract 10 g/l and NaCl 5 g/l) and ampicillin (100 µg/ml) overnight. Subsequently, optical density at 600 nm was measured and adjusted to ~8. Flasks with 50 ml of medium 2×YT and ampicillin (100 µg/ml) were inoculated with 1 ml of the correspondent overnight culture and left to grow (37℃, 200 rpm) in a shaker till OD600 reached ~0.3-0.5. At this point PHA production was induced by adding arabinose (0.2% (w/v)) and prewarmed substrate in 50% ethanol (final concentration 0.5% (w/v)).

For this work, sodium tetradecanoate was used as substrate. The culture was left to grow for 48 hours after induction. Biomass was collected by centrifugation (4700 rpm, 15 min) then washed with 10 ml of prewarmed ethanol (50℃) (centrifuged 8000 rpm, 10 min) to eliminate the residual substrate and then with 10 ml of distilled water (centrifuged 4700 rpm, 15 min). After this, biomass was left to oven-dry overnight at 50℃.

The cultivation of these 6 strains under these conditions was done 3 times in total in 3 different batches and a control with no plasmid was also added to the set.

3.2.6. Gas chromatography analysis

Dry biomass was dissolved with 1 ml chloroform with 1 mg/ml benzoic acid (as internal standard). Then 1 ml of acidified methanol was added (15% (v/v) H_2SO_4) and the solution was vortexed and incubated at 100℃ for 3 hours. The sample was cooled on ice and 0.5 ml of ddH_2O was added. The solution was vortexed and then allowed to sit at room temperature to allow phases to separate. The organic phase (bottom layer) was used for measurement in the GC equipment.

3.2.7. Statistical analysis

All the statistical analysis was calculated with 95% confidence level using the software STATGRAPHICS Centurion XV.11[290] using at least 3 replicates of completely different cultivations. The Tukey HSD test was used to evaluate the honest significant difference between cultivations. Homogeneity of variances was confirmed in each case using the Bartlett's test.

One-way analysis of variance (ANOVA) and Multifactor ANOVA were also performed where necessary.

3.3 Results

3.3.1. Plasmid construction, bacteria transformation, and clone check.

For this **Chapter 3**, a new backbone using the same pBAD inducible promoter was built to test our *phaC* genes again. Unlike **Chapter 2**, for this **Chapter 3** the plasmid was built in our laboratory and the gene sequences were codon optimized for expression in *Escherichia coli* K-12. This time the integrity of the sequence was also confirmed using Sanger sequencing.

With the purpose of testing the restriction enzymes, the pBAD cloning vector went through single digestion with BamHI-HF and EcoRV-HF and then through double digestion with these same enzymes, which resulted in the successful linearization of the fragment and the observation of one single band of 5,629 bp. (**Figure 38** lanes **1,2,3,4** and **5**) The double digested fragment was extracted from the gel for subsequent ligation.

Similarly, the 3 synthetic genes were separated from their commercial backbone (pUC19) by digestion using EcoRV-HF and BamHI-HF and produced 2 fragments of different sizes: The fragment equal to 1, 695 bp corresponds to the *phaC* and the 2,686 bp corresponds to the plasmid backbone in which the synthetic gene was delivered. The 1, 695 bp *phaC* fragment was extracted from the agarose gel for subsequent cloning. (**Figure 39**, lanes **6,7,8,9,10** and **11**).

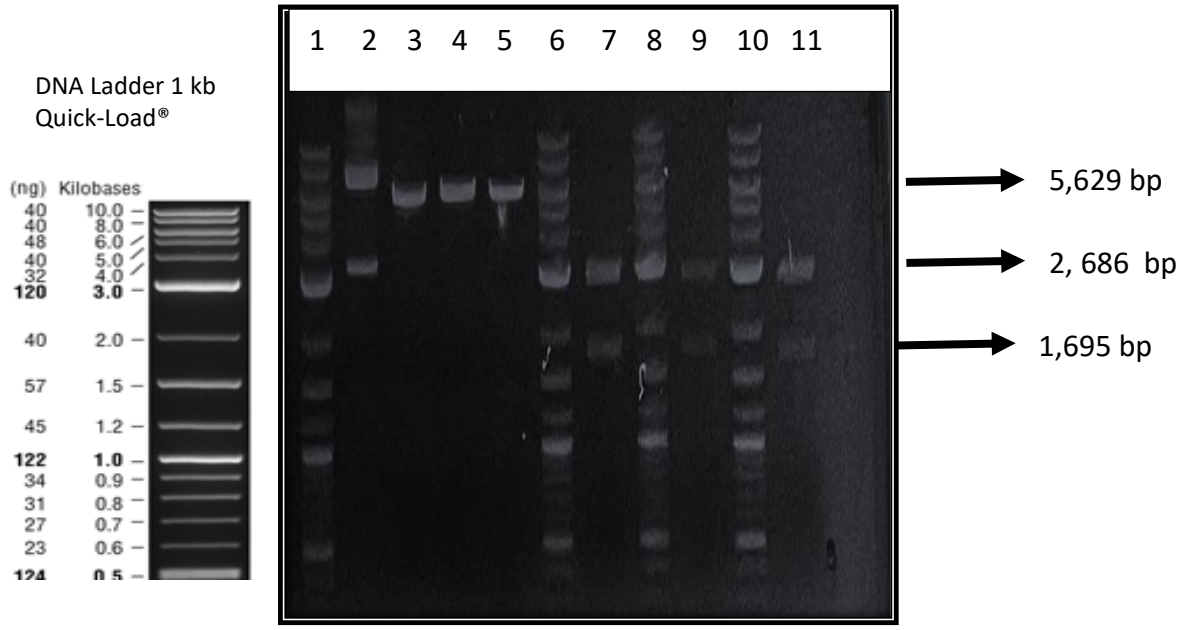

***Figure 38**. Electrophoresis gel of the digestion of the cloning vector pBAD and of the synthetic genes PmePhaC, PstzPhaC and PpuPhaC using EcoRV and BamHI enzymes. The figure lanes show the following:*
***1)** ladder, **2)** Undigested plasmid pBAD, **3)** pBAD digested with BamHI, **4)** pBAD digested with EcoRV **5)** pBAD double digested, **6)** ladder, **7)** backbone and PmePhaC fragments, **8)** ladder, **9)** backbone and PstzPhaC, **10)** ladder, **11)** backbone and PpuPhaC fragment.*

Ligation was performed using T4 ligase for the 3 PhaCs and the pBAD backbone and ligation product was successfully transformed into *Escherichia coli* DH5α and shown in **Figure 39.** The number of colonies obtained per transformant are also indicated. pBAD conferred the cells resistance to ampicillin (100 μg/ml) which was used for selection in the plates.

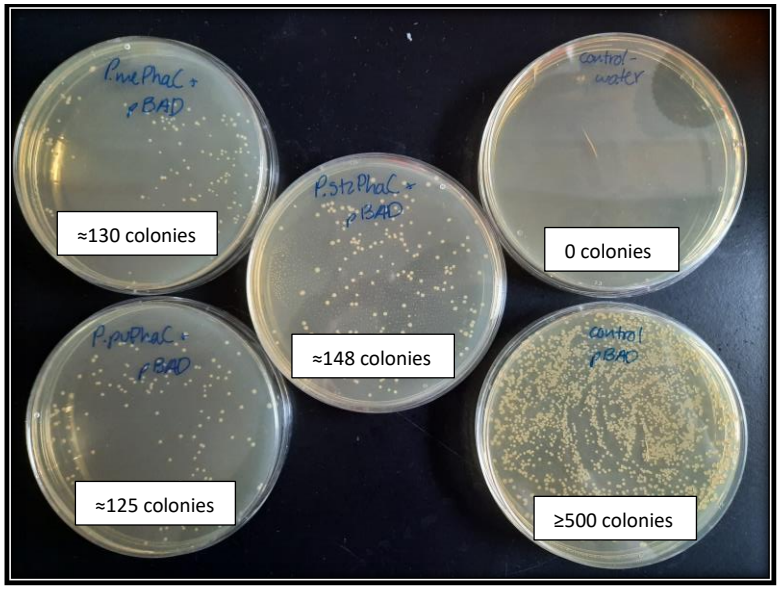

Figure 39. *Transformation of Escherichia coli DH5a with the ligation products pBAD-PmePhaC, pBAD-PstzPhaC and pBAD-PpuPhaC. Intact cloning vector pBAD was used as positive control whereas distilled water was used as negative control. The number of colonies is shown.*

To confirm that the fragment of interest (PhaC) was indeed cloned inside the pBAD vector, clone check was done for 2-3 colonies of each of the 3 PhaCs cloned (Colonies shown in **Figure 39**) using colony PCR. Positive colonies were expected to produce a 1886 bp-long PCR product using the pre-designed pBAD forward and reverse primers.(**Table 21**). Results showed that at least 1 out of the 2 colonies checked for each PhaC was indeed a clone (50% success) (**Figure 40 lanes 1 -8**) .

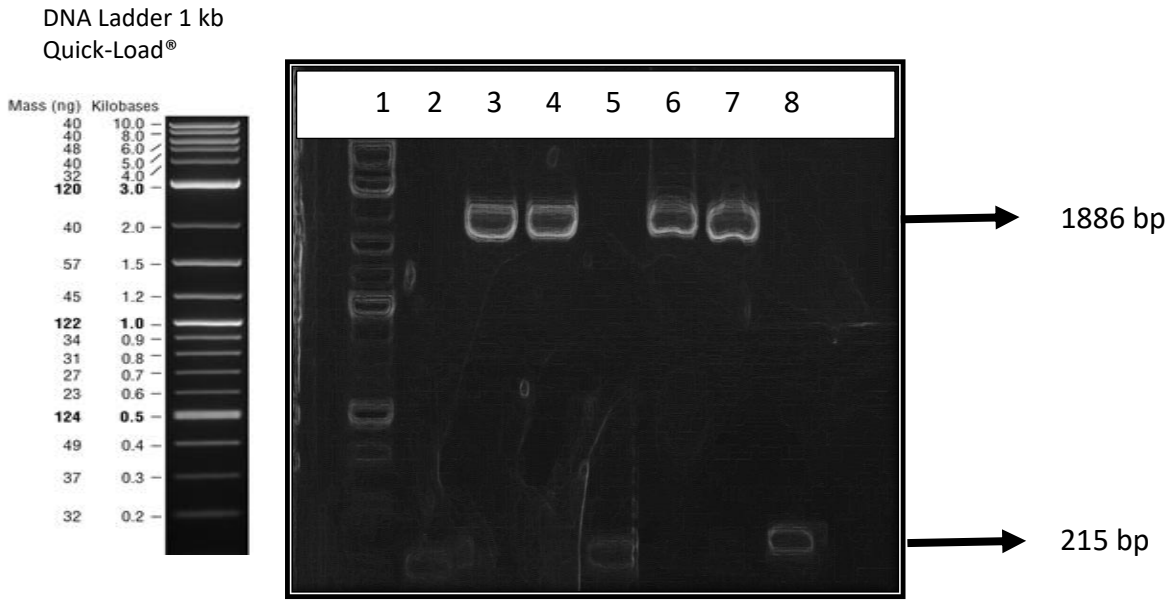

Figure 40. *Clone check using colony PCR and electrophoresis for the cloning of PmePhaC, PstzPhaC and PpuPhaC inside pBAD cloning vector. 2 colonies were screened for each PhaC used. Positive clones present a 1886 bp PCR product whereas negative colonies present a 200 bp product. The figure shows in lane* ***1)*** *Ladder****, 2)*** *pBAD-PmePhaC colony 1 → negative,* ***3)*** *pBAD-PmePhaC colony 2 → positive,* ***4)*** *pBAD-PstzPhaC colony 1 → positive,* ***5)*** *pBAD-PstzPhaC colony 2 → negative,* ***6)*** *pBAD-PpuPhaC colony 1 → positive,* ***7)*** *pBAD-PpuPhaC colony 2 → positive,* ***8)*** *pBAD-control negative.*

Sanger sequence results of the newly constructed plasmids show 100% match with the original sequence for all 3 *phaC* cloned genes. Therefore, there are no polymorphisms in the sequences. For the reaction, pBAD forward and reverse primers were used.

3.3.2. Proteomic profile of *Escherichia coli's* transformants.

The proteomic profiles of recombinant *E. coli* DH5α harbouring the constructed plasmids: pBAD-*PmePhaC*, pBAD-*PstzPhaC* and pBAD-*PpuPhaC* respectively were built and showed in **Figure 41**. PhaC protein is ≈ 62.8 kD. SDS-PAGE shows no clear band with this size in any of the recombinant strains.

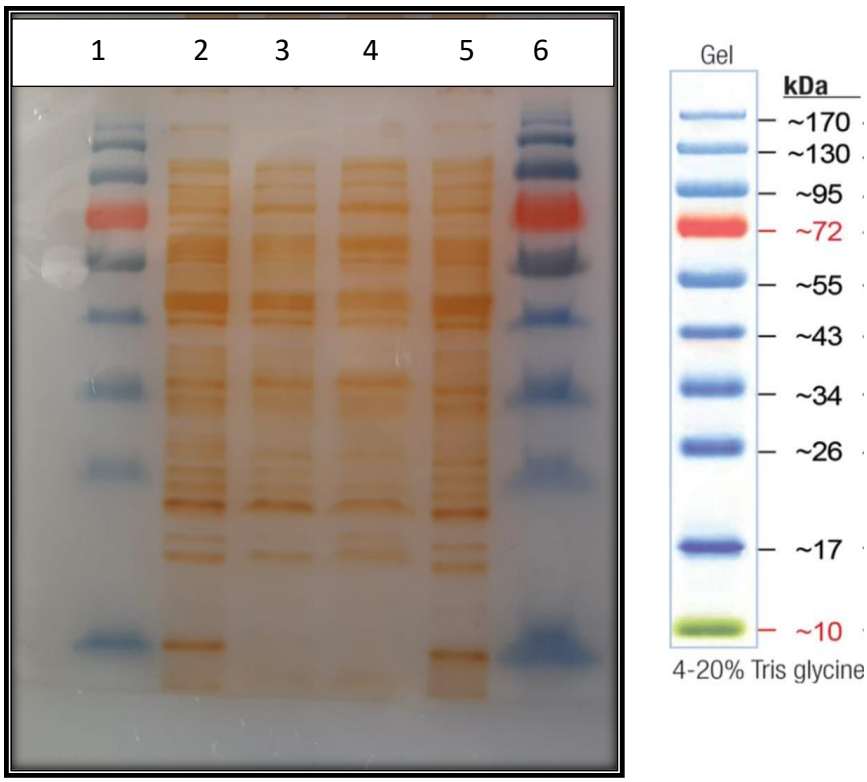

***Figure 41**. Proteomic profile of recombinant Escherichia coli where lane **1)** is the ladder, **2)** is E. coli expressing pBAD-PmePhaC, **3)** pBAD-PstzPhaC**, 4)** pBAD-PpuPhaC, **5)** control and **6**) ladder.*

3.3.3. Bacteria cultivation, PHA production and Gas chromatography analysis.

Dry biomass from the cultivation of recombinant *Escherichia coli* DH5α and from the *E. coli*-K12 *fadA* knockout expressing the plasmids pBAD-*PmePhaC*, pBAD-*PstzPhaC* and pBAD-*PuPhaC* and in the presence of sodium tetradecanoate (C14) as substrate were weighted and compared statistically according to Tukey (P≤0.05) and presented in **Table 22** and **Figure 42 A** and **B.**

Results show no statistically significant difference between the biomass weight of any of the cultures grown in this chapter.

All the biomass was digested and analysed using GC-FID but there was no PHA found in detectable levels. (**Table 22**)

Table 22. Comparison of different PhaCs using sodium tetradecanoate as substrate. Cultures were incubated 37℃, 200 rpm for 48 hours after arabinose induction (0.2% (w/v)).

Host	PhaC source	Substrate 0.5% (w/v)	CDW (g/l)	wt%
DH5α	*P. putida*	C14	1.930± 0.235 a	Non-detectable levels
	P. stutzeri	C14	1.756± 0.363 **a**	Non-detectable levels
	P. mendocina	C14	1.389± 0.317 **a**	Non-detectable levels
	control	C14	1.435± 0.153 **a**	Non-detectable levels
***fadA* Knockout**	*P. putida*	C14	0.931± 0.164 **a**	Non-detectable levels
	P. stutzeri	C14	0.534± 0.038 **a**	Non-detectable levels
	P. mendocina	C14	0.596± 0.065 **a**	Non-detectable levels
	control	C14	0.678± 0.209 **a**	Non-detectable levels

Each culture was grown three times and the value presented is the mean ± the standard deviation. . Means with different letters are significantly different according to Tukey (P≤0.05). Abbreviation: CDW, cell dried weight; wt%, percentage of cell dried weight that corresponds to PHA analysed by GC. Experiments were done in triplicate.

E. coli DH5α

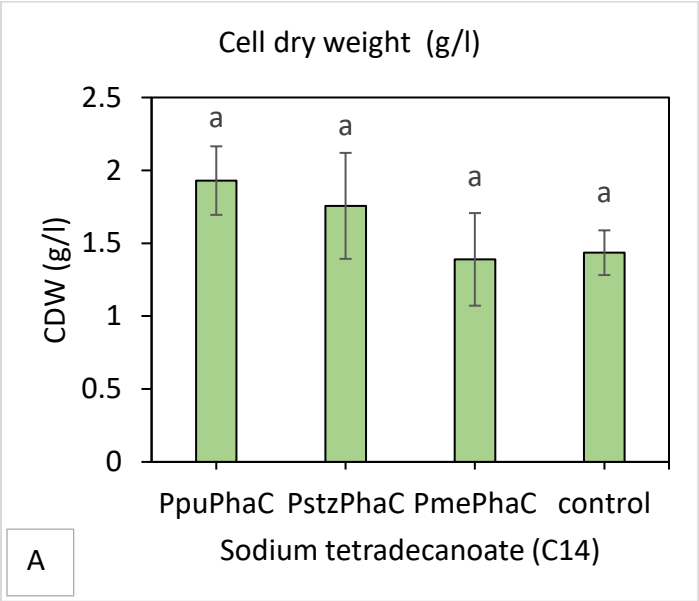

E. coli K-12 *fadA* knockout

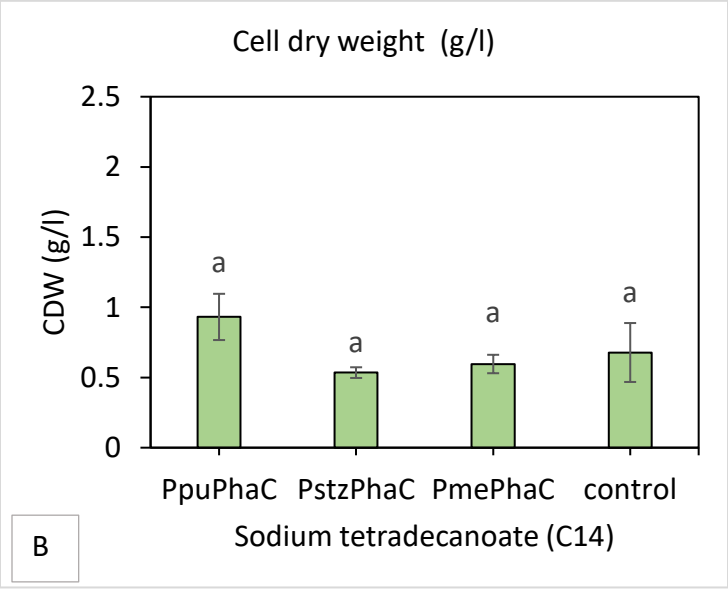

Figure 42. *Bars with the same letter are statistically equal according to Tukey (P≤0.05). A) shows the comparison of cell dry weight between E. coli DH5α transformed with different PhaCs from Pseudomonas B) Shows the comparison of cell dry weight between the knockout fadA. Data was collected from 3 parallel experiments.*

3.4 Discussion and future perspectives

The proteomic profile does not show a clear band on the protein of interest with respect to the control: It was expected to find a clear band with the weight of 62.8 KDa for *P. mendocina* (*PmePhaC*), 62.8 kDa for *P. stutzeri* (PstzPhaC) and 62.25 KDa for *P. putida* (PpuPhaC). However, this was not the case for this work. This result is contrary to the findings of Venkateswar Reddy, Mawatari, Onodera, Nakamura, Yajima and Chang [323] who found a clear band in between the 55 and 69 kDa marker when analyzing crude protein extract of *Pseudomonas palleroni* through SDS-PAGE. On the other hand, the same band was not clearly visible when the same authors analyzed the protein crude extract of *Pseudomonas pseudoflava* (Both strains were grown with the purpose of treating wastewaters using the same conditions). They also made an interesting correlation between a weaker SDS-PAGE band and less enzyme activity and less PHA accumulation inside the cell when comparing *P. palleroni* and *P. pseudoflava*. This information raises the hypothesis that , in this work, even though we have changed expression vector, there still might be an expression problem of all 3 proteins: PmePhaC, PstzPhaC and PpuPhaC.

Observation between the **Figure 42A** and **Figure 42B** makes evident that the biomass produced by DH5α is higher than the biomass produced by the *fadA* knockout, which is consistent with the results shown in **Chapter 2** where it was hypothesized that the substrate (sodium tetradecanoate C14) was not transformed into biomass in the *fadA* knockout because the β-oxidation pathway is incomplete and that this effect is not related to the accumulation of PHA or to the type of vector used. But, although this statement is still true for this **Chapter 3,** when comparing the total biomass accumulation of **Chapter 2** versus the biomass accumulation of **Chapter 3** for both strains, we see that the first one ranges from 2.48 to 3.99 g/l for DH5α and from 0.913 to 1.25 g/l for *fadA* whereas for this **Chapter 3** the ranges go from 1.389 to 1.930 g/l and from 0.534 to 0.931 respectively . And while, the evident decrease in biomass production in this chapter versus the previous one

might be attributed to the fact that a different vector was used, it is important to notice that, due to technical reasons, some culture conditions changed between experiments.

Another important observation is that , **in Chapter 2,** when statistically comparing PhaC activity, there is a higher statistical difference between the biomass of the *E. coli* DH5α culture expressing PpuPhaC in comparison with the cultures expressing the other 2 PhaCs (PmePhaC and PstzPhaC) using tetradecanoate as substrate, whereas in this **Chapter 3** the biomass produced when expressing PpuPhaC is numerically higher for both strains (DH5α and Δ*fadA*), using the same substrate, but it is not reflected statistically according to Tukey ($P \leq 0.05$). Which might indicate that this PhaC is more active than the other two when using a different vector.

Regarding PHA accumulation, even though for this **Chapter 3** the PhaC sequences were codon-optimized, and the sequences were checked using Sanger method, the newly constructed plasmid pBAD with the 3 different PhaC does not produce polyhydroxyalkanoates in a detectable level when using GC-FID analysis, which is the same finding in the previous chapter when using pBBR1c backbone for the expression of genes.

In future, efforts should continue to engineer *Escherichia coli* to achieve accumulation of the desired PHA above the limit of detection. Techniques to optimize protein expression in *Escherichia coli*, as mentioned before, include, plasmid copy number, promoter type, codon usage, temperature, origin of replication etc. [307, 324] Talking about PHA production specifically, engineering the β-oxidation metabolic pathway, in order to channel more intermediates of this route into PHA production, has proven to be effective in increasing the polymer concentration inside the cell in several organisms such as *Cupriavidus necator* [144], *P. putida* [146] and *Escherichia coli* [151] This approach will be applied in the subsequent chapters.

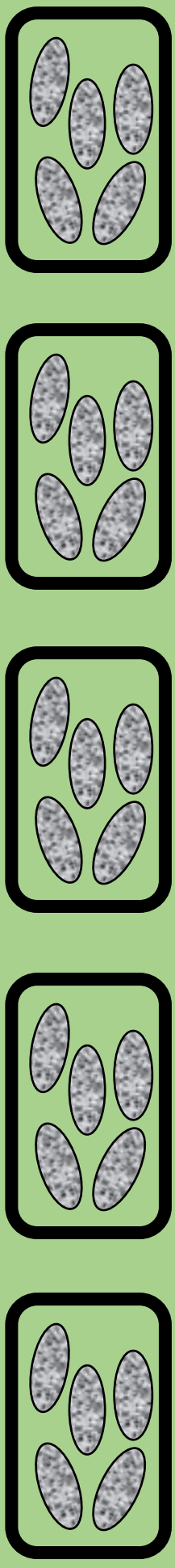

CHAPTER 4

FabG evaluation

Comparison of FabG from *Mycobacterium tuberculosis* and FabG from *Escherichia coli* K-12 to produce polyhydroxyalkanoates with high hydroxytetradecanoate monomer composition

CHAPTER 4 FabG EVALUATION. Comparison of FabG from *Mycobacterium tuberculosis* and FabG from *Escherichia coli* K-12 to produce polyhydroxyalkanoates with high hydroxydodecanoate and hydroxytetradecanoate monomer composition.

4.1. Introduction

(R)-3-hydroxyacyl-CoA is an intermediate metabolite of the β-oxidation pathway that can be channeled into the polymerization of medium chain length polyhydroxyalkanoates by the PhaC (PHA synthase) . This metabolite can be formed inside the cell using different enzymes from 3 different substrates from this pathway (refer to **Figure 43**) : 1) from 3-keto-acyl-CoA using FabG enzyme 2) from (S)-3-hydroxyacyl-CoA using an epimerase and 3) from trans-2-enoyl-CoA using PhaJ enzyme.[325] Additionally, the intermediate (R)-3-hydroxyacyl-ACP from the fatty acid biosynthesis pathway can also be also converted into (R)-3- hydroxyacyl-CoA and in turn channeled to mcl-PHA production through PhaG and Alkk.[326]

For this study, Δ*fadA* knockout *E. coli* was used as host and sodium tetradecanoate (sodium salt version of the fatty acid tetradecanoic acid) (C14) was used as β-oxidation substrate to produce mcl-PHA. As a consequence, there is expected to be a surplus of the intermediate metabolite 3-ketoacyl-CoA (C14) inside the cell and therefore it was decided to overexpress the ketoacyl-acyl carrier protein reductase, commonly referred to as FabG which is , as mentioned before, capable of transforming 3-ketoacyl-CoA into the mcl-PHA substrate (R) 3-hydroxyacyl-CoA. However, it is important to note that FabG was originally known to convert 3-ketoacyl-ACP to (R) -3- hydroxyacyl-ACP from the fatty acid biosynthesis pathway but was later observed to act over 3-ketoacyl-CoA as well. This means that

overexpression of FabG could have a double enhancing effect over PHA yield and composition for this work. (Also **Figure 43**). [152, 327-329]

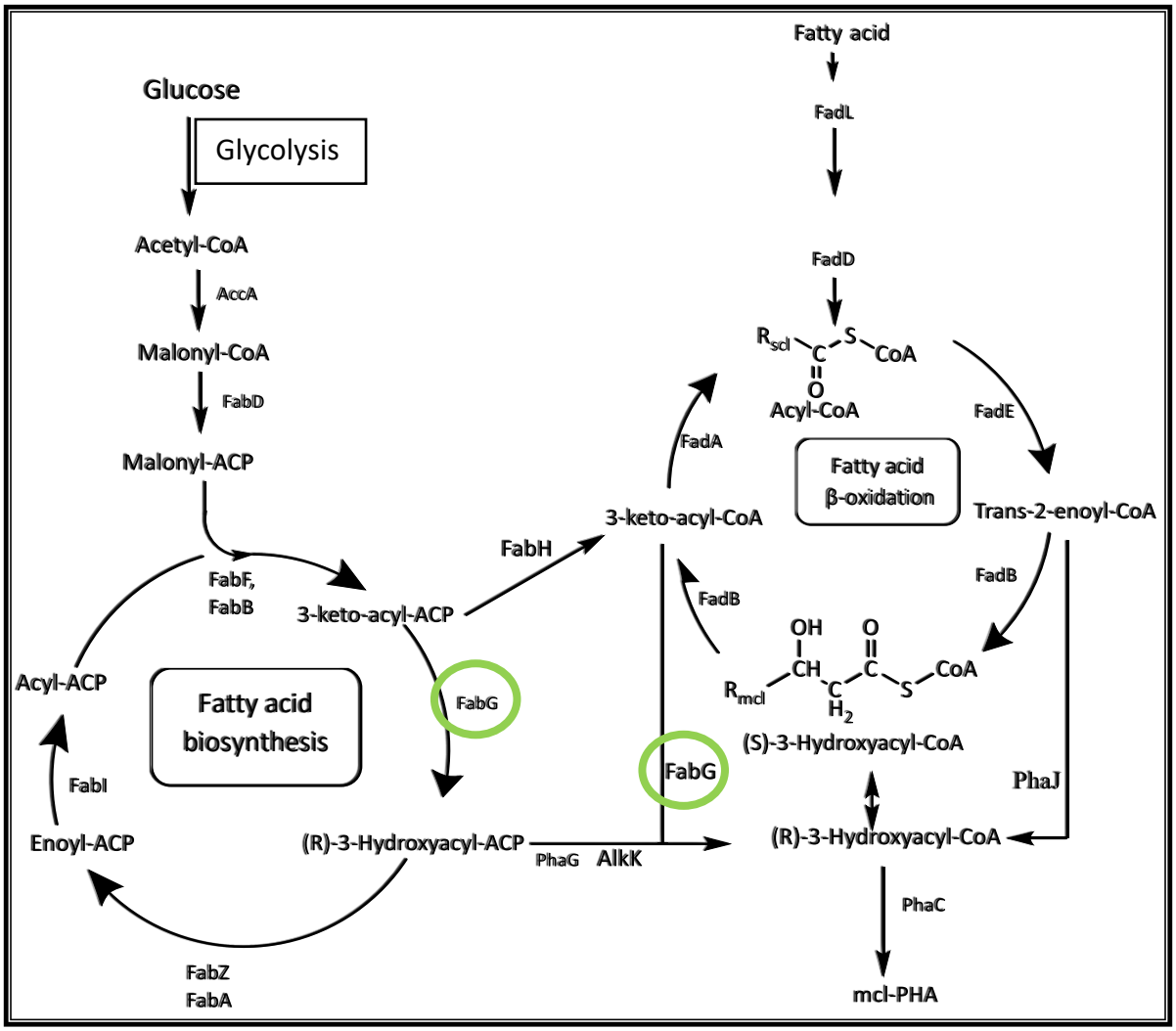

***Figure 43**. Pathways in which the fabG is involved for PHA production: Fatty acid biosynthesis pathway[326] and B-oxidation pathway [325]. fabG (ketoacyl-acyl carrier protein reductase) is circled in green. Diagram was modelled with ChemDraw.*

It is also important to remember that PHA yield and monomer composition are not only dependent on the availability of the substrate but also, among other things, on the specificity and activity (conversion rate) of the several enzymes involved in the conversion of the substrate (fatty acid) into the final product (PHA). [170, 305] For example, Nomura

Christopher, Taguchi, Gan, Kuwabara, Tanaka, Takase and Doi [330] observed that the FabG from *E. coli* JM109 has higher preference for C10-C12 substrates whereas FabG from *Pseudomonas* sp. 61-3 has a preference for C6, C8 fatty acids and that this difference in substrate specificities were reflected in the monomer composition of the polymer produced by recombinant *E. coli.* Consistently with this study, Park, Park and Lee [152] also compared FabGs from these 2 organisms (*E. coli* WA101 and *Pseudomonas aeruginosa* PAO1) for production of PHA with monomers of 10 carbons and also found higher accumulation of the monomer C10 when using EcolifabG.

Additionally, in another study, Yuan, Jia, Tian, Snell, Müh, Sinskey, Lambalot, Walsh and Stubbe [166] demonstrated that the affinity (K_m) of the PhaC changes depending on the substrate provided. High K_m means lower affinity and specificity which, in turn, affects the enzyme activity (conversion rate) and ultimately the yield of mcl-PHA.

In *Mycobacterium tuberculosis*, FabG was first identified by Banerjee, Sugantino, Sacchettini and Jacobs [331] in 1998 and was named MabA that stands for mycolic acid biosynthesis A. MabA then became a protein of medical interest as a target for the antituberculosis drugs isoniazid (INH) and ethionamide (ETH) [331-333] because ,by attacking MabA, this drugs interfere with the fatty-acid elongation system called FAS-II that synthesize mycolic acid [334, 335] which are very long-chain fatty acids (in between 60 and 90 carbons) that play a vital role in the architecture and permeability of the cell envelope in the genus Mycobacterium [332, 336], thus, killing the cell.

In this study, a completely new application for MabA(FabG1) is proposed . Given the fact that MabA is believed to have specificity for long chain fatty acids, the use of this enzyme to produce PHAs with high (≥30%) hydroxytetradecanoate (C14) monomer composition in recombinant *E. coli* is investigated in this chapter. Therefore, in this study, for the first time, this enzyme was co- expressed with 3 different PhaCs from *Pseudomonas*

and cultivated in the presence of sodium tetradecanoate as β-oxidation pathways substrate. FabG from *E. coli* was also cloned and coexpressed with the same 3 PhaCs.

4.2. Materials and Methods

4.2.1. Materials

List of detailed information on the materials used (reagents, kits, equipment, software, media preparation and miscellaneous) can be found in **Appendix 1-5.** Strains, plasmids and primers are shown in **Table 23.**

Table 23. *Lists of strains and plasmids used for this* ***Chapter 5****.*

Strains	Relevant genotype	Source or reference
DH5α	F-, Δ(argF-lac)169, ϕ80dlacZ58(M15), ΔphoA8, glnX44(AS), λ-, deoR481, rfbC1?, gyrA96(NalR), recA1, endA1, thiE1, hsdR17	Thermofisher
Δ*fadA*- *E. coli* K-12	F-, *Δ(araD-araB)567*, *ΔlacZ4787*(::rrnB-3), *λ*$^{-}$, *rph-1*, *Δ(rhaD-rhaB)568*, *hsdR514, ΔfadA, Kan*^{R}	[260]
Plasmids		
pBAD-*PmePhaC-EcolifabG*	P_{BAD} promoter, *phaC* from *P. mendocina*, *fabG* from *E. coli* K-12 Amp^{R}	This study
pBAD-*PstzPhaC-EcolifabG*	P_{BAD} promoter, *phaC* from *P. stutzeri*, *fabG* from *E. coli* K-12 Amp^{R}	This study
pBAD-*PpuPhaC-EcolifabG*	P_{BAD} promoter, *phaC* from *P. putida*, *fabG* from *E. coli* Amp^{R}	This study
pBAD-*PmePhaC-MtubfabG*	P_{BAD} promoter, *phaC* from *P. mendocina*, *fabG* from *M. tuberculosis* Amp^{R}	This study
pBAD-*PstzPhaC-MtubfabG*	P_{BAD} promoter, *phaC* from *P. stutzeri*, *fabG* from *M. tuberculosis* Amp^{R}	This study

pBAD-*PpuPhaC-MtubfabG*	P_{BAD} promoter, *phaC* from *P. putida*, *fabG* from *M. tuberculosis* Amp^R	This study
Primers		
pBAD forward	ATGCCATAGCATTTTTATCC	
reverse	GATTTAATCTGTATCAGG	
To add SacI site for,	AAAACAGCCAAGGGATC	
reverse	TATAGAGCTCGGATGAGAGAAGATTTTCAG	
To amplify *EcolifabG* forward	ATATACGGATCCTTTGTTTAACTTTAAGAAGGAG ATAG	
reverse	TATATATGAGCTCTCAGACCATGTAC	

Plasmids used in this chapter were induced with arabinose 0.2% (w/v). *Escherichia coli* is naturally capable of metabolising arabinose [261] however *Escherichia coli*-K12 has those genes deleted. DH5α strain was only used for cloning purposes in this chapter.

4.2.2. *fabG* gene selection

Mcl-PHA producing *Pseudomonas* studied in **Chapter 3** were also used for *in silico* analysis in this **Chapter 4.** *fabG* sequences of 7 of those strains were chosen for sequence alignment and phylogenetic tree construction. The enzymes belong to *Pseudomonas putida* KT2440, *Pseudomonas mendocina* NK-01, *Pseudomonas entomophila* L48, *P. mediterranea* DSM 16733, *P. corrugate*, *P. chlororaphis* qlu-1 and *P. oleovorans.* Similarly, the *fabG* sequence from *C. necator* H16 was also used in this chapter.

Additionally , it was decided that *fabG* from *Escherichia coli* was also going to be studied *in silico* and cloned and tested *in vivo* because, as mentioned earlier, Nomura Christopher, Taguchi, Gan, Kuwabara, Tanaka, Takase and Doi [330] observed that the FabG from *E. coli* has higher preference for C10-C12 substrates whereas FabG from *Pseudomonas* sp. 61-3 has a preference for C6, C8 fatty acids and that this difference in substrate

specificities were reflected in the monomer composition of the polymer produced by recombinant *E. coli.*

fabG from *Mycobacterium tuberculosis* was also chosen because, although it has never been used before for PHA production, literature shows that it is involved in long-chain fatty acid biosynthesis[332] and we hypothesize that it could provide PhaC with precursors to produce longer mcl-PHAs.

4.2.3. Nucleotide sequence accession numbers

The *fabG* (oxoacyl reductase) sequence from *Mycobacterium tuberculosis* H37rv was taken from the database KEGG: Kyoto Encyclopedia of Genes and Genomes [284] using the entry Rv1483 while *fabG* from *Cupriavidus necator* H16 was taken from The National Center for Biotechnology Information (NCBI) using the accession number QCC01434.1. As for the *Escherichia coli* K-12 BW25113 FabG enzyme, the full bacteria genome was downloaded using Snapgene with the accession number NZ_CP009273.1 from NCBI. The enzyme FabG can be found in the genome using the locus tag BW25113_1093.

From these 3 sequences, only *fabG* from *M. tuberculosis* (*MtubfabG*) was codon optimized using the bioinformatic Codon Optimization Tool from Integrated DNA Technologies and then purchased as synthetic genes using this same company while *fabG* from *Escherichia coli* (*EcolifabG*) was isolated directly from the bacteria for cloning.

The sequence of *fabG* from *C. necator* H16 was not used experimentally, only added to the alignment and phylogenetic tree as a benchmark given that this strain is of industrial importance to produce PHAs. [101]

4.2.1. FabG alignment and comparison of sequences.

The three FabG amino acid sequences mentioned before (from *M. tuberculosis*, *E. coli* K-12 and *C. necator* H16) were aligned and compared against each other using the software Jalview. [291] The alignment and coloring was done using Clustal OWS. [292] The coloring criteria was ≥ 75% identity threshold and ≥75% conservation threshold using the color code (ClustalX) [292] which is shown in **Figure 44.**

A phylogenetic tree was also constructed to investigate the evolutionary relationship between the 3 same FabG sequences. Sequences were compared using the neighbor joining method [3] and the BLOSUM62 alignment score matrix [9]

Category	Colour	Residue at position
Hydrophobic	BLUE	A,I,L,M,F,W,V
		C
Positive charge	RED	K,R
Negative charge	MAGENTA	E
		D
Polar	GREEN	N
		Q
		S,T
Cysteines	PINK	C
Glycines	ORANGE	G
Prolines	YELLOW	P
Aromatic	CYAN	H,Y
Unconserved	WHITE	any / gap

***Figure 44**. Clustal X colour scheme for amino acids.*

4.2.2. Insertion of the sacI restriction site in the pBAD vector.

pBAD plasmid has 2 restriction sites only in the multiple cloning site between the ribosome binding site and the terminator (EcoRV and BamHI) which were used to clone each of the 3 PhaCs from *Pseudomonas* as described in **Chapter 3**. Therefore, to clone and co-express any of the 2 *fabG* genes for this **Chapter 4** along with the already existent *phaC* gene **,** it was necessary to add an extra restriction site in each of the plasmids created in **Chapter 3**: pBAD-*PmePhaC*, pBAD-*PstzPhaC* and pBAD-*PpuPhaC*.

To add the chosen restriction site (SacI), the appropriate primers shown in **Table 23** were used to amplify the entire vector (7 300 bp fragment) through PCR.

4.2.3. Isolation of the *fabG* gene from *Escherichia coli* K-12

The *fabG* gene from *Escherichia coli- K12* was the only gene from this thesis that was not bought as a synthetic gene. Instead, it was isolated directly from the parental strain using colony PCR and *EcolifabG* primers from **Table 23**. Each colony was suspended in 25 µl of distilled water and heated at 98 °C for 10 min, then centrifuged at 4000 g for 5 min. The supernatant was used as the DNA template for PCR.

4.2.4. Plasmid construction, bacteria transformation, and clone check

All plasmids were derived from the commercial pBAD LIC cloning vector (pBAD LIC cloning vector (8A) was a gift from Scott Gradia (Addgene plasmid # 37501)) which contains the inducible P_{BAD} promoter and ampicillin resistance gene. In **Chapter 3**, 3 synthetic genes that code for polyhydroxyalkanoate synthase (PhaC) from *Pseudomonas stutzeri* 1317 (*PstzPhaC*), *P. putida* KT2440 (*PpuPhaC*) and *P. mendocina* NK-01 (*PmePhaC*) were cloned

independently into this vector. For **Chapter 4,** the isolated *fabG* gene from *E. coli (EcolifabG)* and the synthetic *fabG* gene from *M. tuberculosis (MtubfabG)* were independently added to the above plasmids to co-express both type of enzymes in all possible combinations. The resulting 6 new plasmids (pBAD-*PmePhaC-EcolifabG*, pBAD-*PmePhaC-MtubfabG*, pBAD-*PstzPhaC-EcolifabG*, pBAD-*PstzPhaC-MtubfabG*, pBAD-*PpuPhaC-EcolifabG*, pBAD-*PpuPhaC-MtubFabG*) are represented in **Figure 45.**

Digestion of plasmids and genes was done using BamHI-HF and sacI-HF (New England Biolabs) to then recirculate using T4 ligase (New England Biolabs).

Each of the 6 plasmids constructed was used to transform *E. coli* DH5α using the standard $CaCl_2$ and heat shock method [318] and plated on TYE agar (10 g/L tryptone, 5 g/L yeast extract, 8 g/L NaCl, 15 g/L agar) supplemented with 100 µg/mL of ampicillin for clone selection, and incubated overnight at 37 °C.

Subsequently, clones were confirmed using colony PCR: one colony was suspended in 25 µl of distilled water and heated to 98 °C for 10 min, then centrifuged at 4,000 g for 5 min. 3 µl of the supernatant was used as DNA template for PCR reaction. Commercial default Addgene pBAD primers (shown in **Table 23**) were used.

Clones were stored at -80°C in 25% v/v glycerol.

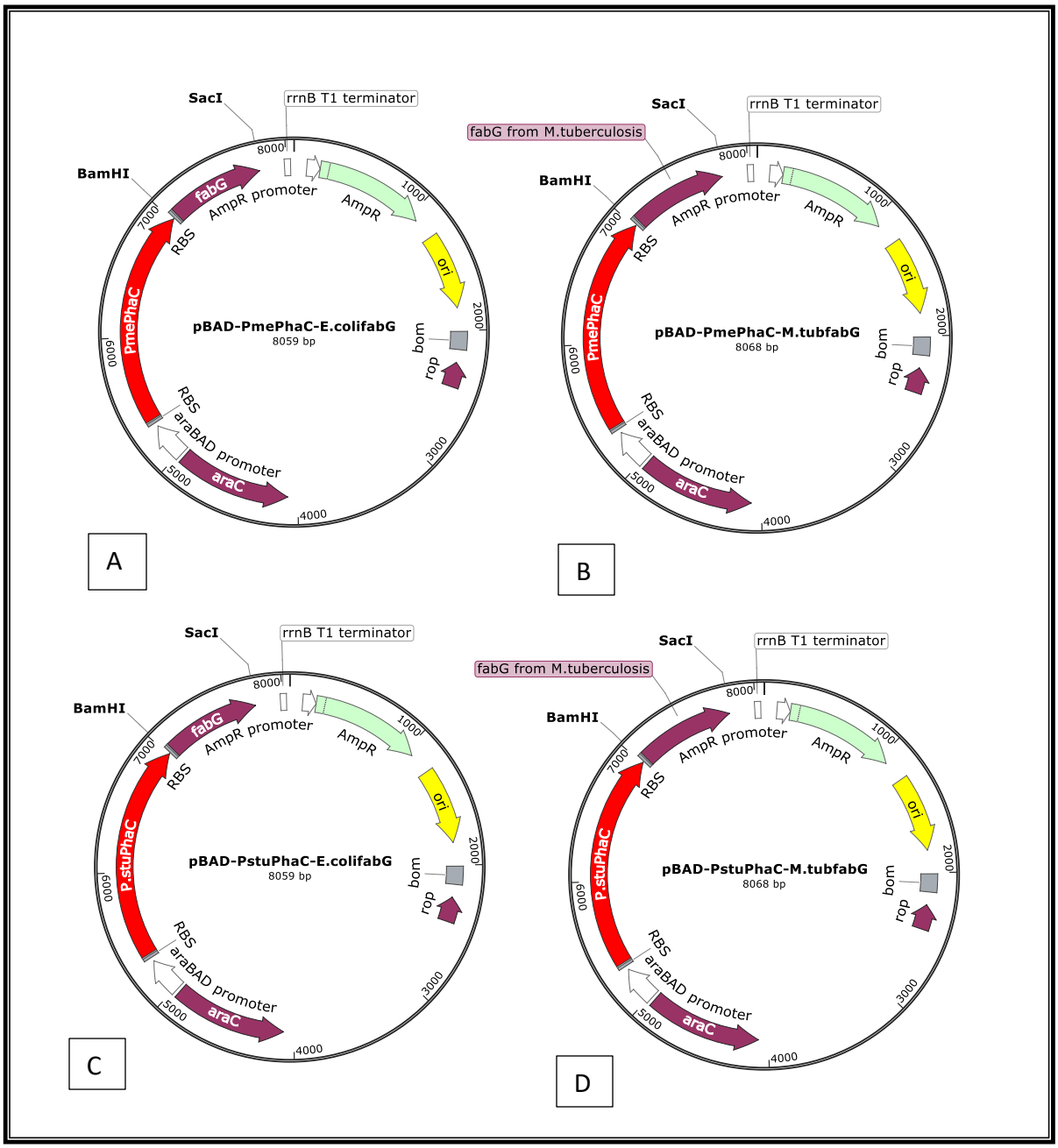
SacI
rrnB T1 terminator
BamHI
fabG
AmpR promoter
AmpR
ori
RBS
PmePhaC
pBAD-PmePhaC-E.colifabG
8059 bp
bom
rop
RBS
araBAD promoter
araC
A
fabG from M.tuberculosis
pBAD-PmePhaC-M.tubfabG
8068 bp
B
P.stuPhaC
pBAD-PstuPhaC-E.colifabG
C
pBAD-PstuPhaC-M.tubfabG
D

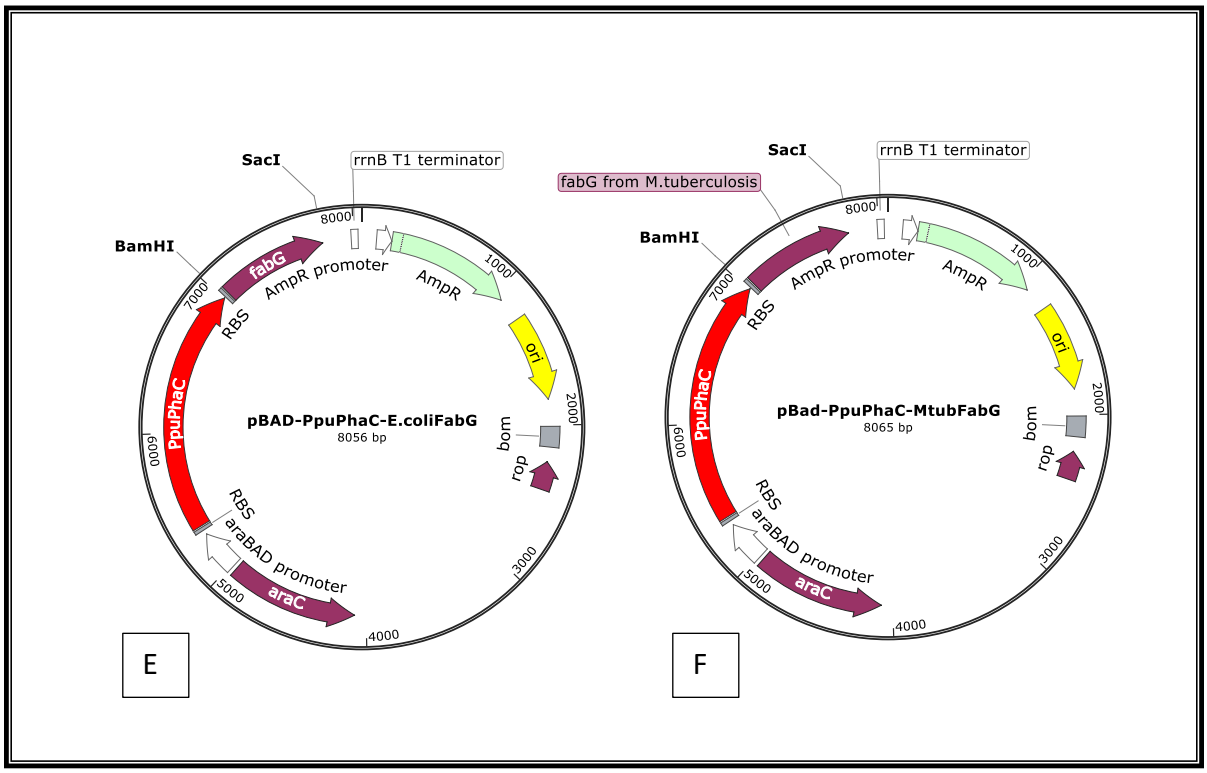

***Figure 45**. Plasmid maps. A) pBAD-PmePhaC-EcolifabG; B) pBAD-PmePhaC-MtubfabG; C)pBAD-PstzPhaC-EcolifabG D) pBAD-PstzPhaC-MtubfabG; E) pBAD-PpuPhaC-EcolifabG; F) pBAD-PpuPhaC-MtubFabG. Maps were built using SnapGene.*

4.2.1. Sanger sequence.

All the newly constructed plasmids were sent for sequencing , using the Sanger sequencing[322] service from GENEWIZ Azenta, to verify the integrity of the *fabG* gene sequences .

4.2.2. Bacteria cultivation and PHA production

The six strains obtained from the transformation of the Δ*fadA* knockout mutant of *E. coli* K-12 BW25113 with the newly constructed plasmids (Refer to **Figure 45**) were used to assess PHA production. Cultivation was done by triplicate using the same procedure explained in **Chapter 3**.

4.2.3. Gas chromatography

PHA accumulation analysis was performed using the same protocol from the previous **Chapters 3** and **2** by triplicate.

4.2.4. Statistical analysis

All the statistical analysis was calculated with 95% confidence level using the software STATGRAPHICS Centurion XV.11[290] .The Tukey HSD test was used to evaluate the honest significant difference between cultivations. Homogeneity of variances was confirmed in each case using the Bartlett's test.

One-way analysis of variance (ANOVA) and Multifactor ANOVA were also performed when necessary.

4.3. Results

4.3.1. FabG alignment and comparison of sequences

The amino acid sequences of the 2 FabG*s* tested (*EcolifabG* BW25113 and *MtubfabG* H37Rv) along with the FabG from *C. necator* and 7 other FabGs from mcl-PHA producing *Pseudomonas strains* pre-selected in **Chapter 2** were aligned and shown in **Figure 46.** Consensus amino acids were colored using the Clustal X colour scheme shown in **Figure 44.** A phylogenetic tree was also constructed and shown in **Figure 47.** The amino acid sequence of FabG from *Cupriavidus necator* H16 was used to both the alignment and the tree as a benchmark of comparison given that this organism is the most studied for PHA production at lab and industrial scale .[65, 101]

The phylogenetic tree (**Figure 47**) shows that MtubfabG is the most distantly-related enzyme of the set whereas EcolifabG and FabG from *Cupriavidus necator* (C.necfabG) are the closest. Therefore, it can be expected for MtubfabG and EcolifabG to behave differently with respect to yield and substrate specificity.

Little has been studied from the microbial FabG amino acid sequences. Squared in black in **Figure 46** are the catalytic triad: Serine, Tyrosine and Lysine as reported by Price, Zhang, Rock and White [337] and Filling, Berndt, Benach, Knapp, Prozorovski, Nordling, Ladenstein, Jörnvall and Oppermann [338]. However, just recently in 2021, Hu, Ma, Chen, Tong, Zhu, Wang and Cronan [339] mutated the sequence of EcolifabG and found that the enzyme remained active when either of the 3 alleged catalytic residues were lacking. This new information suggests that FabG is probably not correctly classified and does not belong to the short-chain alcohol dehydrogenase/reductase (SDR) family as originally thought given than all other members of this family share the same catalytic triad (Ser, Tyr and Lys).

The amino acid sequence alignment of the 2 enzymes evaluated in the lab for this study (EcolifabG and MtubfabG) and the identification of the catalytic triad in the 3D structure is shown in **Figure 48**.

Aditionally, **Figure 46** also presents (squared in red) other important and highly conserved regions between FabGs according to the analysis of Cohen-Gonsaud, Ducasse, Hoh, Zerbib, Labesse and Quemard [332] that might be relevant for the activity of the enzyme.

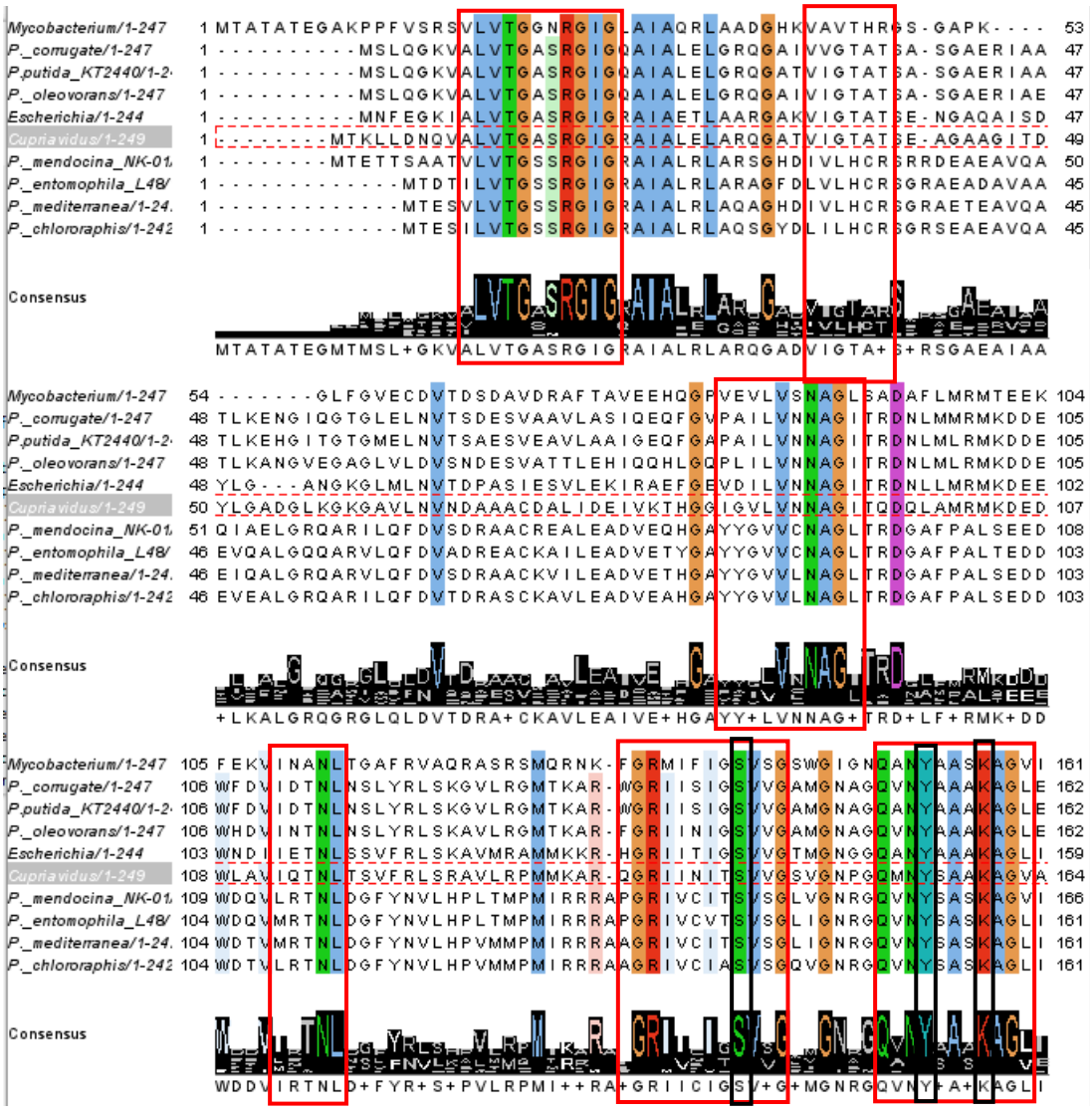

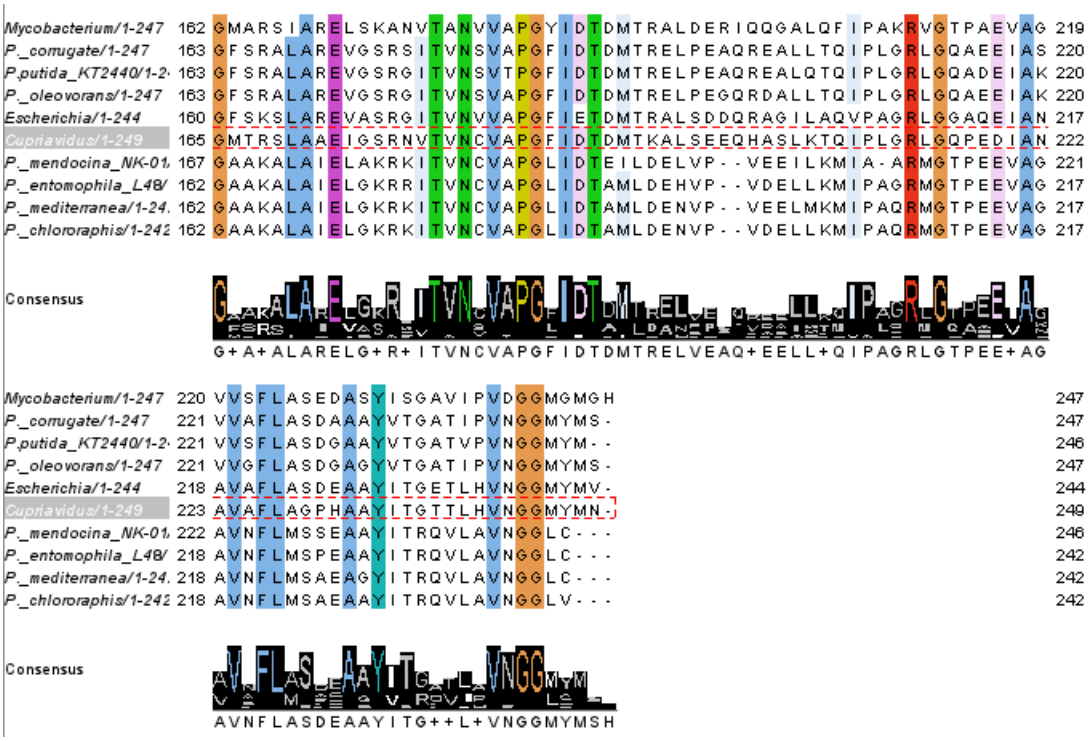

Figure 46*. Squared in red are the highly conserved regions. Squared in black are the catalytic triad: Serine, Tyrosine and Lysine.*

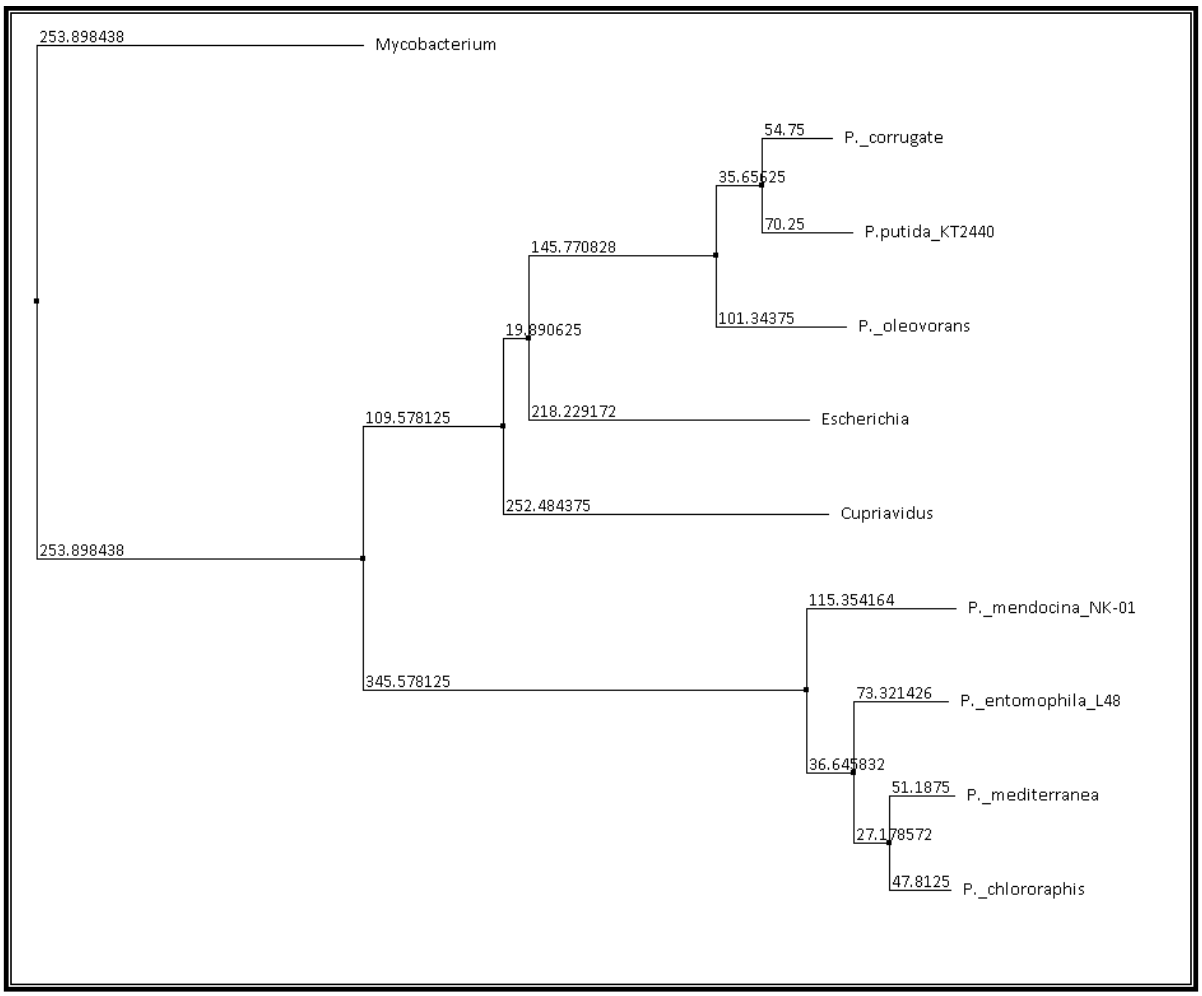

Figure 47. *Phylogenetic tree based on the fabG sequences of 10 different organisms. Sequences were compared using the neighbor joining method [3] and the BLOSUM62 alignment score matrix. [9]*

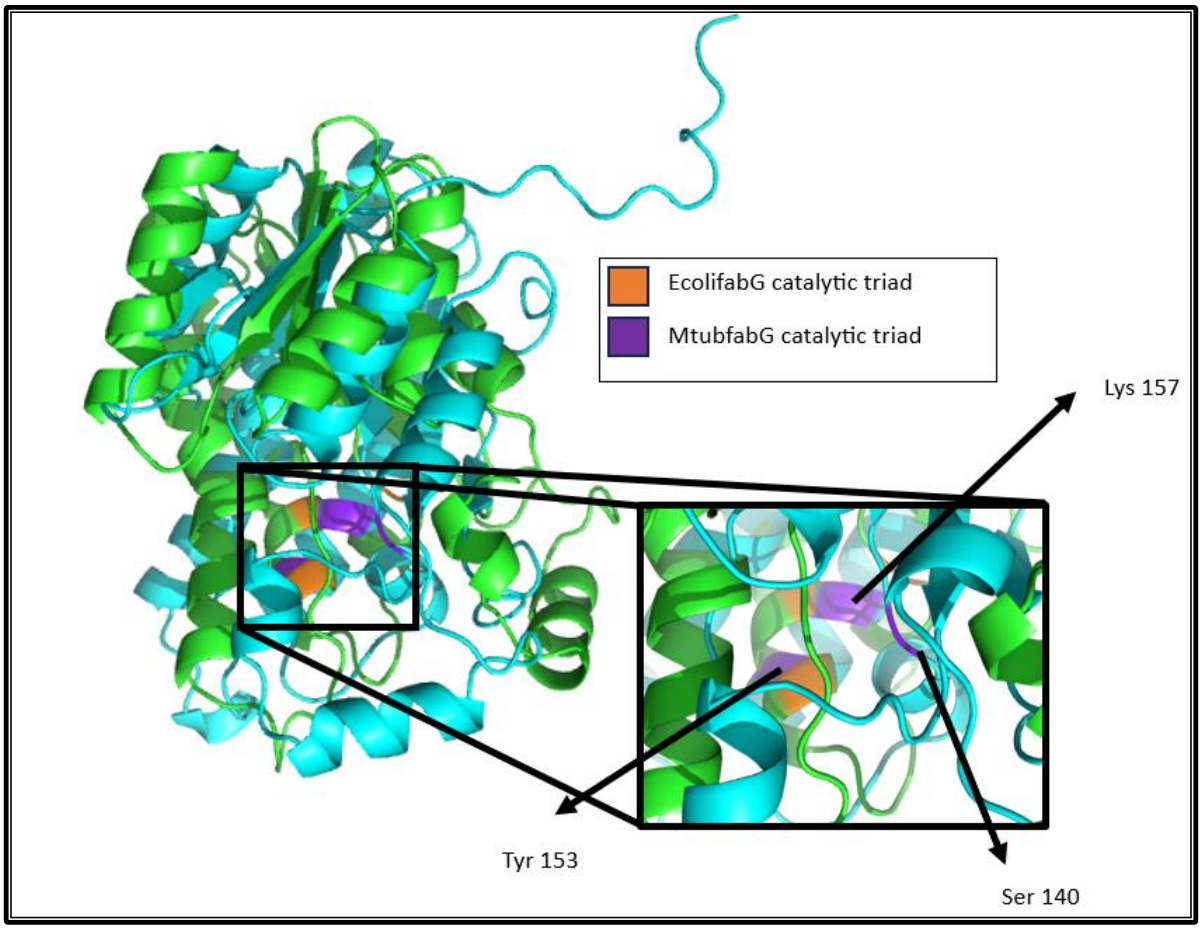

Figure 48. *Pymol structure of 2 aligned FabGs (MtubfabG and EcolifabG) from E. coli BW25113 and M. tuberculosis H37Rv respectively. The catalytic triads Ser, Tyr and Lys are coloured.*

5.4.1. Insertion of the sacI site in the pBAD vector

An extra restriction site was needed to clone *EcolifabG* and *MtubfabG* inside the pBAD-*PpuPhaC*, pBAD-*PmePhaC* and pBAD-*PstzPhaC* plasmids (7300 bp fragment). **Figure 49** shows the successful amplification and therefore successful insertion of the SacI site to the 3 plasmids.

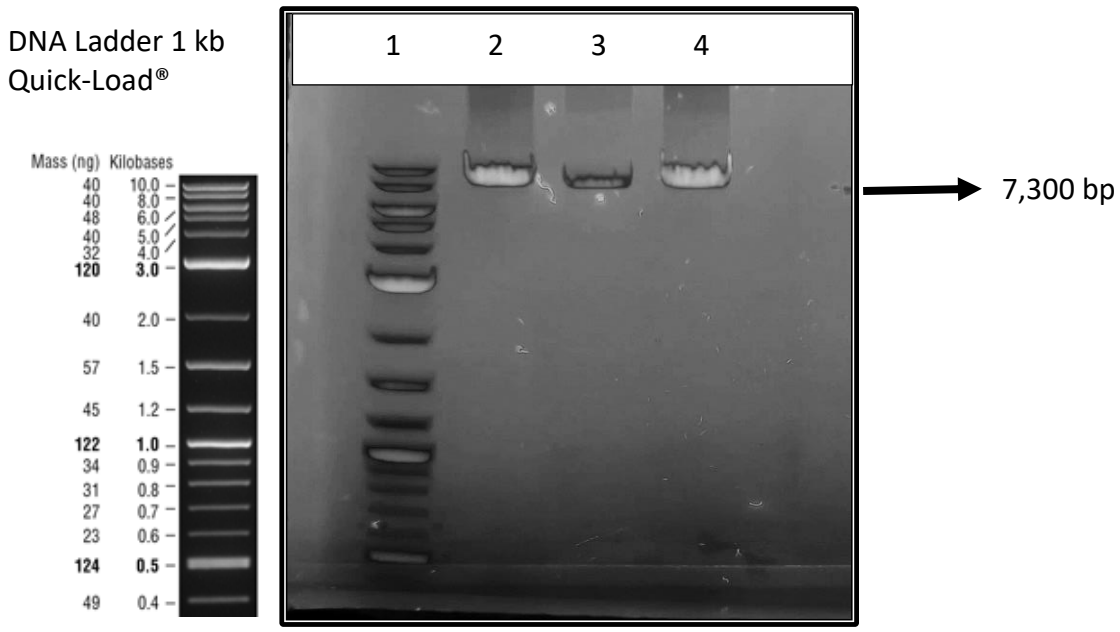

Figure 49. *Electrophoresis gel for the successful addition of the sacI restriction site in the pBAD-PhaC plasmids where 1)ladder, 2) pBAD-PmePhaC, 3)pBAD-PstzPhaC and 4) pBAD-PuPhaC*

4.3.2. Isolation of the *fabG* gene from *Escherichia coli* K-12

Successful isolation of the gene *EcolifabG* (783 bp) (for subsequent cloning in the 3 pBAD-PhaC vectors) using colony PCR was done by triplicate and shown in **Figure 50**. *MtubFabG* was purchased as synthetic gene.

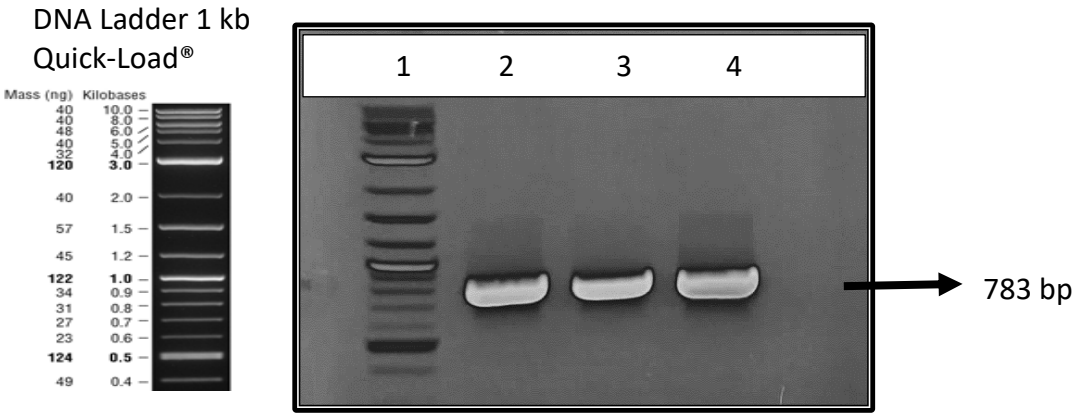

***Figure 50**. Electrophoresis gel showing the successful amplification of the gene fabG from E. coli K-12. 1) ladder 2)3)4) fabG amplified by triplicate.*

4.3.3. Plasmid construction, bacteria transformation, and clone check

Once all 6 plasmids were built and transformed inside *E. coli,* presence of the *fabG* inserts (*EcolifabG* or *MtubfabG*) was confirmed using colony PCR and shown in **Figure 51** and **Figure 52**. Pre-designed commercial pBAD primers (Shown in **Table 23**) were used. Forward primer sits over the araBAD promoter and 124 bp upstream from the start of the *phaC* gene while the reverse primer sits 29 bp downstream from the *fabG* gene and before the terminator. Colony PCR of the cells co-expressing *phaC* and *fabG* resulted in an amplicon that was 2, 642 bp long whereas failure to insert *fabG* inside the vector, resulted in an amplicon of 1, 886 bp. Similarly to **Chapter 3,** each transformant plate had ≈100 colonies but only 2-3 of them were screened for clones and ≈50% were positive.

Sanger sequence results showed 100% match with the original sequence for all 6 *fabG* cloned genes. Therefore there are no polymorphisms in the sequence.

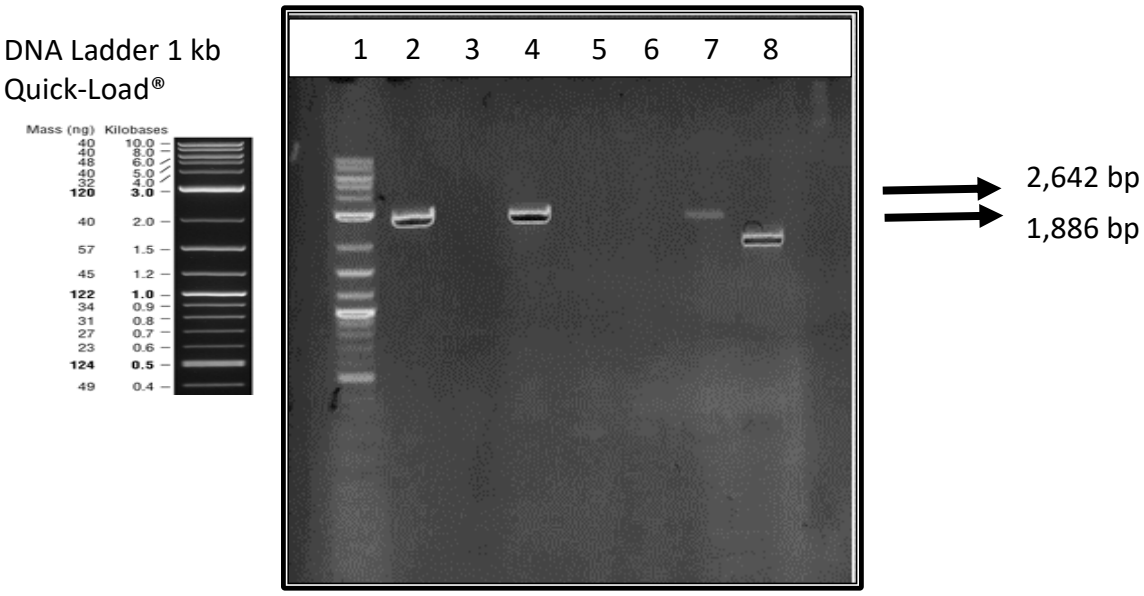

Figure 51. *Electrophoresis of the clone check for the successful construction of pBAD-PhaC-EcolifabG where lane 1) ladder, 2) PmePhaC-EcolifabG colony 1 → positive 3)PmePhaC-EcolifabG colony 2 → negative, 4) PstzPhaC- EcolifabG colony 1 → positive 5)PstzPhaC-EcolifabG colony 2 → negative 6)PpuPhaC-EcolifabG colony 1 →negative, 7) PpuPhaC-EcolifabG colony 2 → positive, 8) PpuPhaC-control*

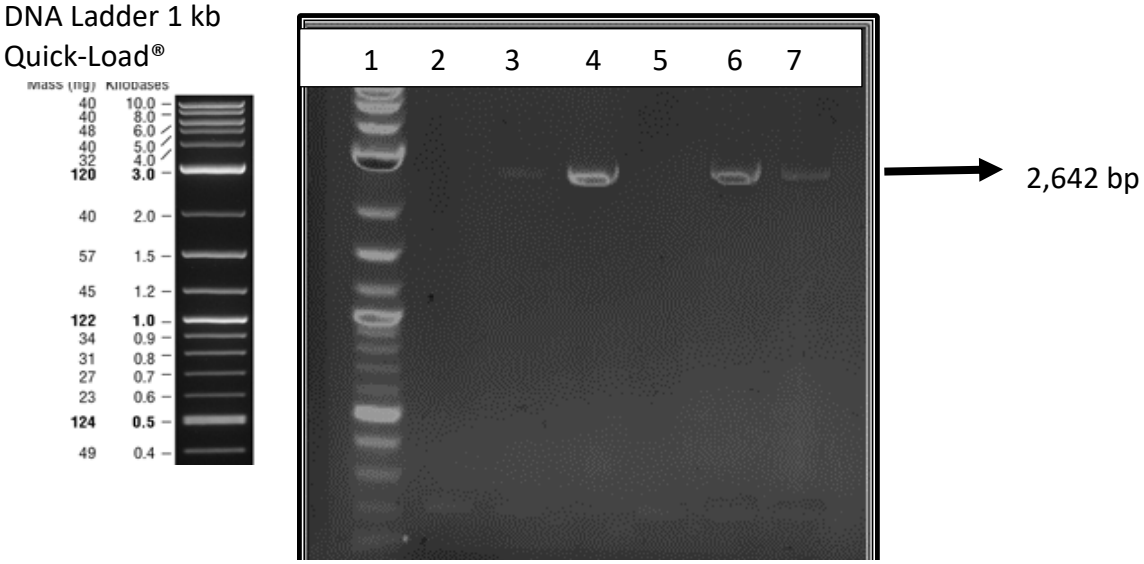

Figure 52*. Electrophoresis gel of the clone check for the successful construction of pBAD-PhaC-MtubfabG where lane 1) ladder, 2) PmePhaC-MtubfabG colony 1 → negative, 3)PmePhaC-MtubfabG colony 2 → positive, 4) PstzPhaC-MtubfabG colony 1 → positive, 5) PstzPhaC- MtubfabG colony 2 → negative, 6) PpuPhaC-MtubfabG colony 1 → positive 7) PpuPhaC-MtubfabG colony 2 → positive.*

4.3.4. Bacteria cultivation and PHA accumulation

Dry biomass from the cultivation of recombinant Δ*fadA Escherichia coli*-K -12 expressing the 6 plasmids pBAD-*PmePhaC-EcolifabG*, pBAD-*PmePhaC-MtubfabG*, pBAD-*PstzPhaC-EcolifabG*, pBAD-*PstzPhaC-MtubfabG*, pBAD-*PpuPhaC-EcolifabG* and pBAD-*PpuPhaC-MtubfabG* in the presence of sodium tetradecanoate (C14) as substrate were weighted and then digested for determination of PHA content. Values for both, biomass accumulation and PHA content, were recorded and presented on **Table 24.** PHA concentration was not detected using GC-FID.

Table 24. Comparison of different pBAD-*PhaC-fabG* plasmids using sodium tetradecanoate as substrate. Cultures were incubated 37°C, 200 rpm for 48 hours after arabinose induction (0.02% (w/v)).

Host	PhaC source	FabG source	Substrate 0.5% (w/v)	CDW (g/l)	GC-FID µg/l
***fadA* Knockout**	*P. mendocina*	*E.coli*	C14	0.439±0.049	Non-detectable
	P. stutzeri	*E.coli*	C14	0.648±0.108	Non-detectable
	P.putida	*E.coli*	C14	0.518± 0.116	Non-detectable
	P.mendocina	*M.tuberculosis*	C14	0.638±0.082	Non-detectable
	P.stutzeri	*M.tuberculosis*	C14	0.7± 0.036	Non-detectable
	P.putida	*M.tuberculosis*	C14	0.646± 0.068	Non-detectable
	Control	control	C14	0.465±0.051	Non-detectable

Each culture was grown three times and the value presented for CDW (g/l) is the mean ± the standard deviation. Abbreviations: CDW, cell dried weight (g/l); GC-FID: concentration of PHA, measured by triplicate, using gas chromatography using flame ionization detector(µg/l) ; GC-MS: concentration of PHA gas chromatography , measured once, using gas chromatography using mass spectrometer as detector (µg/l).

A multifactor ANOVA was also built (95% confidence) using PhaC (*PpuPhaC, PmePhaC, PstzPhaC)* and FabG (*EcolifabG, MtubfabG*) as factors. P values are presented in **Table 25.** Neither of the factors have a P≤0.05 value, which means that they are not statistically significant.

The CDW (g/l) across all the pBAD-PhaC recombinant strains with either EcolifabG or MtubfabG enzyme were graphed and presented on **Figure 53.** Values were also compared statistically according to Tukey (P≤0.05) and both groups resulted to be statistically equal.

Table 25. Multifactorial ANOVA (95% confidence) results for cell dry biomass (g/l). The factors analysed were PhaC and FabG enzymes. P values ≤ 0.05 are statistically significant and are presented in red.

CDW (g/l)		
	Factors	**P-Value**
A	PhaC	0.3106
B	FabG	0.1075
	Interactions	**P-Value**
	AB	0.6847

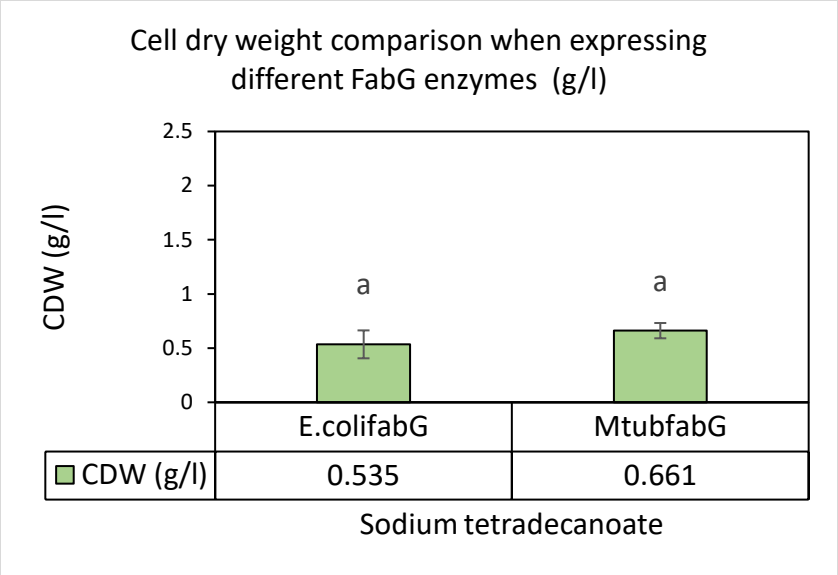

Figure 53. *Comparison of CDW (g/l) accumulation (across all the pBAD-PhaC recombinant cells) with either EcolifabG or MtubfabG* enzyme *using ΔfadA as host and C14 as substrate. The values were also compared statistically according to Tukey (P≤0.05). Same letters represent statistically equal groups. Cultures were done by triplicate*

4.4. Discussion and future perspectives

Unlike the previous **Chapter 3** where only recombinant PhaC was expressed inside *E. coli*, in this **Chapter 4,** PHA production was determined by the activity of two enzymes : PhaC and FabG, therefore it was necessary to run a multifactorial ANOVA (95% confidence) to statistically evaluate cell dry weight of the 6 different recombinant strains constructed . These strains resulted from the combination of the 3 different PhaC (*PmePhaC*, *PstzPhaC, PpuPhaC*) with the 2 different FabG (*EcolifabG* and *MtubfabG)* chosen for this study.

Results show that when comparing *EcolifabG* versus *MtubfabG* for biomass accumulation CDW (g/l), even though the net average value for *MtubfabG* (0.661 g/l) is higher than for *EcolifabG* (0.535 g/l) (**Figure 53**) ,this difference is not statistically significant. As for PHA accumulation, there is no polymer accumulation above the limit of detection when using GC-FID .

Results in the present study differ from the findings from Park, Park and Lee [152] who coexpressed FabG from *E. coli* (EcolifabG) along with the PhaC from *Pseudomonas* sp.61-2 in two different plasmids and achieved a PHA accumulation of 0.22 g/l that was rich in 3-hydroxydecanoate (C10) monomer (93 mol%) using the *fadA* knockout *E. coli* WA101 strain as a host. Production of mcl-PHA when coexpressing FabG and PhaC inside *fadA* mutant *E. coli* was also successful in the study of Ren, Sierro, Witholt and Kessler [329]

In this study *fabG* genes were cloned to supply PhaC with more substrate and it was assumed that, even though protein expression was not distinctly visible using SDS-PAGE in the previous **Chapter 3** there is still expression present but in low quantities. This assumption probably contributed to the failure to produce PHA and in future we need to provide solid evidence that both enzymes are present and active inside the host before further optimizing the plasmid.

Another main difference of the present study versus these studies is the chain length of the target monomer in this study (C14). In this regard, only a handful of studies have been successful in the past at producing mcl-PHAs containing a high hydroxytetradecanoate monomer composition. Examples of these studies are the study of Liu and Chen [150] who, in 2007, produced mcl-PHA consisting of high content of hydroxytetradecanoate (HTD) (≥30%) using the Δ*fadA* Δ*fadB* knockout mutant *Pseudomonas putida* KT2442 termed P. putida KTOY06 grown in tetradecanoic acid. As mentioned before, this mcl-PHA was found to have both higher crystallinity and improved tensile strength compared with that of typical mcl-PHA. Higher crystallinity in PHA with high HTD monomer composition was also confirmed by Chen, Liu, Wang, Zhu, Yu, Chen and Inoue [340] This discovery opened a new door of possibilities for PHA research. A copolymer composed of 12% monomer composition HTD was also synthesized in *Pseudomonas* by Pereira, Araújo, Marques, Neves, Grandfils, Sevrin, Alves, Fortunato, Reis and Freitas [81] from glycerol.

The study of a limited-studied mcl-PHA polymer makes this project both novel and challenging. However, further optimization is still needed to successfully accumulate it inside *Escherichia coli* which is a common chassis for comparison and optimization of enzymes. Several approaches could be taken to achieve this goal , for example, metabolic engineering can be done to further channel β-oxidation intermediates into mcl-PHA synthesis. That is the reason why, in the next chapter, the FadR protein that regulates this pathway will be knocked out.

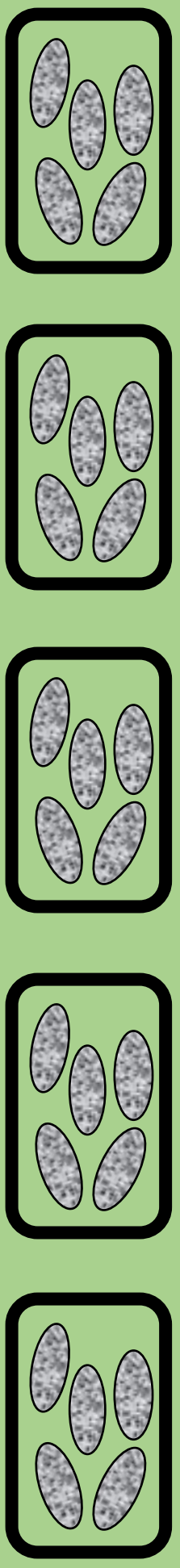

CHAPTER 5

Constitutive expression of the β-oxidation pathway

Construction of the double knockout Δ*fadA*Δ*fadR* to produce polyhydroxyalkanoates with high hydroxytetradecanoate monomer composition.

CHAPTER 5: CONSTITUTIVE EXPRESSION OF THE β-OXIDATION PATHWAY. Construction of the double knockout Δ*fadA*Δ*fadR* to produce polyhydroxyalkanoates with high hydroxytetradecanoate monomer composition.

5.1. Introduction

Regulation of fatty acid metabolism is of vital importance for the cell because fatty acids are the primary components of the cell membrane for all living organisms. The cell membrane surrounds the cell and is responsible for the structure, homeostasis, and transport of substances in and out. [341, 342]

In *Escherichia coli* , the main regulator of fatty acid metabolism is the FadR protein.[343] FadR represses the transcription of every fad gene (*fad*L, *fadD*, *fadE*, *fadBA*, *fadIJ*, *fadH*, *fadM*) by binding to their promoter sequence.[249, 344] Specifically, crystallography reveals that the amino acids Arg35, Arg45 and His65 in FadR formally recognize the palindromic consensus sequence 5'-TGGNNNNNCCA-3' found in the promoter for all these genes, thus repressing the β-oxidation pathway [345] Binding of FadR to the promoter is inhibited by the presence of long chain fatty acyl-CoA (LCFA) compounds (C12 to C18)[344, 346] which means that *E. coli* can only metabolize fatty acids that are equal or longer than 12 carbons. However, medium chain length fatty acids (MCFA) (C6 to C11) can serve as growth substrates for *fadR* mutant strains that constitutively synthesize the fad enzymes. [347-349] Carboxylic acids shorter than C6 (C4 and C5) are referred to as short-chain fatty acids (SCFA) and cannot be metabolized solely via the fad system, [349, 350] the expression of the Ato operon that includes the enzyme genes atoD, atoA and atoB are needed first and a 48-kilodalton protein encoded by atoC is required as an activator of this operon. [351-353]

In contrast with the above, FadR has also long been known to function as a transcription activator of the *fabA* and *fabB* genes that are specifically required to synthesize unsaturated fatty acids. [354-356] Interestingly, it was recently observed that contrary to what was believed, activation of *fab* genes by FadR is not restricted to these 2 genes only (*fabA* and *fabG*) but it also activates almost all remaining fab genes, from the fatty acid biosynthesis pathway, when it is overexpressed inside the cell, resulting in increased yields of all fatty acids acyl chains. [357]

As mentioned before in this work, medium-chain-length PHAs are commonly synthesized from an intermediate of the β-oxidation pathway when the bacteria is fed with fatty acids [135] but they can also be synthesized through the fatty acid biosynthesis pathway using unrelated carbon sources as substrate. [325, 358, 359] and therefore FadR could be considered as a regulator of PHA synthesis as well. Consistently with this statement, Qi, Steinbüchel and Rehm [250] compared several *Escherichia coli* mutants and found that the *fadR* mutant *E. coli* RS3097 has a strong accumulation of PHA contributing to about 60% of cell dry weight, when grown on decanoate and in the presence of the β-oxidation inhibitor acrylic acid, while Rhie and Dennis [113] were able to incorporate significant levels of hydroxyvalerate (HV) into the copolymer polyhydroxybutyrate-co-hydroxyvalerate [P(HB-co-HV)] with a recombinant Δ*fadR* atoC(Constitutive) *Escherichia coli* mutant strain. Yet, more studies are needed to prove if this PHA accumulation enhancement using *fadR* mutant strains would also occur for other monomer-chain-lengths such as C14.

In a last attempt to produce polyhydroxyalkanoate (PHA) with high tetradecanoate monomer composition, in this **Chapter 5** , recombinant Δ*fadA Escherichia coli* expressing pBAD- *PpuPhaC-MtubfabG* was further engineered to channel β-oxidation intermediates to PHA production through the constitutive expression of the β-oxidation pathway (*fadR* mutant) by deleting the gene encoding FadR.

5.2. Materials and methods

List of detailed information on the materials used (reagents, kits, equipment, software, media preparation and miscellaneous) can be found in **Appendix 1-5.** Strains, plasmids and primers are shown in **Table 26.**

Table 26. List of bacterial strains, plasmids and primers used in **Chapter 5**.

Strains	Relevant genotype	Source or reference
E. coli K-12 BW25113 Δ*fadA*	F-, *Δ(araD-araB)567*, *ΔlacZ4787*(::rrnB-3), *λ*- , *rph-1*, *Δ(rhaD-rhaB)568*, *hsdR514, ⊿fadA, Kan*^{R}	260
E.coli K-12 BW25113 Δ*fadR*	F-, *Δ(araD-araB)567*, *ΔlacZ4787*(::rrnB-3), *λ*- , *rph-1*, *Δ(rhaD-rhaB)568*, *hsdR514, ⊿fadR, Kan*^{R}	260
Plasmids		
pBAD-*PpuPhaC*	P_{BAD} promoter, *phaC* from *P. putida*, Amp^R	This study
pSIJ8	araBp-gam-bet-exo, rhaBp-flp, repA101(ts), Amp^R	pSIJ8 was a gift from Alex Nielsen (Addgene plasmid)274
pKD4	FRT-kan-FRT, Amp^R	pKD4 was a gift from Barry L. Wanner (Addgene plasmid # 45605)275
Primers		
KnockoutFadR-for-rev	CCC TCT GGT ATG ATG AGT CC AAA CAA CAA AAA ACC CCT CG	This study
KnockoutFadR-kan,for-locus,rev	GGC TAC CCG TGA TAT TGC TG CGC CAA GAA TGG GAA ATC TG	This study
fadA-for-rev	CTA TGA CGT ATC TGG CAA ACC CGA CCT GAA AAC GGC TTA AG	This study
pBAD for rev	ATG CCA TAG CAT TTT TAT CC GAT TTA ATC TGT ATC AGG	This study

5.2.1. Elimination of the kanamycin resistance from the strain *Escherichia coli* BW25113 Δ*fadA*

The knockout Δ*fadA E. coli* used throughout this thesis is part of the Keio collection from Baba, Ara, Hasegawa, Takai, Okumura, Baba, Datsenko, Tomita, Wanner and Mori [260]. The collection comprises *E. coli*- K12 in-frame single-gene knockout mutants that were built by recombination with a kanamycin gene flanked with a FRT sequence (Flippase recognition target) as originally described by Datsenko and Wanner [360]

In this study, the plasmid pSIJ8 [361],which expresses a flippase enzyme in the presence of rhamnose and a recombinase in the presence of arabinose, was purchased from Addgene and used to delete the kanamycin marker from the strain before knocking out a new gene (FadR), using the same kanamycin marker. This plasmid also confers ampicillin resistance (100 μg/ml) to the cells.

First, the cells are transformed with the pSIJ8 plasmid using the standard heat shock and $CaCl_2$ protocol. [318] Once the plasmid is inside *E. coli,* the procedure followed reads as follows: one colony was grown overnight in 5 ml of 2×YT (tryptone 16 g/l, yeast extract 10 g/l and NaCl 5 g/l) in the presence of 400 μl of L-rhamnose 20% (final concentration 1.6%) and grown at 30 °C, 200 rpm overnight. Subsequently, the culture was diluted 1,000,000 times and plated in 2×YT agar plates with kanamycin (30 μg/ml) (negative control) and with ampicillin (100 μg/ml) (target marker-less colonies) .

From the plate with ampicillin, 5 colonies were picked and tested for the presence/absence of the kanamycin-resistance gene in the genome through colony PCR: each colony was suspended in 25 μl of distilled water and heat to 98°C for 10 min, then centrifuged at 4000 g for 5 min. Three μl of the supernatant was used for the PCR (25 μl reaction). 64°C was used as annealing temperature with the primers *fadA*-for-rev (**Table 26**) . Colonies containing Kan^R are expected to result in a PCR amplicon which is approximately

1800 bp long whereas colonies without Kan^R (desired colonies) are expected to result in a PCR amplicon approximately 400 bp long.

Once the marker-less (no kanamycin resistance) colonies were identified, one of them was re-cultured overnight in the presence of rhamnose 5 more times before plating to ensure the purity of the culture.

This step was necessary because the same marker (kanamycin) is being used for knockout by recombination of *fadR*.

5.2.2. *fadR* gene knockout using the marker-less *Escherichia coli* BW25113 Δ*fadA* as a host.

One colony of marker-less (no Kan^R) Δ*fadA E. coli* harbouring the pSIJ8 plasmid was grown overnight in 5 ml of 2×YT (tryptone 16 g/l, yeast extract 10 g/l and NaCl 5 g/l and ampicillin 100 µg/ml) in the presence of 100 µl of arabinose 20% (w/v) (200 rpm, 30°C) . The next morning 200 µl of this culture was transferred into a new 5 ml 2×YT medium with ampicillin and 50 µl of arabinose. The culture was set to grow for 4.5 hours before transforming with ≈400 ng of linear DNA (H1-FRT-kan^R-FRT-H2) using the standard heat shock and $CaCl_2$ transformation protocol.[318]

Cells were incubated overnight (30 °C) in agar 2×YT with kanamycin (30 µg/ml) as a marker. To confirm replacement of the *fadR* gene with the kanamycin resistance marker, a colony PCR was done using a locus-specific forward primer for the kanamycin gene and a reverse primer from a *fadR* flanking region.

As a last step, the newly constructed double knockout Δ*fadA*Δ*fadR* was cultivated in 5 ml of 2×YT in the presence of kanamycin (30 µg/ml) at 37°C to cure the temperature-resistant plasmid pSIJ8 used. It was then stock with glycerol 25% (v/v) at -80 °C.

5.2.3. Mutants' growth evaluation using sodium hexanoate as substrate.

Bacterial growth curves were constructed to evaluate the influence of the single knockouts Δ*fadA* and Δ*fadR* and the double knockout Δ*fadA*Δ*fadR* over the growth of *Escherichia coli* K-12. Growth curves also evaluated the influence of the presence/ absence of the plasmid pBAD-*PpuPhaC* (expressed with arabinose) over cell growth.

Hence , the following strains were grown overnight in 2×YT medium in the presence of either ampicillin (for pBAD plasmid) or kanamycin (single and double knockouts):

1) Δ*fadA* *E. coli* K-12
2) Δ*fadR E. coli* K-12
3) Δ*fadA* Δ*fadR E. coli* K-12
4) parental *E. coli* K-12
5) Δ*fadA E. coli* K-12- pBAD-*PpuPhaC*
6) Δ*fadR E. coli* K-12 pBAD-*PpuPhaC*
7) Δ*fadA* Δ*fadR E. coli* K-12 pBAD-*PpuPhaC*
8) parental *E. coli* K-12 pBAD-*PpuPhaC*

Subsequently, 50 µl of each of the overnight cultures were transferred to 5 ml of fresh 2×YT with its corresponding antibiotic. 50 µl of arabinose (final 0.2% w/v) was added to induce PhaC expression and 200 µl of sodium hexanoate (C6) was added as substrate for PHA production (final 0.5% w/v).

Lastly, 200 µl of the described culture was added, in triplicate, to a 96-plate microplate reader (TECAN Spark 10M) to build the growth curves for each of the 8 strains at 37 °C with 210 rpm agitation for aeration. Optical density at 600 nm was recorded every 30 minutes for 24 hours. The OD600 values were used to estimate the number of cells using the polynomial degree equation from Mira, Yeh and Hall [362]

5.2.4. Bacteria cultivation and PHA production

The same 8 strains used for the construction of the growth curves were also cultivated for PHA production (by triplicate) using the same methodology from **Chapter 3** and **4.**

5.2.5. Gas chromatography analysis

PHA accumulation analysis was performed using the same acid methanolysis protocol from previous **Chapters 2, 3** and **4.**

5.2.6. Statistical analysis

All the statistical analysis was calculated with 95% confidence level using the software STATGRAPHICS Centurion XV.11[290] using at least 3 replicates of completely different cultivations. The Tukey HSD test was used to evaluate the significant difference between cultivations. Homogeneity of variances was confirmed in each case using the Bartlett's test.

5.3. Results

5.3.1. Elimination of the kanamycin resistance from the strain *Escherichia coli* BW25113 Δ*fadA*

The kanamycin resistance gene from the Δ*fadA E. coli* strain bought from the Keio collection [260] was deleted through the expression of a flippase enzyme using the pSIJ8 plasmid [361]. This step was necessary because the same marker (kanamycin) is being used for knockout by recombination of *fadR*.

Successful deletions can be observed in **Figure 54** where the same volume of culture was plated on **A** and **B,** yet there is a reduced number of colonies in the presence of kanamycin (**Figure 54 B**) due to this resistance loss. Five colonies were selected from the plate **A** (ampicillin 100 µg/ml) to confirm deletions through colony PCR. Also, one colony from the plate in **Figure 54 B** (kanamycin 30 µg/ml) was screened as positive control of the kan^R gene. Results are shown in **Figure 55.** Primers used are shown in **Table 26** as fadA-for-rev. Both primers anneal in regions flanking the *fadA* gene (which was replaced by a kanamycin marker)[260] in the genome (289 bp downstream and 9bp upstream respectively). The PCR resulted in an amplicon of 1 817 bp for presence of the kanamycin gene and 400 bp for absence of it.

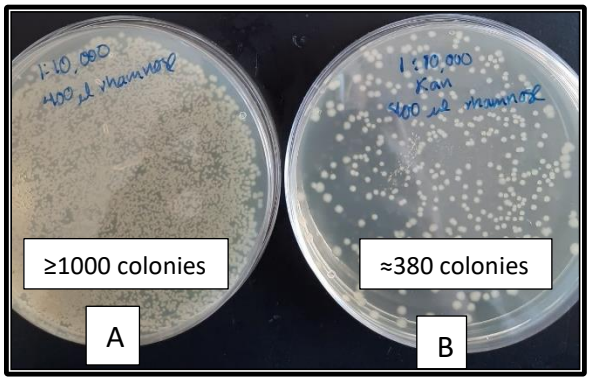

Figure 54*. Loss of the kanamycin resistance gene after overnight induction of flippase by addition of rhamnose. A) Cells plated with no antibiotic after rhamnose induction B)Cells plated in the presence of kanamycin after rhamnose induction.*

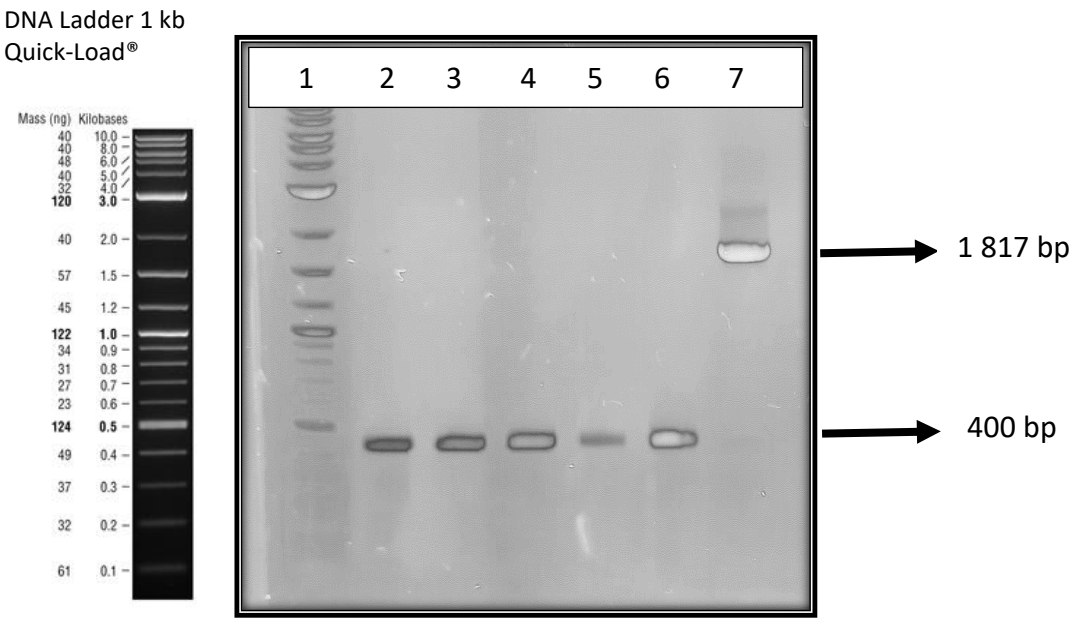

***Figure 55**. Electrophoresis gel showing the successful deletion of the kan^R gene through the expression of a flippase enzyme where lane 1) ladder, 2) colony 1 → negative for kan^R , 3) colony 2 →negative for kan^R, 4) colony 3 → negative for kan ^{R}, 5) colony 4 → negative for kan^R , 6) colony 5 → negative for kan^R and 7) positive control for the presence of kan^R .*

From all the markerless colonies screened (five colonies), one was selected and further purified by re-expressing the flippase enzyme in presence of rhamnose overnight for 5 consecutive times. The culture was plated in the presence of ampicillin and kanamycin to validate the presence of only marker-less cells in the population. Results are shown in **Figure 56.**

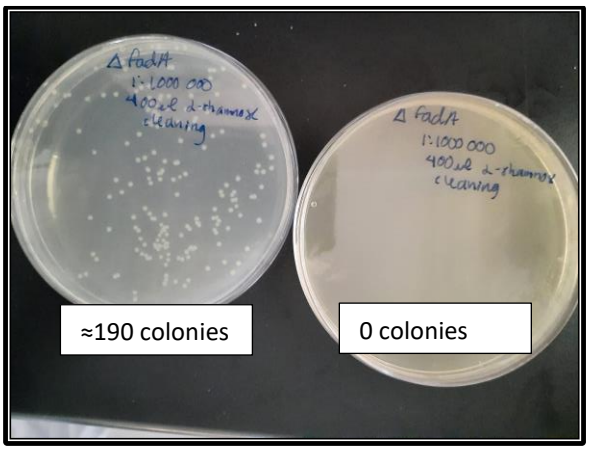

***Figure 56**. Marker-less (no-kan^R) E. coli fadA knockout colonies after 5 consecutive washes with rhamnose to induce flippase expression in the culture. Plate on the left show the colonies growing in the presence of ampicillin (100 µg/ml) whereas plate of the right show no colonies in the presence of kanamycin (30 µg/ml).*

5.3.2. *fadR* gene knockout in the marker-less *Escherichia coli* BW25113 Δ*fadA*.

Once we had obtained a pure culture of marker-less Δ*fadA E. coli* cells, *fadR* gene was deleted using a modified procedure from Jensen, Lennen, Herrgård and Nielsen [361]. Replacement of the *fadR* gene for a kan^R marker was confirmed through PCR and shown in **Figure 57A**. The primers used were a kanamycin locus specific primer and a *fadR* flanking region primer shown in **Figure 57B**. Consequently, negative control colonies that did not had *fadR* replaced with a kanamycin marker did not amplify whereas positive colonies show a 444 bp band. The homologous sequence used for the recombination to take place is also shown in **Figure 57B** (H1 and H2). The full linear DNA sequence used for the recombination has been added in **Annex 6**.

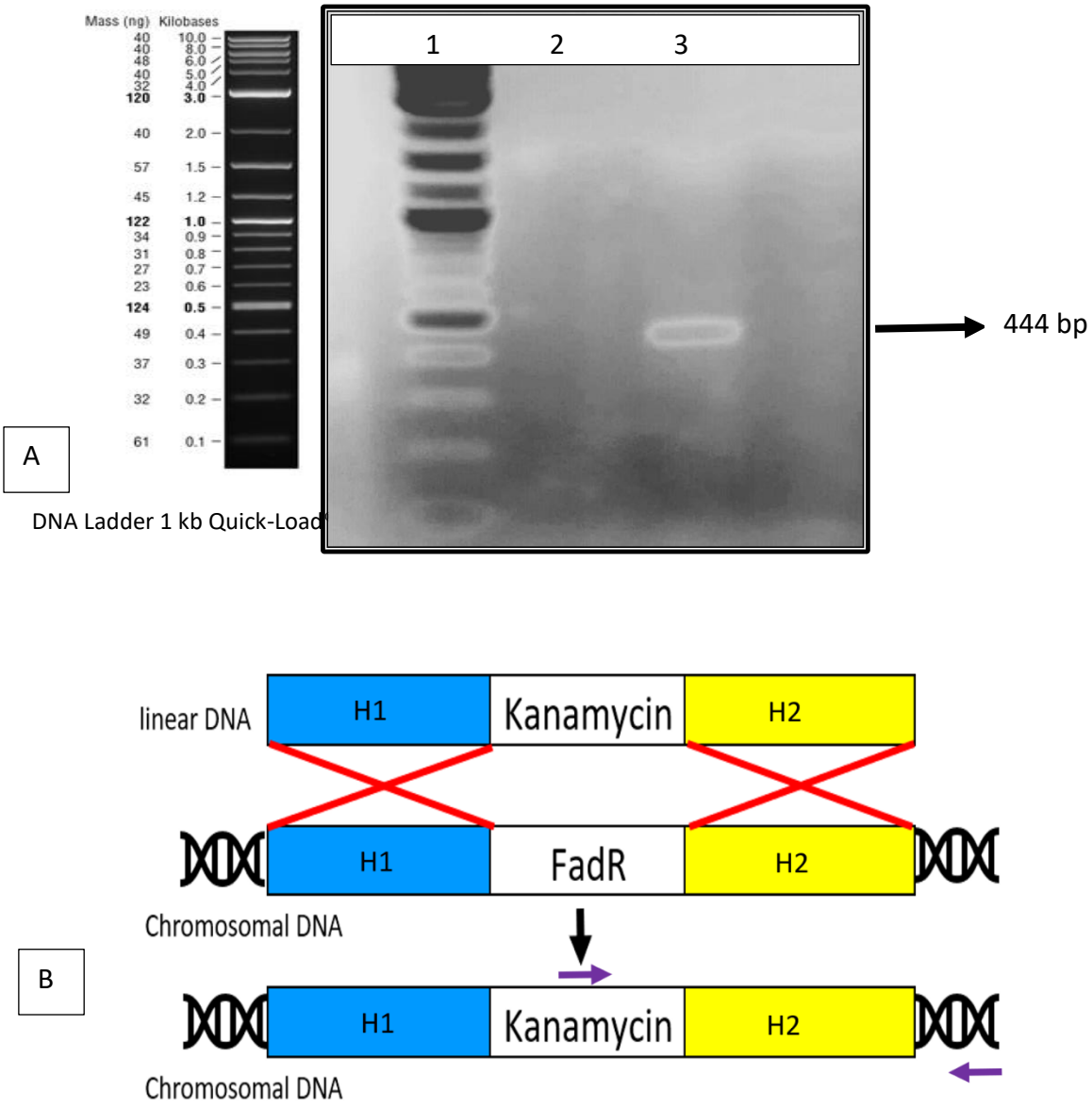

Figure 57. *A) Electrophoresis gel showing the successful deletion of the fadR gene in E.coli K-12. A kanamycin resistance gene was inserted in the place of the fadR gene through recombination and this gene was amplified and shown in this picture through colony PCR. lane 1) represent the ladder, 2) colony 1 → negative for kan ^{R} (negative control), 3) colony 2 → positive for kan^{R} (fadR knockout)*

B) Annealing primers (purple arrows) would only amplify if the recombination took place successfully between the homologous sequences H1 and H2. PCR resulted in a 444 bp product.

5.3.3. Mutant growth evaluation using sodium hexanoate as substrate.

To evaluate the effect of gene deletions over *E. coli's* growth rate and biomass accumulation, the β-oxidation *E. coli* mutants were grown in 2×YT media (tryptone 16 g/l, yeast 10 g/l, NaCl 5 g/l) in the presence of sodium hexanoate as β-oxidation substrate. Growth curves were constructed and shown in **Figure 58**. Biomass was also collected, dried, weighted and graphed in **Figure 59** where it can be observed that the double knockout Δ*fadA*Δ*fadR* strain is statistically lower than the other 2 single mutants and than the parental strain according to Tukey (P≤0.05).

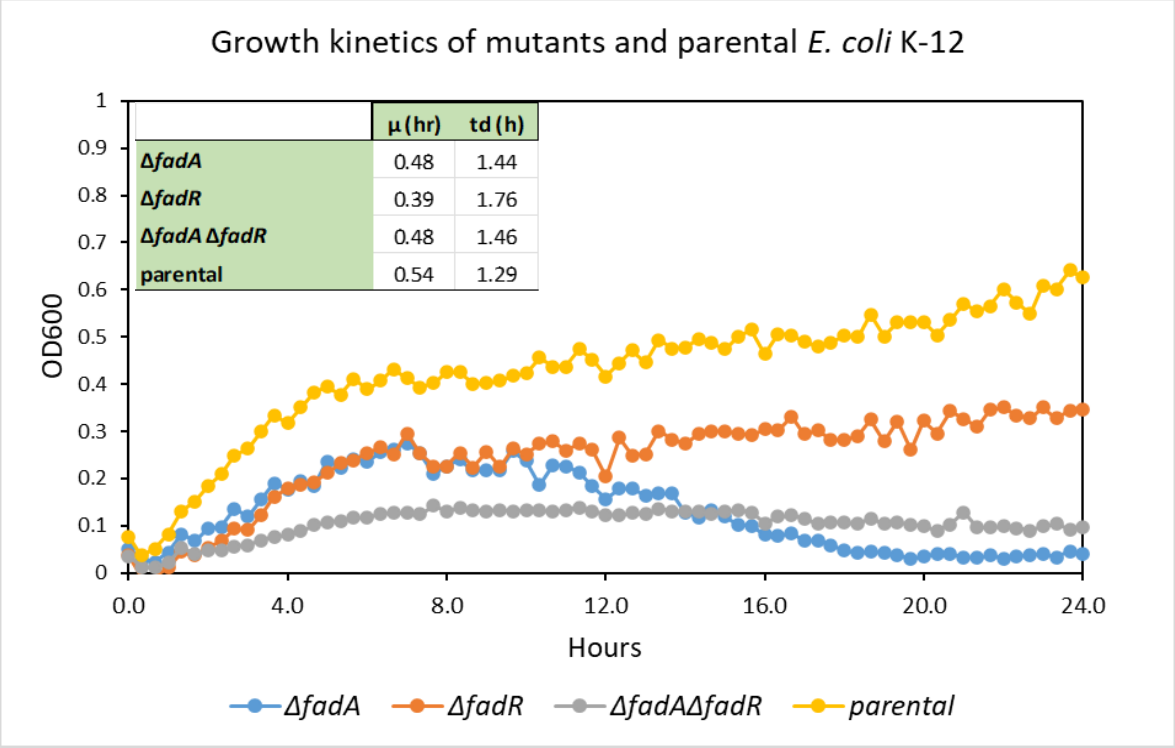

Figure 58. *Growth curve of mutants and parental E. coli-K12. Cells were cultivated in 2xYT and sodium hexanoate 0.5% (w/v) (210 rpm, 37°C) for 24 hours. Growth rate (**μ**) per hour and doubling time (**td**) were estimated from the exponential phase. Growth curves were done in triplicate and the average is presentes.*

C6 is the shortest mcl-PHA. [85]C6 was chosen for this growth curve because, although the intended PHA for this project is C12-C14 carbons long, the corresponding carbon sources are not soluble and interfere with the optical density reading. As mentioned before, binding of the FadR (fatty acid metabolism repressor) [343] can be inhibited by the presence of long chain fatty acyl-CoA (LCFA) compounds (C12 to C18)[344, 346] in *E. coli.* However, (C6-C11) substrates can be metabolized by *fadR* mutants. [347-349]

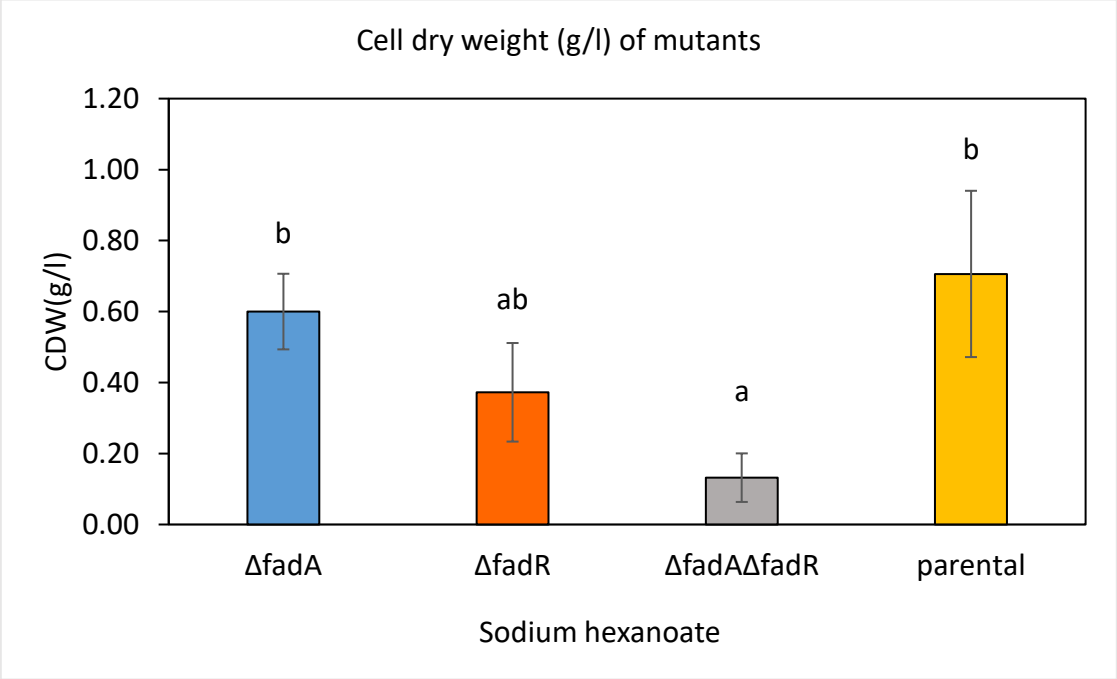

Figure 59*. Comparison of means of the biomass accumulation from the cultivation of E coli-K12 fadA and fadR single mutants, the double fadAfadR mutant and the parental strain. Same letters indicate statistically equal values according to Tukey with 95% confidence. Cultures were done in triplicate*

Furthermore, to evaluate the effects of metabolic burden associated with the heterologous expression of plasmids , the three *E. coli* mutants strains and the parental were transformed with the plasmid pBAD-*PpuPhaC* and once again cultivated in 2×YT media (tryptone 16 g/l, yeast 10 g/l, NaCl 5 g/l) and in the presence of sodium hexanoate as β-oxidation substrate. Growth curves were constructed and shown in **Figure 60**. Biomass was also collected, dried,

weighted graphed and compared in **Figure 61.** In this case, all 4 values are statistically equal according to Tukey (P≤0.05).

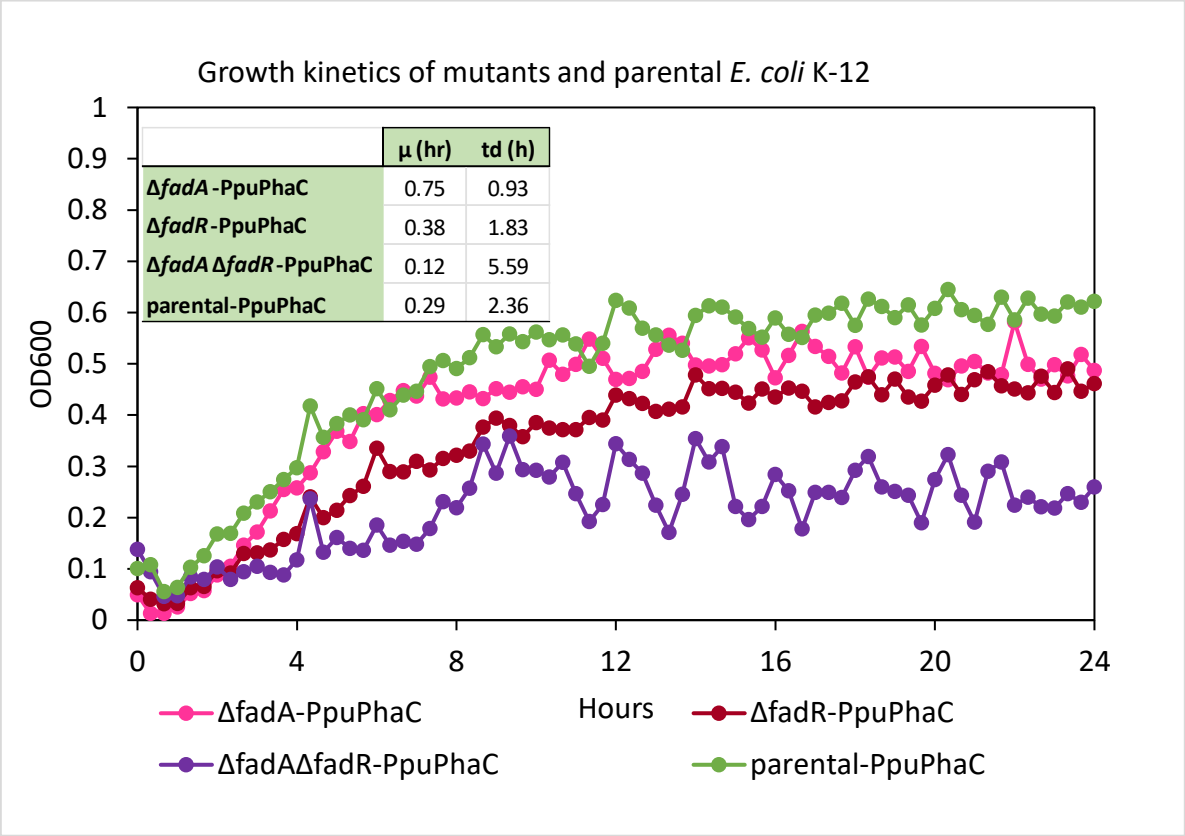

***Figure 60**. Growth curve of mutants and parental E.coli-K12 expressing the pBAD-PpuPhaC plasmid. Cells were cultivated in 2xYT and sodium hexanoate 0.5% (w/v) (210 rpm, 37°C) for 24 hours. The curve was done in triplicate and the average is presented.*

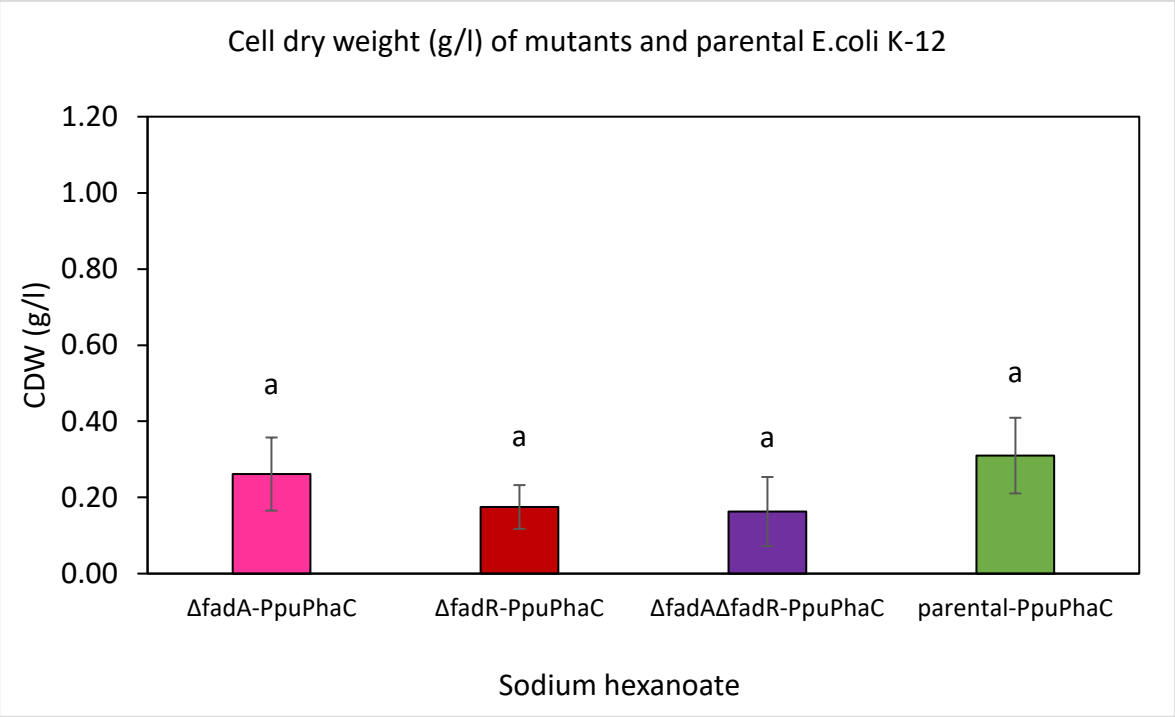

***Figure 61**. Comparison of means of the biomass accumulation from the cultivation of E. coli-K12 fadA and fadR single mutants, the double fadAfadR mutant and the parental strain expressing the plasmid pBAD-PpuPhaC. Same letters indicate statistically equal values whereas different letters indicate statistically different according to Tukey with 95% confidence. Cultivations were done in triplicate.*

5.3.4. Bacteria cultivation and PHA production

Dry biomass from the cultivation of recombinant Δ*fadA*Δ*fadR Escherichia coli*-K -12 expressing the plasmids pBAD -*PmePhaC-MtubfabG* , pBAD - *PstzPhaC-MtubfabG* and pBAD -*PpuPhaC-MtubfabG* in the presence of sodium tetradecanoate (C14) as β-oxidation substrate were weighted and then digested for determination of PHA content. An *E. coli* culture with no plasmid was added as control. Biomass accumulation between the 4 cultures is statistically equal according to Tukey (P≤0.05) (**Figure 62**)

Table 27. Co-expression of *fabG* with different PhaCs using sodium tetradecanoate (C14) as substrate and Δ*fadA*Δ*fadR -E. coli* K-12 as host . Cultures were incubated 37℃, 200 rpm for 48 hours after arabinose induction (0.2% (w/v)).

Host	PhaC source	FabG source	Substrate 0.5% (w/v)	CDW (g/l)	GC-FID µg/l
ΔFadA ΔFadR *E. coli*	*P. mendocina*	*M.tub*	C14	0.487±0.067 a	Non-detectable
	P. stutzeri	*M. tub*	C14	0.483±0.080 a	Non-detectable
	P.putida	*M. tub*	C14	0.661±0.092 a	Non-detectable
	control	*M. tub*	C14	0.590±0.118 a	Non-detectable

Each culture was grown trice and the value presented is the mean ± the standard deviation. Means with different letters are significantly different according to Tukey (P≤0.05). Abbreviation: CDW, cell dried weight; GC-FID, gas chromatography- flame ionization detector; GC-MS, gas chromatography- mass spectrometry.

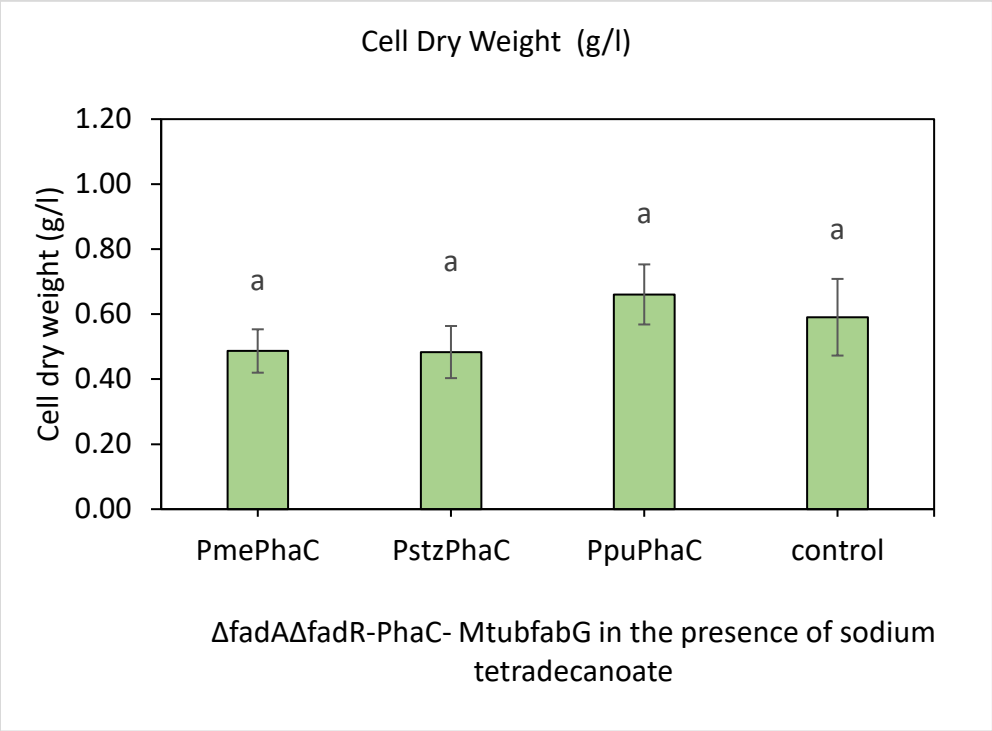

***Figure 62**. Comparison of CDW (g/l) accumulation between cultures of recombinant ΔfadAΔfadR E. coli-K12 expressing fabG from M. tuberculosis and PhaC from 3 different Pseudomonas (P. mendocina, P. stutzeri and P. putida) . Sodium tetradecanoate was used as a β-oxidation substrate. Values were compared statistically according to Tukey (P≤0.05). Same letters represent statistically equal groups.*

5.4. Discussion and future perspectives

For this **Chapter 5,** growth curves were constructed to evaluate the effect of the single mutations Δ*fadA* and Δ*fadR* and of the double mutation Δ*fadA*Δ*fadR* over *Escherichia coli* K12 growth in the presence of the medium chain-length fatty acid (MCFA) sodium hexanoate as β-oxidation substrate. Hexanoate was selected because, unlike sodium tetradecanoate used for previous chapters, it is soluble in water and does not interfere with the optical density measurement of the culture needed to successfully build the curves . However, as mentioned previously, only long chain-length fatty acids (LCFA) bind with the β-oxidation repressor FadR resulting in the activation of this pathway. Therefore, only the single mutant Δ*fadR* strain, expressing the β-oxidation pathway constitutively, was expected to uptake and fully metabolise hexanoate (MCFA) as a carbon source and, as consequence, to accumulate higher biomass than the parental strain, the Δ*fadA* mutant and the Δ*fadA*Δ*fadR* double mutant. Yet, that does not seem to be the case in this study where the parental strain accumulated the highest amount of biomass (0.70 g/l) followed by Δ*fadA* (0.60 g/l), Δ*fadR* (0.37 g/l) and by Δ*fadA*Δ*fadR* (0.13 g/l). These differences were proven to be statistically significant according to Tukey (95% confidence). (**Figure 58** and **59**)

One reason for this could be that even though the β-oxidation pathway is constitutively being expressed in the *fadR* mutant, the pathway is still not being capable of metabolizing sodium hexanoate and, as a result, it is not successfully being converted into biomass. This theory was based on the observations from a previous research that reported a mutant *fadR E. coli* strain growing well on decanoic acid but slow in octanoic acid and failed to grow at all on hexanoic acid [363]

Other possible explanation could be that there is metabolic burden associated with the cell investing energy to constitutively express all the enzymes from the β-oxidation pathway. Metabolic burden is known to reduce growth rate and final cell density [364]

Another observation is that the Δ*fadA* mutant is the only strain that exhibits a death curve after approximately only 8 hours of cultivation. In this strain, because FadA enzyme has been deleted, it is expected to be a surplus of the β-oxidation pathway intermediate 3-keto-acyl-CoA whose presence might be shutting off the pathway entirely resulting in the overaccumulation of fatty acids inside the cell (mainly sodium hexanoate). Excess of fatty acids are toxic for *Escherichia coli* and overaccumulation could be ultimately leading to cell death [365, 366]

The presence of common expression vectors also represents a metabolic burden for the cell [364, 367-369] and this study is no exception. As it can be observed in **Figure 60** and **Figure 61**, biomass collected from recombinant *E. coli* is lower than the one collected from the non-recombinant mutants (**Figures 58** and **59**), which means that there is metabolic burden associated with the presence of the pBAD-*PuPhaC* plasmid inside *E. coli.* [370] Studies have shown that the burden is there for the maintenance of the plasmid whether or not the recombinant protein of interest is being expressed [364]

Finally, for this experimental chapter, the double mutant ΔfadAΔ*fadR* was transformed with the plasmids pBAD-*PpuPhaC-MtubfabG*, pBAD-*PmePhaC-MtubfabG*, and pBAD-*PstzPhaC-MtubfabG* and the 3 cell cultures were fed with sodium tetradecanoate to produce PHA with 14 carbon-chain-length monomer but, unlike other studies, we were nos successful again in producing PHAs. For example, *E. coli* double knockout Δ*fadA*Δ*fadR* strain denominated as JMU194 was used as a host by Ren, Sierro, Witholt and Kessler [329] to coexpress PhaC and FabG from *Pseudomonas* and they found a final PHA accumulation of 20% with a predominant hydroxyoctanoate monomer composition.

In future, the growth curves should be constructed again using a defined culture media instead of the 2×YT used in this study to delete any background fatty acid that could be coming from the yeast. [371] Then, this culture medium should be analysed by GC at

different cultivation times to accurately measure sodium hexanoate consumption by the mutants. Also fatty acids of other chain lengths should be tested to prove if *fadR* mutants confers the host the ability of metabolizing a wider range of fatty acids (MCFA and LCFA) compared with the parental strain (only LCFA) . But, most importantly, the system (double mutant host expressing PhaC and FabG) should be further optimize for production of PHA with high hydroxytetradecanoate monomer composition. To achieve this, several approaches can be adopted, for example : the plasmid can be substituted for a higher copy number plasmid or other PhaCs and FabG can be tested for higher activity and substrate affinity. SDS-PAGE can also be done to monitor the proper expression of both enzymes inside the host.

CHAPTER 6

Expression of PhaCs from
Pseudomonas sp.
in
Escherichia coli.

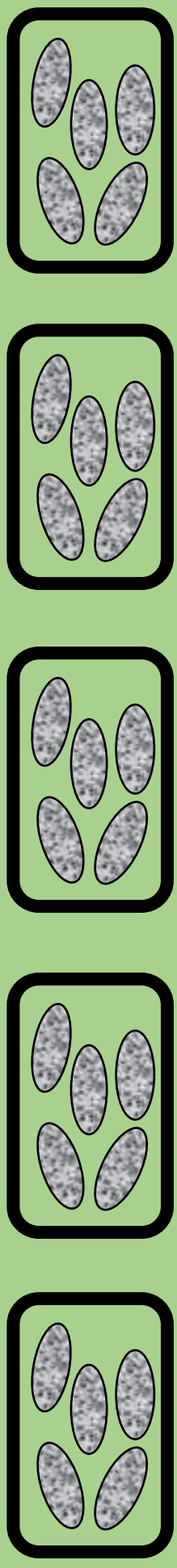

CHAPTER 6: Construction of new plasmids to express PhaC-MtubfabG enzymes

6.1. Introduction

As observed in previous **Chapters 3,4 and 5** of this project, the production of PHA in our cell system remains below quantification levels using GC-FID. As mentioned in these previous chapters one plausible explanation could be the low or lack of PhaC expression from the plasmid. In this regard an alignment between the pBAD promoter in the plasmid used so far and the pBAD promoter of a commercial plasmid expressing the mPlum fluorescent protein[372] was undertaken and a 2 base pair mutation was found in the promoter of the plasmid used in previous chapters (Refer to **Figure 63**).

```
Query  241  ATCTTACCTGACGCTTTTTATCGCAACTCTCTACTGTTTCTCCAT  285
            ||  ||||||||||||||||||||||||||||||||||||||||
Sbjct  241  ATACTACCTGACGCTTTTTATCGCAACTCTCTACTGTTTCTCCAT  285
```

***Figure 63**. Alignment between the araBAD promoter sequence in the plasmid from **Chapters 3,4** and **5** and pBAD promoter from a new plasmid.*

It is possible that this mutation could have been interfering with expression all along. Therefore, for this last experimental **Chapter 6** it was decided to re-build the set of plasmids for co-expression of PhaC and FabG enzymes and detect protein expression.

Another consideration for this **Chapter 6** was the expression of the mPlum fluorescent protein as a positive control of protein expression using the new plasmid.

6.2. Materials and methods

List of detailed information on the materials used (reagents, kits, equipment, software, media preparation and miscellaneous) can be found in **Appendix 1-5.** Strains, plasmids and primers are shown in **Table 29.**

Table 28. Lists of strains and plasmids used for this **Chapter 6**.

Strains	Relevant genotype	Source or reference
E. coli DH5α	F-, Δ(argF-lac)169, ϕ80dlacZ58(M15), ΔphoA8, glnX44(AS), λ-, deoR481, rfbC1?, gyrA96(NalR), recA1, endA1, thiE1, hsdR17	Thermofisher
Plasmids		
pBAD-*mPlum*	P_{BAD} promoter, mPlum fluorescence protein	[372]
pBAD-*PmePhaC-MtubfabG*	P_{BAD} promoter, *phaC* from *P. mendocina*, and *fabG* from *M. tuberculosis* Amp^R	This study
pBAD-*PstzPhaC-MtubfabG*	P_{BAD} promoter, *phaC* from *P. stutzeri*, and *fabG* from *M. tuberculosis* Amp^R	This study
pBAD-*PpuPhaC-MtubfabG*	P_{BAD} promoter, *phaC* from *P. putida and fabG from M. tuberculosis*, Amp^R	This study
Primers		
XhoI-*PpuPhaC* forward	TATAT CTCGAG CATG AGC AAC AAA AAC AAT G	
XhoI-*PmePhaC* forward	ATAAA CTCGAG CATG CGT GAC AAA TCT AAC	
XhoI-*PstzPhaC* forward	ATATA CTCGAG AATG CGT GAC AAA CCG AAC	
EcoRI-*MtubfabG* reverse	TATAT GAATTC CTCT TAA TGC CCC ATC CCC ATC	
pBAD clone check	ATG CCA TAG CAT TTT TAT CC GAT TTA ATC TGT ATC AGG	

6.2.1. Expression of mPlum protein using a new backbone

The purchased pBAD-*mPlum* [372] was shipped already transformed inside *E. coli* DH5α and we proceeded to grow it overnight in 2×YT media (tryptone 16 g/l, yeast 10 g/l, NaCl 5 g/l) (37°C, 200 rpm) with ampicillin (100 µg/ml). The next day the culture was adjusted to an OD_{600}≈0.03 in 100 µl of fresh media, ampicillin (100 µg/ml) and arabinose (0.2% w/v) to induce the fluorescence expression and the culture was left to grow for 24 hours (37°C, 200 rpm) in a 96 well plate reader. A negative control without arabinose was also used. Both growth curves were done by triplicate but only the average was used for the construction of the graphs.

Fluorescence was measured using 584 nm excitation and 620 nm emission wavelengths. Absorbance of cells was measured using optical density at 600 nm and these values were used to estimate the number of cells using the polynomial degree equation from Mira, Yeh and Hall [362]

6.2.2. Construction of new plasmids, and clone check

DNA preparation, construction of new plasmids, clone check and storage were done using the exact same reactants and methods than in previous **Chapter 3** and **Chapter 4.**

For this **Chapter 6** the restriction enzymes chosen were XhoI and EcoRI from New England Biolabs. The plasmid used was a gift from Michael Davidson & Roger Tsien (Addgene plasmid # 54564 ; http://n×t.net/addgene:54564 ; RRID:Addgene_54564). [372]

The *phaC-MtubfabG* fragments used for cloning were amplified using the pBAD-*PhaC-MtubfabG* plasmids from **Chapter 4** as template. Maps of the resulting plasmids are shown in **Figure 64**

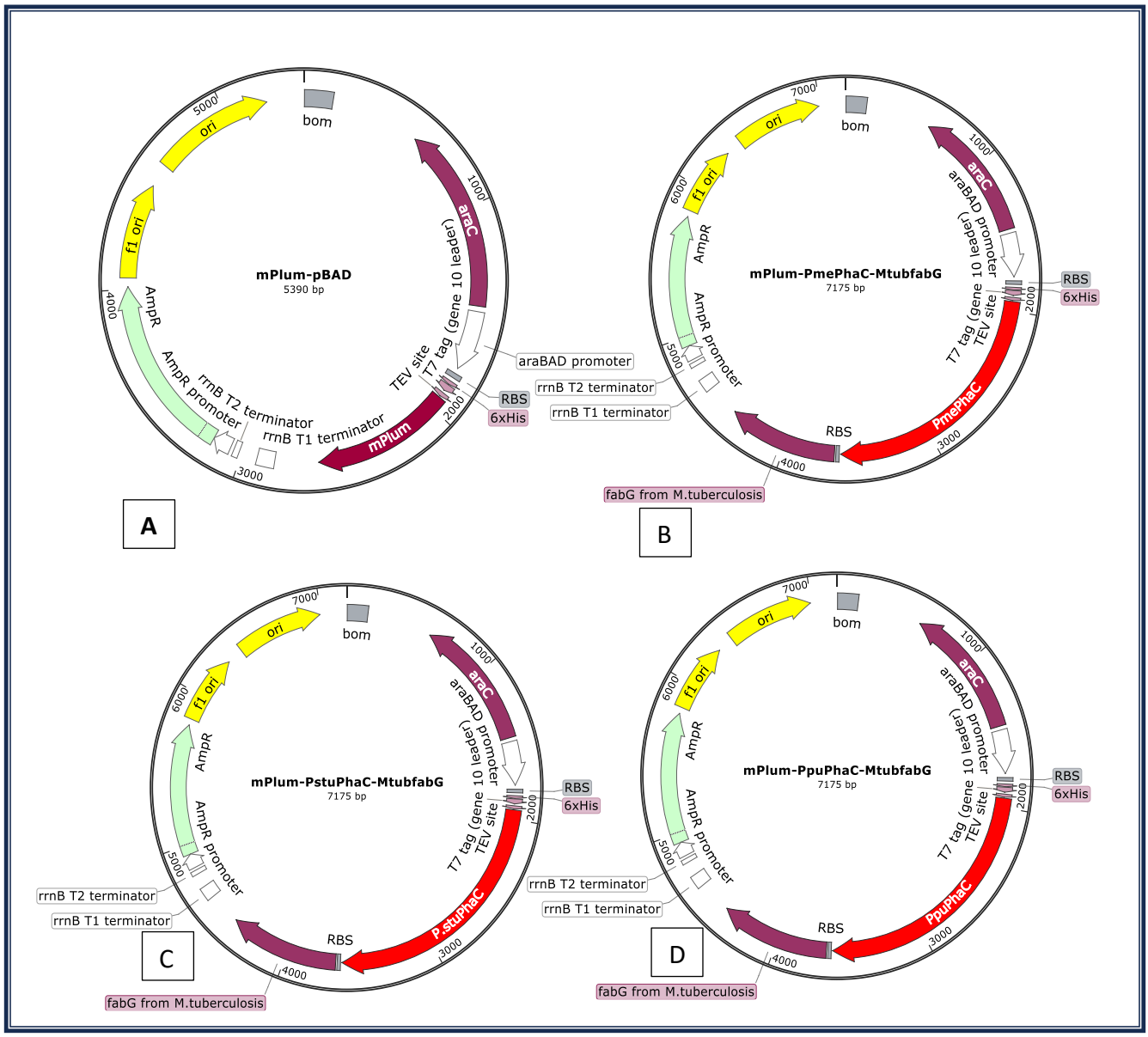

Figure 64. *Plasmids maps were pBAD promoter was used to express A) mPlum fluorescence protein, B) PmePhaC-MtubfabG, C) PstzPhaC-MtubfabG, D) PpuPhaC-MtubfabG*

6.2.3. SDS-PAGE for protein expression

With the purpose of knowing if the different PhaCs are expressed along with FabG from *M. tuberculosis* inside *E. coli* DH5α a proteomic profile was built using SDS-PAGE gel separation. [320] The protocol used to prepare and run the samples was the same described in the methods section from **Chapter 3** with the exception that, for this **Chapter 6**, pBAD-*mPlum* was used as a positive control of protein expression and a transformant cultivated without arabinose was used as a negative control. Another difference is that the gel was revealed using a quicker method with Coomassie Blue [373]

6.3. Results

6.3.1. Expression of mPlum using a new backbone

Growth curves of recombinant *Escherichia coli* DH5α transformed with pBAD-*mPlum* in the presence or absence of the inducer arabinose are shown in **Figure 65** and **Figure 66** respectively. **Figure 65** shows successful expression and fluorescence of the mPlum protein over time in the presence of arabinose, reaching the maximum detectable fluorescence level after only 7 hours of growth. In contrast and as expected, the culture without the inducer arabinose shows no fluorescence over time (**Figure 66**). Both growth curves show similar growth rate, duplication time and reach similar final cell densities measured as OD_{600} (**Figure 65** and **Figure 66**).

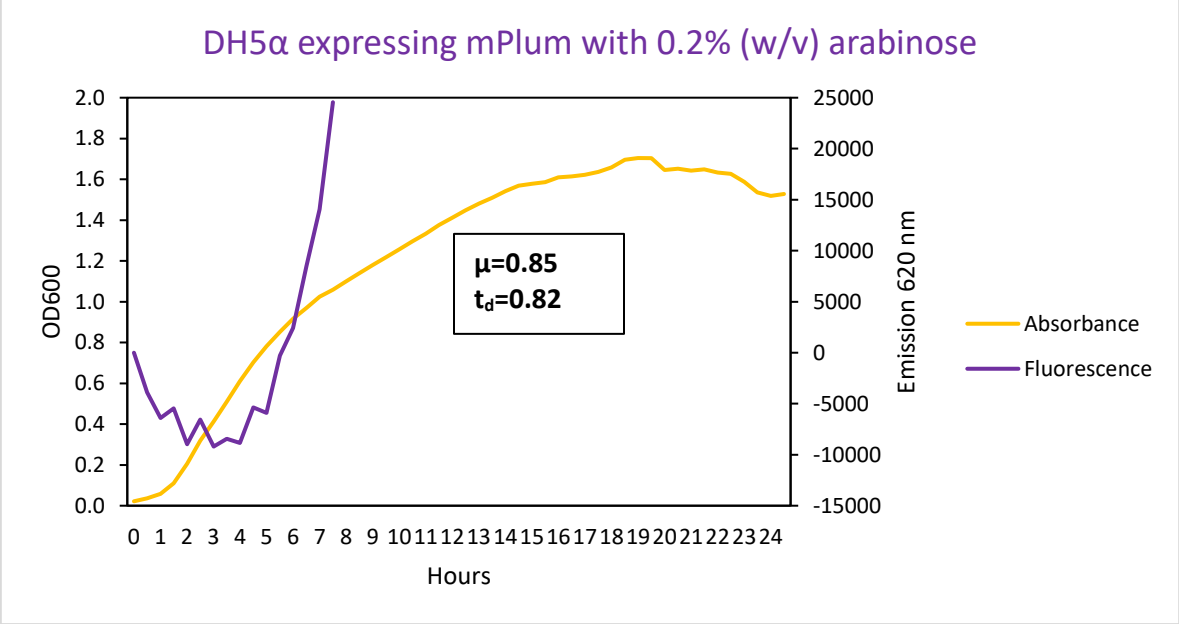

Figure 65. *Growth curve for E. coli DH5α expressing the fluorescence protein mPlum under the pBAD promoter and in the presence of arabinose 0.2% (w/v). Growth rate* ***μ*** *and duplication time* $\boldsymbol{t_d}$ *are indicated. The curves were done in triplicate and the average values were used to build this figure.*

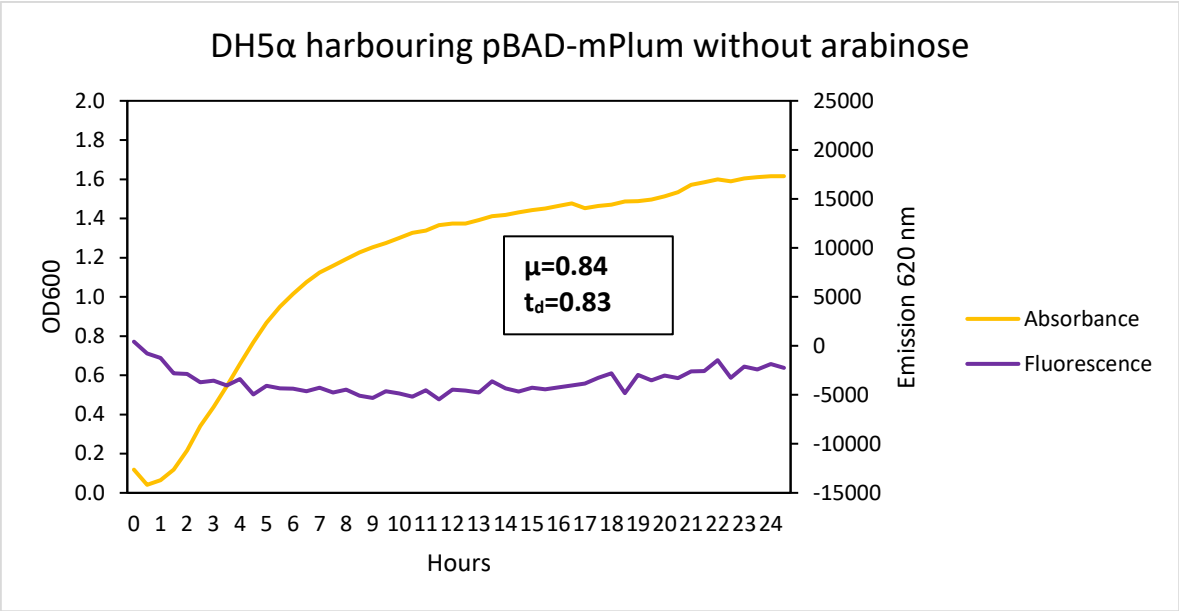

***Figure 66**. Growth curve for E. coli DH5α harbouring the pBAD-mPlum plasmid without arabinose. Growth rate **μ** and duplication time **t_d** are indicated. The curves were done in triplicate and the average values were used to build this figure.*

6.3.2. Construction of new plasmids, and clone check

For this **Chapter 6**, a new backbone pBAD-*mPlum* using the same promoter pBAD but without the 2-base mutation found previously was used. *phaC-MtubfabG* fragments were successfully amplified and cloned into the new backbone using restriction digestion-ligation method. Each transformation resulted in approximately 100 colonies from which 2 to 5 colonies were screened for clone check using the pre-designed pBAD primers from **Table 29** . The forward primer anneals on the araBAD promoter region which is 219 bp upstream from the *phaC* gene and the reverse primer anneals 45 bp downstream from the stop codon of MtubfabG.

Successful colonies resulted in a 2768 bp product while unsuccessful clones resulted in a 983 bp product that corresponded to the *mPlum* gene of the original plasmid. (Refer to **Figure 67**).

DNA Ladder 1 kb
Quick-Load®

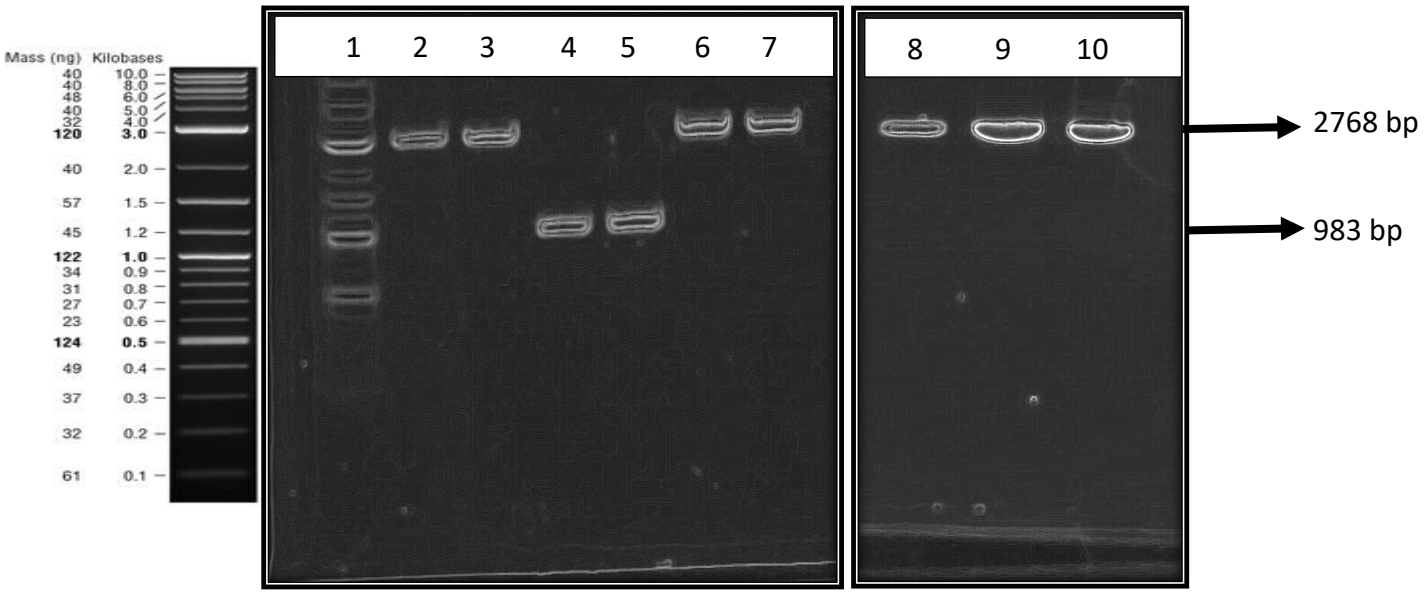

***Figure 67**. Electrophoresis for the successful construction of pBAD-PhaC-MtubfabG plasmids were lane 1) ladder, 2) PmePhaC-MtubfabG colony 1 → positive, 3)PmePhaC-MtubfabG colony 2 → positive, 4) PstzPhaC-MtubfabG colony 1 → negative, 5) PstzPhaC-MtubfabG colony 2 → negative, 6)PpuPhaC-MtubfabG colony 1 → positive, 7)PpuPhaC-MtubfabG colony 2 → positive, 8) PstzPhaC-MtubfabG colony 3 → positive, 9) PstzPhaC-MtubfabG colony 4 → positive, 10)PstzPhaC-MtubfabG colony 5 → positive.*

6.3.3. SDS-PAGE for protein expression.

The proteomic profiles of recombinant *E .coli* DH5α harbouring the constructed new plasmids were investigated using SDS-PAGE and the results are shown in **Figure 68.**

The different lanes correspond (in this order) to the ladder, the plasmids: pBAD-*PmePhaC-MtubfabG* , pBAD-*PstzPhaC-MtubfabG* and pBAD-*PpuPhaC- MtubfabG* plus the positive control pBAD-*mPlum* and a negative control where the recombinant cells harbouring the plasmid pBAD-*PmePhaC-MtubfabG* were grown without the arabinose inducer.

All three PhaC proteins (PmePhaC, PstzPhaC, PpuPhaC) from the 3 different plasmids were successfully expressed and are shown in **Figure 68.** Each protein band weights ≈66 KDa which corresponds to the 62.8 KDa weight of the PhaC enzyme plus ≈3 KDa from the His tag, T7 tag and the TEV site sequences. However the FabG protein (25.7 KDa) is not visible in either of the 3 cases indicating that it might have not been expressed properly. Successful expression of the mPlum protein (25.6 KDa +3 KDa) used as positive control can also be observed in **Figure 68.** Cultivation, induction, and SDS-PAGE was performed in duplicate (Shown in **Annex 7**).

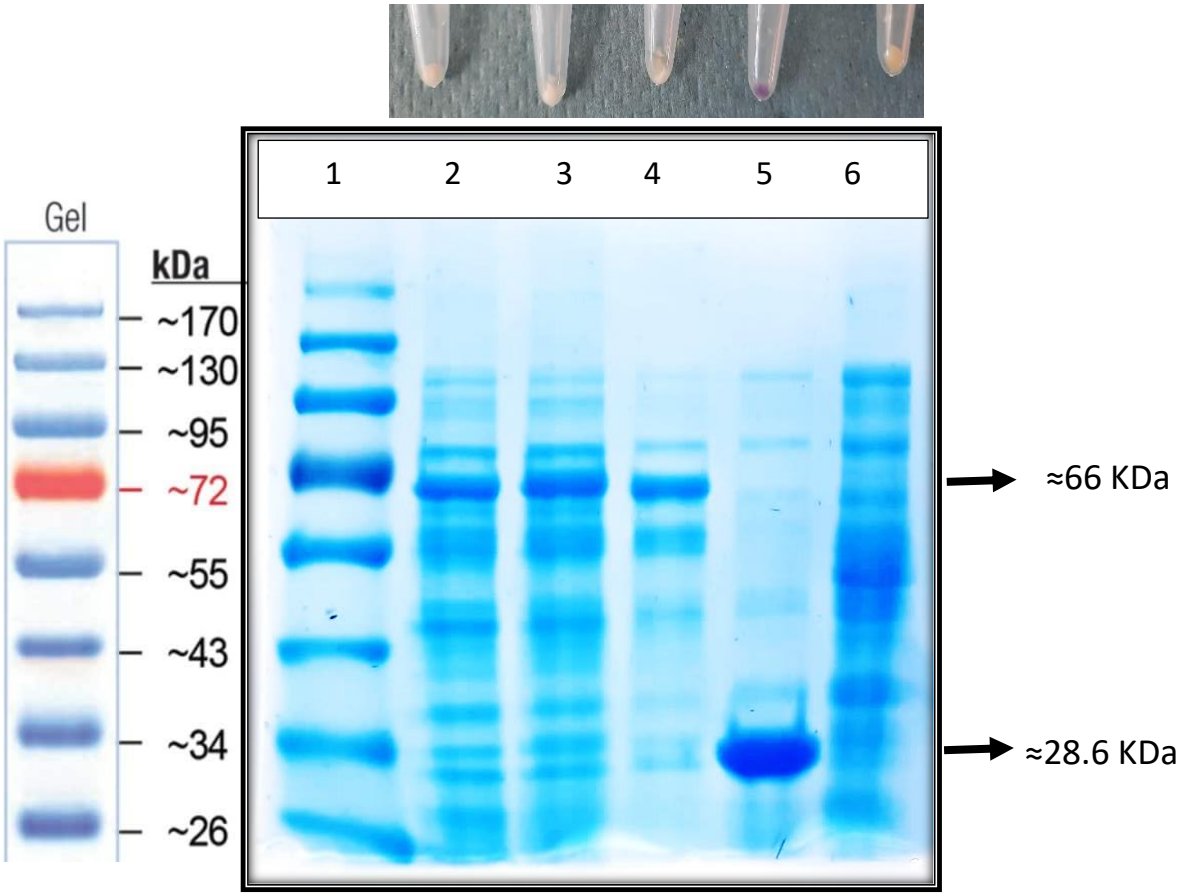

Figure 68. *Proteomic profile of recombinant Escherichia coli where lane 1) is the ladder, 2) E. coli expressing pBAD-PmePhaC-MtubfabG, 3) pBAD-PstzPhaC-MtubfabG, 4) pBAD-PpuPhaC-MtubfabG, 5)pBAD-mPlum 6) control with no arabinose. Cultivation, induction, and SDS-PAGE was done 2 times.*

6.4. Discussion and future perspectives

The pBAD promoter is a commonly used promoter for heterologous protein expression because it has several advantages such as high protein expression levels, induction by the inexpensive monosaccharide L-arabinose and tight regulation of transcription. [294] However, at this point in the project it was discovered that the pBAD promoter used for **Chapter 3, 4** and **5** has a 2-base mutation that might potentially be interfering with proper expression of the proteins of interest, therefore for this **Chapter 6,** it was decided to acquire a new plasmid backbone with the correct pBAD promoter sequence and re-do the gene cloning. It was also decided that a positive control was needed to monitor successful protein expression inside our host.

Results show successful expression of the mPlum fluorescence protein at 620 nm [374] over time and the correspondent 28.6 KDa band is observed using SDS-PAGE. Correspondingly, a 66 KDa band is successfully observed when PhaC is being expressed instead of mPlum using the same backbone. However, the same SDS-PAGE results show the second gene added to the expression cassette is not present in the cell (FabG from *M. tuberculosis*).

There is plenty of evidence on the existence of operons in bacterial cells, which are a cluster of genes under the control of a single promoter [375] Nonetheless, there is also several evidence showing that in an operon the level of protein expression for each gene is not equal and it is directly influenced by the distance between the gene and the promoter being the closest gene the strongest expressed, and so forth. [376, 377] In this case in particular, the second gene seems to be either too weakly expressed to be observed in the gel or not being expressed altogether.

In future experiments an extra promoter could be cloned upstream from the *fabG* gene to ensure its proper and equal level of expression with regards to the *phaC* gene.

Additionally, we could add a Histidine tag for protein purification with a Ni-NTA affinity chromatography column[378] and/or a T7 protein tag for protein detection through immunoblotting, immunoprecipitation or immunostaining. [379] Both tags are already present in the mPlum positive control and in the three *phaCs* but not in *MtubfabG* sequence. Tags would be used to further confirm the expression of our proteins of interest apart from the SDS-PAGE gel.

CHAPTER 7

Concluding remarks
and
future work

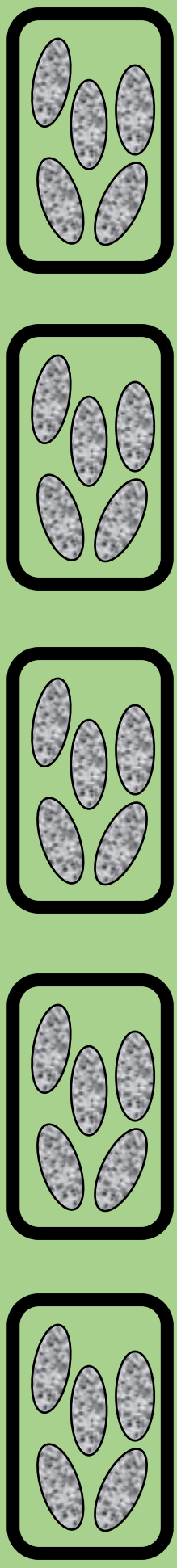

CHAPTER 7 : Concluding remarks and future work.

This study was undertaken with the purpose of engineering the metabolism of *E. coli* for the synthesis of a novel mcl-PHA with high hydroxytetradecanoate (≥30%) monomer composition. The final optimized strain achieved in this thesis was a Δ*fadA*Δ*fadR* mutant recombinant strain and a set of plasmids for the expression of 3 different PhaCs (PHA synthases).

As a first step for the project, and with the purpose of identifying, characterizing and quantifying the PHA present in all samples throughout this thesis project, standard curves were built for all possible PHA monomers (C4, C6, C8, C10, C12 and C14) (**Chapter 2**). Standard curves for the identification of the culture media's fatty acid substrates C12 and C14 were also built. Additionally, an acid methanolysis digestion method was successfully validated for conversion of commercial polyhydroxybutyrate into volatile methyl esters that can be detected through gas chromatography. Standard curves of other carbon-chain-length fatty acids can be constructed, in the future, so that other fatty acid substrates could be tested in the strain constructed.

In following experiments (**Chapter 2 and Chapter 3**) 3 different PHA synthases (*PmePhaC, PstzPhaC, PpuPhaC)* were cloned in DH5α *E. coli* and the Δ*fadA E. coli* K-12 mutant using the β-oxidation substrates sodium dodecanoate (C12) and sodium tetradecanoate (C14) as carbon sources. Effects of the β-oxidation inhibitor sodium acrylate was also evaluated. Results show no PHA at detectable levels in any of the experiments. As intracellular accumulation of PHA can be low due to many factors including low intracellular precursor concentrations, it was decided to engineer *E. coli* to enhance the intracellular concentration of 3-hydroxyacyl-CoA by heterologous expression of FabG from *M. tuberculosis* in *E. coli*. Therefore, in **Chapter 4**, an attempt was made to co-express FabG enzyme along with PhaC in the same plasmid. It was also decided to build the double knockout Δ*fadR*Δ*fadA E. coli* to further increase the availability of substrate inside the cell

for mcl-PHA production (**Chapter 5**). Gene cloning of both genes *phaC* and *fabG* throughout the project and DNA recombination used for *fadR* gene deletion were successful. Unfortunately, the intracellular quantities of PHA measured were still below the limit of quantification indicating that low intracellular precursor concentration may not be the sole bottleneck for mcl-PHA production in the engineered *E. coli* strain.

It was hypothesized that there was a protein expression problem all along our experimental chapters, therefore, as a last attempt to polymerize PHA, the 3 *phaC* genes and *fabG* from *M. tuberculosis* were cloned once more in a new backbone. This time, an extra plasmid coding for the fluorescent protein mPlum was also monitored as a positive control for protein expression in our new construct. SDS-PAGE showed successful expression of the PhaC enzymes in all 3 cases, but FabG expression seems to be absent.

In the near future, further engineering biology strategies could be applied to upregulate the heterologous expression of the cloned *fabG* by adding an extra promoter to our plasmids. Once this has been done, the new constructs must be expressed in Δ*fadA*Δ*fadR E.coli* so that we can proceed to validate, characterize, and quantify PHA production in our novel metabolically engineered *E. coli* system. Other techniques, aside the GC method used in this work, could be used to qualitatively validate PHA presence such as Nile blue/red staining and microscopy.

After the PHA has been successfully produced and extracted, the material must be investigated to determine its specific physical-chemical properties (melting temperature, tensile strength etc.) and deliberate on its potential use in the medical field or as a plastic-replacement in any other field.

To achieve the impact of the extracted PHA in the identified field, subsequent future efforts should focus on setting up scale-up experiments for optimization of the industrial production process. For example, literature suggests that PHA production improves when

cells are grown in a fed-batch bioreactor rather than in continuous bioreactors. [97] Other growing parameters such as temperature, pH and aeration should also be considered for optimization. Efforts should also continue for the use of cost-effective substrates to make the material competitive in the market against petroleum-based plastic.

One of the difficulties of mcl-PHA production industrially using native producers such as *Pseudomonas* is the control of the monomer composition of mcl-PHA because some of these strains contain several copies for each gene of the β-oxidation pathway, for example *P. entomophila* has 6 different genes that code for the FadA enzyme and 2 for FadB [380] and the overall substrate-product flux for all of these enzymes is hard to control. On top of this, PhaC substrates can also be channelled from the fatty acid biosynthesis pathway creating more variability on the final product of the polymer. [326]

The novelty of our work relies on the use of a metabolically simpler host (*E. coli*) which natively only contains one copy of the gene encoding the FadA enzyme. The deletion of this gene would therefore interrupt the cyclical β-oxidation pathway ensuring that monomers containing the same chain length would preferentially accumulate within the *E. coli* host, increasing the probability of producing a homopolymer of mcl-PHA, which would be maintained during scale up under aerobic conditions. The deletion of FadR would further contribute to control the PHA monomer composition and yield because FadR has a dual effect as β-oxidation repressor [249, 344] and a fatty acid biosynthesis activator. [354-356] In other words, our novel Δ*fadA*Δ*fadR* *E. coli* strain expresses an incomplete β-oxidation pathway constitutively and does not express the fatty acid biosynthesis pathways which makes it a valuable host for mcl-PHA homopolymer production.

Additionally, PHA with high C12 and/or C14 monomer composition is a novel polymer that, as mentioned before, is currently not being produced industrially and its study in lab-scale remains limited.[150] Due to constraints in time, PHA production and evaluation using each of the 3 different PhaCs was not possible, however the comparison

of these enzymes and the selection of one for enhanced production of this polymer is a novel idea presented in this project. The potential use of FabG from *M. tuberculosis* to produce a new mcl-PHA is also a novel idea presented in this work that can be used for further research.

REFERENCES

1. Hardin, T., Vol. 2024 (Copyright © Plastic Oceans International, 2022).
2. Das, M., Manda, B. & Katiyar, V. Sustainable routes for synthesis of poly (ε-caprolactone): Prospects in chemical industries. (Springer, Singapore; 2020).
3. Saitou, N. & Nei, M. The neighbor-joining method: a new method for reconstructing phylogenetic trees. *Molecular Biology and Evolution* **4**, 406-425 (1987).
4. Li, G. et al. in Molecules, Vol. 25 (2020).
5. Bhagwat, G. et al. Benchmarking Bioplastics: A Natural Step Towards a Sustainable Future. *Journal of Polymers and the Environment* **28**, 3055-3075 (2020).
6. Siracusa, V. & Blanco, I. in Polymers, Vol. 12 (2020).
7. Evans, D.A. History of the Harvard ChemDraw Project. *Angewandte Chemie International Edition* **53**, 11140-11145 (2014).
8. Hisano, T. et al. The Crystal Structure of Polyhydroxybutyrate Depolymerase from Penicillium funiculosum Provides Insights into the Recognition and Degradation of Biopolyesters. *Journal of Molecular Biology* **356**, 993-1004 (2006).
9. Eddy, S.R. Where did the BLOSUM62 alignment score matrix come from? *Nature Biotechnology* **22**, 1035-1036 (2004).
10. Barletta, M. et al. Poly(butylene succinate) (PBS): Materials, processing, and industrial applications. *Progress in Polymer Science* **132**, 101579 (2022).
11. Jalabert, M., Fraschini, C. & Prud'homme, R.E. Synthesis and characterization of poly(L-lactide)s and poly(D-lactide)s of controlled molecular weight. *Journal of Polymer Science Part A: Polymer Chemistry* **45**, 1944-1955 (2007).
12. Jian, J., Xiangbin, Z. & Xianbo, H. An overview on synthesis, properties and applications of poly(butylene-adipate-co-terephthalate)–PBAT. *Advanced Industrial and Engineering Polymer Research* **3**, 19-26 (2020).
13. Chen, G.-Q., Chen, X.-Y., Wu, F.-Q. & Chen, J.-C. Polyhydroxyalkanoates (PHA) toward cost competitiveness and functionality. *Advanced Industrial and Engineering Polymer Research* **3**, 1-7 (2020).
14. Baker, M.I., Walsh, S.P., Schwartz, Z. & Boyan, B.D. A review of polyvinyl alcohol and its uses in cartilage and orthopedic applications. *Journal of Biomedical Materials Research Part B: Applied Biomaterials* **100B**, 1451-1457 (2012).
15. Rishi, V. et al. Utilization of kitchen waste for production of pullulan to develop biodegradable plastic. *Applied Microbiology and Biotechnology* **104**, 1307-1317 (2020).
16. Guilbert, S., Morel, M.-H., Gontard, N. & Cuq, B. in Feedstocks for the Future, Vol. 921 334-350 (American Chemical Society, 2006).
17. Patni, N., Yadava, P., Agarwal, A. & Maroo, V. An overview on the role of wheat gluten as a viable substitute for biodegradable plastics. **30**, 421-430 (2014).
18. Patnaik, S., Panda, A.K. & Kumar, S. Thermal degradation of corn starch based biodegradable plastic plates and determination of kinetic parameters by isoconversional methods using thermogravimetric analyzer. *Journal of the Energy Institute* **93**, 1449-1459 (2020).
19. Wang, J., Wang, L., Gardner, D.J., Shaler, S.M. & Cai, Z. Towards a cellulose-based society: opportunities and challenges. *Cellulose* **28**, 4511-4543 (2021).

20. Merino, D., Paul, U.C. & Athanassiou, A. Bio-based plastic films prepared from potato peels using mild acid hydrolysis followed by plasticization with a polyglycerol. *Food Packaging and Shelf Life* **29**, 100707 (2021).
21. Zhou, Y., He, Y., Lin, X., Feng, Y. & Liu, M. Sustainable, High-Performance, and Biodegradable Plastics Made from Chitin. *ACS Applied Materials & Interfaces* **14**, 46980-46993 (2022).
22. Gheorghita, R., Gutt, G. & Amariei, S. in Coatings, Vol. 10 (2020).
23. Geyer, R., Jambeck, J.R. & Law, K.L. Production, use, and fate of all plastics ever made. *Science Advances* **3**, e1700782.
24. Zalasiewicz, J. et al. The geological cycle of plastics and their use as a stratigraphic indicator of the Anthropocene. *Anthropocene* **13**, 4-17 (2016).
25. Crutzen, P.J. in Earth System Science in the Anthropocene. (eds. E. Ehlers & T. Krafft) 13-18 (Springer Berlin Heidelberg, Berlin, Heidelberg; 2006).
26. Laist, D.W. in Marine Debris: Sources, Impacts, and Solutions. (eds. J.M. Coe & D.B. Rogers) 99-139 (Springer New York, New York, NY; 1997).
27. Kumar, R. et al. Micro(nano)plastics pollution and human health: How plastics can induce carcinogenesis to humans? *Chemosphere* **298**, 134267 (2022).
28. Atiwesh, G., Mikhael, A., Parrish, C.C., Banoub, J. & Le, T.-A.T. Environmental impact of bioplastic use: A review. *Heliyon* **7**, e07918 (2021).
29. Fredi, G. & Dorigato, A. Recycling of bioplastic waste: A review. *Advanced Industrial and Engineering Polymer Research* **4**, 159-177 (2021).
30. Bioplastics, E. in European Bioplastics, Vol. 2024 (Berlin, Germany.
31. Emadian, S.M., Onay, T.T. & Demirel, B. Biodegradation of bioplastics in natural environments. *Waste Management* **59**, 526-536 (2017).
32. Nandakumar, A., Chuah, J.-A. & Sudesh, K. Bioplastics: A boon or bane? *Renewable and Sustainable Energy Reviews* **147**, 111237 (2021).
33. Jabeen, N., Majid, I. & Nayik, G.A. Bioplastics and food packaging: A review. *Cogent Food & Agriculture* **1**, 1117749 (2015).
34. Zikmanis, P., Kolesovs, S. & Semjonovs, P. Production of biodegradable microbial polymers from whey. *Bioresources and Bioprocessing* **7**, 36 (2020).
35. Rehm, B.H.A. Bacterial polymers: biosynthesis, modifications and applications. *Nature Reviews Microbiology* **8**, 578-592 (2010).
36. Moradali, M.F. & Rehm, B.H.A. Bacterial biopolymers: from pathogenesis to advanced materials. *Nature Reviews Microbiology* **18**, 195-210 (2020).
37. Hazenberg, W. & Witholt, B. Efficient production of medium-chain-length poly(3-hydroxyalkanoates) from octane by Pseudomonas oleovorans: economic considerations. *Applied Microbiology and Biotechnology* **48**, 588-596 (1997).
38. Lenz, R.W. & Marchessault, R.H. Bacterial Polyesters: Biosynthesis, Biodegradable Plastics and Biotechnology. *Biomacromolecules* **6**, 1-8 (2005).
39. Stainer, W.R., Kunisawa, R. & Contopoulou, B. The role of organic substrates in bacterial photosynthesis. *Proceedings Natl. Acad. Science* **45**, 1246-1260 (1959).
40. Lemoigne, M. Produits de deshydration et de polymerisation de l'acide B-oxybutyric. *The Bulletin de la Société Chimique de France* **8**, 770-778 (1926).
41. Jendrossek, D. & Handrick, R. Microbial Degradation of Polyhydroxyalkanoates. *Annual Review of Microbiology* **56**, 403-432 (2002).
42. Steinbüchel, A. & Valentin, H.E. Diversity of bacterial polyhydroxyalkanoic acids. *FEMS Microbiology Letters* **128**, 219-228 (1995).

43. Anjum, A. et al. Microbial production of polyhydroxyalkanoates (PHAs) and its copolymers: A review of recent advancements. *International Journal of Biological Macromolecules* **89**, 161-174 (2016).
44. Noda, I., Green, P.R., Satkowski, M.M. & Schechtman, L.A. Preparation and Properties of a Novel Class of Polyhydroxyalkanoate Copolymers. *Biomacromolecules* **6**, 580-586 (2005).
45. Samrot, A.V., Avinesh, R.B., Sukeetha, S.D. & Senthilkumar, P. Accumulation of Poly[(R)-3-hydroxyalkanoates] in Enterobacter cloacae SU-1 During Growth with Two Different Carbon Sources in Batch Culture. *Applied Biochemistry and Biotechnology* **163**, 195-203 (2011).
46. Kessler, B., Weusthius, R., Witholt, B. & Eggink, G. Production of microbial polyesters: fermentation and downstream processes. *Advances in Biochemical Engineering/ Biotechnology* **71**, 159-182 (2001).
47. Lee, S.Y. Bacterial polyhydroxyalkanoates. *Biotechnology and Bioengineering* **49**, 1-14 (1996).
48. Olivera, E.R., Arcos, M., Naharro, G. & Luengo, J.M. in Plastics from Bacteria: Natural Functions and Applications. (ed. G.G.-Q. Chen) 133-186 (Springer Berlin Heidelberg, Berlin, Heidelberg; 2010).
49. Chen, G.-Q. & Wu, Q. Microbial production and applications of chiral hydroxyalkanoates. *Applied Microbiology and Biotechnology* **67**, 592-599 (2005).
50. Lu, J., Tappel, R. & Nomura, C. Mini-Review: Biosynthesis of Poly(hydroxyalkanoates). *Journal of Macromolecular Science®* **Part C: Polymer Reviews**, 226-248 (2009).
51. Wong, P.A.L., Chua, H., Lo, W., Lawford, H.G. & Yu, P.H. Production of specific copolymers of polyhydroxyalkanoates from industrial waste. *Applied Biochemistry and Biotechnology* **98**, 655-662 (2002).
52. Aragao, G.M.F., Lindley, N.D., Uribelarrea, J.L. & Pareilleux, A. Maintaining a controlled residual growth capacity increases the production of polyhydroxyalkanoate copolymers by Alcaligenes eutrophus. *Biotechnology Letters* **18**, 937-942 (1996).
53. Bates, F.S. & Fredrickson, G.H. Block Copolymer Thermodynamics: Theory and Experiment. *Annual Review of Physical Chemistry* **41**, 525-557 (1990).
54. Mantzaris, N.V., Kelley, A.S., Daoutidis, P. & Srienc, F. A population balance model describing the dynamics of molecular weight distributions and the structure of PHA copolymer chains. *Chemical Engineering Science* **57**, 4643-4663 (2002).
55. Stubbe, J. & Tian, J. Polyhydroxyalkanoate (PHA) homeostasis: the role of the PHA synthase. *Natural Product Reports* **20**, 445-457 (2003).
56. Jurasek, L. & Marchessault, R.H. Polyhydroxyalkanoate (PHA) granule formation in Ralstonia eutropha cells: a computer simulation. *Applied Microbiology and Biotechnology* **64**, 611-617 (2004).
57. López-Cortés, A., Lanz-Landázuri, A. & García-Maldonado, J.Q. Screening and Isolation of PHB-Producing Bacteria in a Polluted Marine Microbial Mat. *Microbial Ecology* **56**, 112-120 (2008).
58. Spiekermann, P., Rehm, B.H.A., Kalscheuer, R., Baumeister, D. & Steinbüchel, A. A sensitive, viable-colony staining method using Nile red for direct screening of bacteria that accumulate polyhydroxyalkanoic acids and other lipid storage compounds. *Archives of Microbiology* **171**, 73-80 (1999).
59. Hartman, T.L. The Use of Sudan Black B as a Bacterial Fat Stain. *Stain Technology* **15**, 23-28 (1940).

60. Porras, M.A., Villar, M.A. & Cubitto, M.A. Improved intracellular PHA determinations with novel spectrophotometric quantification methodologies based on Sudan black dye. *Journal of Microbiological Methods* **148**, 1-11 (2018).
61. MarketsandMarkets Polyhydroxyalkanoate (PHA) Market by Type (Short Chain Length, Medium Chain Length), Production Method (Sugar Fermentation, Vegetable Oil Fermentation, Methane Fermentation), Application, and Region - Global Forecast to 2024. *Markets and Markets*, 155 (2019).
62. Xanthos, D. & Walker, T.R. International policies to reduce plastic marine pollution from single-use plastics (plastic bags and microbeads): A review. *Marine Pollution Bulletin* **118**, 17-26 (2017).
63. in EU Circular Economy Package Vol. 2019 (
64. Chen, G.-Q. in Plastics from Bacteria: Natural Functions and Applications. (ed. G.G.-Q. Chen) 121-132 (Springer Berlin Heidelberg, Berlin, Heidelberg; 2010).
65. Chen, G.-Q. A microbial polyhydroxyalkanoates (PHA) based bio- and materials industry. *Chemical Society Reviews* **38**, 2434-2446 (2009).
66. Technavio 1-29 (2017).
67. Bio-on, Vol. 2019 (2019).
68. Bucci, D.Z., Tavares, L.B.B. & Sell, I. PHB packaging for the storage of food products. *Polymer Testing* **24**, 564-571 (2005).
69. Pachekoski, W.M., Agnelli, J.A.M. & Belem, L.P. Thermal, mechanical and morphological properties of poly (hydroxybutyrate) and polypropylene blends after processing. *Materials Research* **12**, 159-164 (2009).
70. Kourmentza, C. et al. Recent Advances and Challenges towards Sustainable Polyhydroxyalkanoate (PHA) Production. *Bioengineering* **4** (2017).
71. Jiang, G. et al. Carbon Sources for Polyhydroxyalkanoates and an Integrated Biorefinery. *Int J Mol Sci* **17**, 1157 (2016).
72. Danimerscientific in PHA culture and manufacturing Vol. 2019 (2019).
73. TianAn, Vol. 2019 (2019).
74. TianjinGreenBio, Vol. 2019 (2019).
75. Williams, S.F., Martin, D.P. & Skraly, F.A., Vol. US6838493B2 27 (Metabolix, Inc., Cambridge, MA (US), United States; 2005).
76. Dilkes-Hoffman, L.S., Lant, P.A., Laycock, B. & Pratt, S. The rate of biodegradation of PHA bioplastics in the marine environment: A meta-study. *Marine Pollution Bulletin* **142**, 15-24 (2019).
77. Chamas, A. et al. Degradation Rates of Plastics in the Environment. *ACS Sustainable Chemistry & Engineering* **8**, 3494-3511 (2020).
78. Kumar, M. et al. Bacterial polyhydroxyalkanoates: Opportunities, challenges, and prospects. *Journal of Cleaner Production* **263**, 121500 (2020).
79. Wang, Y., Yin, J. & Chen, G.-Q. Polyhydroxyalkanoates, challenges and opportunities. *Current Opinion in Biotechnology* **30**, 59-65 (2014).
80. Muthuraj, R., Valerio, O. & Mekonnen, T.H. Recent developments in short- and medium-chain- length Polyhydroxyalkanoates: Production, properties, and applications. *International Journal of Biological Macromolecules* **187**, 422-440 (2021).
81. Pereira, J.R. et al. Demonstration of the adhesive properties of the medium-chain-length polyhydroxyalkanoate produced by Pseudomonas chlororaphis subsp. aurantiaca from glycerol. *International Journal of Biological Macromolecules* **122**, 1144-1151 (2019).
82. Panaitescu, D.M. et al. Medium Chain-Length Polyhydroxyalkanoate Copolymer Modified by Bacterial Cellulose for Medical Devices. *Biomacromolecules* **18**, 3222-3232 (2017).

83. Ansari, S., Sami, N., Yasin, D., Ahmad, N. & Fatma, T. Biomedical applications of environmental friendly poly-hydroxyalkanoates. *International Journal of Biological Macromolecules* **183**, 549-563 (2021).
84. Sun, J., Dai, Z., Zhao, Y. & Chen, G.-Q. In vitro effect of oligo-hydroxyalkanoates on the growth of mouse fibroblast cell line L929. *Biomaterials* **28**, 3896-3903 (2007).
85. Rai, R., Keshavarz, T., Roether, J.A., Boccaccini, A.R. & Roy, I. Medium chain length polyhydroxyalkanoates, promising new biomedical materials for the future. *Materials Science and Engineering: R: Reports* **72**, 29-47 (2011).
86. Xu, X.-Y. et al. The behaviour of neural stem cells on polyhydroxyalkanoate nanofiber scaffolds. *Biomaterials* **31**, 3967-3975 (2010).
87. Braunegg, G., Sonnleitner, B. & Lafferty, R.M. A rapid gas chromatographic method for the determination of poly-β-hydroxybutyric acid in microbial biomass. *European journal of applied microbiology and biotechnology* **6**, 29-37 (1978).
88. Jiang, X.J., Sun, Z., Ramsay, J.A. & Ramsay, B.A. Fed-batch production of MCL-PHA with elevated 3-hydroxynonanoate content. *AMB Express* **3**, 50 (2013).
89. Hiroe, A., Watanabe, S., Kobayashi, M., Nomura, C.T. & Tsuge, T. Increased synthesis of poly(3-hydroxydodecanoate) by random mutagenesis of polyhydroxyalkanoate synthase. *Applied Microbiology and Biotechnology* **102**, 7927-7934 (2018).
90. Bhatia, S.K. et al. Production of (3-hydroxybutyrate-co-3-hydroxyhexanoate) copolymer from coffee waste oil using engineered Ralstonia eutropha. *Bioprocess and Biosystems Engineering* **41**, 229-235 (2018).
91. Watanabe, Y. et al. Development and validation of an HPLC-based screening method to acquire polyhydroxyalkanoate synthase mutants with altered substrate specificity. *Journal of Bioscience and Bioengineering* **113**, 286-292 (2012).
92. Randriamahefa, S., Renard, E., Guérin, P. & Langlois, V. Fourier Transform Infrared Spectroscopy for Screening and Quantifying Production of PHAs by Pseudomonas Grown on Sodium Octanoate. *Biomacromolecules* **4**, 1092-1097 (2003).
93. Song, J., Yoon, S., Yu, S. & Lenz, R. Differential scanning calorimetric study of poly(3-hydroxyoctanoate) inclusions in bacterial cells. *International journal of biological macromolecules* **23**, 165-173 (1998).
94. Liu, Z. et al. Domain-centric dissection and classification of prokaryotic poly(3-hydroxyalkanoate) synthases. *bioRxiv*, 693432 (2019).
95. Wang, L. et al. Bioinformatics Analysis of Metabolism Pathways of Archaeal Energy Reserves. *Scientific Reports* **9**, 1034 (2019).
96. Lane, C.E. & Benton, M.G. Detection of the enzymatically-active polyhydroxyalkanoate synthase subunit gene, phaC, in cyanobacteria via colony PCR. *Molecular and Cellular Probes* **29**, 454-460 (2015).
97. Blunt, W., Levin, D.B. & Cicek, N. in Polymers, Vol. 10 (2018).
98. Xie, C.-H. & Yokota, A. Reclassification of Alcaligenes latus strains IAM 12599T and IAM 12664 and Pseudomonas saccharophila as Azohydromonas lata gen. nov., comb. nov., Azohydromonas australica sp. nov. and Pelomonas saccharophila gen. nov., comb. nov., respectively. *International Journal of Systematic and Evolutionary Microbiology* **55**, 2419-2425 (2005).
99. Lee, S.Y. Plastic bacteria? Progress and prospects for polyhydroxyalkanoate production in bacteria. *Trends in Biotechnology* **14**, 431-438 (1996).
100. Díaz-Barrera, A., Urtuvia, V., Padilla-Córdova, C. & Peña, C. Poly(3-hydroxybutyrate) accumulation by Azotobacter vinelandii under different oxygen transfer strategies. *Journal of Industrial Microbiology & Biotechnology* **46**, 13-19 (2019).

101. Sohn, Y.J. et al. Chemoautotroph Cupriavidus necator as a potential game-changer for global warming and plastic waste problem: A review. *Bioresource Technology* **340**, 125693 (2021).
102. Vandamme, P. & Coenye, T. Taxonomy of the genus Cupriavidus: a tale of lost and found. *International Journal of Systematic and Evolutionary Microbiology* **54**, 2285-2289 (2004).
103. Schlegel, H., Gottschalk, G. & Von Bartha, R. Formation and utilization of poly-β-hydroxybutyric acid by Knallgas bacteria (Hydrogenomonas). *Nature* **191**, 463 (1961).
104. Cramm, R. Genomic View of Energy Metabolism in Ralstonia eutropha H16. *Journal of Molecular Microbiology and Biotechnology* **16**, 38-52 (2009).
105. Pohlmann, A. et al. Genome sequence of the bioplastic-producing "Knallgas" bacterium Ralstonia eutropha H16. *Nature Biotechnology* **24**, 1257-1262 (2006).
106. Yu, J. in Bioprocessing for Value-Added Products from Renewable Resources. (ed. S.-T. Yang) 585-610 (Elsevier, Amsterdam; 2007).
107. Zhang, M., Kurita, S., Orita, I., Nakamura, S. & Fukui, T. Modification of acetoacetyl-CoA reduction step in Ralstonia eutropha for biosynthesis of poly(3-hydroxybutyrate-co-3-hydroxyhexanoate) from structurally unrelated compounds. *Microbial Cell Factories* **18**, 147 (2019).
108. Mifune, J., Nakamura, S. & Fukui, T. Engineering of pha operon on Cupriavidus necator chromosome for efficient biosynthesis of poly(3-hydroxybutyrate-co-3-hydroxyhexanoate) from vegetable oil. *Polymer Degradation and Stability* **95**, 1305-1312 (2010).
109. Ng, K.-S., Wong, Y.-M., Tsuge, T. & Sudesh, K. Biosynthesis and characterization of poly(3-hydroxybutyrate-co-3-hydroxyvalerate) and poly(3-hydroxybutyrate-co-3-hydroxyhexanoate) copolymers using jatropha oil as the main carbon source. *Process Biochemistry* **46**, 1572-1578 (2011).
110. Raberg, M., Volodina, E., Lin, K. & Steinbüchel, A. Ralstonia eutropha H16 in progress: Applications beside PHAs and establishment as production platform by advanced genetic tools. *Critical Reviews in Biotechnology* **38**, 494-510 (2018).
111. LiebergeseII, M. & SteinbÜChel, A. Cloning and nucleotide sequences of genes relevant for biosynthesis of poly(3-hydroxybutyric acid) in Chromatium vinosum strain D. *European Journal of Biochemistry* **209**, 135-150 (1992).
112. Slater, S.C., Voige, W.H. & Dennis, D.E. Cloning and expression in Escherichia coli of the Alcaligenes eutrophus H16 poly-beta-hydroxybutyrate biosynthetic pathway. *Journal of Bacteriology* **170**, 4431 (1988).
113. Rhie, H.G. & Dennis, D. Role of fadR and atoC(Con) mutations in poly(3-hydroxybutyrate-co-3-hydroxyvalerate) synthesis in recombinant pha+ Escherichia coli. *Applied and Environmental Microbiology* **61**, 2487 (1995).
114. Andreeßen, B., Lange, A.B., Robenek, H. & Steinbüchel, A. Conversion of Glycerol to Poly(3-Hydroxypropionate) in Recombinant <em>Escherichia coli</em&gt. *Applied and Environmental Microbiology* **76**, 622 (2010).
115. Langenbach, S., Rehm, B.H.A. & Steinbüchel, A. Functional expression of the PHA synthase gene phaC1 from Pseudomonas aeruginosa in Escherichia coli results in poly(3-hydroxyalkanoate) synthesis. *FEMS Microbiology Letters* **150**, 303-309 (1997).
116. Klinke, S., Ren, Q., Witholt, B. & Kessler, B. Production of Medium-Chain-Length Poly(3-Hydroxyalkanoates) from Gluconate by Recombinant <em>Escherichia coli</em&gt. *Applied and Environmental Microbiology* **65**, 540 (1999).
117. Follonier, S., Panke, S. & Zinn, M. A reduction in growth rate of Pseudomonas putida KT2442 counteracts productivity advances in medium-chain-length polyhydroxyalkanoate production from gluconate. *Microbial Cell Factories* **10**, 25 (2011).

118. Fontaine, P., Mosrati, R. & Corroler, D. Medium chain length polyhydroxyalkanoates biosynthesis in Pseudomonas putida mt-2 is enhanced by co-metabolism of glycerol/octanoate or fatty acids mixtures. *International Journal of Biological Macromolecules* **98**, 430-435 (2017).
119. Le Meur, S., Zinn, M., Egli, T., Thöny-Meyer, L. & Ren, Q. Production of medium-chain-length polyhydroxyalkanoates by sequential feeding of xylose and octanoic acid in engineered Pseudomonas putida KT2440. *BMC Biotechnology* **12**, 53 (2012).
120. Davis, R. et al. Conversion of grass biomass into fermentable sugars and its utilization for medium chain length polyhydroxyalkanoate (mcl-PHA) production by Pseudomonas strains. *Bioresource Technology* **150**, 202-209 (2013).
121. Poblete-Castro, I., Binger, D., Oehlert, R. & Rohde, M. Comparison of mcl-Poly(3-hydroxyalkanoates) synthesis by different Pseudomonas putida strains from crude glycerol: citrate accumulates at high titer under PHA-producing conditions. *BMC biotechnology* **14**, 962-962 (2014).
122. Fu, J., Sharma, U., Sparling, R., Cicek, N. & Levin, D.B. Evaluation of medium-chain-length polyhydroxyalkanoate production by Pseudomonas putida LS46 using biodiesel by-product streams. *Canadian Journal of Microbiology* **60**, 461-468 (2014).
123. Salvachúa, D. et al. Metabolic engineering of Pseudomonas putida for increased polyhydroxyalkanoate production from lignin. *Microbial Biotechnology* **13**, 290-298 (2020).
124. Santhanam, A. & Sasidharan, S. Microbial production of polyhydroxyalkanoates (PHA) from Alcaligens spp. and Pseudomonas oleovorans using different carbon sources *African journal of biotechnology* **9**, 3144-3150 (2010).
125. Poltronieri, P., Mezzolla, V. & D'Urso, O.F. PHB Production in biofermentors assisted through biosensor applications. *Proceedings* **2017** (2016).
126. Khosravi-Darani, K., Mokhtari, Z.-B., Amai, T. & Tanaka, K. Microbial production of poly(hydroxybutyrate) from C1 carbon sources. *Applied Microbiology and Biotechnology* **97**, 1407-1424 (2013).
127. Passanha, P., Kedia, G., Dinsdale, R.M., Guwy, A.J. & Esteves, S.R. The use of NaCl addition for the improvement of polyhydroxyalkanoate production by Cupriavidus necator. *Bioresource Technology* **163**, 287-294 (2014).
128. Du, G. & Yu, J. Green technology for conversion of food scraps to biodegradable thermoplastic polyhydroxyalkanoates. *Environmental Science and Technology* **36**, 5511-5516 (2002).
129. Nikodinovic-Runic, J. et al. in Advances in Applied Microbiology, Vol. 84. (eds. S. Sariaslani & G.M. Gadd) 139-200 (Academic Press, 2013).
130. Yu, P.H., Chua, H., Huang, A.L., Lo, W. & Chen, G.Q. Conversion of food industrial wastes into bioplastics. *Applied Biochemistry and Biotechnology* **70**, 603-614 (1998).
131. Pakalapati, H., Chang, C.-K., Show, P.L., Arumugasamy, S.K. & Lan, J.C.-W. Development of polyhydroxyalkanoates production from waste feedstocks and applications. *Journal of Bioscience and Bioengineering* **126**, 282-292 (2018).
132. Sudesh, K. in Polyhydroxyalkanoates from Palm oil: biodegradable plastics, Vol. 1. (ed. S.i. Microbiology) 63-70 (Springer, Berlin, Heidelberg, Berlin; 2013).
133. Serafim, L.S., Lemos, P.C., Albuquerque, M.G.E. & Reis, M.A.M. Strategies for PHA production by mixed cultures and renewable waste materials. *Applied Microbiology and Biotechnology* **81**, 615-628 (2008).
134. Werker, A. et al. Consistent production of high quality PHA using activated sludge harvested from full scale municipal wastewater treatment – PHARIO. *Water Science and Technology* **78**, 2256-2269 (2018).

135. Thomson, N., Roy, I., Summers, D. & Sivaniah, E. In vitro production of polyhydroxyalkanoates: achievements and applications. *Journal of Chemical Technology & Biotechnology* **85**, 760-767 (2010).
136. Chen, J.-Y., Song, G. & Chen, G.-Q. A lower specificity PhaC2 synthase from Pseudomonas stutzeri catalyses the production of copolyesters consisting of short-chain-length and medium-chain-length 3-hydroxyalkanoates. *Antonie van Leeuwenhoek* **89**, 157-167 (2006).
137. Kumari, A. in Sweet Biochemistry. (ed. A. Kumari) 17-19 (Academic Press, 2018).
138. Lu, X., Zhang, J., Wu, Q. & Chen, G.-Q. Enhanced production of poly(3-hydroxybutyrate-co-3-hydroxyhexanoate) via manipulating the fatty acid β-oxidation pathway in E. coli. *FEMS Microbiology Letters* **221**, 97-101 (2003).
139. Liu, Q., Luo, G., Zhou, X.R. & Chen, G.-Q. Biosynthesis of poly(3-hydroxydecanoate) and 3-hydroxydodecanoate dominating polyhydroxyalkanoates by β-oxidation pathway inhibited Pseudomonas putida. *Metabolic Engineering* **13**, 11-17 (2011).
140. Meng, D.-C. & Chen, G.-Q. in Synthetic Biology – Metabolic Engineering. (eds. H. Zhao & A.-P. Zeng) 147-174 (Springer International Publishing, Cham; 2018).
141. Vo, M.T., Lee, K.-W., Jung, Y.-M. & Lee, Y.-H. Comparative effect of overexpressed phaJ and fabG genes supplementing (R)-3-hydroxyalkanoate monomer units on biosynthesis of mcl-polyhydroxyalkanoate in Pseudomonas putida KCTC1639. *Journal of Bioscience and Bioengineering* **106**, 95-98 (2008).
142. Flores-Sánchez, A., Rathinasabapathy, A., López-Cuellar, M.d.R., Vergara-Porras, B. & Pérez-Guevara, F. Biosynthesis of polyhydroxyalkanoates from vegetable oil under the co-expression of fadE and phaJ genes in Cupriavidus necator. *International Journal of Biological Macromolecules* **164**, 1600-1607 (2020).
143. Budde, C.F., Riedel, S.L., Willis, L.B., Rha, C. & Sinskey, A.J. Production of poly(3-hydroxybutyrate-co-3-hydroxyhexanoate) from plant oil by engineered Ralstonia eutropha strains. *Applied and environmental microbiology* **77**, 2847-2854 (2011).
144. Wong, Y.-M., Brigham, C.J., Rha, C., Sinskey, A.J. & Sudesh, K. Biosynthesis and characterization of polyhydroxyalkanoate containing high 3-hydroxyhexanoate monomer fraction from crude palm kernel oil by recombinant Cupriavidus necator. *Bioresource Technology* **121**, 320-327 (2012).
145. Fukui, T., Abe, H. & Doi, Y. Engineering of Ralstonia eutropha for Production of Poly(3-hydroxybutyrate-co-3-hydroxyhexanoate) from Fructose and Solid-State Properties of the Copolymer. *Biomacromolecules* **3**, 618-624 (2002).
146. Tripathi, L., Wu, L.-P., Chen, J. & Chen, G.-Q. Synthesis of Diblock copolymer poly-3-hydroxybutyrate -block-poly-3-hydroxyhexanoate [PHB-b-PHHx] by a β-oxidation weakened Pseudomonas putida KT2442. *Microbial cell factories* **11**, 44-44 (2012).
147. Li, M. et al. Engineering Pseudomonas entomophila for synthesis of copolymers with defined fractions of 3-hydroxybutyrate and medium-chain-length 3-hydroxyalkanoates. *Metabolic Engineering* **52**, 253-262 (2019).
148. Ouyang, S.-P. et al. Production of Polyhydroxyalkanoates with High 3-Hydroxydodecanoate Monomer Content by fadB and fadA Knockout Mutant of Pseudomonas putida KT2442. *Biomacromolecules* **8**, 2504-2511 (2007).
149. Zhao, F. et al. Metabolic engineering of Pseudomonas mendocina NK-01 for enhanced production of medium-chain-length polyhydroxyalkanoates with enriched content of the dominant monomer. *International Journal of Biological Macromolecules* **154**, 1596-1605 (2020).
150. Liu, W. & Chen, G.-Q. Production and characterization of medium-chain-length polyhydroxyalkanoate with high 3-hydroxytetradecanoate monomer content by fadB and

fadA knockout mutant of Pseudomonas putida KT2442. *Applied Microbiology and Biotechnology* **76**, 1153-1159 (2007).
151. Agnew, D.E., Stevermer, A.K., Youngquist, J.T. & Pfleger, B.F. Engineering Escherichia coli for production of C12–C14 polyhydroxyalkanoate from glucose. *Metabolic Engineering* **14**, 705-713 (2012).
152. Park, S.J., Park, J.P. & Lee, S.Y. Metabolic engineering of Escherichia coli for the production of medium-chain-length polyhydroxyalkanoates rich in specific monomers. *FEMS Microbiology Letters* **214**, 217-222 (2002).
153. Tan, H.T. et al. Evaluation of BP-M-CPF4 polyhydroxyalkanoate (PHA) synthase on the production of poly(3-hydroxybutyrate-co-3-hydroxyhexanoate) from plant oil using Cupriavidus necator transformants. *International Journal of Biological Macromolecules* **159**, 250-257 (2020).
154. Rehm, B.H.A. Polyester synthases: natural catalysts for plastics. *Biochemical Journal* **376**, 15-33 (2003).
155. Mezzolla, V., D'Urso, F.O. & Poltronieri, P. Role of PhaC Type I and Type II Enzymes during PHA Biosynthesis. *Polymers* **10** (2018).
156. Chen, J.-Y., Liu, T., Zheng, Z., Chen, J.-C. & Chen, G.-Q. Polyhydroxyalkanoate synthases PhaC1 and PhaC2 from Pseudomonas stutzeri 1317 had different substrate specificities. *FEMS Microbiology Letters* **234**, 231-237 (2006).
157. Bhubalan, K. et al. Characterization of the Highly Active Polyhydroxyalkanoate Synthase of Chromobacterium sp. Strain USM2. *Applied and Environmental Microbiology* **77**, 2926 (2011).
158. Matsusaki, H., Abe, H. & Doi, Y. Biosynthesis and Properties of Poly(3-hydroxybutyrate-co-3-hydroxyalkanoates) by Recombinant Strains of Pseudomonas sp. 61-3. *Biomacromolecules* **1**, 17-22 (2000).
159. Tsuge, T., Hyakutake, M. & Mizuno, K. Class IV polyhydroxyalkanoate (PHA) synthases and PHA-producing Bacillus. *Applied Microbiology and Biotechnology* **99**, 6231-6240 (2015).
160. Altschul, S.F. et al. Gapped BLAST and PSI-BLAST: a new generation of protein database search programs. *Nucleic Acids Research* **25**, 3389-3402 (1997).
161. Wittenborn, E.C., Jost, M., Wei, Y., Stubbe, J. & Drennan, C.L. Structure of the Catalytic Domain of the Class I Polyhydroxybutyrate Synthase from Cupriavidus necator. *J Biol Chem* **291**, 25264-25277 (2016).
162. Nambu, Y., Ishii-Hyakutake, M., Harada, K., Mizuno, S. & Tsuge, T. Expanded Amino Acid Sequence of the PhaC Box in the Active Center of Polyhydroxyalkanoate Synthases. *FEBS Letters* **n/a** (2019).
163. Zhang, S., Yasuo, T., Lenz, R.W. & Goodwin, S. Kinetic and Mechanistic Characterization of the Polyhydroxybutyrate Synthase from Ralstonia eutropha. *Biomacromolecules* **1**, 244-251 (2000).
164. Schrödinger, L. & DeLano, W. (2020).
165. Stubbe, J. et al. NONTEMPLATE-DEPENDENT POLYMERIZATION PROCESSES: Polyhydroxyalkanoate Synthases as a Paradigm. *Annual Review of Biochemistry* **74**, 433-480 (2005).
166. Yuan, W. et al. Class I and III Polyhydroxyalkanoate Synthases from Ralstonia eutropha and Allochromatium vinosum: Characterization and Substrate Specificity Studies. *Archives of Biochemistry and Biophysics* **394**, 87-98 (2001).

167. Antonio, R.V., Steinbüchel, A. & Rehm, B.H.A. Analysis of in vivo substrate specificity of the PHA synthase from Ralstonia eutropha: formation of novel copolyesters in recombinant Escherichia coli. *FEMS Microbiology Letters* **182**, 111-117 (2000).
168. Chen, Y., Jr., Tsai, P.-C., Hsu, C.-H. & Lee, C.-Y. Critical residues of class II PHA synthase for expanding the substrate specificity and enhancing the biosynthesis of polyhydroxyalkanoate. *Enzyme and Microbial Technology* **56**, 60-66 (2014).
169. Shen, X.-W., Shi, Z.-Y., Song, G., Li, Z.-J. & Chen, G.-Q. Engineering of polyhydroxyalkanoate (PHA) synthase PhaC2Ps of Pseudomonas stutzeri via site-specific mutation for efficient production of PHA copolymers. *Applied Microbiology and Biotechnology* **91**, 655-665 (2011).
170. Tsuge, T. Fundamental factors determining the molecular weight of polyhydroxyalkanoate during biosynthesis. *Polymer Journal* **48**, 1051-1057 (2016).
171. Zou, H. et al. Natural and engineered polyhydroxyalkanoate (PHA) synthase: key enzyme in biopolyester production. *Applied Microbiology and Biotechnology* **101**, 7417-7426 (2017).
172. Nomura, C.T. & Taguchi, S. PHA synthase engineering toward superbiocatalysts for custom-made biopolymers. *Applied Microbiology and Biotechnology* **73**, 969-979 (2007).
173. Takase, K., Taguchi, S. & Doi, Y. Enhanced Synthesis of Poly(3-hydroxybutyrate) in Recombinant Escherichia coli by Means of Error-Prone PCR Mutagenesis, Saturation Mutagenesis, and In Vitro Recombination of the Type II Polyhydroxyalkanoate Synthase Gene. *The Journal of Biochemistry* **133**, 139-145 (2003).
174. Tajima, K. et al. In vitro synthesis of polyhydroxyalkanoate (PHA) incorporating lactate (LA) with a block sequence by using a newly engineered thermostable PHA synthase from Pseudomonas sp. SG4502 with acquired LA-polymerizing activity. *Applied Microbiology and Biotechnology* **94**, 365-376 (2012).
175. Sheu, D.-S. & Lee, C.-Y. Altering the Substrate Specificity of Polyhydroxyalkanoate Synthase 1 Derived from Pseudomonas putida GPo1 by Localized Semirandom Mutagenesis. *Journal of Bacteriology* **186**, 4177 (2004).
176. Rehm, B.H.A., Antonio, R.V., Spiekermann, P., Amara, A.A. & Steinbüchel, A. Molecular characterization of the poly(3-hydroxybutyrate) (PHB) synthase from Ralstonia eutropha: in vitro evolution, site-specific mutagenesis and development of a PHB synthase protein model. *Biochimica et Biophysica Acta (BBA) - Protein Structure and Molecular Enzymology* **1594**, 178-190 (2002).
177. Taguchi, S., Nakamura, H., Hiraishi, T., Yamato, I. & Doi, Y. In Vitro Evolution of a Polyhydroxybutyrate Synthase by Intragenic Suppression-Type Mutagenesis1. *The Journal of Biochemistry* **131**, 801-806 (2002).
178. Niamsiri, N., Delamarre, S.C., Kim, Y.-R. & Batt, C.A. Engineering of Chimeric Class II Polyhydroxyalkanoate Synthases. *Applied and Environmental Microbiology* **70**, 6789 (2004).
179. Tsuge, T. et al. Combination of N149S and D171G mutations in Aeromonas caviae polyhydroxyalkanoate synthase and impact on polyhydroxyalkanoate biosynthesis. *FEMS Microbiology Letters* **277**, 217-222 (2007).
180. Sun, J. et al. Production of P(3-hydroxybutyrate-co-3-hydroxyhexanoate-co-3-hydroxyoctanoate) Terpolymers Using a Chimeric PHA Synthase in Recombinant Ralstonia eutropha and Pseudomonas putida. *Bioscience, Biotechnology, and Biochemistry* **74**, 1716-1718 (2010).
181. Matsumoto, K.i., Takase, K., Yamamoto, Y., Doi, Y. & Taguchi, S. Chimeric Enzyme Composed of Polyhydroxyalkanoate (PHA) Synthases from Ralstonia eutropha and

Aeromonas caviae Enhances Production of PHAs in Recombinant Escherichia coli. *Biomacromolecules* **10**, 682-685 (2009).
182. Yang, T.H. et al. Tailor-made type II Pseudomonas PHA synthases and their use for the biosynthesis of polylactic acid and its copolymer in recombinant Escherichia coli. *Applied Microbiology and Biotechnology* **90**, 603-614 (2011).
183. Yang, T.H. et al. Biosynthesis of polylactic acid and its copolymers using evolved propionate CoA transferase and PHA synthase. *Biotechnology and Bioengineering* **105**, 150-160 (2010).
184. Chen, Y., Jr. Critical residues of class II PHA synthase for expanding the substrate specificity and enhancing the biosynthesis of polyhydroxyalkanoate. *Enzyme and microbial technology* **v. 56**, pp. 7-66-2014 v.2056 (2014).
185. Choi, S.Y. et al. One-step fermentative production of poly(lactate-co-glycolate) from carbohydrates in Escherichia coli. *Nature Biotechnology* **34**, 435-440 (2016).
186. Ren, Y. et al. Microbial synthesis of a novel terpolyester P(LA-co-3HB-co-3HP) from low-cost substrates. *Microbial Biotechnology* **10**, 371-380 (2017).
187. Shozui, F. et al. A New Beneficial Mutation in Pseudomonas sp. 61-3 Polyhydroxyalkanoate (PHA) Synthase for Enhanced Cellular Content of 3-Hydroxybutyrate-Based PHA Explored Using Its Enzyme Homolog as a Mutation Template. *Bioscience, Biotechnology, and Biochemistry* **74**, 1710-1712 (2010).
188. Han, X., Satoh, Y., Tajima, K., Matsushima, T. & Munekata, M. Chemo-enzymatic synthesis of polyhydroxyalkanoate by an improved two-phase reaction system (TPRS). *Journal of Bioscience and Bioengineering* **108**, 517-523 (2009).
189. Thomson, N.M. et al. Efficient Production of Active Polyhydroxyalkanoate Synthase in Escherichia coli by Coexpression of Molecular Chaperones. *Applied and Environmental Microbiology* **79**, 1948 (2013).
190. Valentin, H.E. & Steinbüchel, A. Application of enzymatically synthesized short-chain-length hydroxy fatty acid coenzyme A thioesters for assay of polyhydroxyalkanoic acid synthases. *Applied Microbiology and Biotechnology* **40**, 699-709 (1994).
191. de Roo, G., Ren, Q., Witholt, B. & Kessler, B. Development of an improved in vitro activity assay for medium chain length PHA polymerases based on CoenzymeA release measurements. *Journal of Microbiological Methods* **41**, 1-8 (2000).
192. Fukui, T. et al. Enzymatic synthesis of poly-β-hydroxybutyrate inZoogloea ramigera. *Archives of Microbiology* **110**, 149-156 (1976).
193. Gerngross, T.U. et al. Overexpression and Purification of the Soluble Polyhydroxyalkanoate Synthase from Alcaligenes eutrophus: Evidence for a Required Posttranslational Modification for Catalytic Activity. *Biochemistry* **33**, 9311-9320 (1994).
194. Kraak, M.N., Kessler, B. & Witholt, B. In vitro Activities of Granule-Bound Poly[(R)-3-Hydroxyalkanoate] Polymerase C1 of Pseudomonas oleovorans. *European Journal of Biochemistry* **250**, 432-439 (1997).
195. Burns, K.L., Oldham, C.D., Thompson, J.R., Lubarsky, M. & May, S.W. Analysis of the in vitro biocatalytic production of poly-(β)-hydroxybutyric acid. *Enzyme and Microbial Technology* **41**, 591-599 (2007).
196. Martínez-Tobón, D.I., Gul, M., Elias, A.L. & Sauvageau, D. Polyhydroxybutyrate (PHB) biodegradation using bacterial strains with demonstrated and predicted PHB depolymerase activity. *Applied Microbiology and Biotechnology* **102**, 8049-8067 (2018).
197. de Eugenio, L.I. et al. Biochemical Evidence That phaZ Gene Encodes a Specific Intracellular Medium Chain Length Polyhydroxyalkanoate Depolymerase in Pseudomonas putida

KT2442: CHARACTERIZATION OF A PARADIGMATIC ENZYME**This work was supported by the Comisio´n Interministerial de Ciencia y Tecnologi´a (Grants GEN2001-4698-C05-02, BIO2003-05309-C04-01/02 and CTM2006-04007) and by the European Union (Grant 6FP-026515-2). The costs of publication of this article were defrayed in part by the payment of page charges. This article must therefore be hereby marked “advertisement” in accordance with 18 U.S.C. Section 1734 solely to indicate this fact. *Journal of Biological Chemistry* **282**, 4951-4962 (2007).

198. Ouyang, S.-P., Liu, Q., Fang, L. & Chen, G.-Q. Construction of pha-Operon-Defined Knockout Mutants of Pseudomonas putida KT2442 and their Applications in Poly(hydroxyalkanoate) Production. *Macromolecular Bioscience* **7**, 227-233 (2007).
199. Borrero-de Acuña, J.M., Rohde, M., Saldias, C. & Poblete-Castro, I. Fed-Batch mcl-Polyhydroxyalkanoates Production in Pseudomonas putida KT2440 and ΔphaZ Mutant on Biodiesel-Derived Crude Glycerol. *Frontiers in Bioengineering and Biotechnology* **9** (2021).
200. Elbanna, K., Lütke-Eversloh, T., Jendrossek, D., Luftmann, H. & Steinbüchel, A. Studies on the biodegradability of polythioester copolymers and homopolymers by polyhydroxyalkanoate (PHA)-degrading bacteria and PHA depolymerases. *Archives of Microbiology* **182**, 212-225 (2004).
201. Mergaert, J. & Swings, J. Biodiversity of microorganisms that degrade bacterial and synthetic polyesters. *Journal of Industrial Microbiology and Biotechnology* **17**, 463-469 (1996).
202. Knoll, M., Hamm, T.M., Wagner, F., Martinez, V. & Pleiss, J. The PHA Depolymerase Engineering Database: A systematic analysis tool for the diverse family of polyhydroxyalkanoate (PHA) depolymerases. *BMC Bioinformatics* **10**, 89 (2009).
203. Jaeger, K.E., Steinbüchel, A. & Jendrossek, D. Substrate specificities of bacterial polyhydroxyalkanoate depolymerases and lipases: bacterial lipases hydrolyze poly(omega-hydroxyalkanoates). *Applied and environmental microbiology* **61**, 3113-3118 (1995).
204. Behrends, A., Klingbeil, B. & Jendrossek, D. Poly(3-hydroxybutyrate) depolymerases bind to their substrate by a C-terminal located substrate binding site. *FEMS Microbiology Letters* **143**, 191-194 (1996).
205. Saito, T., Iwata, A. & Watanabe, T. Molecular structure of extracellular poly(3-hydroxybutyrate) depolymerase fromAlcaligenes faecalis T1. *Journal of environmental polymer degradation* **1**, 99-105 (1993).
206. Ohura, T., Kasuya, K.-I. & Doi, Y. Cloning and Characterization of the Polyhydroxybutyrate Depolymerase Gene of Pseudomonas stutzeri and Analysis of the Function of Substrate-Binding Domains. *Applied and Environmental Microbiology* **65**, 189 (1999).
207. Papaneophytou, C.P., Pantazaki, A.A. & Kyriakidis, D.A. An extracellular polyhydroxybutyrate depolymerase in Thermus thermophilus HB8. *Applied Microbiology and Biotechnology* **83**, 659-668 (2009).
208. Wakadkar, S., Hermawan, S., Jendrossek, D. & Papageorgiou, A.C. The structure of PhaZ7 at atomic (1.2 A) resolution reveals details of the active site and suggests a substrate-binding mode. *Acta Crystallogr Sect F Struct Biol Cryst Commun* **66**, 648-654 (2010).
209. Kellici, T.F., Mavromoustakos, T., Jendrossek, D. & Papageorgiou, A.C. Crystal structure analysis, covalent docking, and molecular dynamics calculations reveal a conformational switch in PhaZ7 PHB depolymerase. *Proteins: Structure, Function, and Bioinformatics* **85**, 1351-1361 (2017).

210. Wang, Y.-L., Lin, Y.-T., Chen, C.-L., Shaw, G.-C. & Liaw, S.-H. Crystallization and preliminary crystallographic analysis of poly(3-hydroxybutyrate) depolymerase from Bacillus thuringiensis. *Structural biology communications* **70**, 1421-1423 (2014).
211. Mukai, K., Yamada, K. & Doi, Y. Kinetics and mechanism of heterogeneous hydrolysis of poly[(R)-3-hydroxybutyrate] film by PHA depolymerases. *International Journal of Biological Macromolecules* **15**, 361-366 (1993).
212. Kasuya, K.-i., Inoue, Y. & Doi, Y. Adsorption kinetics of bacterial PHB depolymerase on the surface of polyhydroxyalkanoate films. *International Journal of Biological Macromolecules* **19**, 35-40 (1996).
213. Fujita, M. et al. Interaction between Poly[(R)-3-hydroxybutyrate] Depolymerase and Biodegradable Polyesters Evaluated by Atomic Force Microscopy. *Langmuir* **21**, 11829-11835 (2005).
214. Hiraishi, T., Hirahara, Y., Doi, Y., Maeda, M. & Taguchi, S. Effects of Mutations in the Substrate-Binding Domain of Poly[(R)-3-Hydroxybutyrate] (PHB) Depolymerase from Ralstonia pickettii T1 on PHB Degradation. *Applied and Environmental Microbiology* **72**, 7331 (2006).
215. Kasuya, K.-i., Ohura, T., Masuda, K. & Doi, Y. Substrate and binding specificities of bacterial polyhydroxybutyrate depolymerases. *International Journal of Biological Macromolecules* **24**, 329-336 (1999).
216. Gowda U. S, V. & Shivakumar, S. Poly(-β-hydroxybutyrate) (PHB) depolymerase PHAZPenfrom Penicillium expansum: purification, characterization and kinetic studies. *3 Biotech* **5**, 901-909 (2015).
217. Shivakumar, S. Polyhydroxybutyrate (PHB) Depolymerase from Fusarium solani Thom. *Journal of Chemistry* **2013**, 9 (2013).
218. Shivakumar, S., Jagadish, S.J., Zatakia, H. & Dutta, J. Purification, Characterization and Kinetic Studies of a Novel Poly(β) Hydroxybutyrate (PHB) Depolymerase PhaZPenfrom Penicillium citrinum S2. *Applied Biochemistry and Biotechnology* **164**, 1225-1236 (2011).
219. Tanio, T. et al. An Extracellular Poly(3-Hydroxybutyrate) Depolymerase from Alcaligenes faecalis. *European Journal of Biochemistry* **124**, 71-77 (1982).
220. Madison, L.L. & Huisman, G.W. Metabolic Engineering of Poly(3-Hydroxyalkanoates): From DNA to Plastic. *Microbiology and Molecular Biology Reviews* **63**, 21 (1999).
221. Hiraishi, T., Komiya, N. & Maeda, M. Y443F mutation in the substrate-binding domain of extracellular PHB depolymerase enhances its PHB adsorption and disruption abilities. *Polymer Degradation and Stability* **95**, 1370-1374 (2010).
222. Tan, L.-T., Hiraishi, T., Sudesh, K. & Maeda, M. Effects of mutation at position 285 of Ralstonia pickettii T1 poly[(R)-3-hydroxybutyrate] depolymerase on its activities. *Applied Microbiology and Biotechnology* **98**, 7061-7068 (2014).
223. Huisman, G.W. et al. Metabolism of poly(3-hydroxyalkanoates) (PHAs) by Pseudomonas oleovorans. Identification and sequences of genes and function of the encoded proteins in the synthesis and degradation of PHA. *Journal of Biological Chemistry* **266**, 2191-2198 (1991).
224. Schirmer, A., Jendrossek, D. & Schlegel, H.G. Degradation of poly(3-hydroxyoctanoic acid) [P(3HO)] by bacteria: purification and properties of a P(3HO) depolymerase from Pseudomonas fluorescens GK13. *Applied and Environmental Microbiology* **59**, 1220 (1993).
225. Ramsay, B.A., Saracovan, I., Ramsay, J.A. & Marchessault, R.H. A method for the isolation of microorganisms producing extracellular long-side-chain poly (β-hydroxyalkanoate) depolymerase. *Journal of environmental polymer degradation* **2**, 1-7 (1994).

226. Williamson, D.H., Mellanby, J. & Krebs, H.A. Enzymic determination of d(−)-β-hydroxybutyric acid and acetoacetic acid in blood. *Biochemical Journal* **82**, 90-96 (1962).
227. Kobayashi, T. & Saito, T. Catalytic triad of intracellular poly(3-hydroxybutyrate) depolymerase (PhaZ1) in Ralstonia eutropha H16. *Journal of Bioscience and Bioengineering* **96**, 487-492 (2003).
228. Kasuya, K.-i., Inoue, Y., Yamada, K. & Doi, Y. Kinetics of surface hydrolysis of poly[(R)-3-hydroxybutyrate] film by PHB depolymerase from Alcaligenes faecalis T1. *Polymer Degradation and Stability* **48**, 167-174 (1995).
229. Kasuya, K. et al. Biochemical and molecular characterization of the polyhydroxybutyrate depolymerase of Comamonas acidovorans YM1609, isolated from freshwater. *Applied and Environmental Microbiology* **63**, 4844 (1997).
230. Handrick, R. et al. A New Type of Thermoalkalophilic hydrolase of Paucimonas lemoignei with high specificity for amorphous polyesters of short chain-length hydroxyalkanoic acids. . *The Journal of Biological Chemistry* **276**, 36215-36224 (2001).
231. Jendrossek, D. Peculiarities of PHA granules preparation and PHA depolymerase activity determination. *Applied Microbiology and Biotechnology* **74**, 1186 (2007).
232. Molitoris, H.P., Moss, S.T., de Koning, G.J.M. & Jendrossek, D. Scanning electron microscopy of polyhydroxyalkanoate degradation by bacteria. *Applied Microbiology and Biotechnology* **46**, 570-579 (1996).
233. Spyros, A., Kimmich, R., Briese, B.H. & Jendrossek, D. H NMR Imaging Study of Enzymatic Degradation in Poly(3-hydroxybutyrate) and Poly(3-hydroxybutyrate-co-3-hydroxyvalerate). Evidence for Preferential Degradation of the Amorphous Phase by PHB Depolymerase B from Pseudomonas lemoignei. *Macromolecules* **30**, 8218-8225 (1997).
234. Oh, J.S., Choi, M.H. & Yoon, S. In vivo 13C-NMR spectroscopic study of polyhydroxyalkanoic acid degradation kinetics in bacteria. *Journal of Microbiology and Biotechnology* **15**, 1330-1336 (2005).
235. Taidi, B., Mansfield, D.A. & Anderson, A.J. Turnover of poly(3-hydroxybutyrate) (PHB) and its influence on the molecular mass of the polymer accumulated by Alcaligenes eutrophus during batch culture. *FEMS Microbiology Letters* **129**, 201-205 (1995).
236. De Eugenio, L.I. et al. Biochemical evidence that phaZ gene encodes a specific intracellular medium chain length polyhydroxyalkanoate depolymerase in Pseudomonas putida KT2442: characterization of a paradigmatic enzyme. *Journal of Biological Chemistry* (2006).
237. Tokiwa, Y. & Calabia, B.P. Review Degradation of microbial polyesters. *Biotechnology Letters* **26**, 1181-1189 (2004).
238. Sharma, P.K., Mohanan, N., Sidhu, R. & Levin, D.B. Colonization and degradation of polyhydroxyalkanoates by lipase-producing bacteria. *Canadian Journal of Microbiology* **65**, 461-475 (2019).
239. Mohamed, R.A., Salleh, A.B., Leow, A.T.C., Yahaya, N.M. & Abdul Rahman, M.B. Ability of T1 Lipase to Degrade Amorphous P(3HB): Structural and Functional Study. *Molecular Biotechnology* **59**, 284-293 (2017).
240. Mok, P.-S., Ch'ng, D.H.-E., Ong, S.-P., Numata, K. & Sudesh, K. Characterization of the depolymerizing activity of commercial lipases and detection of lipase-like activities in animal organ extracts using poly(3-hydroxybutyrate-co-4-hydroxybutyrate) thin film. *AMB Express* **6**, 97 (2016).
241. Ch'ng, D.H.-E. & Sudesh, K. Densitometry based microassay for the determination of lipase depolymerizing activity on polyhydroxyalkanoate. *AMB Express* **3**, 22 (2013).

242. Rodríguez-Contreras, A., Calafell-Monfort, M. & Marqués-Calvo, M.S. Enzymatic degradation of poly(3-hydroxybutyrate-co-4-hydroxybutyrate) by commercial lipases. *Polymer Degradation and Stability* **97**, 597-604 (2012).
243. Mendes, A.A. et al. Evaluation of immobilized lipases on poly-hydroxybutyrate beads to catalyze biodiesel synthesis. *International Journal of Biological Macromolecules* **50**, 503-511 (2012).
244. Yang, T.H. et al. In Situ Immobilized Lipase on the Surface of Intracellular Polyhydroxybutyrate Granules: Preparation, Characterization, and its Promising Use for the Synthesis of Fatty Acid Alkyl Esters. *Applied Biochemistry and Biotechnology* **177**, 1553-1564 (2015).
245. Haywood, G.W., Anderson, A.J. & Dawes, E.A. A survey of the accumulation of novel polyhydroxyalkanoates by bacteria. *Biotechnology Letters* **11**, 471-476 (1989).
246. Doi, Y., Kitamura, S. & Abe, H. Microbial Synthesis and Characterization of Poly(3-hydroxybutyrate-co-3-hydroxyhexanoate). *Macromolecules* **28**, 4822-4828 (1995).
247. Hiroe, A., Ushimaru, K. & Tsuge, T. Characterization of polyhydroxyalkanoate (PHA) synthase derived from Delftia acidovorans DS-17 and the influence of PHA production in Escherichia coli. *Journal of Bioscience and Bioengineering* **115**, 633-638 (2013).
248. Thijsse, G.J.E. Fatty-acid accumulation by acrylate inhibition of β-oxidation in an alkane-oxidizing pseudomonas. *Biochimica et Biophysica Acta (BBA) - Specialized Section on Lipids and Related Subjects* **84**, 195-197 (1964).
249. Pavoncello, V., Barras, F. & Bouveret, E. in Biomolecules, Vol. 12 (2022).
250. Qi, Q., Steinbüchel, A. & Rehm, B.H.A. Metabolic routing towards polyhydroxyalkanoic acid synthesis in recombinant Escherichia coli (fadR): inhibition of fatty acid β-oxidation by acrylic acid. *FEMS Microbiology Letters* **167**, 89-94 (1998).
251. Alvarez, H.M., Souto, M.F., Viale, A. & Pucci, O.H. Biosynthesis of fatty acids and triacylglycerols by 2,6,10,14-tetramethyl pentadecane-grown cells of Nocardia globerula 432. *FEMS Microbiology Letters* **200**, 195-200 (2001).
252. Alvarez, H.M., Kalscheuer, R. & Steinbüchel, A. Accumulation of storage lipids in species of Rhodococcus and Nocardia and effect of inhibitors and polyethylene glycol. *Lipid / Fett* **99**, 239-246 (1997).
253. Green, P.R. et al. Formation of Short Chain Length/Medium Chain Length Polyhydroxyalkanoate Copolymers by Fatty Acid β-Oxidation Inhibited Ralstonia eutropha. *Biomacromolecules* **3**, 208-213 (2002).
254. Alves, L.P.S. et al. A simple and efficient method for poly-3-hydroxybutyrate quantification in diazotrophic bacteria within 5 minutes using flow cytometry. *Brazilian Journal of Medical and Biological Research* **50** (2017).
255. Koller, M. & Rodríguez-Contreras, A. Techniques for tracing PHA-producing organisms and for qualitative and quantitative analysis of intra- and extracellular PHA. *Engineering in Life Sciences* **15**, 558-581 (2015).
256. Nomura, C.T., Taguchi, K., Taguchi, S. & Doi, Y. Coexpression of Genetically Engineered 3-Ketoacyl-ACP Synthase III (fabH) and Polyhydroxyalkanoate Synthase (phaC) Genes Leads to Short-Chain-Length-Medium-Chain-Length Polyhydroxyalkanoate Copolymer Production from Glucose in Escherichia coli JM109. *Applied and Environmental Microbiology* **70**, 999 (2004).
257. Tariq, M. et al. Identification, FT-IR, NMR (1H and 13C) and GC/MS studies of fatty acid methyl esters in biodiesel from rocket seed oil. *Fuel Processing Technology* **92**, 336-341 (2011).

258. Kamatou, G.P.P. & Viljoen, A.M. Comparison of fatty acid methyl esters of palm and palmist oils determined by GCxGC–ToF–MS and GC–MS/FID. *South African Journal of Botany* **112**, 483-488 (2017).
259. Santos, I.C. et al. Analysis of bacterial FAMEs using gas chromatography – vacuum ultraviolet spectroscopy for the identification and discrimination of bacteria. *Talanta* **182**, 536-543 (2018).
260. Baba, T. et al. Construction of Escherichia coli K-12 in-frame, single-gene knockout mutants: the Keio collection. *Mol Syst Biol* **2**, 2006.0008-2006.0008 (2006).
261. Desai, T.A. & Rao, C.V. Regulation of Arabinose and Xylose Metabolism in Escherichia coli. *Applied and Environmental Microbiology* **76**, 1524-1532 (2010).
262. Liu, M.-H., Chen, Y., Jr. & Lee, C.-Y. Characterization of medium-chain-length polyhydroxyalkanoate biosynthesis by Pseudomonas mosselii TO7 using crude glycerol. *Bioscience, Biotechnology, and Biochemistry* **82**, 532-539 (2018).
263. Chen, Y., Jr., Huang, Y.-C. & Lee, C.-Y. Production and characterization of medium-chain-length polyhydroxyalkanoates by Pseudomonas mosselii TO7. *Journal of Bioscience and Bioengineering* **118**, 145-152 (2014).
264. Licciardello, G., Catara, A.F. & Catara, V. in Bioengineering, Vol. 6 (2019).
265. Licciardello, G. et al. Transcriptome analysis of Pseudomonas mediterranea and P. corrugata plant pathogens during accumulation of medium-chain-length PHAs by glycerol bioconversion. *New Biotechnology* **37**, 39-47 (2017).
266. Solaiman, D.K.Y., Ashby, R.D. & Foglia, T.A. Physiological Characterization and Genetic Engineering of Pseudomonas corrugata for Medium-Chain-Length Polyhydroxyalkanoates Synthesis from Triacylglycerols. *Current Microbiology* **44**, 189-195 (2002).
267. Sharma, P.K. et al. Genome features of Pseudomonas putida LS46, a novel polyhydroxyalkanoate producer and its comparison with other P. putida strains. *AMB Express* **4**, 37 (2014).
268. Cerrone, F. et al. Medium chain length polyhydroxyalkanoate (mcl-PHA) production from volatile fatty acids derived from the anaerobic digestion of grass. *Applied Microbiology and Biotechnology* **98**, 611-620 (2014).
269. Zhao, F. et al. Screening of endogenous strong promoters for enhanced production of medium-chain-length polyhydroxyalkanoates in Pseudomonas mendocina NK-01. *Scientific Reports* **9**, 1798 (2019).
270. Guo, W. et al. Comparison of medium-chain-length polyhydroxyalkanoates synthases from Pseudomonas mendocina NK-01 with the same substrate specificity. *Microbiological Research* **168**, 231-237 (2013).
271. Pereira, J.R. et al. Production of medium-chain-length polyhydroxyalkanoates by Pseudomonas chlororaphis subsp. aurantiaca: Cultivation on fruit pulp waste and polymer characterization. *International Journal of Biological Macromolecules* **167**, 85-92 (2021).
272. Meneses, L. et al. in Molecules, Vol. 26 (2021).
273. Wang, Y., Chung, A. & Chen, G.-Q. Synthesis of Medium-Chain-Length Polyhydroxyalkanoate Homopolymers, Random Copolymers, and Block Copolymers by an Engineered Strain of Pseudomonas entomophila. *Advanced Healthcare Materials* **6**, 1601017 (2017).
274. Liu, Y., Yang, S. & Jia, X. Construction of a “nutrition supply–detoxification” coculture consortium for medium-chain-length polyhydroxyalkanoate production with a glucose–xylose mixture. *Journal of Industrial Microbiology and Biotechnology* **47**, 343-354 (2020).
275. Możejko-Ciesielska, J. & Serafim, L.S. Proteomic Response of Pseudomonas putida KT2440 to Dual Carbon-Phosphorus Limitation during mcl-PHAs Synthesis. *Biomolecules* **9** (2019).

276. Yang, S., Li, S. & Jia, X. Production of medium chain length polyhydroxyalkanoate from acetate by engineered Pseudomonas putida KT2440. *Journal of Industrial Microbiology and Biotechnology* **46**, 793-800 (2019).
277. Heinrich, D. et al. Synthesis Gas (Syngas)-Derived Medium-Chain-Length Polyhydroxyalkanoate Synthesis in Engineered Rhodospirillum rubrum. *Applied and Environmental Microbiology* **82**, 6132-6140 (2016).
278. Hokamura, A. et al. Biosynthesis of poly(3-hydroxybutyrate-co-3-hydroxyalkanoates) by recombinant Escherichia coli from glucose. *Journal of Bioscience and Bioengineering* **120**, 305-310 (2015).
279. Borrero-de Acuña, J.M. et al. Production of medium chain length polyhydroxyalkanoate in metabolic flux optimized Pseudomonas putida. *Microbial Cell Factories* **13**, 88 (2014).
280. Guzik, M.W. et al. Identification and characterization of an acyl-CoA dehydrogenase from Pseudomonas putida KT2440 that shows preference towards medium to long chain length fatty acids. *Microbiology* **160**, 1760-1771 (2014).
281. Fonseca, P., de la Peña, F. & Prieto, M.A. A role for the regulator PsrA in the polyhydroxyalkanoate metabolism of Pseudomonas putida KT2440. *International Journal of Biological Macromolecules* **71**, 14-20 (2014).
282. Poblete-Castro, I., Binger, D., Oehlert, R. & Rohde, M. Comparison of mcl-Poly(3-hydroxyalkanoates) synthesis by different Pseudomonas putida strains from crude glycerol: citrate accumulates at high titer under PHA-producing conditions. *BMC Biotechnology* **14**, 962 (2014).
283. Guo, W. et al. Complete Genome of Pseudomonas mendocina NK-01, Which Synthesizes Medium-Chain-Length Polyhydroxyalkanoates and Alginate Oligosaccharides. *Journal of Bacteriology* **193**, 3413-3414 (2011).
284. Kanehisa, M. & Goto, S. KEGG: Kyoto Encyclopedia of Genes and Genomes. *Nucleic Acids Research* **28**, 27-30 (2000).
285. Sayers, E.W. et al. Database resources of the national center for biotechnology information. *Nucleic Acids Research* **50**, D20-D26 (2022).
286. Johnson, A.O., Gonzalez-Villanueva, M., Tee, K.L. & Wong, T.S. An Engineered Constitutive Promoter Set with Broad Activity Range for Cupriavidus necator H16. *ACS Synthetic Biology* **7**, 1918-1928 (2018).
287. Dagert, M. & Ehrlich, S.D. Prolonged incubation in calcium chloride improves the competence of Escherichia coli cells. *Gene* **6**, 23-28 (1979).
288. Hui, C.-Y., Guo, Y., Zhang, W. & Huang, X.-Q. Rapid monitoring of the target protein expression with a fluorescent signal based on a dicistronic construct in Escherichia coli. *AMB Express* **8**, 81 (2018).
289. Juengert, J.R., Bresan, S. & Jendrossek, D. Determination of Polyhydroxybutyrate (PHB) Content in Ralstonia eutropha Using Gas Chromatography and Nile Red Staining. *Bio-protocol* **8**, e2748 (2018).
290. Statgraphics Technologies, I. (The Plains, Virginia 2022).
291. Waterhouse, A.M., Procter, J.B., Martin, D.M.A., Clamp, M. & Barton, G.J. Jalview Version 2—a multiple sequence alignment editor and analysis workbench. *Bioinformatics* **25**, 1189-1191 (2009).
292. Higgins, D.G. & Sharp, P.M. CLUSTAL: a package for performing multiple sequence alignment on a microcomputer. *Gene* **73**, 237-244 (1988).
293. Ushani, U., Sumayya, A.R., Archana, G., Rajesh Banu, J. & Dai, J. in Food Waste to Valuable Resources. (eds. J.R. Banu, G. Kumar, M. Gunasekaran & S. Kavitha) 211-233 (Academic Press, 2020).

294. Széliová, D., Krahulec, J., Šafránek, M., Lišková, V. & Turňa, J. Modulation of heterologous expression from PBAD promoter in Escherichia coli production strains. *Journal of Biotechnology* **236**, 1-9 (2016).
295. Jain, A. & Srivastava, P. Broad host range plasmids. *FEMS Microbiology Letters* **348**, 87-96 (2013).
296. Maloy, S.R., Ginsburgh, C.L., Simons, R.W. & Nunn, W.D. Transport of long and medium chain fatty acids by Escherichia coli K12. *Journal of Biological Chemistry* **256**, 3735-3742 (1981).
297. Nunn, W.D. & Simons, R.W. Transport of long-chain fatty acids by Escherichia coli: mapping and characterization of mutants in the fadL gene. *Proceedings of the National Academy of Sciences* **75**, 3377-3381 (1978).
298. Kim, Y.-G., Lee, J.-H., Park, S., Kim, S. & Lee, J. Inhibition of polymicrobial biofilm formation by saw palmetto oil, lauric acid and myristic acid. *Microbial Biotechnology* **15**, 590-602 (2022).
299. Luli, G.W. & Strohl, W.R. Comparison of growth, acetate production, and acetate inhibition of Escherichia coli strains in batch and fed-batch fermentations. *Applied and Environmental Microbiology* **56**, 1004-1011 (1990).
300. Hanahan, D. Studies on transformation of Escherichia coli with plasmids. *Journal of Molecular Biology* **166**, 557-580 (1983).
301. Song, Y. et al. Determination of single nucleotide variants in Escherichia coli DH5α by using short-read sequencing. *FEMS Microbiology Letters* **362**, fnv073 (2015).
302. Sekse, C., Bohlin, J., Skjerve, E. & Vegarud, G.E. Growth comparison of several Escherichia coli strains exposed to various concentrations of lactoferrin using linear spline regression. *Microbial Informatics and Experimentation* **2**, 5 (2012).
303. Ahmad, A. et al. Modeling the growth dynamics of multiple Escherichia coli strains in the pig intestine following intramuscular ampicillin treatment. *BMC Microbiology* **16**, 205 (2016).
304. Jiang, X., Sun, Z., Marchessault, R.H., Ramsay, J.A. & Ramsay, B.A. Biosynthesis and Properties of Medium-Chain-Length Polyhydroxyalkanoates with Enriched Content of the Dominant Monomer. *Biomacromolecules* **13**, 2926-2932 (2012).
305. Han, J., Qiu, Y.-Z., Liu, D.-C. & Chen, G.-Q. Engineered Aeromonas hydrophila for enhanced production of poly(3-hydroxybutyrate-co-3-hydroxyhexanoate) with alterable monomers composition. *FEMS Microbiology Letters* **239**, 195-201 (2004).
306. Casillas-Vargas, G. et al. Antibacterial fatty acids: An update of possible mechanisms of action and implications in the development of the next-generation of antibacterial agents. *Progress in Lipid Research* **82**, 101093 (2021).
307. Weickert, M.J., Doherty, D.H., Best, E.A. & Olins, P.O. Optimization of heterologous protein production in Escherichia coli. *Current Opinion in Biotechnology* **7**, 494-499 (1996).
308. Gruber, S., Hagen, J., Schwab, H. & Koefinger, P. Versatile and stable vectors for efficient gene expression in Ralstonia eutropha H16. *Journal of Biotechnology* **186**, 74-82 (2014).
309. Ruiz, N. & Silhavy Thomas, J. How Escherichia coli Became the Flagship Bacterium of Molecular Biology. *Journal of Bacteriology* **204**, e00230-00222 (2022).
310. Leong, Y.K., Show, P.L., Ooi, C.W., Ling, T.C. & Lan, J.C.-W. Current trends in polyhydroxyalkanoates (PHAs) biosynthesis: Insights from the recombinant Escherichia coli. *Journal of Biotechnology* **180**, 52-65 (2014).
311. Burgess-Brown, N.A. et al. Codon optimization can improve expression of human genes in Escherichia coli: A multi-gene study. *Protein Expression and Purification* **59**, 94-102 (2008).

312. Menzella, H.G. Comparison of two codon optimization strategies to enhance recombinant protein production in Escherichia coli. *Microbial Cell Factories* **10**, 15 (2011).
313. Guzman, L.M., Belin, D., Carson, M.J. & Beckwith, J. Tight regulation, modulation, and high-level expression by vectors containing the arabinose PBAD promoter. *Journal of Bacteriology* **177**, 4121-4130 (1995).
314. Schleif, R. AraC protein, regulation of the l-arabinose operon in Escherichia coli, and the light switch mechanism of AraC action. *FEMS Microbiology Reviews* **34**, 779-796 (2010).
315. Schleif, R., Hess, W., Finkelstein, S. & Ellis, D. Induction kinetics of the L-arabinose operon of Escherichia coli. *J Bacteriol* **115**, 9-14 (1973).
316. Hirsh, J. & Schleif, R. In vivo experiments on the mechanism of action of l-arabinose C gene activator and lactose repressor. *Journal of Molecular Biology* **80**, 433-444 (1973).
317. Johnson, C.M. & Schleif, R.F. In vivo induction kinetics of the arabinose promoters in Escherichia coli. *Journal of Bacteriology* **177**, 3438-3442 (1995).
318. Rahimzadeh, M., Sadeghizadeh, M., Najafi, F., Arab, S. & Mobasheri, H. Impact of heat shock step on bacterial transformation efficiency. *Mol Biol Res Commun* **5**, 257-261 (2016).
319. Lowry, O.H., Rosebrough, N.J., Farr, A.L. & Randall, R.J. Protein measurement with the Folin phenol reagent. *J Biol Chem* **193**, 265-275 (1951).
320. Walker, J.M., Vol. 1. (ed. H. Press) (2002).
321. Couto, N., Barber, J. & Gaskell, S.J. Matrix-assisted laser desorption/ionisation mass spectrometric response factors of peptides generated using different proteolytic enzymes. *Journal of Mass Spectrometry* **46**, 1233-1240 (2011).
322. Men, A.E., Wilson, P., Siemering, K. & Forrest, S. in Next Generation Genome Sequencing 1-11 (2008).
323. Venkateswar Reddy, M. et al. Polyhydroxyalkanoates (PHA) production from synthetic waste using Pseudomonas pseudoflava: PHA synthase enzyme activity analysis from P. pseudoflava and P. palleronii. *Bioresource Technology* **234**, 99-105 (2017).
324. Francis, D.M. & Page, R. Strategies to Optimize Protein Expression in E. coli. *Current Protocols in Protein Science* **61**, 5.24.21-25.24.29 (2010).
325. Jimenez-Diaz, L., Caballero, A. & Segura, A. in Aerobic Utilization of Hydrocarbons, Oils and Lipids. (ed. F. Rojo) 1-23 (Springer International Publishing, Cham; 2017).
326. Cronan, J.E. & Thomas, J. Bacterial fatty acid synthesis and its relationships with polyketide synthetic pathways. *Methods Enzymol* **459**, 395-433 (2009).
327. Rock, C.O. & Cronan, J.E. Escherichia coli as a model for the regulation of dissociable (type II) fatty acid biosynthesis. *Biochimica et Biophysica Acta (BBA) - Lipids and Lipid Metabolism* **1302**, 1-16 (1996).
328. Taguchi, K., Aoyagi, Y., Matsusaki, H., Fukui, T. & Doi, Y. Co-expression of 3-ketoacyl-ACP reductase and polyhydroxyalkanoate synthase genes induces PHA production in Escherichia coli HB101 strain. *FEMS Microbiology Letters* **176**, 183-190 (1999).
329. Ren, Q., Sierro, N., Witholt, B. & Kessler, B. FabG, an NADPH-Dependent 3-Ketoacyl Reductase ofPseudomonas aeruginosa, Provides Precursors for Medium-Chain-Length Poly-3-Hydroxyalkanoate Biosynthesis inEscherichia coli. *Journal of Bacteriology* **182**, 2978-2981 (2000).
330. Nomura Christopher, T. et al. Expression of 3-Ketoacyl-Acyl Carrier Protein Reductase (fabG) Genes Enhances Production of Polyhydroxyalkanoate Copolymer from Glucose in Recombinant Escherichia coli JM109. *Applied and Environmental Microbiology* **71**, 4297-4306 (2005).

331. Banerjee, A., Sugantino, M., Sacchettini, J.C. & Jacobs, W.R. The mabA gene from the inhA operon of Mycobacterium tuberculosis encodes a 3lketoacyl reductase that fails to confer isoniazid resistance. *Microbiology* **144**, 2697-2704 (1998).
332. Cohen-Gonsaud, M. et al. Crystal Structure of MabA from Mycobacterium tuberculosis, a Reductase involved in Long-chain Fatty Acid Biosynthesis. *Journal of Molecular Biology* **320**, 249-261 (2002).
333. Banerjee, A. et al. inhA, a Gene Encoding a Target for Isoniazid and Ethionamide in Mycobacterium tuberculosis. *Science* **263**, 227-230 (1994).
334. Marrakchi, H., Lanéelle, G. & Quémard, A.K. InhA, a target of the antituberculous drug isoniazid, is involved in a mycobacterial fatty acid elongation system, FAS-II. *Microbiology (Reading)* **146 (Pt 2)**, 289-296 (2000).
335. Quémard, A., Lacave, C. & Lanéelle, G. Isoniazid inhibition of mycolic acid synthesis by cell extracts of sensitive and resistant strains of Mycobacterium aurum. *Antimicrob Agents Chemother* **35**, 1035-1039 (1991).
336. Daffé, M. & Draper, P. in Advances in Microbial Physiology, Vol. 39. (ed. R.K. Poole) 131-203 (Academic Press, 1997).
337. Price, A.C., Zhang, Y.M., Rock, C.O. & White, S.W. Structure of beta-ketoacyl-[acyl carrier protein] reductase from Escherichia coli: negative cooperativity and its structural basis. *Biochemistry* **40**, 12772-12781 (2001).
338. Filling, C. et al. Critical residues for structure and catalysis in short-chain dehydrogenases/reductases. *J Biol Chem* **277**, 25677-25684 (2002).
339. Hu, Z. et al. Escherichia coli FabG 3-ketoacyl-ACP reductase proteins lacking the assigned catalytic triad residues are active enzymes. *Journal of Biological Chemistry* **296**, 100365 (2021).
340. Chen, S. et al. Polymorphic crystallization of fractionated microbial medium-chain-length polyhydroxyalkanoates. *Polymer* **50**, 4378-4388 (2009).
341. Zhang, Y.-M. & Rock, C.O. Transcriptional regulation in bacterial membrane lipid synthesis. *Journal of Lipid Research* **50**, S115-S119 (2009).
342. Yèagle, P.L. Lipid regulation of cell membrane structure and function. *The FASEB Journal* **3**, 1833-1842 (1989).
343. Fujita, Y., Matsuoka, H. & Hirooka, K. Regulation of fatty acid metabolism in bacteria. *Molecular Microbiology* **66**, 829-839 (2007).
344. DiRusso, C.C., Heimert, T.L. & Metzger, A.K. Characterization of FadR, a global transcriptional regulator of fatty acid metabolism in Escherichia coli. Interaction with the fadB promoter is prevented by long chain fatty acyl coenzyme A. *Journal of Biological Chemistry* **267**, 8685-8691 (1992).
345. Xu, Y., Heath, R.J., Li, Z., Rock, C.O. & White, S.W. The FadR·DNA Complex: TRANSCRIPTIONAL CONTROL OF FATTY ACID METABOLISM INESCHERICHIA COLI*. *Journal of Biological Chemistry* **276**, 17373-17379 (2001).
346. Salanitro, J.P. & Wegener, W.S. Growth of Escherichia coli on short-chain fatty acids: growth characteristics of mutants. *J Bacteriol* **108**, 885-892 (1971).
347. Weeks, G., Shapiro, M., Burns, R.O. & Wakil, S.J. Control of Fatty Acid Metabolism I. Induction of the Enzymes of Fatty Acid Oxidation in Escherichia coli. *Journal of Bacteriology* **97**, 827-836 (1969).
348. Simons, R.W., Egan, P.A., Chute, H.T. & Nunn, W.D. Regulation of fatty acid degradation in Escherichia coli: isolation and characterization of strains bearing insertion and temperature-sensitive mutations in gene fadR. *J Bacteriol* **142**, 621-632 (1980).

349. Salanitro Joseph, P. & Wegener Warner, S. Growth of Escherichia coli on Short-Chain Fatty Acids: Growth Characteristics of Mutants. *Journal of Bacteriology* **108**, 885-892 (1971).
350. Clark David, P. & Cronan John, E. Two-Carbon Compounds and Fatty Acids as Carbon Sources. *EcoSal Plus* **1**, 10.1128/ecosalplus.1123.1124.1124 (2005).
351. Jenkins, L.S. & Nunn, W.D. Regulation of the ato operon by the atoC gene in Escherichia coli. *Journal of Bacteriology* **169**, 2096-2102 (1987).
352. Jenkins, L.S. & Nunn, W.D. Genetic and molecular characterization of the genes involved in short-chain fatty acid degradation in Escherichia coli: the ato system. *J Bacteriol* **169**, 42-52 (1987).
353. Chen, C.Y., Hogarth, L.A. & Shanley, M.S. Regulatory sequences controlling short chain fatty acid metabolism in Escherichia coli. *SAAS Bull Biochem Biotechnol* **4**, 22-26 (1991).
354. My, L. et al. Transcription of the Escherichia coli Fatty Acid Synthesis Operon fabHDG Is Directly Activated by FadR and Inhibited by ppGpp. *Journal of Bacteriology* **195**, 3784-3795 (2013).
355. Campbell, J.W. & Cronan, J.E., Jr. Escherichia coli FadR positively regulates transcription of the fabB fatty acid biosynthetic gene. *J Bacteriol* **183**, 5982-5990 (2001).
356. Nunn, W.D., Giffin, K., Clark, D. & Cronan, J.E. Role for fadR in unsaturated fatty acid biosynthesis in Escherichia coli. *Journal of Bacteriology* **154**, 554-560 (1983).
357. Cronan, J.E. The Escherichia coli FadR transcription factor: Too much of a good thing? *Molecular Microbiology* **115**, 1080-1085 (2021).
358. Agnew, D.E. & Pfleger, B.F. Synthetic biology strategies for synthesizing polyhydroxyalkanoates from unrelated carbon sources. *Chemical Engineering Science* **103**, 58-67 (2013).
359. Tappel, R.C. et al. Engineering Escherichia coli for Improved Production of Short-Chain-Length-co-Medium-Chain-Length Poly[(R)-3-hydroxyalkanoate] (SCL-co-MCL PHA) Copolymers from Renewable Nonfatty Acid Feedstocks. *ACS Sustainable Chemistry & Engineering* **2**, 1879-1887 (2014).
360. Datsenko, K.A. & Wanner, B.L. One-step inactivation of chromosomal genes in Escherichia coli K-12 using PCR products. *Proceedings of the National Academy of Sciences* **97**, 6640 (2000).
361. Jensen, S.I., Lennen, R.M., Herrgård, M.J. & Nielsen, A.T. Seven gene deletions in seven days: Fast generation of Escherichia coli strains tolerant to acetate and osmotic stress. *Scientific Reports* **5**, 17874 (2015).
362. Mira, P., Yeh, P. & Hall, B.G. Estimating microbial population data from optical density. *PLOS ONE* **17**, e0276040 (2022).
363. Iram, S.H. & Cronan, J.E. The β-Oxidation Systems of Escherichia coli and Salmonella enterica Are Not Functionally Equivalent. *Journal of Bacteriology* **188**, 599-608 (2006).
364. Ow, D.S.-W., Nissom, P.M., Philp, R., Oh, S.K.-W. & Yap, M.G.-S. Global transcriptional analysis of metabolic burden due to plasmid maintenance in Escherichia coli DH5α during batch fermentation. *Enzyme and Microbial Technology* **39**, 391-398 (2006).
365. Sherkhanov, S., Korman, T.P. & Bowie, J.U. Improving the tolerance of Escherichia coli to medium-chain fatty acid production. *Metabolic Engineering* **25**, 1-7 (2014).
366. Hatton, P.V. & Kinderlerer, J.L. Toxicity of medium chain fatty acids to Penicillium crustosum Thom and their detoxification to methyl ketones. *Journal of Applied Bacteriology* **70**, 401-407 (1991).

367. Bentley, W.E., Mirjalili, N., Andersen, D.C., Davis, R.H. & Kompala, D.S. Plasmid-encoded protein: The principal factor in the “metabolic burden” associated with recombinant bacteria. *Biotechnology and Bioengineering* **35**, 668-681 (1990).
368. Rozkov, A. et al. Characterization of the metabolic burden on Escherichia coli DH1 cells imposed by the presence of a plasmid containing a gene therapy sequence. *Biotechnology and Bioengineering* **88**, 909-915 (2004).
369. Pasini, M. et al. Using promoter libraries to reduce metabolic burden due to plasmid-encoded proteins in recombinant Escherichia coli. *New Biotechnology* **33**, 78-90 (2016).
370. Glick, B.R. Metabolic load and heterologous gene expression. *Biotechnology Advances* **13**, 247-261 (1995).
371. Sundaramahalingam, M.A., Sivashanmugam, P., Rajeshbanu, J. & Ashokkumar, M. A review on contemporary approaches in enhancing the innate lipid content of yeast cell. *Chemosphere* **293**, 133616 (2022).
372. Wang, L., Jackson, W.C., Steinbach, P.A. & Tsien, R.Y. Evolution of new nonantibody proteins via iterative somatic hypermutation. *Proceedings of the National Academy of Sciences* **101**, 16745-16749 (2004).
373. Kurien, B.T. & Scofield, R.H. in Protein Electrophoresis: Methods and Protocols. (eds. B.T. Kurien & R.H. Scofield) 471-479 (Humana Press, Totowa, NJ; 2012).
374. Yoon, E., Konold, P.E., Lee, J., Joo, T. & Jimenez, R. Far-Red Emission of mPlum Fluorescent Protein Results from Excited-State Interconversion between Chromophore Hydrogen-Bonding States. *The Journal of Physical Chemistry Letters* **7**, 2170-2174 (2016).
375. Osbourn, A.E. & Field, B. Operons. *Cellular and Molecular Life Sciences* **66**, 3755-3775 (2009).
376. Chizzolini, F., Forlin, M., Cecchi, D. & Mansy, S.S. Gene Position More Strongly Influences Cell-Free Protein Expression from Operons than T7 Transcriptional Promoter Strength. *ACS Synthetic Biology* **3**, 363-371 (2014).
377. Lim, H.N., Lee, Y. & Hussein, R. Fundamental relationship between operon organization and gene expression. *Proceedings of the National Academy of Sciences* **108**, 10626-10631 (2011).
378. Spriestersbach, A., Kubicek, J., Schäfer, F., Block, H. & Maertens, B. in Methods in Enzymology, Vol. 559. (ed. J.R. Lorsch) 1-15 (Academic Press, 2015).
379. Studier, F.W. & Moffatt, B.A. Use of bacteriophage T7 RNA polymerase to direct selective high-level expression of cloned genes. *Journal of Molecular Biology* **189**, 113-130 (1986).
380. Chung, A.-L. et al. Biosynthesis and Characterization of Poly(3-hydroxydodecanoate) by β-Oxidation Inhibited Mutant of Pseudomonas entomophila L48. *Biomacromolecules* **12**, 3559-3566 (2011).

APPENDICES

Appendix 1: List of reagents

List of Reagents	Catalogue #; Manufacturer details
PHA standards	
Methyl (R)-3-hydroxybutyrate	Cat#: 243159-1G; Sigma Aldrich, St. Louis, Missouri, United States
Methyl (R)-3-hydroxyhexanoate	Cat#:77938-100MG; Sigma Aldrich, St. Louis, Missouri, United States
Methyl(R)-3-hydroxyoctanoate	Cat#:1746-25 mg; Cambridge Bioscience,
Methyl (R)-3-hydroxydecanoate	Cat#:1728-25 mg; Cambridge Bioscience,
Methyl (R)-3-hydroxydodecanoate	Cat#:1732-25 mg; Cambridge Bioscience,
Methyl(R)-3-hydroxytetradecanoate	Cat#:1736-25 mg; Cambridge Bioscience,
methyl-myristate	Cat#:M3378-1G; Sigma Aldrich, St. Louis, Missouri, United States
methyl-laurate	Cat#:234591-2.5G; Sigma Aldrich, St. Louis, Missouri, United States
polyhydroxybutyrate	Cat#:363502-10G; Sigma Aldrich, St. Louis, Missouri, United States
Antibiotics	
Chloramphenicol	Cat#: CLA01; FORMEDIUM, Norfolk, UK
Kanamycin	Cat#: A1493,0025; AppliChem, Cheshire, UK
Ampicillin	Cat#: A1593-25G; Sigma Aldrich, St. Louis, Missouri, United States
Media components	
Tryptone	Cat#: TRP02; FORMEDIUM, Norfolk, UK
Yeast extract	Cat#: YEA03, FORMEDIUM, Norfolk, UK
Sodium chloride (NaCl)	Cat#: NAC02; FORMEDIUM, Norfolk, UK

Agar	Cat#: AGR03; FORMEDIUM, Norfolk, UK
Sodium tetradecanoate	Cat#: M8005; Sigma Aldrich, Missouri, United States
Sodium dodecanoate	Cat#: L9755; Sigma Aldrich, Missouri, United States
Miscellaneous	
Calcium chloride ($CaCl_2 \bullet H_2O$)	Cat#: 437055N; VWR, Leicestershire, UK
Sodium acrylate	Cat#:408220; Sigma Aldrich, Missouri, United States
L-Arabinose	Cat#: SC-221794B; ChemCruz, Heidelberg, Germany
Glycerol	Cat#: 444485B; VWR, Leicestershire, UK
Sodium dodecyl sulphate (SDS)	Cat#: 444464T; VWR, Leicestershire, UK
Acetic acid	Cat#: 20104.334; VWR, Leicestershire, UK
Tris Molecular Biology grade	Cat#: BP152-1; Fisher Chemical, Loughborough, UK
EDTA DISODIUM	Cat#: EDTA500; FORMEDIUM, Norfolk, UK
Agarose	Cat#: 50004; Lonza, Slough, UK
Ethidium bromide	Cat#: HC001596; MERCK, Darmstadt, Germany
Gel Loading Dye Blue (6×)	Cat#: B707 S; New England Biolabs, Massachusetts, US
DNA Ladder 1 kb Quick-Load®[50 µg/ml]	Cat#: N0468S; New England Biolabs, Massachusetts, US
T4 DNA ligase 10× Buffer with 10 mM ATP	Cat#: B0202S; New England Biolabs, Massachusetts, US
10× CutSmart buffer	Cat#: B7204S; New England Biolabs, Massachusetts, US
Enzymes	
T4 DNA ligase [400,000 U/ml]	Cat#: M0202; New England Biolabs, Herts, UK
NdeI [20,000 U/ml]	Cat#: R0111S; New England Biolabs, Herts, UK
BamHI [20,000 U/ml]	Cat#: R0136S; New England Biolabs, Herts, UK
EcoRV-HF	Cat#:R3195S; New Englad Biolabs, Massachusetts, US
BamHI-HF	Cat#:R3136S; New Englad Biolabs, Massachusetts, US
SacI-HF	Cat#: R3156S;New Englands Biolabs, Massachusetts, US
EcoRI-HF	Cat#: R3101S;New Englands Biolabs, Massachusetts, US

XhoI	Cat#: R0146S;New Englands Biolabs, Massachusetts, US
PCR reagents	
Q5 HF DNA Polimerasa [2.0 U/µl]	Cat#: M0491S; New England Biolabs, Herts, UK
Primers	Integrated DNA technologies, Coralville, Iowa, United States
5× Q5 Reaction Buffer	Cat#: B9027S; New England Biolabs, Massachusetts, US
5× Q5 High GC Enhancer	Cat#: M0491S; New England Biolabs, Massachusetts, US
Q5® High-Fidelity PCR Kit	Cat#:E0555S; New England Biolabs, Massachusetts, US

Appendix 2: List of kits

Experiment	**Catalogue #; Manufacturer details**
Isolation of plasmid	Cat#: D6942-01; E.Z.N.A.® Plasmid Mini Kit I, Omega Bio-Tek, Norcross, USA
Gel and PCR purification	Cat#: 740609.250; NucleoSpin® Gel and PCR Clean-up Macherey-Nagel, Düren, Germany

Appendix 3: List of equipment

Experiment	**Details**
Bacterial cultivation	For 37℃ à ES-20 shaker-incubator; Grant Instruments, Shepreth, UK
Optical density (OD_{600})	BioPhotometer Plus UV/Vis photometer; Eppendorf, Stevenage, UK
Biomass weight	Analytical balance XA204, Delta Range; Mettler Toledo, Ohio, United States
DNA concentration	VersaWave Spectrophotometer; Expedeon, Cambridge, UK
PCR	Eppendorf Mastercycler; Eppendorf, Stevenage, UK
Electrophoresis	Mini-Sub Cell GT Systems; Bio-Rad, Hertfordshire, UK

Bacteria transformation	For heat shock à Eppendorf Thermomixer C; Eppendorf, Stevenage, UK
PHA characterization	Gas chromatography GC-2010Pro; Shimadzu, Kyoto, Japan
Gel documentation system	Genosmart2, VWR, Leicestershire, UK
Knockout growth curves	Spark® Multimode Microplate Reader by Tecan, Tecan Trading AG, Switzerland
Biomass digestion for GC	Block heater DRB 200, Hach Company, Colorado, USA

Appendix 4: List of software

Experiment	Details
Protein graphics	PyMOL Version 2.0, Schrödinger, Inc. New York, New York
DNA design and analysis	SnapGene 5.3.2, Insightful Science, LLC. San Diego, California.
Statistical analysis	STATGRAPHICS Centurion XV.11, Statgraphics Technologies, Inc. The Plains, Virginia.
Organic chemistry figures design	Chemdraw, PerkinElmer. Waltham, Massachusetts.
Alignment of sequences	Jalview, Version 2[291]

Appendix 5: Media preparation

Media	Preparation
2× YT	Per 1 L 16 g Tryptone 10 g Yeast extract 5 g NaCl
TYE Agar plate	Per 1 L 10 g Tryptone

	5 g Yeast extract
	8 g NaCl
	15 g Agar

ANNEXES

Annex 1: Gas chromatography analysis for the 15 well experiment in **Chapter 2**.

Well 1			
Peak	**Time(min)**	**Area (µV*s)**	**Identification**
1	0.967	19149.96	air
2	1.1	66195.2	chloroform
3	1.898	364.41	C4
4	2.082	23.93	
5	5.895	412.44	int.standard

Well 2			
Peak	**Time(min)**	**Area (µV*s)**	**Identification**
1	0.965	18137.6	air
2	1.097	68824.55	chloroform
3	1.894	363.6	C4
4	5.887	418.86	int.standard

Well 3			
Peak	**Time(min)**	**Area (µV*s)**	**Identification**
1	0.964	18608.32	air
2	1.095	69397.5	chloroform
3	1.892	356.88	C4
4	5.885	423.7	int.standard

Well 4			
Peak	**Time(min)**	**Area (µV*s)**	**Identification**
1	0.963	18757.19	air
2	1.096	68886.2	chloroform
3	1.891	328.29	C4
4	5.881	426.78	int.standard

Well 5			
Peak	**Time(min)**	**Area (µV*s)**	**Identification**
1	0.967	19858.29	air
2	1.099	70837.33	chloroform
3	1.896	355.15	C4
4	2.079	23.07	
5	5.883	422.89	int.standard

Well 6			
Peak	**Time(min)**	**Area (µV*s)**	**Identification**
1	0.961	19128.62	air
2	1.092	69874.99	chloroform
3	1.889	387.94	C4
4	2.071	24.33	
5	5.878	418	int.standard

Well 7			
Peak	**Time(min)**	**Area (µV*s)**	**Identification**
1	0.966	16012.78	air
2	1.097	71371.5	chloroform
3	1.422	18.02	
4	1.893	477.49	C4
5	2.074	33.24	
6	5.878	506.47	int.standard

Well 8			
Peak	**Time(min)**	**Area (µV*s)**	**Identification**
1	0.964	19105.79	air
2	1.096	69300.49	chloroform
3	1.888	312.3	C4
4	2.072	21.12	
5	5.873	415.49	int.standard

Well 9			
Peak	Time(min)	Area (µV*s)	Identification
1	0.964	19084.42	air
2	1.096	68005.2	chloroform
3	1.889	320.97	C4
4	2.072	22.4	
5	5.875	407.94	int.standard

Well 10			
Peak	Time(min)	Area (µV*s)	Identification
1	0.962	19186.07	air
2	1.094	68422.51	chloroform
3	1.887	311.24	C4
4	5.875	416.63	int.standard

Well 11			
Peak	Time(min)	Area (µV*s)	Identification
1	0.963	19350.6	air
2	1.096	68060.29	chloroform
3	1.888	311.65	C4
4	2.072	21.82	
5	5.874	414.79	int.standard

Well 12			
Peak	Time(min)	Area (µV*s)	Identification
1	0.964	18181.9	air
2	1.096	68135.96	chloroform
3	1.887	286.62	C4
4	5.876	421.2	int.standard

Well 13			
Peak	Time(min)	Area (µV*s)	Identification
1	0.961	18747.98	air
2	1.093	68505.17	chloroform
3	1.885	304.37	C4
4	2.06	20.06	
5	5.872	424.35	int.standard

Well 14			
Peak	Time(min)	Area (µV*s)	Identification
1	0.963	19330.02	air
2	1.095	68622.6	chloroform
3	1.889	353.42	C4
4	2.072	25.58	
5	5.876	421.45	int.standard

Well 15			
Peak	Time(min)	Area (µV*s)	Identification
1	0.964	10409.6	air
2	1.094	73852.6	chloroform
3	1.419	19.85	
4	1.891	534.18	C4
5	2.07	36.47	
6	5.874	564.99	int.standard

Annex 2. *Escherichia coli* growth kinetics from **Chapter 2**

	0 h	1 h	2 h	3 h	4 h	5 h	6 h	7 h	8 h	9 h	24 h
DH5α	0.161	0.376	0.865	2.385	3.380	4.720	4.925	6.145	7.190	7.960	8.280
FadA⁻	0.161	0.552	1.490	3.590	5.425	6.520	7.400	7.530	9.050	9.600	10.255
DH5α-*PmePhaC*	0.161	0.275	0.749	1.495	2.365	4.465	4.520	5.905	6.260	7.180	9.170
FadA⁻ PmePhaC	0.161	0.458	1.246	3.445	4.955	6.630	7.390	7.985	9.290	9.690	11.670

Annex 3. Equation to calculate concentration of PHT (µg/l) from the area under the curve obtained using GC-MS

$$\mu g \text{ of } C14 = SI(AC14/AS) \times 3.956$$

$$(\mu g \text{ of } C14) \times 20 = \mu g/l$$

- SI =standard injected = 1.738 g
- AC14= area under the curve of methyl-hydroxytetradecanoate GC-MS
- AS= area under the curve of internal standard GC-MS
- 3.956= (Area under the curve for 1.738 g of C14 GC-FID)/(Area under the curve for 1.738 g of internal standard using GC-FID)

Annex 4. Standard curve for the methyl-3-hydroxyalkanoates of C6, C8, C10 , C12 and C14 carbon-chain- lengths and their retention time (RT)

The standard curves for commercial methyl-3-hydroxyalkanoates of different chain lengths (C6, C8, C10, C12 and C14 carbons) were prepared and then analyzed in three, totally

independent, replicates and the linear regression equation was elucidated from the average of these replicates with a $R^2 \geq 0.94$ The standard curves were also graphed and shown in **Figures to 69 to 73** where concentration of methyl ester in chloroform (µg/µl) was chosen for the "x" axis and area under the peak of the chromatogram (µV*s) for "y".

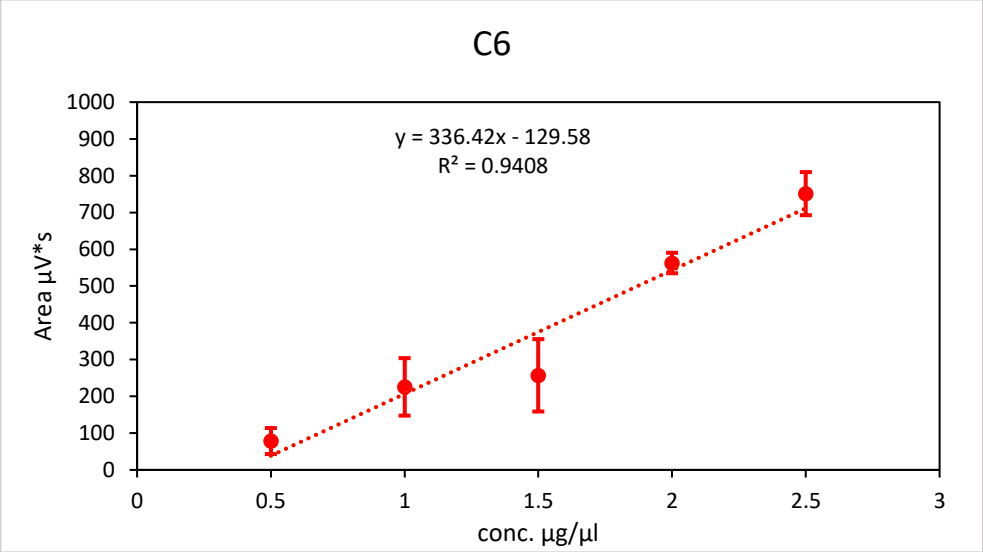

***Figure 69**. Standard curve of the monomer methyl-3-hydroxyhexanoate. Retention time: 4.92 ±0.043 min. The dashed line represents the linear trendline (used to build the linear equation) between the points of the curve. Each concentration (µg/µl) was prepared by triplicate and measured using GC.*

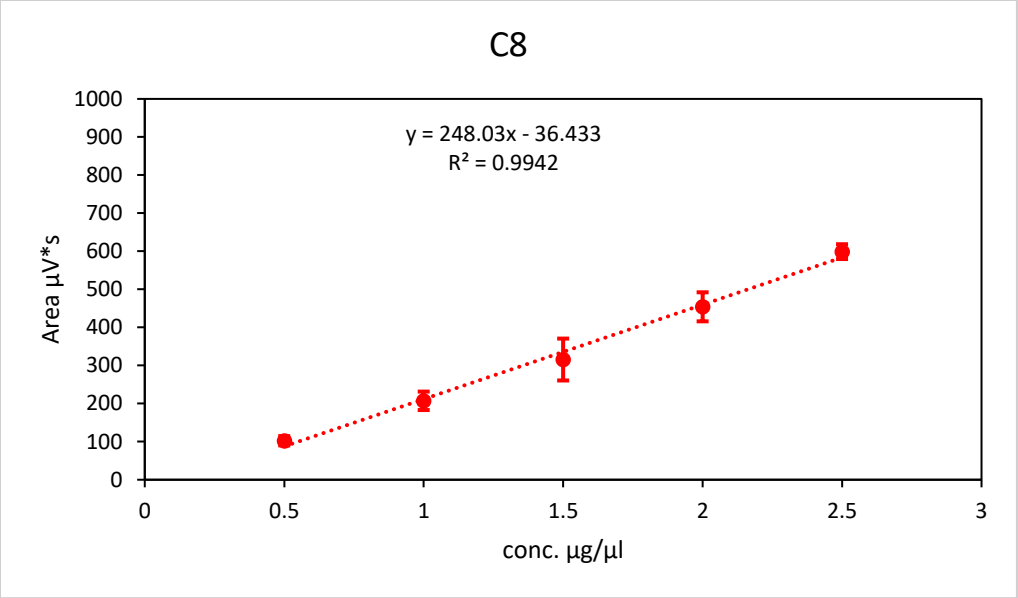

Figure 70. *Standard curve of the monomer methyl-3-hydroxyoctanoate. Retention time: 8.10 ±0.005 min The dashed line represents the linear trendline (used to build the linear equation) between the points of the curve. Each concentration (µg/µl) was prepared by triplicate and measured using GC.*

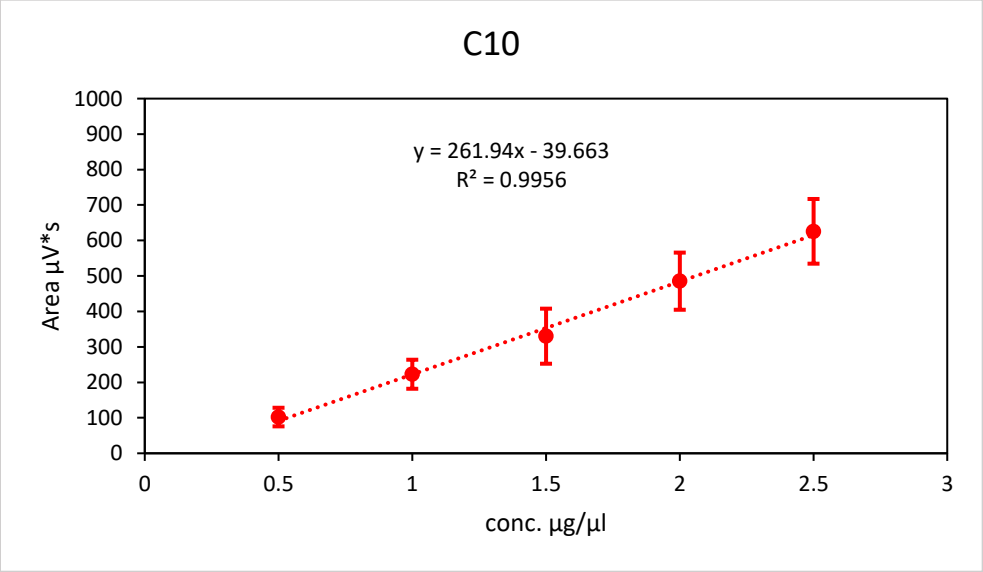

Figure 71. *Standard curve of the monomer methyl-3-hydroxydecanoate. Retention time: 9.78 ±0.009 min. The dashed line represents the linear trendline (used to build the linear equation) between the points of the curve. Each concentration (µg/µl) was prepared by triplicate and measured using GC.*

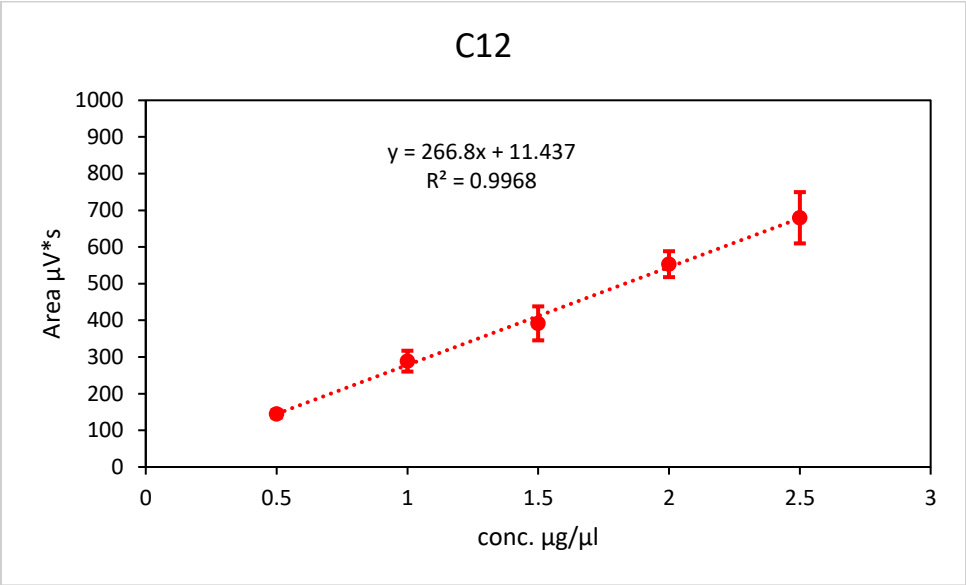

Figure 72. *Standard curve of methyl-3-hydroxydodecanoate. Retention time: 11.08 ±0.010 min. The dashed line represents the linear trendline (used to build the linear equation) between the points of the curve. Each concentration (µg/µl) was prepared by triplicate and measured using GC.*

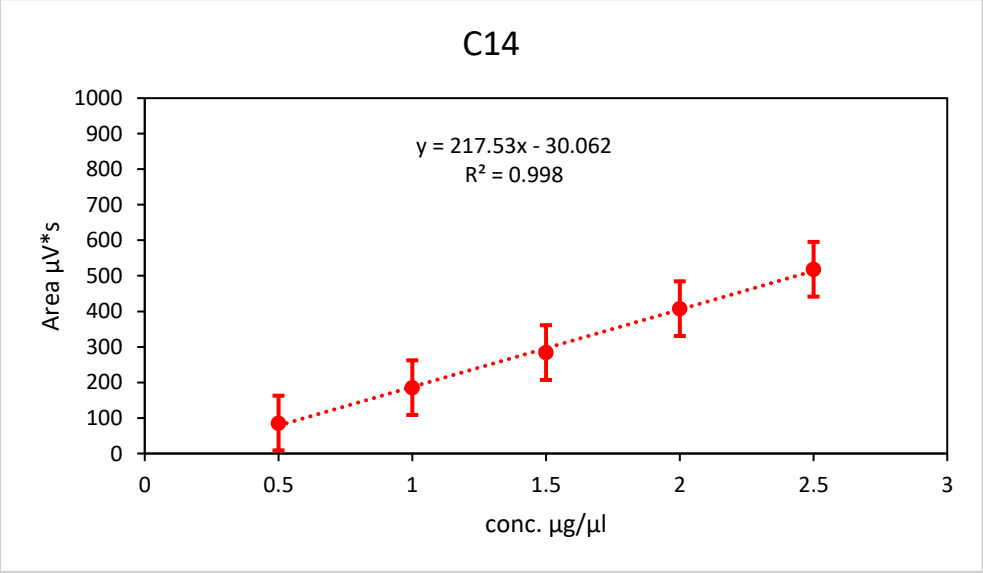

Figure 73. *Standard curve of methyl-3-hydroxytetradecanoate. Retention time: 12.21±0.005 min. The dashed line represents the linear trendline (used to build the linear equation) between the points of the curve. Each concentration (µg/µl) was prepared by triplicate and measured using GC*

Retention time analysis

The GC retention time (RT) for the methyl ester of each standard curve constructed was recorded and the average and standard deviation was calculated from 5 replicates and shown in **Table 11.**

Table 29. Retention times of methyl-3-hydroxyalkanoates with different carbon lengths being analysed through Gas Chromatography.

Carbons	Retention time (min)	SD
C4	1.91	±0.013
C6	4.92	±0.043
C8	8.10	±0.005
C10	9.78	±0.009
C12	11.08	±0.010
C14	12.21	±0.005

It was observed that the RT increased proportionally with the length of the carbon number, therefore making it possible to build a linear regression model between RT and number of carbons as shown in **Figure 27.**

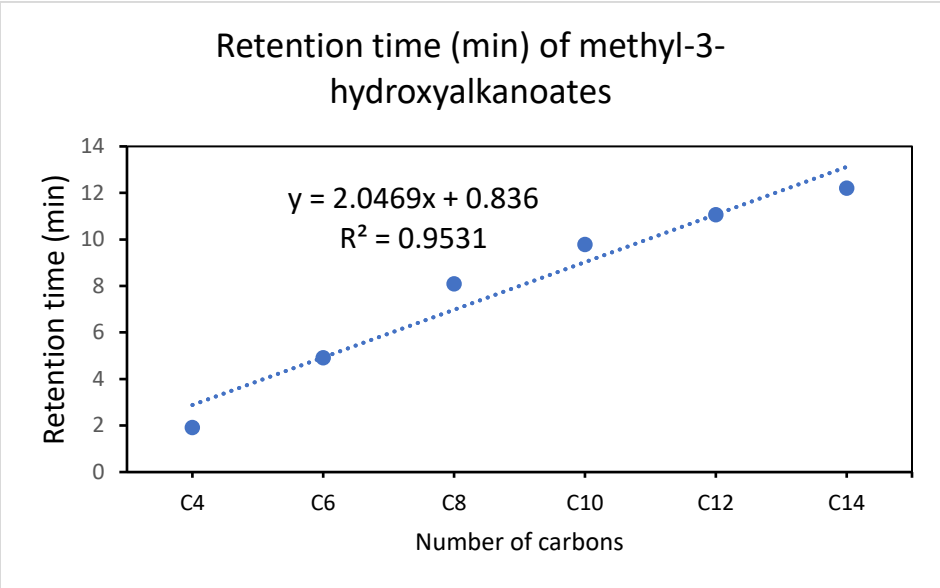

Figure 74. *Retention time (min) of methyl-3-hydroxyalkanoates with different carbon lengths. The dashed line represents the linear trendline (used to build the linear equation) between the points of the curve.*

Annex 5. Standard curve for methyl alkanoates of C12 and C14 carbons and their retention time (RT)

Fatty acid methyl esters (FAMEs) of 12 and 14 carbons were diluted in chloroform and then analyzed in three, totally independent, replicates and the linear regression equation was elucidated from the average of these replicates with a $R^2 \geq 0.94$ The standard curves were also graphed and shown in **Figure 77 and 78** where concentration of methyl ester in chloroform (µg/µl) was chosen for the "x" axis and area under the peak of the chromatogram (µV*s) for "y". The retention time observed for methyl-laurate (C12) was 10.18 ±0.004 while the retention time for methyl-myristate (C14) was 11.40 ± 0.0019. It is important to note that these values differ from the retention times 11.08±0.010 and 12.21±0.005 from methyl-hydroxydodecanoate (C12) and methyl-hydroxytetradecanoate (C14) respectively.

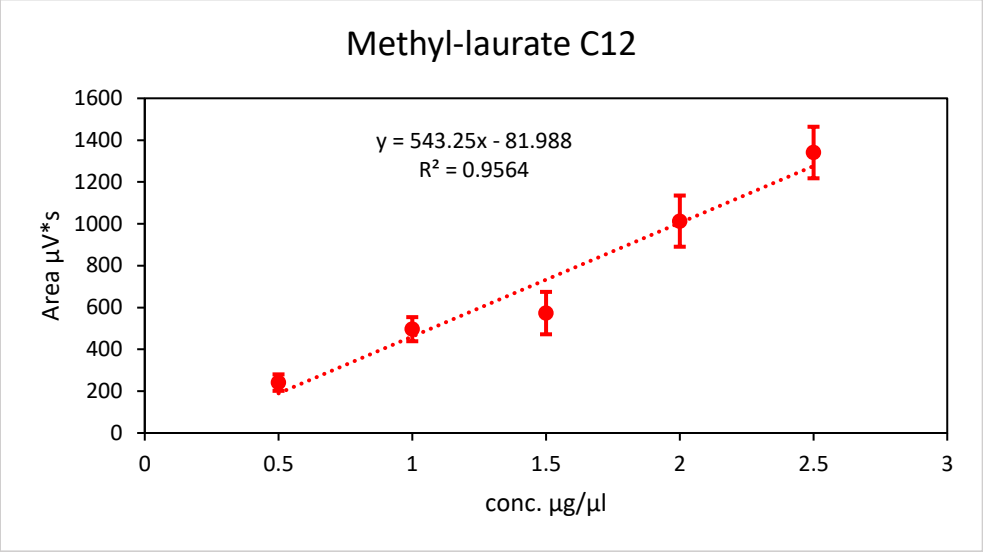

Figure 75. *Standard curve of the monomer methyl-laurate. Retention time: 10.18 ±0.004 min. The dashed line represents the linear trendline (used to build the linear equation) between the points of the curve. Each concentration (µg/µl) was prepared by triplicate and measured using GC.*

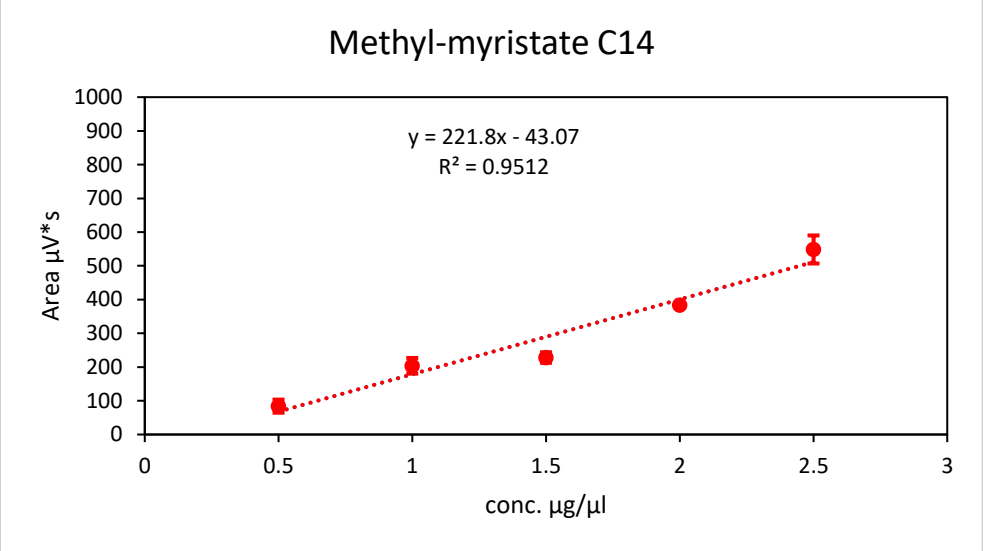

Figure 76*. Standard curve of the monomer methyl-myristate. Retention time: 11.40 ± 0.0019 min. The dashed line represents the linear trendline (used to build the linear equation) between the points of the curve. Each concentration (µg/µl) was prepared by triplicate and measured using GC.*

Annex 6. Plasmids and gene sequences.

CHAPTER 2: Comparison of different PhaCs from *Pseudomonas* to produce PHA with high hydroxydodecanoate and hydroxytetradecanoate monomer composition and the effect of the β-oxidation inhibitor sodium acrylate.

These plasmids were constructed by Johnson, Gonzalez-Villanueva, Tee and Wong [286] [286]

>*PmePhaC*

ATGCGGGATAAGTCGAACCCGGCCTCGCTGCCGGCCCCGGCGACCTTCATGAATGCCCAG
AGCGCGGTGGTCGGTGTGCGCGGTCGCGATCTGCTCAGCACCATGCGGCTGCTGGCCGC
CCAATCGCTGAAGAATCCGGTGCGCAGCGGTCGCCATCTGCTGGCGTTTGGTGGCCAGCT
CGGTCGCGTGCTGCTGGGTGATACGCTGCACAAAGTCAACCCCCAAGACGCGCGCTTCGC
CGATCCGACGTGGCATCTGAACCCGTTCTACCGCCGGTCGCTGCAAGCCTATCTGGCGTG
GCAGAAACAGCTGGCCGCGTGGATCGATGATTCGGACCTCGCGGCCGACGACCGCGCCC
GCGCGCGCTTTCTGGCCTCGCTGATGTCGGATGCGCTGTCGCCGTCGAACAGCCCGCTGA
ACCCCCAAGCGGTCAAAGAACTGTTCAACACGGGTGGTTCGTCGGCCTTCAAGGGCCTCC
GCCATCTGCTGGACGATCTGCTCCACAACGACGGTCTGCCCTCGCAAGTGTCGAAGCATG
CCTTCGAAGTGGGTCGCAACCTCGCGTGCACCCCGGGTGCGGTGGTGTTCCGCAATGAGC
TGCTGGAGCTCATCCAGTACAAGCCCATGTCGGAGAAGCAATACCTCCGCCCGCTGCTCA
TCGTGCCGCCGCAGATCAACAAGTACTACATCTTCGACCTCTCGAACGACAAAAGCTTCGT
CCAGTACGCGCTGAAGAACGGTCTGCAGACGTTCATGATTAGCTGGCGGAATCCCGACCC
GCGCCATCGGGAATGGGGTCTGTCGTCGTACGTGCAAGCCGTCGAAGAGGCCGTCGATG
CGTGCCGCACCATTACCGGTTCGAAGGATGTCAATCTGCTGGGTGCGTGTGCCGGTGGTC
TGACCATCGCCGCGCTGCAAGGTCATCTGCAAGCGCGGCGCCAACTGCGCAAAGTGGCC
TCGGCCACCTACATGGTGTCGCTGCTGGACTCGCAGATCGATTCGCCGGCCATGCTGTTC
GCCGATGAGGAGACGCTGGAGTCGGCCAAACGGCGCTCGTACCAGCATGGCGTGCTGG
ACGGTCGCGATATGGCCCGCGTCTTTGCGTGGATGCGCCCCAACGACCTCATTTGGAACT
ACTGGATCAACAACTATCTGCTCGGCAAACAGCCCCCCGCGTTCGACATCCTCTACTGGAA
CAACGACAATACGCGGCTGCCCGCCGCCCTCCATGGCGATCTGATCGACTTCTTCAAACAC

AACCCGCTGTCGCGGGCCGGCGGTCTGGAGGTGTGTGGCACCCCGGTGGATCTGGCGAA
GGTGAATGTGGATTCGTTCTCGGTCGCCGGTATTAATGACCACATCACCCCGTGGGACGC
CGTGTATCGGTCGACGCTGCTGCTCGGTGGCAATCGGCGGTTCATTCTGAGCAACTCGGG
CCACATTCAGTCGATTCTGAACCCGCCCGGCAATCCGAAGGCCAACTATTACGAAAACAC
GAAGCTGACCAGCGACCCGCGCGCGTGGTACCATGATGCCCAGCACCAGCAAGGCAGCT
GGTGGCCGCAATGGCTGGAGTGGATTCAAGCCCGCAGCGGTGAACAGCGGGAAACCGT
GATGGCGCTGGGCAACCAGAACCATCCGGCGATGGAAACCGCGCCCGGCACGTATGTGC
ACATCCGCTAA

>*PstzPhaC*

ATGCGCGATAAGCCCAACTCGGGCGCGCTGCCCACGCCGGCGACGTTCATGAACGCGCA
GTCGGCCGTCGTGGGTGTGCGCGGTCGCGATCTGCTGTCGACCGTCCGGCTGCTGGCCG
TGCAAGGTCTGAAGCATCCGGTGCGCAGCAGCCGCCATCTGCTGGCGTTTGGTGGCCAAC
TCGGTCGCGTGCTGCTGGGCGATACGCTGCACAAGACCAACCCGCAAGACGCGCGCTTC
GCCGACCCGACGTGGCAGCTCAACCCCTTCTATCGCCGGTCGCTCCAAGCGTATCTCGCGT
GGCAGAAACAGCTGGGCGCGTGGATCGATGATTCGGAGCTCAGCGCCGACGACCGCGC
GCGGGCGCGCTTTCTGGCCGCCATTCTGTCGGATGCGCTGGCCCCGTCGAACTCGCTGCT
GAACCCGCTGGCGCTGAAGGAGCTCTTCAACAGCGGCGGTAGCTCGCTGTTCAAGGGCA
TGCGCCATCTGCTGGACGATCTGCTGCACAACGACGGTCTGCCCTCGCAAGTGAGCAAAC
ACGCCTTCGAAGTGGGTCGCAATCTGGCGTGCACCCCCGGTGCGGTGGTCTTTCGGAACG
AGCTGCTGGAACTCATCCAGTACCGCCCGATGAGCGAAAAACAGTATGTCCGCCCGCTGC
TGATCGTCCCGCCCCAAATCAACAAGTACTACATCTTCGATCTGTCGAACGACAAGTCGTT
CGTGCAGTACGCGCTGAAGAACGGTCTCCAGACCTTCATGATCTCGTGGCGGAATCCCGA
TGCCCGCCATCGCGAGTGGGGTCTGTCGTCGTACGTCCAAGCCGTGGAACAAGCCGTGG
ACGCGTGTCGGGCGATTACCGGCTCGAAGGACGTGAATCTGCTGGGTGCGTGCGCCGGT
GGTCTCACCATTGCCGCGCTGCAAGGCCATCTGCAAGCGAAGCGCCAACTGCGGAAGGT
GGCCAGCGCCACCTACATGGTGTCGCTGCTGGACTCGCAGATCGATTCGCCGGCCATGCT
GTTCGCGGACGAGCAGACGCTGGAAAGCGCCAAGCGGCGGAGCTATCAGCGCGGTGTG

CTGGATGGTCGCGACATGGCGAAGGTGTTTGCGTGGATGCGCCCGAACGATCTGATCTG
GAACTACTGGGTGAACAACTATCTGCTGGGCAAACAGCCCCCGGCCTTCGACATCCTCTA
CTGGAACAACGATAATACCCGGCTGCCGGCCGCGCTGCACGGTGATCTGATCGACTTCTT
CAAGCACAACCCGCTGTCGCGCGCGGGTGGTCTGGAAGTGTGCGGTACGCCCGTCGACC
TCTCGAAGGTGGCGGTGGATAGCTTCTCGGTCGCCGGCATCAACGATCACATCACCCCGT
GGGACGCCGTCTATCGCTCGGCGCTGCTGCTCGGCGGTGAACGCCGGTTTATTCTGTCGA
ACTCGGGTCACATCCAGAGCATTCTGAACCCGCCCGGCAATCCGAAGGCCAACTACTACG
AGAACGGCAAACTGACCAGCGACCCGCGCGCGTGGTACCATGATGCCCGCCACGTGCAA
GGCAGCTGGTGGCCGCAATGGCTGGAGTGGATTCAAGCCCGCAGCGGTGAACAGCGGG
AAACGCTGCTGGCGCTGGGTGACCAGAAACATCCGCCGCAAGAAGCCGCGCCGGGTACG
TACGTGCACATCCGGTAA

>*PpuPhaC*

ATGTCGAACAAGAACAACGACGAGCTGCAGCGCCAAGCCTCGGAGAACACCCTCGGTCT
GAATCCGGTGATCGGCATCCGCCGCAAGGATCTGCTGTCGAGCGCGCGGACCGTCCTCC
GCCAAGCGGTCCGCCAACCGCTGCACTCGGCCAAACACGTCGCCCATTTCGGTCTGGAAC
TGAAGAACGTGCTGCTGGGTAAGTCGTCGCTGGCCCCGGACTCGGATGACCGGCGCTTC
AATGACCCCGCGTGGTCGAACAACCCGCTGTATCGCCGCTATCTGCAGACCTATCTGGCG
TGGCGCAAGGAGCTGCAAGACTGGGTGTCGAGCTCGGATCTGTCGCCGCAAGACATTTC
GCGCGGCCAGTTCGTCATCAATCTGATGACGGAGGCGATGGCCCCCACGAATACGCTCA
GCAATCCGGCCGCCGTGAAGCGGTTTTTTGAGACGGGCGGCAAATCGCTGCTGGACGGC
CTCTCGAACCTCGCCAAGGACATGGTGAACAACGGCGGCATGCCGTCGCAAGTGAACAT
GGACGCCTTTGAGGTCGGCAAGAATCTGGGTACCAGCGAGGGCGCGGTCGTGTATCGGA
ACGACGTGCTGGAACTGATTCAGTACTCGCCCATCACCGAACAAGTGCATGCGCGGCCGC
TGCTGGTGGTGCCCCCGCAGATCAACAAGTTCTACGTGTTCGATCTGAGCCCGGAAAAGT
CGCTGGCGCGGTTTTGCCTCCGCTCGCAGCAACAGACCTTCATCATCAGCTGGCGGAACC
CCACGAAAGCCCAACGCGAATGGGGTCTGTCGACCTACATTGACGCGCTCAAAGAAGCG
GTGGACGCCGTGCTGAGCATCACCGGCAGCAAGGATCTGAACATGCTGGGCGCGTGCTC

GGGTGGCATCACGTGCACCGCGCTGGTGGGCCATTACGCGGCCATTGGCGAGAACAAGG
TGAACGCGCTGACGCTGCTGGTGTCGGTGCTCGACACCACGATGGACAACCAAGTGGCG
CTGTTCGTCGACGAACAGACGCTGGAAGCCGCGAAACGCCATTCGTACCAAGCCGGCGT
GCTGGAAGGCAGCGAAATGGCCAAGGTGTTCGCGTGGATGCGCCCGAACGACCTCATCT
GGAACTACTGGGTCAACAACTATCTGCTCGGTAACGAGCCGCCGGTGTTCGACATTCTGT
TCTGGAACAATGACACCACCCGCCTCCCGGCCGCCTTTCACGGCGATCTGATCGAGATGTT
CAAGTCGAACCCGCTGACCCGGCCCGATGCCCTCGAAGTGTGTGGTACGGCCATTGATCT
GAAGCAAGTGAAGTGCGACATCTATAGCCTCGCCGGCACGAATGATCACATCACCCCGTG
GCCCAGCTGTTACCGCTCGGCGCATCTGTTCGGCGGCAAGATCGAATTCGTGCTGAGCAA
CAGCGGCCACATTCAGAGCATTCTGAACCCGCCGGGTAACCCGAAAGCCCGCTTTATGAC
CGGCGCCGATCGCCCGGGTGACCCGGTGGCGTGGCAAGAGAACGCCATCAAGCACGCG
GATAGCTGGTGGCTCCACTGGCAATCGTGGCTGGGTGAACGCGCGGGTGCGCTGAAAAA
AGCGCCGACCCGCCTCGGTAATCGGACGTATGCCGCCGGTGAAGCCTCGCCGGGCACGT
ATGTGCATGAGCGGTAA

CHAPTER 3: Comparison of different PhaCs from *Pseudomonas* using a different plasmid backbone to produce PHA with high hydroxytetradecanoate (HTD) monomer composition.

Backbone is no longer available in Addgene.

>*PstzPhaC*

ATGCGTGACAAACCGAATTCCGGAGCCTTGCCTACTCCTGCGACCTTCATGAACGCCCAAT
CTGCAGTAGTGGGGGTACGTGGGCGTGACTTATTATCGACAGTGCGCTTGCTTGCCGTTC
AGGGACTTAAACACCCTGTACGCTCGTCACGCCATTTATTAGCATTCGGAGGGCAGCTGG
GGCGCGTGTTATTAGGGGATACGCTGCATAAAACGAATCCCCAAGACGCTCGTTTTGCAG
ATCCTACTTGGCAACTGAACCCCTTTTACCGCCGTTCTCTGCAGGCTTACTTAGCTTGGCAG
AAACAGCTGGGCGCATGGATCGACGACTCTGAATTGAGTGCGGACGACCGTGCACGCGC
TCGTTTTTTAGCAGCAATCTTGTCAGACGCCTTGGCACCTTCAAATAGCTTACTGAATCCCT
TAGCGTTAAAGGAACTGTTTAATTCCGGCGGGAGTTCTCTTTTCAAAGGGATGCGTCACTT
GCTGGATGATCTGTTACATAACGACGGATTACCCTCTCAGGTTTCAAAACACGCGTTTGAG
GTAGGTCGCAACCTTGCGTGTACACCAGGCGCAGTTGTATTTCGCAACGAGTTGCTTGAA
CTTATTCAGTACCGCCCCATGTCAGAAAAACAGTATGTGCGCCCCCTTTTGATCGTTCCTCC
ACAGATCAACAAGTATTACATTTTTGATCTGAGCAACGATAAGTCGTTCGTCCAGTATGCT
CTGAAGAATGGCTTACAGACTTTTATGATCTCCTGGCGTAACCCCGACGCGCGCCACCGC
GAGTGGGGACTTAGCTCGTACGTCCAAGCTGTAGAGCAGGCAGTCGATGCCTGCCGCGC
TATTACCGGCTCCAAAGACGTCAATCTTCTTGGGGCCTGCGCGGGGGGACTGACTATTGC
GGCCCTGCAAGGACACTTACAAGCTAAGCGCCAGCTTCGTAAGGTAGCATCTGCTACATA
TATGGTGTCTCTTCTTGACAGCCAGATCGACTCGCCCGCCATGTTGTTTGCCGACGAACAA
ACATTGGAATCAGCAAAGCGTCGTAGCTATCAACGCGGAGTATTGGATGGTCGTGACAT
GGCGAAGGTTTTCGCGTGGATGCGTCCGAATGATCTTATTTGGAACTACTGGGTTAACAA
CTATTTGCTGGGTAAGCAACCTCCTGCATTTGACATCCTGTATTGGAACAACGATAACACT
CGCCTGCCTGCGGCGCTGCACGGAGATCTTATTGATTTCTTCAAGCACAATCCCCTTTCAC
GTGCGGGGGGGCTGGAGGTCTGCGGTACCCCTGTAGATTTGTCTAAAGTGGCGGTTGAC
TCCTTCAGCGTAGCGGGAATCAACGACCACATCACGCCGTGGGACGCGGTGTACCGTTCA

GCCCTTCTGCTGGGTGGTGAGCGCCGTTTCATCTTAAGTAACAGTGGCCATATCCAAAGT
ATCCTGAACCCACCAGGCAATCCTAAGGCAAATTATTATGAGAATGGGAAGCTTACTTCT
GACCCACGTGCATGGTATCACGATGCGCGCCATGTTCAAGGTTCTTGGTGGCCACAATGG
TTGGAGTGGATTCAGGCGCGCAGTGGTGAGCAGCGCGAAACCCTTCTGGCACTTGGCGA
TCAGAAGCATCCTCCTCAGGAGGCAGCCCCAGGTACCTATGTTCATATTCGCTAA

>*PpuPhaC*

ATGAGCAACAAAAACAATGATGAGTTACAGCGTCAAGCGAGTGAGAATACGCTTGGTTT
GAATCCGGTAATCGGTATCCGCCGCAAAGATCTTTTATCGAGTGCACGCACAGTTCTTCGT
CAGGCGGTCCGCCAGCCACTGCACAGTGCAAAGCACGTAGCTCACTTCGGCTTAGAGCTG
AAAAATGTGCTTTTGGGAAAAAGTAGCTTAGCACCCGACTCTGATGATCGTCGTTTCAAT
GACCCAGCATGGTCAAATAATCCTCTTTACCGCCGCTACCTTCAGACGTATTTGGCATGGC
GCAAGGAGCTGCAGGATTGGGTAAGTTCGAGCGATTTGTCCCCACAAGATATTTCACGTG
GGCAATTCGTGATTAACTTAATGACGGAGGCCATGGCCCCGACTAACACCTTGAGTAACC
CCGCAGCTGTCAAGCGTTTCTTCGAAACTGGCGGAAAATCTTTGCTGGACGGTCTTTCCAA
TCTTGCCAAGGACATGGTAAACAACGGTGGGATGCCCAGCCAAGTGAACATGGATGCCTT
TGAAGTAGGGAAGAATTTGGGAACTTCAGAAGGAGCAGTCGTCTACCGCAATGACGTTC
TGGAGTTGATCCAATATAGTCCGATCACTGAACAGGTACACGCACGCCCGTTGTTAGTAG
TCCCTCCCCAAATTAACAAATTTTATGTGTTTGATCTTTCCCCTGAGAAGAGCCTGGCGCG
CTTCTGTCTGCGCAGCCAACAACAGACGTTCATCATCAGCTGGCGTAATCCCACGAAGGC
CCAGCGTGAGTGGGGGCTGTCCACGTATATTGATGCCTTAAAGGAAGCAGTCGATGCCG
TCCTGAGCATTACTGGTAGTAAGGATTTGAATATGTTGGGAGCATGTTCCGGGGGAATCA
CATGTACTGCTCTTGTTGGTCATTACGCTGCGATTGGGGAGAACAAAGTTAATGCGCTGA
CCCTGCTTGTAAGTGTCTTAGACACTACAATGGACAACCAAGTTGCTTTGTTTGTGGATGA
ACAGACGTTAGAAGCCGCGAAGCGTCACTCATATCAAGCCGGTGTATTGGAGGGTTCAG
AAATGGCTAAGGTCTTCGCTTGGATGCGCCCAAACGATCTGATCTGGAATTACTGGGTGA
ACAATTATCTGTTAGGGAATGAGCCTCCAGTGTTCGACATCCTGTTTTGGAATAATGACAC
GACACGCTTGCCCGCCGCTTTCCACGGAGACCTGATCGAAATGTTTAAGTCTAACCCACTT
ACGCGTCCCGACGCTTTAGAGGTGTGTGGTACCGCGATTGACTTGAAGCAAGTGAAGTG
CGATATTTACAGTCTGGCGGGAACAAATGACCACATTACACCGTGGCCGTCGTGTTATCG

TAGCGCACATTTATTCGGCGGCAAAATTGAGTTCGTCTTAAGTAATAGCGGCCATATCCAA
TCTATCTTAAATCCTCCCGGCAACCCAAAAGCCCGTTTTATGACCGGTGCGGATCGTCCGG
GCGATCCTGTGGCGTGGCAAGAAAACGCTATCAAGCACGCCGATTCGTGGTGGCTTCACT
GGCAATCTTGGTTAGGGGAGCGCGCAGGTGCTTTGAAGAAGGCACCAACGCGCTTGGGT
AACCGTACCTACGCCGCCGGCGAGGCTTCTCCCGGAACTTACGTGCACGAACGCTAA

>*PmePhaC*

ATGCGTGACAAATCTAACCCCGCTTCTTTACCGGCGCCCGCTACTTTCATGAATGCGCAGT
CCGCCGTAGTAGGCGTTCGCGGGCGTGACCTTCTGAGCACTATGCGCCTTCTTGCTGCCC
AGAGTCTTAAAAATCCGGTCCGTAGTGGGCGCCATTTGCTGGCCTTTGGGGGCCAGTTAG
GGCGTGTTTTGTTAGGGGATACGTTACATAAGGTTAATCCCCAGGATGCCCGTTTCGCGG
ACCCTACGTGGCACCTTAATCCGTTTTATCGCCGTAGTTTGCAGGCGTATCTGGCATGGCA
AAAACAGCTGGCTGCTTGGATCGACGATTCTGATCTGGCGGCCGATGACCGTGCGCGTGC
CCGTTTCCTGGCTAGCTTGATGTCAGATGCTCTGAGCCCCAGCAATAGCCCGCTTAATCCT
CAAGCGGTGAAAGAATTGTTTAACACCGGAGGATCGTCCGCATTTAAAGGCTTACGTCAT
CTGTTAGACGATCTTCTTCATAACGACGGTTTACCCTCGCAGGTCTCTAAGCACGCATTTG
AAGTGGGCCGCAACCTTGCGTGCACCCCGGGGGCTGTAGTTTTTCGCAACGAGTTGTTAG
AGTTAATTCAATATAAGCCCATGAGCGAAAAGCAGTACTTGCGCCCCCTGTTAATCGTACC
CCCCCAGATCAACAAGTACTACATCTTTGATCTTTCGAACGACAAGAGCTTTGTGCAATAC
GCCCTGAAGAATGGACTTCAGACGTTCATGATCAGCTGGCGTAATCCTGATCCTCGCCAC
CGCGAGTGGGGGTTGAGCAGTTACGTGCAAGCTGTGGAAGAAGCCGTCGATGCTTGTCG
TACGATCACGGGCAGTAAGGACGTCAACTTGTTGGGGGCATGTGCTGGAGGTCTGACCA
TTGCCGCACTGCAAGGTCACCTTCAAGCGCGTCGCCAGTTGCGTAAAGTCGCATCTGCGA
CATATATGGTTAGTCTGCTTGACAGTCAGATCGATAGCCCCGCCATGTTGTTCGCAGACGA
AGAGACCTTGGAAAGTGCGAAACGTCGCTCGTATCAACACGGCGTGTTGGATGGTCGCG
ATATGGCCCGCGTCTTCGCTTGGATGCGCCCAAACGACCTGATTTGGAACTATTGGATTAA
CAATTACTTACTGGGAAAGCAGCCCCCTGCTTTTGATATTCTGTACTGGAATAACGACAAT
ACTCGCTTACCTGCCGCGTTACACGGCGACCTGATTGATTTTTTCAAACACAACCCCCTTTC
CCGTGCTGGAGGTCTTGAGGTATGCGGAACTCCTGTCGACTTGGCAAAAGTAAATGTCGA
TTCGTTCAGTGTCGCCGGAATCAACGATCACATTACCCCCTGGGACGCGGTATATCGCTCG

ACGTTGTTACTGGGGGGAAATCGTCGCTTTATTTTGTCGAATAGTGGGCATATTCAGTCG
ATTTTAAATCCCCCTGGCAATCCCAAGGCCAACTACTATGAAAATACTAAATTGACTTCTG
ACCCCCGCGCGTGGTACCACGATGCGCAACACCAACAGGGCAGCTGGTGGCCTCAATGG
CTTGAGTGGATTCAGGCCCGCTCTGGAGAGCAACGTGAGACGGTTATGGCGTTGGGTAA
CCAGAACCACCCCGCCATGGAGACGGCCCCCGGAACATACGTACACATTCGTTAA

CHAPTER 4: Comparison of FabG from Mycobacterium tuberculosis and FabG from Escherichia coli K-12 to produce polyhydroxyalkanoates with high hydroxytetradecanoate monomer composition.

Backbone is no longer available in Addgene.

>*MtubfabG*

ATGACGGCAACAGCGACGGAAGGCGCAAAACCTCCATTCGTAAGCCGCTCGGTATTGGTT
ACCGGCGGGAATCGTGGAATTGGATTGGCTATCGCTCAGCGCTTGGCTGCCGATGGGCA
TAAGGTCGCGGTGACACACCGTGGAAGTGGTGCGCCTAAGGGTCTGTTTGGAGTCGAAT
GTGATGTTACGGACAGTGATGCGGTAGATCGCGCATTTACCGCGGTCGAGGAGCACCAG
GGCCCCGTTGAAGTGCTTGTTTCAAATGCTGGACTGTCTGCGGATGCCTTTCTGATGCGTA
TGACGGAGGAGAAATTCGAGAAAGTCATCAACGCGAATTTAACAGGAGCATTTCGCGTA
GCCCAACGCGCGAGTCGCTCCATGCAACGTAACAAGTTCGGCCGTATGATTTTCATCGGT
AGCGTATCCGGCTCATGGGGTATTGGCAACCAAGCGAATTACGCGGCCTCGAAGGCTGG
CGTAATCGGTATGGCACGTAGTATCGCACGCGAACTTTCAAAGGCAAACGTGACCGCAAA
TGTCGTTGCTCCAGGCTATATCGACACCGATATGACTCGTGCTTTGGATGAACGCATCCAG
CAGGGGGCTCTTCAATTCATCCCCGCTAAGCGCGTGGGGACACCTGCCGAGGTAGCTGGT
GTTGTAAGTTTTCTTGCATCTGAGGATGCATCCTATATCTCGGGGGCTGTCATTCCAGTGG
ATGGGGGGATGGGGATGGGGCATTAA

>EcolifabG

ATGAATTTTGAAGGAAAAATCGCACTGGTAACCGGTGCAAGCCGCGGAATTGGCCGCGC
AATTGCTGAAACGCTCGCAGCCCGTGGCGCGAAAGTTATTGGCACTGCGACCAGTGAAA
ATGGCGCTCAGGCGATCAGTGATTATTTAGGTGCCAACGGCAAAGGTCTGATGTTGAATG
TGACCGACCCGGCATCTATCGAATCTGTTCTGGAAAAAATTCGCGCAGAATTTGGTGAAG
TGGATATCCTGGTCAATAATGCCGGTATCACTCGTGATAACCTGTTAATGCGAATGAAAG
ATGAAGAGTGGAACGATATTATCGAAACCAACCTTTCATCTGTTTTCCGTCTGTCAAAAGC
GGTAATGCGCGCTATGATGAAAAAGCGTCATGGTCGTATTATCACTATCGGTTCTGTGGT
TGGTACCATGGGAAATGGCGGTCAGGCCAACTACGCTGCGGCGAAAGCGGGCTTGATCG
GCTTCAGTAAATCACTGGCGCGCGAAGTTGCGTCACGCGGTATTACTGTAAACGTTGTTG
CTCCGGGCTTTATTGAAACGGACATGACACGTGCGCTGAGCGATGACCAGCGTGCGGGT
ATCCTGGCGCAGGTTCCTGCGGGTCGCCTCGGCGGCGCACAGGAAATCGCCAACGCGGT
TGCATTCCTGGCATCCGACGAAGCAGCTTACATCACGGGTGAAACTTTGCATGTGAACGG
CGGGATGTACATGGTCTGA

CHAPTER 5: Construction of the double knockout ΔfadAΔfadR to produce polyhydroxyalkanoates with high hydroxytetradecanoate monomer composition.

>H1(fadR)-FRT-kan-FRT-H2(fadR)

The forward primer is squared in the sequence **GGCTACCCGTGATATTGCTG**

CCCTCTGGTATGATGAGTCCAACTTTGTTTTGCTGTGTTATGGAAATCTCACCTGCTTCGAA
GTTCCTATACTTTCTAGAGAATAGGAACTTCGGAATAGGAACTTCAAGATCCCCTCACGCT
GCCGCAAGCACTCAGGGCGCAAGGGCTGCTAAAGGAAGCGGAACACGTAGAAAGCCAG
TCCGCAGAAACGGTGCTGACCCCGGATGAATGTCAGCTACTGGGCTATCTGGACAAGGG
AAAACGCAAGCGCAAAGAGAAAGCAGGTAGCTTGCAGTGGGCTTACATGGCGATAGCTA
GACTGGGCGGTTTTATGGACAGCAAGCGAACCGGAATTGCCAGCTGGGGCGCCCTCTGG
TAAGGTTGGGAAGCCCTGCAAAGTAAACTGGATGGCTTTCTTGCCGCCAAGGATCTGATG

GCGCAGGGGATCAAGATCTGATCAAGAGACAGGATGAGGATCGTTTCGCATGATTGAAC
AAGATGGATTGCACGCAGGTTCTCCGGCCGCTTGGGTGGAGAGGCTATTCGGCTATGACT
GGGCACAACAGACAATCGGCTGCTCTGATGCCGCCGTGTTCCGGCTGTCAGCGCAGGGG
CGCCCGGTTCTTTTTGTCAAGACCGACCTGTCCGGTGCCCTGAATGAACTGCAGGACGAG
GCAGCGCGGCTATCGTGGCTGGCCACGACGGGCGTTCCTTGCGCAGCTGTGCTCGACGTT
GTCACTGAAGCGGGAAGGGACTGGCTGCTATTGGGCGAAGTGCCGGGGCAGGATCTCCT
GTCATCTCACCTTGCTCCTGCCGAGAAAGTATCCATCATGGCTGATGCAATGCGGCGGCT
GCATACGCTTGATCCGGCTACCTGCCCATTCGACCACCAAGCGAAACATCGCATCGAGCG
AGCACGTACTCGGATGGAAGCCGGTCTTGTCGATCAGGATGATCTGGACGAAGAGCATC
AGGGGCTCGCGCCAGCCGAACTGTTCGCCAGGCTCAAGGCGCGCATGCCCGACGGCGAG
GATCTCGTCGTGACCCATGGCGATGCCTGCTTGCCGAATATCATGGTGGAAAATGGCCGC
TTTTCTGGATTCATCGACTGTGGCCGGCTGGGTGTGGCGGACCGCTATCAGGACATAGCG
TT**GGCTACCCGTGATATTGCTG**AAGAGCTTGGCGGCGAATGGGCTGACCGCTTCCTCGT
GCTTTACGGTATCGCCGCTCCCGATTCGCAGCGCATCGCCTTCTATCGCCTTCTTGACGAG
TTCTTCTGAGCGGGACTCTGGGGTTCGAAATGACCGACCAAGCGACGCCCAACCTGCCAT
CACGAGATTTCGATTCCACCGCCGCCTTCTATGAAAGGTTGGGCTTCGGAATCGTTTTCCG
GGACGCCGGCTGGATGATCCTCCAGCGCGGGGATCTCATGCTGGAGTTCTTCGCCCACCC
CAGCTTCAAAAGCGCTCTGAAGTTCCTATACTTTCTAGAGAATAGGAACTTCGGAATAGG
AACTAAGGAGGATATCCCTTCCGTTTAAAGAGCAAACCCCTCAAACGAGGGGTTTTTTGTT
GTTT

CHAPTER 6: Construction of new plasmids to express *phaC-MtubfabG* genes.

Sequence is available in **Addgene** Catalog number **54564**

mPlum-pBAD was a gift from Michael Davidson & Roger Tsien (Addgene plasmid # 54564 ; http://n2t.net/addgene:54564 ; RRID:Addgene_54564) [372]

PhaC sequences and MtubfabG sequence are the same shown for **Chapters 3,4, and 5**

Annex 7. SDS-PAGE for Chapter 6.